Investigation of the Function Of *YOL093W*

in *Saccharomyces cerevisae*

Meng-Ya Chang

A Thesis Presented for the Degree of

Doctor of Philosophy

University of Edinburgh

May 2004

Declaration

I hereby declare that this thesis was composed by myself and the research presented is my own, expect where otherwise stated.

Meng-Ya Chang

May 2004

Acknowledgements

I would like to thank David Leach for the opportunity to work on this research and for his patience and help. Thank Jean Beggs for the opportunity to carry out my experiments in her laboratory. I would also like to thank John Connelly and Richard Grainger for all the guidance and for doing the corrections for my writing.

Thanks also go to the members of the Leach group and the Beggs group for being great friends. They have made my time in Edinburgh so enjoyable and special.

An enormous thank must go to my big family for their love and encouragement.

Chih-Jui for all the good food he made, his funny jokes, and his support.

Finally, I would like to thank the Darwin Trust of Edinburgh for funding this work.

Abstract

Resolution of four-way junction (Holliday junction, HJ) structures is a key event during recombination. The enzymatic activities that promote Holliday junction formation and resolution have been extensively characterized in bacteria. However, much less is known in eukaryotic cells and to identify similar activities in eukaryotes have been difficult. In this thesis, we aimed to identify HJ resolvases through protein sequence alignment. We identified *Saccharomyces cerevisiae* Yol093wp by the PSI-BLAST search with the sequence of the yeast mitochondrial resolvase Cce1p or Ydc2p. Yol093wp homologs are widely found in eukaryotes. Each sequence of the Yol093wp family has diverged substantially from every other with relatively small sizes, and contains some conserved acidic residues, which might contribute to the binding site catalytic metal ion(s). These are similar to those observed among the families of known resolvases. In this work, a variety of general and specific approaches were used to characterize the functions of *YOL093W*. We have shown that His-tagged Yol093wp expressed in *E. coli* and has been enriched, and the Yol093wp extracts might have DNA binding properties. Interestingly, *in vitro* studies revealed the preferential binding of Yol093wp extracts to a mobile four-way junction than to a 60 nt-ssDNA or a 60 bp-dsDNA. The basis of this binding activity is still unclear. Further analysis will be required to elucidate the specificity of this DNA binding. Cells lacking Yol093wp have no obvious growth defects under standard growth conditions. Meiotic recombination assays showed that *YOL093W* deletion has no effect on meiotic recombination. A yeast two-hybrid screen and TAP

tag purification were utilised to identify Yol093wp-interacting proteins. In the two-hybrid screen, Mtl1p that is involved in cell wall biogenesis was retrieved with relatively low significance. The TAP purification of Yol093wp complex showed that the Yol093w protein was synthesized in the TAP-tagged strain, and could be purified followed the TAP purification precedure. However, the identities of the potential interacting proteins identified did not throw much light on the function of Yol093wp. Finally, the immunofluorescence micrographs of Yol093wp-GFP and Yol093wp-13myc in conjunction with DAPI straining suggested that the Yol093w fusion proteins are located in the nucleus. All of these data may be indicative of the function of Yol093wp.

Common Abbreviations

aa	Amino acid(s)
Amp	Ampicillin
ARS	Autonomous Replication Sequence
ATP	Adenosine 5'-triphosphate
bp	Base-pair
°C	Degree Celsius
cDNA	Complementary Deoxyribonucleic Acid
CEN	Centromere Sequence
cpm	Counts per Minutes
cm	centimeter
Da	Dalton
dATP	Deoxyadenosine triphosphate
dCTP	Deoxycytidine triphosphate
dGTP	Deoxyguanosine triphosphate
dTTP	Deoxythymine triphosphate
DMSO	Dimehtyl Sulfate
DNA	deoxyribonucleic acid
DTT	Dithiothreitol
ECL	Enhanced Chemi-Luminescence
EDTA	Ethylenediaminetetraacetic acid
g	gram(s)
h	hour(s)
HA	Haemagglutinin HA-1 protein epitope
HEPES	*N*-2-hydroxyethylpiperazine-*N'*-2-ethanesulfonic acid
hph	Hygromycin B
HRP	Horseradish Peroxidase
kb	kilobase
kDa	kilodalton
kV	kilovolt(s)
L	Litter(s)
LB	Luria Broth (medium)
M	Molar
mA	milliampere(s)
mg	milligram(s)

mM	millimolar
mmol	millimole(s)
min	minute(s)
ml	milliliter(s)
mRNA	Messenger Ribonucleic Acid
MOPS	3-[N-Morpholino]-propanesulphonic acid
MW	Molecular Weight
NP-40	Nonident P-40 detergent
ng	nanogram(s)
nm	nanometer(s)
nt	nucleotide
OD_{600}	Optical Density at 600 nm
ORF	Open Reading Frame
PAGE	Polyacryamide Gel Electrophoresis
PCR	Polymerase Chain Reaction
pmol	picomole(s)
RNA	Ribonucleic Acid
RT	Room Temperature
rpm	Revolutions per minute
SDS	Sodium Dodecyl Sulphate
TAE	Tris/Acetate (buffer)
TBS	Tris-buffered Saline
TEMED	*N,N,N',N'*-tetramethyl-ethylenediamine
tRNA	transfer Ribonucleic acid
Tris	Tris(hydroxymethyl)aminomethane
µg	microgram(s)
µl	microliter(s)
µm	micrometer(s)
U	Unit(s)
V	Volt(s)
v/v	Volume per unit volume
w/v	Weight per unit volume
YMM	Yeast Minimal medium
YPDA	Yeast/Peptone/Dextrose/Adenine (medium)

Amino Acid Abbreviations

Amino acid	3-letter code	1-letter code
Alanine	Ala	A
Arginine	Arg	R
Asparagine	Asn	N
Aspartate	Asp	D
Cystenine	Cys	C
Glutamate	Glu	E
Glutamine	Gln	Q
Glycine	Gly	G
Histidine	His	H
Isoleucine	Ile	I
Leucine	Leu	L
Lysine	Lys	K
Methionine	Met	M
Phenylalanine	Phe	F
Proline	Pro	P
Serine	Ser	S
Threonine	Thr	T
Tryptophan	Trp	W
Tyrosine	Tyr	Y
Valine	Val	V

Table of Contents

List of Figures

List of Tables

CHAPTER ONE

Introduction

1.1 Homologous Recombination

1.1.1 Introduction

Homologous recombination (HR) is a process for genetic exchange between DNA sequences that share homology. It is a fundamental biological process that promotes genetic diversity and the maintenance of genome integrity in prokaryotic and eukaryotic organisms. Several processes employ the mechanism of homologous recombination: the repair of broken replication forks or DNA lesions (Kowalczykowski, 2000), the reassortment of alleles, and the correct segregation of chromosomes during meiosis (Roeder, 1997). In meiosis, the primary function of recombination is to establish a physical connection between homologous chromosomes to ensure their correct disjunction at the first meiotic division. In

addition, meiotic recombination contributes to diversity by creating new linkage arrangements between genes, or parts of genes (Roeder, 1997). It is now widely recognized that the primary function of homologous recombination in mitotic cells is to repair DSBs that form as a result of replication fork collapse, from processing of spontaneous damage, and from exposure to DNA-damaging agents (Kogoma, 1997; Aguilera et al., 2000; Cox, 2001; Kuzminov, 2001). Recombination is also required to repair the DSBs that initiate programmed rearrangements, such as mating-type switching in *Saccharomyces cerevisiae* (Strathern et al., 2000).

Recombination can be initiated by several types of DNA damage: single-strand DNA (ssDNA) lesions may result during DNA replication or during repair, after UV irradiation or the alkylation or cross-linking of DNA bases, or from intermediates of type I topoisomerases; double-strand breaks (DSBs) can appear as a consequence of ionizing radiation, by mechanical stress, by endonucleases, or by replication of a single-stranded nicked chromosome (Friedberge et al., 1995; Lindahl and West, 1995; Smith and Jones, 2000). If unrepaired, DSBs will result in broken chromosomes and loss of genetic material, genomic alterations or cell death. If repaired incorrectly, they can cause genetic alterations that can lead to cancer (Haber, 1999; Jackson, 1999; Thacker 1986; Jeggo, 1998[a]; Kanaar and Hoeijmakers, 1998). For these reasons, DSBs must be efficiently repaired to restore the integrity and functionality of the genome.

A single-strand DNA lesion can be repaired using the information present on the remaining intact strand, but a double-strand lesion cannot be repaired in this way. In

eukaryotic cells, repair can be carried out either by homologous recombination or by non-homologous end joining (NHEJ) (reviewed in Pastink and Lohman, 1999; Pastink et al., 2001; Bosch et al., 2002; Symington, 2002). These pathways differ in their requirement for a homologous DNA template and the fidelity of the repair reaction. Homologous recombination uses an intact sister duplex as the template for repair, so the reaction occurs with high fidelity. By contrast, NHEJ occurs without a template, and involves the simple religation of the broken termini. Any sequences that are lost at the break site will be fixed as a mutation or deletion in the rejoined product. These repair mechanisms have been conserved through evolution and operate in a wide range of organisms, including both prokaryotes and eukaryotes, however, significantly differs depending on the organism. While homologous recombination plays a major role in DSB repair in prokaryotes and lower eukaryotes, it operates rather rarely in somatic cells of higher eukaryotes. Instead, in somatic cells of higher eukaryotes including, DSB are repaired primarily through NHEJ (Jeggo, 1998[b]; Critchlow and Jackson, 1998). The importance of each pathway also depends on the stage of the cell cycle, with NHEJ dominating in G1, and homologous recombination making a greater contribution in the S and G2 phases (Liang et al., 1998; Takata et al., 1998; Essers et al., 2000). In addition, in muticellular organisms, it also depends on the cell type and the stage of development. Furthermore, the involvement of each pathway may be influenced by the complexity and/or the quality of the break (Pastink and Lohman, 1999; Pastink et al., 2001; van den Bosch et al., 2002).

The processes by which damaged DNA is repaired and the mechanisms of genetic recombination are intimately related. Much of what we know about these events has come from studies of the yeast *Saccharomyces cerevisiae*, for which the development of new molecular biological and genetic approaches has made it possible to appreciate the many different pathways used by eukaryotic cells. The study of these processes in a simple, unicellular eucaryote has the obvious advantages of the ease of manipulation of DNA sequences and the possibility of studying specific repair and recombination events induced synchronously in a large proportion of cells. Equally important is the growing conviction that the processes that one can study with relative ease in yeast are identical in most respects to the ways in which human cells repair DNA damage and generate genetic diversity. The expanding list of human genetic diseases associated with defects in DNA metabolism makes it especially important in understanding how these processes occur. Moreover, defining these mechanisms has taken on added importance in the quest to develop more efficient mechanisms of gene targeting and gene replacement in mammalian cells (Paques and Haber, 1999).

1.1.2 Current Model of Homologous Recombination

Although with different biological meaning and genetic control, both mitotic and meiotic recombination uses common factors and steps. For years, the model most commonly used to explain the molecular mechanism of recombination has been the double-strand break repair (DSBR) model (Figure 1.1) (Szostak et al., 1983). The repair processes commences as single-stranded (ss) degradation of the broken DNA molecule exposes protruding 3'-OH ends. In all organisms, the early steps of

recombination involving homologous pairing and strand exchange are promoted by proteins belonging to the RecA/RAD51 family of recombinases. The 5'-ends on either side of the break is resected to produce single-stranded (ss) 3'-tails. The D-loop created by single-end invasion (SEI) may enter the double-strand-break repair (DSBR) pathway and form a double Holliday junction (dHJ) (Hunter and Kleckner, 2001; Allers and Lichten, 2001b), which can be resolved to crossover (CO) and non-crossover (NCO) products. Resolution to crossover requires a symmetric cleavage of both Holliday junctions in opposite orientations by a Holliday junction resolvase. Resolution to non-crossovers can also be achieved by the resolvase (cleavage of both junctions in the same orientation) or by collapsing the dHJ to a hemi-catenane followed by resolution involving a type I topoisomerase activity. Alternatively, the D-loop enters the synthesis-dependent strand annealing (SDSA) pathway. After extension by DNA polymerase, the invading strand retreats to reanneal with the single-stranded DNA tail that did not form a D-loop. In its simplest version, SDSA leads only to NCO products (as shown in Figure 1.1). More complex versions of SDSA involve dHJ formation, which can be resolved by a Holliday junction resolvase to CO and NCO products (Paques and Haber, 1999).

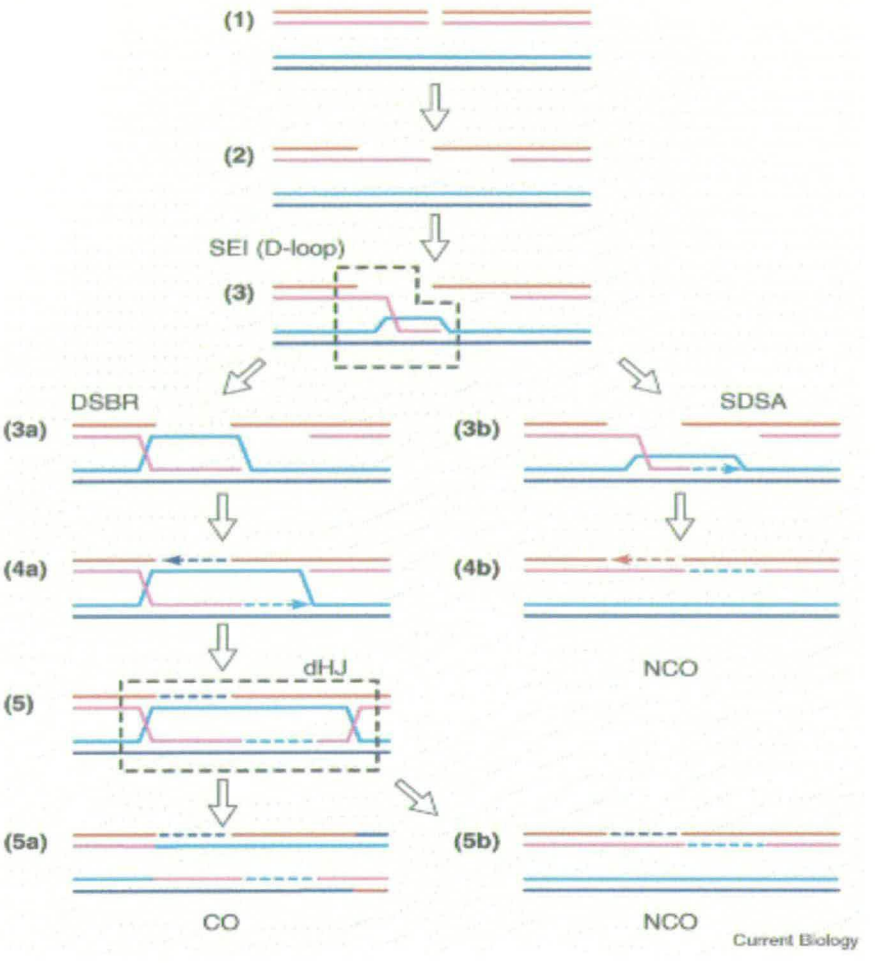

Figure 1.1 Double-strand-break Repair (DSBR) and Synthesis-Dependent Strand Annealing (SDSA) Models for Meiotic Recombination (Heyer, 2004)

Meiotic recombination is initiated by Spo11-generated double-stranded DNA breaks (DSBs) (step 1). After DSB processing by the Mre11–Rad50–Xrs2 complex and other enzymes (step 2), RPA, Rad52 and Rad55–Rad57 orchestrate formation of the Rad51 nucleoprotein filament capable of homology search and DNA strand invasion (step 3). Rad54 augments Rad51-mediated recombination in D-loop formation and is also thought to allow access of DNA polymerases to the invading 3'-OH by displacing Rad51 from the product heteroduplex DNA (steps 3b, 4a). The D-loop created by single-end invasion (SEI) may enter the DSBR pathway (step 3a) and form a double Holliday junction (dHJ; steps 4a, 5), which can be resolved to crossover (CO; step 5a) and non-crossover (NCO; step 5b) products. Resolution to CO requires a symmetric cleavage of both Holliday junctions in opposite orientations by Holliday junction resolvase. Resolution to NCOs can also be achieved by the resolvase (cleavage of both junctions in the same orientation) and by collapsing the dHJ to a hemi-catenane followed by resolution involving a type I topoisomerase activity. Alternatively, the D-loop enters the SDSA pathway (step 3b). After extension by DNA polymerase, the invading strand retreats to reanneal with the single-stranded DNA tail that did not form a D-loop (step 4b). In its simplest version, SDSA leads only to NCO products (as shown).

1.1.2.1 Homologous Recombination in *Escherichia coli*

The molecular mechanism of Homologous recombination (HR) is best understood in *Escherichia coli* (Roca and Cox, 1997; Cox, 1999). The principal recombination protein in this organism is the RecA protein and almost all DSB repair by HR is through the RecBCD pathway (Kowalczykowski et al., 1994). In the initiating step, DSB are specifically recognized by the RecBCD heterotrimer (exonuclease V), which has both exonuclease and helicase activities. In the presence of Mg^{2+} and ATP, the RecBCD complex binds to the end of a double-stranded DNA (dsDNA) substrate, unwinds processively and degrades preferentially the 3'-ending strand until it encounters a Chi (χ)-site sequences that create recombination hot spots. After interaction with the χ-site, the nuclease activity of the enzyme is altered so that degradation of the 3'-terminal strand is downregulated and the nuclease activity at the 5'-terminated strand is upregulated, whilst helicase activity remains unaltered. Finally, the χ-modified RecBCD enzyme produces resected dsDNA with a 3'-ssDNA tail terminating at the χ-sequence (Bianco and Kowalczykowski, 1997; Amundsen et al., 2000). Another helicase, RecQ, has also been shown to be able to initiate recombination by providing the RecA protein with a suitable substrate (Harmon and Kowalczykowski, 1998). In the presence of ATP, RecA coats a 3'-ssDNA tail and polymerizes head-to-tail, forming a right-handed presynaptic helical nucleoprotein filament. Upon modification of nuclease activity, RecBCD enzyme coordinates the preferential loading of RecA onto the resultant 3'-ssDNA tail downstream of χ (Arnold and Kowalczykowski, 2000). In this process, RecBCD promotes displacement of single-strand binding (SSB) protein from ssDNA by RecA. SSB plays a dual role in RecA-mediated strand exchange (Meyer and Laine, 1990).

Firstly, by binding to ssDNA, it removes any secondary structure and allows RecA to form a continuous filament. Secondly, as strand exchange proceeds, it binds to the released single-stranded DNA, and therefore stabilizes the joint molecule and prevents reinitiation (Roman et al., 1991). Additional proteins, RecF, RecO and RecR, help RecA to overcome inhibition of binding by the SSB protein (Umezu and Kolodner, 1994; Morimatsu and Kowalczykowski, 2003). The RecA nucleoprotein filament then recognizes and invades the homologous sequence in duplex DNA, thereby creating hDNA (West, 1996). Additional factors, including RuvA, RuvB and RecG proteins, bind to the Holliday junctions and promote branch migration (West, 1996; Whitby and Lloyd, 1998). The RuvA protein specifically recognizes the Holliday junction, whereas RuvB is necessary for branch migration. RecG protein, like RuvA–RuvB, also promotes branch migration but the reaction is weaker. The Holliday junction can be resolved by the Holliday junction resolvase, RuvC (West, 1996). In the absence of RuvC, another Holliday junction resolvase, RusA, can be activated and act on Holliday junction. Suppression function of RusA, however, critically depends on RecG protein (Mahdi et al., 1996). RuvC endonuclease binds to the RuvA–RuvB complex and then cuts the DNA intermediate at two sites. Subsequent ligation generates recombinant (or non-recombinant) molecules containing a segment of hDNA. Alternatively, the double Holliday junction might be resolved by reverse branch migration (Bianco et al., 1998).

As expected, cells lacking the RecA protein show nearly no recombination events (Cox, 1999; Kowalczykowski et al., 1994). Nevertheless, *recA* mutants have 50% viability when grown in liquid cultures (Capaldo et al., 1974). The *recA* mutants

exhibit various defects in recombination, repair and SOS response and are sensitive to a variety of DNA damaging agents (reviewed in Cox, 1999; Kowalczykowski et al., 1994).

1.1.2.2 Homologous Recombination in *Saccharomyces cerevisiae*

As shown by Siede *et al.* (Siede et al., 1996), HR is the favored DSB repair pathway in *S. cerevisiae*, whereas NHEJ is only of minor importance. These authors found that in cells competent for HR, deletion of NHEJ component did not result in increased sensitivity to IR or to MMS and DSB repair was not impaired. However, if HR was disabled, inactivation of NHEJ led to an additional sensitization to IR and MMS. Hence, in *S. cerevisiae* NHEJ activity can be demonstrated only in the absence of HR and it may thus serve only as a backup system.

In the *S. cerevisiae*, the genes implicated in HR belong to the *RAD52* epistasis group, which includes *RAD50*, *RAD51*, *RAD52*, *RAD54*, *RAD55*, *RAD57*, *RAD59*, *RDH54/TID1*, *MRE11* and *XRS2* genes (Pastink and Lohman, 1999; Pastink et al., 2001; van den Bosch et al., 2002; Symington, 2002; Paques and Haber, 1999; Sung et al., 2000). Cells mutated in these genes are in general sensitive to IR, but not to ultraviolet (UV) irradiation, unable to repair DSB, and defective in mitotic and/or meiotic recombination (Petes et al., 1989). However, there is a considerable variability among the *RAD52* epistasis group members with respect to the repair defect conferred by the particular mutation. Subdivision of the *RAD52* epistasis group members into several families was therefore suggested (Paques and Haber,

1999). Since the *RAD52* gene is required for virtually all HR events, it stands alone. The uniqueness of the *RAD52* gene product is well established by the IR sensitivity of the *rad52* mutant: the *rad52* single mutant is as IR sensitive as a double mutant of *rad52* combined with a mutation in one of the other *RAD* genes (Game and Mortimer, 1974). The *rad51*, *rad54*, *rad55* and *rad57* mutants have common phenotypes, and the corresponding gene products constitute a family that has been designated the *RAD51* family. Contrary to *RAD52*, the *RAD51* family is necessary for some HR events, but dispensable for others. Furthermore, the IR sensitive phenotype of the *RAD51* family mutants is much less severe than that of the *rad52* mutant. The *rad50*, *mre11* and *xrs2* mutants also display identical phenotypes and therefore the respective genes constitute another family. There are homologues of the *RAD52* and *RAD54* genes, designated *RAD59* and *RDH54/TID1*, respectively, which may represent the separate subgroups because of their specific functions in HR.

1.1.2.3 Homologous Recombination in Higher Eukaryotes

For many years, HR had been considered to be a minor pathway that acts on DSB in higher eukaryotes. This opinion was based on the fact that none of the cell lines displaying an IR sensitive phenotype and/or DSB repair defects were found to be mutated in any of the genes encoding the HR proteins. Moreover, some of the HR mutants are lethal in vertebrate cell lines and therefore they could not be further tested for the particular mutation. It was therefore believed that DSB repair in higher eukaryotes is almost exclusively undertaken by the NHEJ pathway. Recently, however, it has been established that HR also contributes considerably to DSB repair

in these cells (reviewed in van den Bosch et al., 2002; Morrison and Takeda, 2000; Johnson and Jasin, 2001; Thompson and Schild, 2001). This conclusion has come mainly from the identification of relevant mammalian HR genes either through cloning genes that complement cell lines that are sensitive to DNA damaging agents or through homology searches (Morita et al., 1993; Shinohara et al., 1993; Park, 1995; Petrini et al., 1995; Tebbs et al., 1995; Albala et al., 1997; Tambini et al., 1997; Cartwright et al., 1998; Dosanjh et al., 1998; Liu et al., 1998; Pittman et al., 1998; Tanaka et al., 2000; Leasure et al., 2001), or from generating HR gene knockout mutants of the chicken B lymphocyte cell line, DT40. Furthermore, the generation of homozygous HR gene knockout mice (Lim and Hasty, 1996; Tsuzuki et al., 1996; Essers et al., 1997; Rijkers et al., 1998; Luo et al., 1999; Shu et al., 1999; Deans et al., 2000; Pittman and Schimenti, 2000) and embryonic stem (ES) cells has also highlighted the importance of the HR pathway in DSB repair in higher eukaryotes (Lim and Hasty, 1996; Tsuzuki et al., 1996; Deans et al., 2000; Luo et al., 1999).

In addition to the HR genes described for *S. cerevisiae*, mammalian cells contain some additional HR factors. Thus, there are five *RAD51*-like genes, namely *RAD51B/RAD51L1/hREC2/R51H2*, *RAD51C/RAD51L2*, *RAD51D/RAD51L3*, *XRCC2* and *XRCC3*. In addition, the breast cancer susceptibility proteins, Brca1 and Brca2, seem to be directly involved in the HR process in mammalian cells (reviewed in Thompson and Schild, 1999; van den Bosch et al., 2002; Morrison and Takeda, 2000; Thompson and Schild, 2001).

1.1.3 Crossover verses Non-crossover Recombination

Recent advances indicate, however, that the decision of whether a recombination event will result in a CO or NCO chromosome occurs much earlier, soon after DSB formation (Allers and Lichten, 2001b; Hunter and Kleckner, 2001; Clyne et al., 2003). Several observations challenge the idea that the orientation of Holliday junction resolution accounts for the relative frequencies of COs and NCOs. First, several mutants have been identified that retain high levels of DSBs and NCOs, but reduced levels of COs (Engebrecht et al., 1990; and references for the genes/proteins discussed below in Borner et al., 2004; Fung et al., 2004). Proteins implicated specifically in promoting meiotic CO recombination include (1) a DNA helicase Mer3; (2) Msh4 and Msh5, relatives of *E. coli* MutS not involved in mismatch repair; (3) Zip1, a structural component of the central region of the synaptonemal complex; and (4) Zip2 and Zip3, two proteins required for initiating Zip1 polymerization along homologs. Mutation of any member of this group reduces CO (but not NCO) frequency. These findings suggested that COs form via a more elaborate mechanism than NCOs. Second, the configuration of heteroduplex DNA on NCO recombinants did not conform to expectations of the DSBR model (Figure 1.1) (Gilbertson and Stahl, 1996 and Porter et al., 1993). Third, Allers and Lichten (Allers and Lichten, 2001a) used physical detection methods to provide evidence that most or all of the dHJ intermediates are pre-CO intermediates rather than intermediates on the road to forming either COs or NCOs. Forth, two new studies in budding yeast show that the positions of COs are determined much earlier in prophase than the stage at which Holliday junction resolution occurs. These new studies support and extend an earlier proposition based on timing of dHJ resolution relative to that of recombination

nodule appearance (Storlazzi et al., 1996). These studies, particularly the work from the Kleckner and Lichten labs, support an "Early CO decision" (ECD) model of meiotic recombination (Figure 1.2).

Allers and Lichten (Allers and Lichten, 2001a) suggested that NCO recombinants form by a pathway that does not involve a Holliday junction intermediate (see Figure 1.2). They proposed that NCOs form by transient invasion of one or both of the two DNA ends formed by a DSB. Such transient invasion could allow an invading 3' end to be extended via limited DNA synthesis using the invaded duplex as template. Following ejection of the extended ends, annealing of partner ends could then lead to repair of the DSB. Evidence that such a recombination pathway can occur has been found in several mitotic systems and is referred to as "synthesis-dependent strand annealing" (SDSA) (reviewed in Nassif et al., 1994 and Paques and Haber, 1999). While it remains to be determined if meiotic NCOs form via SDSA, this hypothesis is attractive and accounts for available data. The mechanism through which recombination intermediates can be assigned a CO fate prior to Holliday junction resolution is, at present, mysterious.

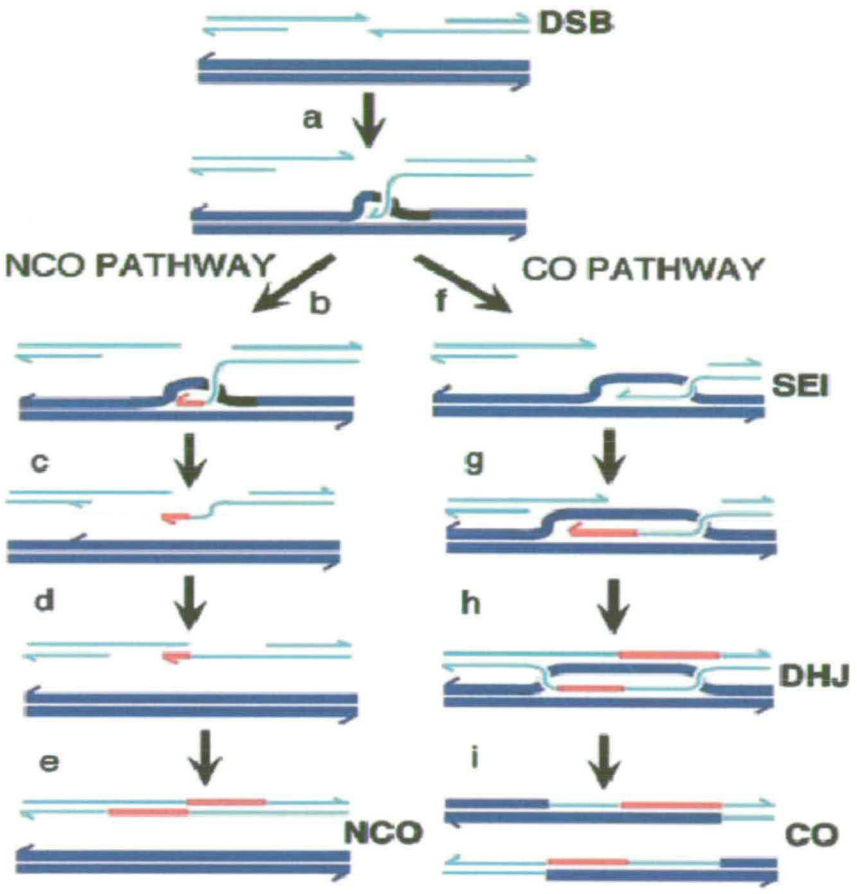

Figure 1.2 The Early Crossover Decision (ECD) Models of Meiotic Recombination

(a) DSB end forms an unstable ("nascent") interaction with a homologous chromatid. (b) En route to forming an NCO, the end involved in the nascent interaction is extended by DNA synthesis. This intermediate is either unstable or too transient to detect by current 2D gel methods. (c) The extended end is ejected from the nascent joint. (d) The extended end anneals with its partner. (e) DNA synthesis and ligation completes formation of the NCO. (f) En route to forming a CO, the nascent end is stabilized to form an SEI intermediate that can be detected by 2D gels. (g) The second end engages the SEI via strand invasion or annealing. (h) DNA synthesis from the invading ends fills in regions lost by end resection, ligation of extended strands forms two Holliday junctions. (i) Resolution of Holliday junctions occurs such that only a CO is formed.

In addition, studies of a newly discovered endonuclease, Mus81, indicate that, in addition to dHJ resolution, COs may be formed by the processing of non-dHJ intermediates (Heyer et al., 2003; Osman et al., 2003) (Figure 1.3). The decision of which crossover pathway to use appears to vary between organisms and may be evolutionarily significant (De Los Santos et al., 2003).

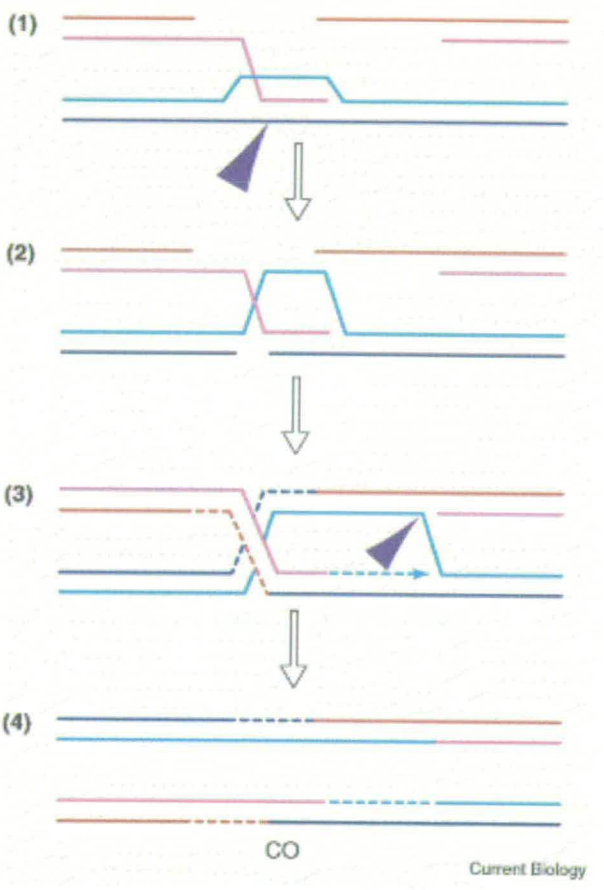

Figure 1.3 A Model for Crossovers Formation without Resolution of Double Holliday Junctions (Osman et al., 2003)
After single-end invasion, Mus81–Eme1 cleaves the D-loop, which should topologically stabilize single-end invasion. Second-end capture and DNA synthesis produces a nicked Holliday junction subject to a second, possibly independent, cleavage by Mus81–Eme1. The potential Mus81–Eme1/Mms4 cleavage sites are indicated by arrowheads. Processing of the cleavage products to accommodate possible flaps and ligation will always lead to crossovers. Osman *et al.* (Osman et al., 2003) propose this alternative crossover model based on the *in vitro* substrate specificity of Mus81–Eme1. This model was independently (Heyer et al., 2003) derived from the proposed function of XPF–ERCC1 in gene targeting (Niedernhofer et al., 2001). XPF–ERCC1 is related to Mus81–Eme1/Mms4, the enzymes having a similar subunit structure and sequence homology in their active sites (Heyer et al., 2003).

1.1.4 Non-homologous End Joining

In eukaryotes, double-strand break repair mediated by homologous recombination occurs mainly during the late S and G2 phases of the cell cycle, when sister chromatids are present. Another repair pathway, NHEJ, is operational throughout the cell cycle but may be more important during G1, prior to DNA replication, or in cells that are no longer cycling (Hendrickson, 1997). The genetic requirements for this pathway were elucidated in mammalian cell lines, and two protein complexes were shown to be required. The first is the DNA-dependent protein kinase complex (DNA-PK), the components of which are Ku70 and Ku80 (a heterodimer that binds DNA ends) and the DNA-PK catalytic subunit (DNA-PKcs). The second complex required is a heterodimer comprising DNA ligase IV and the product of the *XRCC4* gene (Tsukamoto and Ikeda, 1998 and Critchlow and Jackson, 1998). Mutations in genes encoding components of these complexes result in immune and DNA repair deficiencies (Hendrickson, 1997; Ochiai et al., 2001; Riballo et al., 2001). Ku70/Ku80 are thought to stimulate end-joining by binding to DNA ends, recruiting DNA-PKcs to this site, and activating its DNA-dependent kinase activity. This complex in turn is believed to act by protecting the DNA from nonspecific nucleases and by recruiting DNA ligase IV/Xrcc4 to covalently join the broken DNA ends.

The *S. cerevisiae* homologs of Ku70/Ku80 (Hdf1/Hdf2) and the DNA ligase IV/Xrcc4 complex (Dnl4/Lif1) have been shown to belong to the same epistasis group as the MRX complex (Chen et al., 2001) demonstrated that these proteins can stimulate the intermolecular end-joining of linear double-strand DNA molecules

containing cohesive ends. Their results suggest a model (that may be applicable to NHEJ) in which Hdf1/Hdf2 binds DNA ends and facilitates end-bridging by the MRX complex; the MRX complex in turn specifically stimulates Dnl4/Lif4-mediated end-joining. The observations of de Jager et al., 2001 make a model in which DNA end-joining is mediated by a protein complex containing Rad50/Mre11 even more attractive. Using scanning force microscopy, they showed directly that the human MR complex can tether the ends of two linear double-strand DNA molecules, and suggested that this observation might explain the importance of the Rad50/Mre11 complexes in a number of processes involving DNA ends. In the presence of DNA ligase IV and Xrcc4, purified hMre11 alone can stimulate the ligation of DNA molecules containing nonhomologous ends (Paull and Gellert, 2000).

NHEJ is not considered a major pathway of DSB repair in prokaryotes. However, DNA sequences encoding homologs of Ku, the DNA binding component of eukaryotic DNA-PK, have been found to exist in various bacteria (Aravind and Koonin, 2001 and Doherty et al., 2001). Sequence similarity is greatest to eukaryotic Ku70 and Ku80 proteins in the central core domain that is responsible for heterodimerization and DNA binding. Very often these genes are found in association with an ATP-dependent DNA ligase, raising the possibility that bacteria possess a NHEJ pathway.

1.1.5 DNA Damage Checkpoint Proteins

When a chromosome is broken, cells must sense the presence of damage, activate the course of events that will eventually restore genomic integrity and then return to normal growth. Checkpoint proteins link repair and cell cycle by delaying cell cycle transitions, and also by causing changes in chromatin structure, transcriptional induction and post-traslational modifications of repair genes (Hartwell and Weinert, 1989; Kiser and Weinert, 1996; Aboussekhra et al., 1996; Bashkirov et al., 2000; Scott and Plon, 2003). The DNA damage checkpoint is a signal transduction network consisting of sensors, transducers and effectors.

The checkpoint sensor protein Rad24 forms an alternative RFC complex with Rfc2/3/4/5 and recruits a PCNA-like complex, Rad17/Mec3/Ddc1 (Naiki et al., 2000; Venclovas et al., 2002; Green et al., 2000) to sites of damaged chromatin. This signal activates downstream-acting kinases. The Rad9 protein also acts as a DNA damage sensor and is hyperphosphorylated in response to damage (Schwartz et al., 2002; Gilbert et al., 2001).

The ATM-like kinase Mec1p together with Ddc2p form a complex on chromatin in response to DNA damage, thus playing an important role in damage sensing, as well as in signal transduction (Melo and Toczyski, 2002; Rouse and Jackson, 2002; Paciotti et al., 1998). Phosphorylation of some Mec1p targets occurs independently of the RFC and PCNA-like complexes (Rouse and Jackson, 2002; Kondo et al., 2001), however these complexes are necessary for the Mec1p-dependent

phosphorylation of Rad53p to instigate a full cellular checkpoint response (Zou et al., 2002).

The sensor proteins activate signal transducers, such as the Rad53p, Chk1p and Dun1p protein kinases (Carr, 2002; Gardner et al., 1999). This signal transduction eventually leads to cell cycle arrest and transcriptional induction of repair genes (Aboussekhra et al., 1996). Recently, the DNA damage response has been shown to control additional processes including direct activation of DNA repair and processing of DNA damage (Aylon and Kupiec, 2003). These processes may play critical roles in the survival of cells in response to DNA damage (Aylon and Kupiec, 2003).

1.2 Holliday Junctions (HJ)

Holliday junction has been considered a central intermediate in homologous recombination ever since Robin Holliday proposed their existence and suggested that crossovers result from their resolution (Holliday, 1964). While recombination models have evolved since that time, the Holliday junction - more precisely the double Holliday junction (Szostak et al., 1983) - is still held as the critical intermediate in crossover formation (Paques and Haber, 1999) (Figure 1.1). Once Holliday junctions are formed, they must be removed from the genome to allow replication and transcription to continue unhindered, and enable chromosomes to segregate at cell division. The resolution of recombination intermediates by endonucleolytic cleavage is a central part of the recombination process in all organisms and it has been retained throughout evolution (Shinohara et al., 1993). Failure to repair damaged

DNA is associated at the cellular level with sensitivity to radiation, increased mutation rates, DNA and chromosomal aberrations, and reduced viability.

Work to identify a Holliday junction resolvase with the correct junction-cleavage activity began in earnest two decades ago. Early research was accelerated by new methods to prepare plasmid substrates bearing authentic Holliday junctions and to synthesize structures from oligonucleotides that resemble these junctions. The molecular pathways of homologous recombination have been studied extensively in *E. coli* (Kowalczykowski et al., 1994; Lloyd, 1996; West, 1992). Heteroduplex intermediates are usually formed by the RecA filament, a structure that overcomes the natural tendency for Watson-Crick strands to remain paired and at the same time makes use of this property to exchange single strands between duplex molecules in a way that secures homologous alignment (West, 1992). Pioneering work in West's laboratory led to the discovery of a Holliday junction resolvase encoded by the *ruvC* gene in the bacterium *Escherichia coli* (West, 1996). The four-way junction processing is mediated by the RuvA, RuvB and RuvC proteins. A single tetramer of RuvA binds the junction and holds it in an open conformation that enables two hexameric rings of RuvB helicase to assemble on diametrically opposed arms (Rafferty et al., 1996; West, 1997). RuvC binds the exposed face of the junction between the two RuvB rings, forming a "resolvasome" complex in which ATP-dependent branch migration by RuvAB locates the junction at sequences that can be cleaved by RuvC (Davies and West, 1998; van Gool et al., 1998; Whitby et al., 1996; Zerbib et al., 1998). RuvC is a homodimeric endonuclease that converts junctions into duplex products by dual strand incision. In a RuvABC resolvasome, RuvB

directs RuvC to cleave target sequences that lie in the strands passing 5'→3' through the RuvB rings to the junction (van Gool et al., 1999) (Figure 1.4).

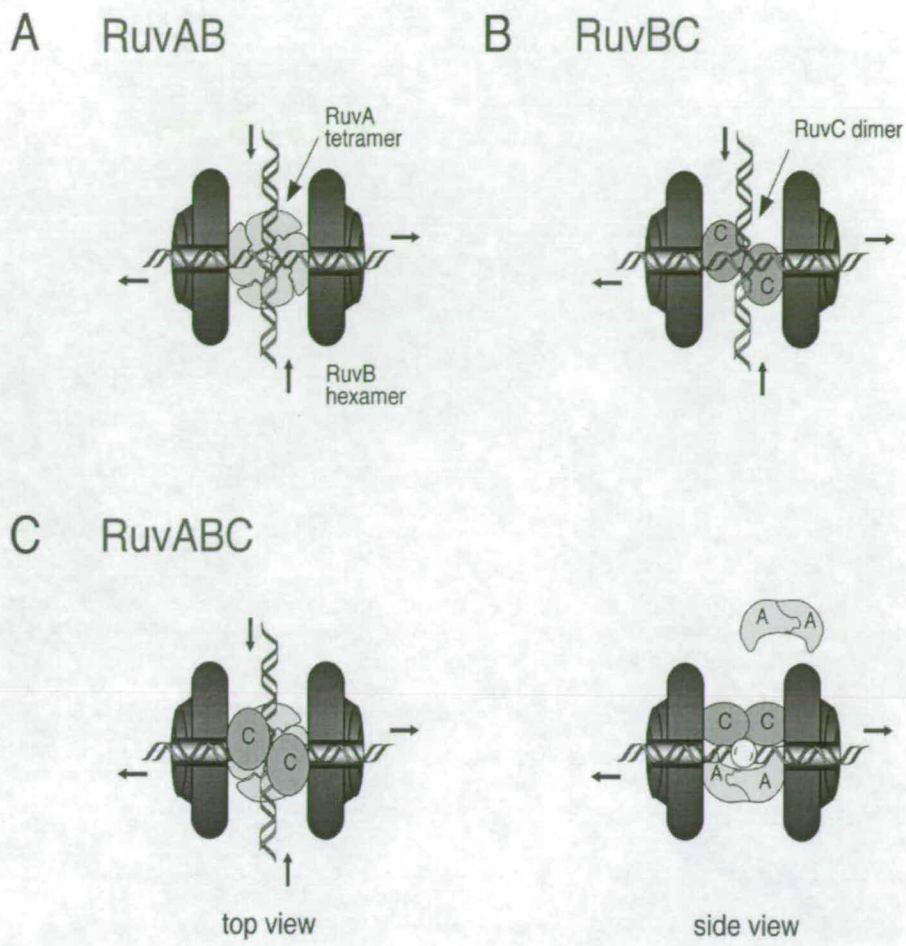

Figure 1.4 Model indicating the interactions between the RuvA, RuvB and RuvC proteins and the Holliday junction (van Gool et al., 1998)
(A) Model of the RuvAB branch migration complex, in which RuvA binds the junction and holds it in an unfolded square planar configuration. RuvB hexameric rings, which are oppositely oriented and lie diametrically opposed on two DNA arms, drive branch migration using their DNA helicase activities. Although physical studies indicate that the junction is bound by two tetramers (Yu et al., 1997), one on either face of the junction, in this diagram only one RuvA tetramer is shown for purposes of clarity. Drawing adapted from Parsons *et al.* (Parsons et al., 1995) and Rafferty *et al.* (Rafferty et al., 1996). The arrows indicate the direction of DNA movement during branch migration. (B) Proposed structure of a RuvBC complex capable of limited branch migration and elevated junction-resolution efficiency. In this diagram, a RuvC dimer is shown binding the junction and interacting with two RuvB hexamers. (C) Two views of a hypothetical RuvABC complex in which RuvA and RuvC bind opposite faces of the Holliday junction and stabilise the binding of two RuvB rings. It is proposed that the RuvC dimer may displace a RuvA tetramer, as indicated. In this model, RuvAB promote branch migration, as shown in (A), driving DNA into and through the complex. The RuvC dimer `scans' DNA sequences as they pass through the complex, resulting in efficient resolution at preferred sites. The complex is shown from above and in side view.

The RuvABC complex has proved a valuable system for understanding movement and resolution of Holliday junctions, but efforts to identify similar activities in eukaryotes have not been as fruitful. Early efforts to purify a cruciform cleaving activity from yeast resulted in the identification of Cce1p, an enzyme that works in mitochondria (Lockshon et al., 1995). Other studies reported Holliday junction cleavage in extracts of yeast and mammalian tissues that contain a protein known as Mus81p (Elborough and West, 1988; Constantinou et al., 2001). Paul Russell's laboratory (Boddy et al., 2001) showing that *S. pombe mus81* mutants were defective in a late stage of meiotic recombination, and that this defect could be partially overcome by expression of a bacterial Holliday junction resolvase (Boddy et al., 2001). Moreover, complexes containing Mus81p were shown to resolve Holliday junctions and fork structures *in vitro* (Boddy et al., 2001). Detailed biochemical studies with purified recombinant Mus81 and its partner protein (Mms4 in *S. cerevisiae* or Eme1 in *S. pombe*) showed that Mus81 shares sequence homology with the Rad1/XPF subunits of structure-specific endonucleases that function in nucleotide excision repair (Interthal and Heyer, 2000; Boddy et al., 2000), therefore, the endonucleases actually show a much greater specific activity with 3'-flap or replication-fork structures than with Holliday junctions (Kaliraman et al., 2001; Doe et al., 2002). Similar results were obtained with purified fractions containing Mus81 from human cells (Constantinou et al., 2002). However, it was shown that *S. cerevisiae mus81* mutants, in contrast to those from *S. pombe*, did not have such a profound meiotic-recombination deficiency (de los Santos et al., 2001). Although *mus81* mutants are sensitive to agents that block replication-fork progression, they do not show defects in DSB repair. Moreover, purified recombinant Mus81 complexes

show considerably greater activities with various substrates that mimic flap structures and replication forks than they do with Holliday junctions (Constantinou et al., 2002; Kaliraman et al., 2001; Doe et al., 2002). Whether or not Mus81 functions as a true resolvase is, at present, a topic of some debate (Haber and Heyer, 2001; Heyer et al., 2003).

For years, efforts to determine the identity of any proteins required for resolvasome activity have been unsuccessful until 2004. In new work, Liu and colleagues (Liu et al., 2004) followed up on the observation that partially purified HeLa cell fractions catalyze ATP-dependent branch migration and resolution of Holliday junctions. Their most exciting finding was that this activity requires RAD51C, a key recombination/repair protein, but not other proteins known to be involved in resolution or branch migration (MUS81, WRN, or BLM). Depletion of RAD51C with a highly specific monoclonal antibody reduced resolution and branch migration to almost background levels; resolvase activity could be reconstituted by adding back recombinant protein complexes containing RAD51C to the depleted fraction. Furthermore, they discovered that Chinese hamster ovary cell lines lacking RAD51C, or its binding partner XRCC3, had greatly reduced resolvase activity. Together, these *in vitro* results provide compelling evidence that, in eukaryotic cells, the Holliday junction resolvase is either RAD51C itself or another protein that is activated by RAD51C.

The resolvases studied to date share certain common features and biochemical characteristics (Lilley and White, 2000). Resolving enzymes function as dimers, resolving the four-way DNA junction by the introduction of paired nicks in opposing strands with a metal ion-dependent endonuclease activity. Despite these functional similarities, the junction resolvases are structurally diverse with no detectable sequence similarity between any of the known families. Structural studies have emphasized this diversity because the crystal structures of *E. coli* RuvC (Ariyoshi et al., 1994), bacteriophage T4 endonuclease VII (Raaijmakers et al., 1999), bacteriophage T7 endonuclease I (Hadden et al., 2001), archaeal Hjc form *Sulfolobus solfataricus* (Bond et al., 2001) and *Pyrococcus feriosus* (Nishino et al., 2001), *Schizosaccharomyces pombe* mitochondial YDC2 (Ceschini et al., 2001) and lambdoid prophage RusA (Rafferty et al., 2003) have radically different folds. These observations have led to the suggestion that Holliday junction resolving enzymes have arisen several times during the course of evolution, perhaps by recruitment of nucleases with other cellular roles. Nonetheless, they are all metal ion-dependent endonucleases and seem to have a conserved catalytic mechanism. Recent sequence alignment analyses suggest that peering into the more distant evolutionary past, there are intriguing similarities between the metal-ion-binding sites of the integrase and nuclease superfamilies. Most of the junction-resolving enzymes can be fitted into these two main superfamilies of proteins with two outliers (T4 endonuclease VII and lambdoid prophage RusA). RuvC, the A22 pox virus resolvase and the yeast mitochondrial enzymes are related and form a subfamily within the integrase superfamily, whereas T7 endonuclease I and Hjc are classed with nucleases (Aravind et al., 2000; Garcia et al., 2000; Lilley and White, 2000; Lilley and White, 2001;

Rafferty et al., 2003). Differences in the topology of the central β-sheet in RuvC compared with the restriction endonucleases have led to the suggestion that any similarities between them are due to convergent rather than divergent evolution (Venclovas and Siksnys, 1995). A family tree that is consistent with the relationships is shown in Figure 1.5. Junction-resolving enzymes bind four-way DNA junctions in dimeric form. Binding is highly structure selective, but all the enzymes significantly distort the structure of the DNA on binding. Some of the resolving enzymes also have pronounced sequence selectivity at the cleavage stage; this can effectively ensure cleavage of Holliday junctions and not other branched DNA structures.

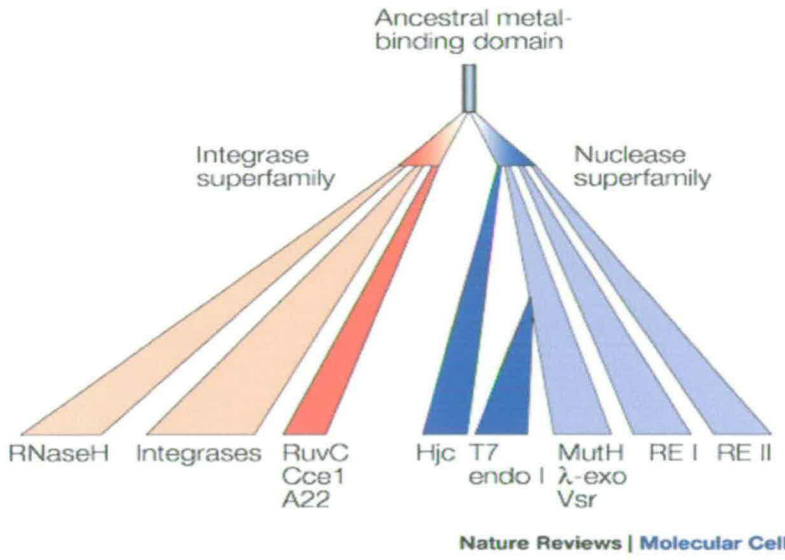

Figure 1.5 Family Tree of Junction-resolving Enzymes (Lilley and White, 2001)

These enzymes are found in two superfamilies. The integrase superfamily includes the sequence-dependent resolving enzymes RuvC and Cce1, which probably share a eubacterial lineage. By contrast, archaeal Hjc and the phage T7 endonuclease I enzymes are members of a large nuclease superfamily. Other family members include the type I and type II restriction enzymes (RE) and repair proteins such as Vsr, MutH and λ-exonuclease. All share a common metal-ion-binding domain that is required for catalysis, but these domains are arranged differently to accommodate the wide variety of substrate specificities of these enzymes. Despite some differences in strand topology, the nuclease and integrase superfamilies might themselves be related through a shared ancestral metal-ion-binding domain. The positions of branch points in this figure are not intended to indicate the degree of relatedness between family members.

1.3 This thesis

1.3.1 Gene Identification via PSI-BLAST Searches

Despite the low levels of absolute sequence identity, which have obscured the relationships between these resolvases to date, we found that PSI-BLAST searches initiated with the sequence of the mitochondrial resolvase Cce1p from *Saccharomyces cerevisiae* (Figure 1.6A) or Ydc2p from *Schizosaccharomyces pombe* identified the Yol093wp putative protein from the *S. cerevisiae*, despite of the limited homology. It suggested that Yol093wp potentially might be a member of a resolvase family. The sequences alignment of Cce1p with Yol093wp is shown in Figure 1.6B. The hypothetical protein *YOL093W* is 882 nucleotides in length, and encodes protein of 293 amino acids with a predicted molecular weight of 34.5 kDa. No functional data were available for this protein in database searches. Iterative BLAST searches showed that Yol093wp is a member of a family of proteins found widely in all free-living eukaryotes (Figure 1.7). This family of proteins has been described in both the PFAM database and the COGs (Cluster of Orthologous Groups) database as being conserved, with no ascribed function. There are some conserved acidic residues in this family, which might contribute to the binding site catalytic metal ion(s). However, sequence comparisons have failed so far to link the *YOL093W* family conserved domains to the same domains that show homology to Cce1p, therefore, this will need further investigations from bioinformaticians allows new connections to be made. The protein family revealed that each sequence has diverged substantially from every other with relatively small sizes, which are similar to those observed among the known resolvases. These homologues have not been characterised and therefore did not help in determining the function of Yol093wp.

(A)

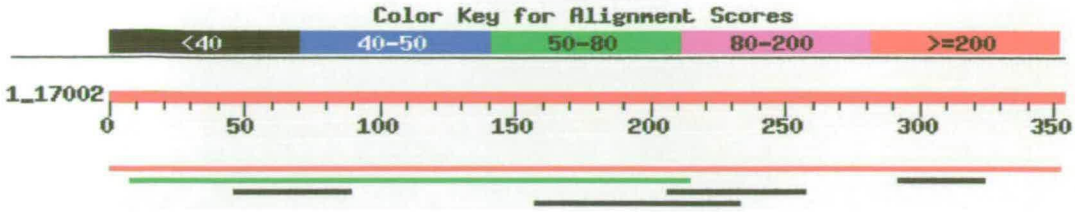

>gi|6324479|ref|NP_014548.1| Yol093wp Length = 293

Score = 26.2 bits (56), Expect = 8.3
Identities = 16/44 (36%), Positives = 23/44 (52%)

```
Yol093wp:   IQEQCEFLEKLRQQKIREGRINILSMDAGVSNFAFSKMQLLNND 90
            IQE  +  E++ Q+ IRE RIN+    D+G+           L ND
Cce1p:      IQEYIDRGEEVPQELIREPRINVNQTDSGIEIILDCSFDELMND 109
```

http://www.ncbi.nlm.nih.gov/BLAST/

(B)

```
Yol093wp    (20)-PVPEGMSKKQWKKMCKRQRWEENKAKYNAERRVKKKRLRHERSAKIQEYIDRGEEVPQE 99
Cce1p           MSTAQKAKILQLIDSCCQNAKSTQLKSLSFVIGAVNGTTKEAKRTYIQEQCEFLEKLRQQ 60
                 ...:  .  *  . * ::  . :  . .    . :   :. : : *** :  *:: *:

Yol093wp        LIREPRINVNQTDSGIEIILDCSFDELMND---------------------------- 129
Cce1p           KIREGRINILSMDAGVSNFAFSKMQLLNNDPLPKVLDWQKINLEEKFFQNLKKLSLNPAE 120
                 *** ***: . *:*:. :  ..:: * **

Yol093wp        ------------------KEIVSLSNQVTRAYSANRRANHFAEIKVAP--FDKRLKQRFE 169
Cce1p           TSELVFNLTEYLFESMPIPDMFTIERQRTRTMSSRHILDPILKVNILEQILFSNLENKMK 180
                                  ::.::..* **: *:.:  : : ::::    : ..*:::::

Yol093wp        TTLKNTNYENWNHFKFLPDDKIMFGDEHISKD----KIVYLTADTEEKLEKLEPGMRYIV 225
Cce1p           YTNKIPNTSKLRYMVCSSDPHRMTSYWCIPREETPTSSKKLKSNKHSKDSRIKLVKKILS 240
                 * * .* .: .::   .* : * .   *.::    .   *.::..* .:::   : :

Yol093wp        GGIVDKN--------RYKELCLKKAQKMGIPTRRLPIDEYINLEGRR-VLTTTHVVQLML 276
Cce1p           TSILEGNSTSSTKLVEFIGVWNNRIRNALTKKKSFKLCDILEIQDNSGVRKDDDLADSFL 300
                 .*:: *        .:  :  :: ::    .: : : : ::::..  * .  .:.: :*

Yol093wp        KYFDDHNWKNAFESVLPPRKLDAEAKSAS-------SSPAPKDT--------- 293
Cce1p           HCLSWMEWLKNYESITELLNSKTLVKTQFGQVFEFCENKVQKLKFLQNTYNND 353
                : :.  :* : :**:    : .: .*:         .. . * .
```

Figure 1.6 Sequence Identification of Yol093wp by BLAST Search Initialled with the *S. cerevisiae* Cce1p (A), and the Sequence Alignment of Yol093wp with Cce1p (B)

Proposed homologoues were identified by NCBI nr peptide sequence database. Sequences were aligned using the Clustal W alignment program. Stars highlight identical residues, and dots indicate the conservation of the nature of the amino acids at that site. The number in parentheses before the alignment indicate the numbers of amino acids from individual sequences not included in the alignment for clarity of presentation.

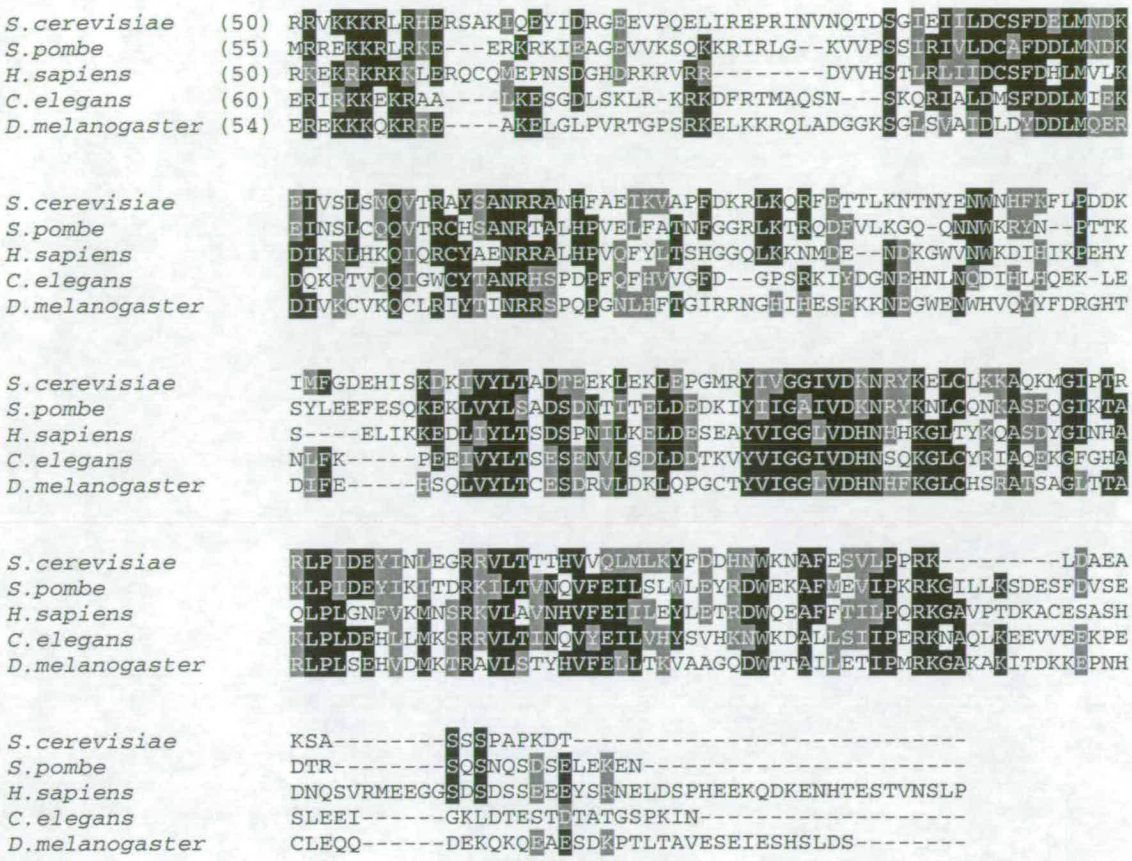

Figure 1.7 Sequence Alignment of Yol093wp with Putative Homologues in other Eukaryotes

Proposed homologoues were identified using BLAST searches. Sequences were aligned using the EMBL ClustalW program. A representative alignment is shaded to a 50% consensus using BoxShade, and indicates residues that are similar (grey background) or identical across species (black background). The number in parentheses before the alignment indicate the numbers of amino acids from individual sequences not included in the alignment for clarity of presentation. Sequences are: *S. cerevisiae* Yol093wp; *S. pombe* hypothetical protein SPAC6B12.09 (pir no: T39016); *H. sapiens* unknown (gb no: AAD210.19); *C. elegans* hypothetical protein F25H8.1 (pir no: T21368); *D. melanogaster* CG14618 gene product (gb no: AAF5059.1).

1.3.2 Yeast Research

The yeast *Saccharomyces cerevisiae* is recognized as an ideal eukaryotic microorganism for biological studies. Although yeasts have greater genetic complexity than bacteria, they share many of the technical advantages that permitted rapid progress in the molecular genetic of prokaryotes and their viruses. Some of these properties make yeast particularly suitable for biological studies. Strains of *S. cerevisiae* have both a stable haploid and diploid state, and they are viable with a great many auxotrophic markers. The development of DNA transformation has made yeast particularly accessible to gene cloning and genetic engineering techniques. In addition, homologous recombination coupled with the high levels of gene conversion in yeasts has led to the development of techniques for the direct replacement of genetically engineered DNA sequences into normal chromosome locations. This approach, which relies on the great efficiency and accuracy of mitotic recombination in *S. cerevisiae*, results in the precise deletion of the entire gene. The phenotypes arising after disruption of yeast genes have contributed significantly toward understanding the functions of certain proteins *in vivo*.

Because of the redundancy (the existence of sets of two or more genes encoding proteins with identical or very similar sequences) problem in the *S. cerevisiae* genome, and to enable the study of gene interactions, it will also be necessary to construct multiply deleted strains; easy methods to achieve this are already in hand (Langle-Rouault and Jacobs, 1995; Guldener et al., 1996). All these approaches should make *S. cerevisiae* the eukaryote of choice for the study of functions common to all eukaryotic cells, by reversing the traditional path of genetic research to one in

which the study of the gene (or DNA sequence) leads to an understanding of biological function, rather than a change in function leading to the identification of a gene.

1.3.3 Work Objectives

In this work, a variety of approaches have been used to characterize *YOL093W*. To get first clues about the function of the protein, a gene deletion was performed to find out whether the protein is required for cell viability. The *YOL093W*-disrupted strains could be used for further studies in order to check if disruption of this gene led to a detectable phenotype. Additionally, the interactions between Yol093wp and other factors were investigated using either a two-hybrid screen or Tandem Affinity Purification (TAP) tag purification. This would help us to further understand the biological functions of *YOL093W*. The subcellular localization of Yolo93w protein was assessed. Furthermore, the purified protein was also used to investigate the general biochemical properties of *YOL093W*.

CHAPTER TWO

Materials and Methods

2.1 Materials

2.1.1 General Reagents

2.1.1.1 Chemicals

Chemicals were purchased from the following sources, except where stated otherwise: Amersham, Fisher, Melford Labs, Scotlab, Sigma.

2.1.1.2 Enzymes

Restriction enzymes, DNA and RNA polymerases and other enzymes were purchased from the following sources unless otherwise stated; Epicentre Technologies, Gibco BRL, New England Biolabs (NEB), Pharmacia, Promega, QIAGEN, and Roche.

2.1.1.3 Growth Reagents

Reagents for all growth media were purchased from the following sources: Beta Lab, Difco Laboratories, Gibco BRL, Oxoid and Sigma.

2.1.1.4 Antibiotics

Ampicillin, Hygromycin (hph), Kanamycin (G418 sulphate, kan) were purchased from Beecham Research, Roche and Sigma respectively.

2.1.2 Bacterial and Yeast Growth Media

2.1.2.1 General Information

All liquid growth media were autoclaved prior to use, and stored at room temperature. For solid media, 2% (w/v) agar was added prior to autoclaving. Solid media were stored at 4°C.

2.1.2.2 Bacterial Media

Table 2.1 Bacterial Media

Medium	Components
Luria-Broth (LB)	1% (w/v) Bacto-tryptone 0.5% (w/v) Yeast extract 0.5% (w/v) sodium chloride pH adjusted to 7.2 with sodium hydroxide

2.1.2.3 Yeast Media

Table 2.2 Yeast Media

Medium	Components
YPDA	2% (w/v) Bacto-peptone 1% (w/v) Yeast extract 2% (w/v) Glucose 0.004% (w/v) Adenine sulphate
Drop-out	0.67% (w/v) Yeast nitrogen base without amino acids 2% (w/v) Glucose 0.2% (w/v) drop-out powder 1 pellet of NaOH per 500ml
Sporulation (for BMA38 strains)	0.1% (w/v) Bacto-yeast eatract 1% (w/v) Potassium acetate 0.05% (w/v) Glucose (supplemented with nutrients as required)
Sporulation Liquid (for W303 strains)	0.02% Raffinose 1% (w/v) Potassium acetate (supplemented with nutrients as required)
YPA Media	2% Potassium Acetate 2% Peptone 1% Yeast Extract

* For solid media, 2% (w/v) agar was added prior to antoclaving.

2.1.2.4 Antibiotics

Antibiotics were added to liquid media immediately prior to use, whereas for solid media antibiotics were added after autoclaving. Ampicillin was stored at –20°C, hygromycin B was stored at 4°C, and G418 sulphate was stored at RT.

Table 2.3 Antibiotics

Medium	Abbreviation	Solvent	Final concentration (μg/ml)
Ampicillin	Amp	H_2O	100
Hygromycin B	hph	PBS*	300
G418 sulphate	kan	H_2O	250
Tetracycline	Tet	Ethanol	15

* Dissolved in PBS (405 mg/ml) when purchased.

2.1.2.5 Drop-out powder

Drop-out powder was prepared by added and mixing 2 g of each of the following nutrients: adenine, alanine, arginine, asparagine, aspartic acid, cysteine, glutamic acid, glutamine, glycine, histidine, isoleucine, lysine, methionine, phenylalanine, proline, serine, threonine, tyrosine, tryptophan, uracil and valine. In addition, 4 g of leucine were added to the drop-out powder when required. For a specific drop-out powder, the relevant nutrients were omitted. This mix was then ground with a mortar and pestle to ensure complete mixing and was added to yeast media to a final concentration of 0.2% (w/v). One pellet of NaOH was added to each 500 ml of media containing drop-out powder, in order to adjust the pH.

2.1.3 Commonly Used Buffers

Table 2.4 Commonly Used Buffers

Buffer	Components
X10 TAE	0.4 M Tris-acetate, pH7.5 20 mM EDTA
X10 TE	0.1 M Tris-HCl, pH7.5 10 mM EDTA
X10 TBE	0.9 M Tris-borate, pH8.3 20 mM EDTA
X10 TBST	0.5 M Tris-HCl, pH7.5 1.5 M NaCl 1% (w/v) Tween-20
X20 MOPS	1 M MOPS 1 M Tris base 2% (w/v) SDS 20 mM EDTA

2.1.4 *Escherichia coli* Strains

Bacterial strains utilized during this work are listed in table 2.5 below. DH5αF' was used for all cloning procedures and propagation of plasmid DNA, and for the propagation of plasmid DNA rescued from yeast cells (section 2.3.2.4). BL21(DE3) cells were utilized for the expression of recombinant *S. cerevisiae* proteins in *E. coli.*

Table 2.5 *Escherichia coli* Strains

Strain	Genotype	Source
DH5αF'	*F'*, ϕ80*dlacZΔM15*, Δ(*lacZYA-argF*) *U169*, *deo*R *recA1*, *endA1*, *hsdR17* (r_k^-, m_k^+), *supE44*, λ^-, *thi*-1, gyrA96, *relA1*.	Gibco BRL
BL21 (DE3)	F^-, *omp*T, *hsdS*$_B$ (r_B^-, m_B^+), *gal*, *dem (DE3)*	Novagen

2.1.5 *Saccharomyces cerevisiae* Strains

The strains used during this work are listed in table 2.6.

Table 2.6 *Saccharomyces cerevisiae* Strains

Strain	Genotype	Source
BMA38α	*MATα, his3Δ200, leu2-3, -112, ura3-1, trp1Δ1, ade2-1,can1-100*	A.E. Mayes (J. Beggs Lab)
BMA38a	*MATa, his3Δ200, leu2-3, -112, ura3-1, trp1Δ1, ade2-1,can1-100*	M. Albers (J. Beggs Lab)
BMA38 (2n)	*MATa/α, his3Δ200, leu2-3, -112, ura3-1, trp1Δ1, ade2-1,can1-100*	B. Dujon Institute Pasteur
MYY1	*MATa/α, his3Δ200, leu2-3, -112, ura3-1, trp1Δ1, ade2-1,can1-100, YOL093W/yol093wΔkan*	This work
MYY2	*MATa/α, his3Δ200, leu2-3, -112, ura3-1, trp1Δ1, ade2-1,can1-100, YOL093W/yol093wΔhph*	This work
MYY3	*MATa/α, his3Δ200, leu2-3, -112, ura3-1, trp1Δ1, ade2-1,can1-100, yol093wΔkan /yol093wΔkan*	This work
BMA38a/ *YOL093W-TAP*	*MATa, his3Δ200, leu2-3, -112, ura3-1, trp1Δ1, ade2-1,can1-100, YOL093W:TAP*	This work
MYY3/pRS316-*YOL093W* (CEN)	*MATa/α, his3Δ200, leu2-3, -112, ura3-1, trp1Δ1, ade2-1,can1-100, yol093wΔkan /yol093wΔkan [pRS316/YOL093W, URA3]*	This work
MYY3/ pYEplac195-*YOL093W* (2μ)	*MATa/α, his3Δ200, leu2-3, -112, ura3-1, trp1Δ1, ade2-1,can1-100, yol093wΔkan /yol093wΔkan [pYEplac195/YOL093W, URA3]*	This work
MYY3/pRS316-*SPO21* (CEN)	*MATa/α, his3Δ200, leu2-3, -112, ura3-1, trp1Δ1, ade2-1,can1-100, YOL093W/yol093wΔhph [pRS316/SPO21, URA3]*	This work

Table 2.6 *Saccharomyces cerevisiae* Strains continued

Strain	Genotype	Source
MYY3/pRS426-*SPO21* (2μ)	*MATa/α, his3Δ200, leu2-3, -112, ura3-1, trp1Δ1, ade2-1,can1-100, yol093wΔkan /yol093wΔkan [pRS426/SPO21, URA3]*	This work
MYY3/pBL419-*RFC4* (CEN)	*MATa/α, his3Δ200, leu2-3, -112, ura3-1, trp1Δ1, ade2-1,can1-100, yol093wΔkan /yol093wΔkan [pBL419/RFC4, URA3]*	This work
EUF153-RAD5$^+$	*MATa, his3-11, leu2-3, -112, ura3-1, trp1-Δ2 ade2-1, ade1::ADE2, can1-100, lys2-nde3', RAD 5$^+$*	Philip Jordan (This lab)
EUF180-RAD5$^+$	*MATα, his3-11, leu2-3, -112, URA3, trp1-Δ2 ade2-1, ADE1, CAN, lys2-nde5', RAD 5$^+$*	Philip Jordan (This lab)
L40ΔG	*MATa, his3Δ200, trp1-901, leu2-3112, ade2, LYS2::(4lexAop-HIS3), URA3::(8lexAop-lacZ,) GAL4Δ::Kan*	Hollenberg et al., 1995
L40ΔG/ pBTM116-*YOL093W*	*MATa, his3Δ200, trp1-901, leu2-3,112, ade2, LYS2::(4lexAop-HIS3), URA3::(8lexAop-lacZ), GAL4Δ::Kan, [pBTM116/YOL093W, TRP1]*	This work
Y187	*MATα, his3-200, trp1-901, leu2-3,112, ade2-101,, ura3-52, gal4Δ, met$^-$,gal80Δ URA2::GAL1$_{UAS}$-GAL1$_{TATA}$-lacZ*	Clontech
BMA38a/ *YOL093W-GFP*	*MATa, his3Δ200, leu2-3, -112, ura3-1, trp1Δ1, ade2-1,can1-100, YOL093W:GFP*	This work
BMA38α/ *YOL093W-MYC*	*MATα, his3Δ200, leu2-3, -112, ura3-1, trp1Δ1, ade2-1,can1-100, YOL093W:13MYC*	This work

2.1.6 Oligonucleotides

Oligonucleotides that were used in this study are listed below. All oligonucleotides were synthesized and purchased from MWG Biotech

Table 2.7 General and Cloning Oligonucleotides

Name	Sequence (5'-3')	Description
YOL093W-KO-1	CTTTCAAGGTAAATAATTAAGT GTCAATCTGCAGGCAAAACAA CCGGATCCCCGGGTTAATTAA	Used for ORF deletion of *YOL093W* with *kan* or *hph* (forward)
YOL093W-KO-2	ACTATTTTGCTATTCAGTTACT AATAATACTACAGTGATGGCT GCTCGATGAATTCGAGCTCGTT	Used for ORF deletion of *YOL093W* with *kan* or *hph* (reversed)
R-hygromycin B	GAATTCCCCAATGTCAAGCAC	Hygromycin B internal primer (reversed)
R-Kan	CATATGTAACATCATTGGCA	Kanamycin internal primer (reversed)
SC093W-test1	GTGGTTGGTTTTCCCACCTT	Used for checking *YOL093W* deletion (forward)
SC093W-test2	CCCACGGCCCTACATTAGAT	Used for checking *YOL093W* deletion or tagging (reverse)
F-Kan	GCAGTTTCATTTGATGCTC GA	Kanamycin internal primer (forward)
R-3HA	ATACGGATAGCCCGCATAGTC	HA internal primer (reversed)

Table 2.7 General and Cloning Oligonucleotides continued

Name	Sequence (5'-3')	Description
Yol093w-13myc1	GCGGAAGCAAAATCCGCAAGCT CTTCGCCAGCTCCAAAGGACAC ACGGATCCCCGGGTTAAT TAA	Used for ORF tagging of *YOL093W* with*13myc* or GFP (forward)
Yol093w-13myc2	ACTATTTTGCTATTCAGTTACT AATAATACTACAGTGATGGCT GCGAATTCGAGCTCGTTTAAAC	Used for ORF tagging of *YOL093W* with*13myc* or GFP (reversed)
Yol093w-tap1	GCGGAAGCAAAATCCGCAAGC TCTTCGCCAGCTCCAAAGGACA CATCCATGGAAAAGAGAAG	Used for ORF tagging of *YOL093W* with TAP (forward)
Yol093w-tap2	ACTATTTTGCTATTCAGTTACTA ATAATACTACAGTGATGGCTGC TACGACTCACTATAGGG	Used for ORF tagging of *YOL093W* with TAP (reverse)
YOL093W-TAP-test	CGCCAGCTCCA AAGGACACA	YOL093W internal primer; Used for checking the *YOL093W* tagging (forward)
SC093W-R	ACTATTTTGC TATTCAGTTA CTAATAATAC TACAGTGATG GCTGCGAATTCGAGCTCGTT TAAAC	Used for ORF deletion of *YOL093W* with *kan* or *hph* (forward)
SC093W-F	CTTTCAAGGTAAATAATTAA GTGTCAATCTGCAGGCAAAA CAACCGGATCCCCGGGTTAA	Used for ORF deletion of *YOL093W* with *kan* or *hph* (forward)
NdeI-XbaI-YOL093 promoter-R	GACATATGTCTAGAGTTTTGC CTGCAGATTG	*YOL093W* PCR forward primer (with Ned I and XbaI site)

Table 2.7 General and Cloning Oligonucleotides continued

Name	Sequence (5'-3')	Description
YOL093W-KO-3	CATTGTCTTTAAGAGAGATG GTGATGTTTAATATAGCGTA AAGCGGATCCCCGGGTTAAT TAA	Used for ORF deletion of *YOL093W* with *kan* or *hph* (forward; 45bp upstream than SC093W-F)
YOL093W-KO-4	GTATCTCTGACATCAATATA CACCTATTGTAGCTACGGAG ACTATTTCGATGAATTCGAG CTCGTT	Used for ORF deletion of *YOL093W* with *kan* or *hph* (forward; 45bp downstream than SC093W -R)
F-hph-1004	GCACTCGTCCGAGGGCAAA GGA	Hygromycin B internal primer (forward)
XbaI-YOL093W-F	GCTCTAGAATGTCCAATGATG AGATAAAC	*YOL093W* PCR forward primer (with XbaI site)
EcoRI-YOL093W polyA-R	CGGAATTCTAATTGAGGTCGTC GAGCGA	*YOL093W* polyA signal PCR primer (reverse)
BamHI-YOL093W -promoter-F	CGGGATCCGGGCATGTTACCAT CTTTAG	*YOL093W* promoter PCR primer (forward)
KpnI-YOL093W prompter-F	GGGGTACCGAGCAAGGCAATG TACCGAA	*YOL093W* promoter PCR primer (forward)
Sfi-YOL093W-F	CGGGGCCGGACGGGCCATGTC CAATGATGAGATAAA	Two-hybrid primer (forward)
Sfi-YOL093W-R	AGGGGCCCCAGTGGCCCTATG TGTCCTTTGGAGCTG	Two-hybrid primer (reversed)

Table 2.7 General and Cloning Oligonucleotides continued

Name	Sequence (5'-3')	Description
J26-1	CCGCTACCAGTGATCACCAAT GGATTGCTAGGACATCTTTGC CCACCTGCAGGTTCACCC	Oligonucleotides for HJ
J26-2	TGGGTGAACCTGCAGGTGGGC AAAGATGTCCTAGCAATCCAT TGTCTATGACGTCAAGCT	Oligonucleotides for HJ
J26-3	GATCTTGACGTCATAGACAAT GGATTTCTATGACACTTTGCC GTCTTCTCAATATCGGC	Oligonucleotides for HJ
J26-4	TGCCGATATTGACAAGACGGC AAAGATGTCCTAGCAATCCAT TGGTGATCACTGGTAGCG	Oligonucleotides for HJ
J26-2-COMP	AGCTTGACGTCATAGACAATG GATTGCTAGTACATCTTTGCC CACCTGCAGGTTCACCCA	Oligonucleotides for HJ
R-FA6a-MX6	GCGCCACTTCTA AATAAGCG	Reverse primer for checking myc or GFP cassette

2.1.7 Antisera

The antisera used in this study are described in Table 2.8 below.

Table 2.8 Antisera

Antibody	Description	Reference
Anti-HA	Rabbit polyclonal antibodies raised against the Haemagglutinin HA-1 protein epitope of the influenza virus. 1:1000 dilution for Western blotting.	Santa Cruz Biotechnology
PAP (Anti-protein A)	Peroxidase Anti-Peroxidase (PAP) Soluble Complex antibody produced in rabbit. 1:1000 dilution for Western blotting.	Sigma Biotechnology
Anti-Rabbit IgG-HRP	Donkey Anti-rabbit IgG covalently linked to horseradish peroxidase. 1:5000 dilution for Western blotting.	Amersham
Anti-c-Myc (A-14)	Rabbit polyclonal antibodies raised against the carboxy-terminus of human c-Myc. 1:1000 dilution for Western blotting.	Santa Cruz Biotechnology

2.1.8 Plasmids

The plasmids used during this work are listed in tables 2.9 and 2.10.

Table 2.9 Cloning Vectors

Plasmid	Features	Source
pBTM116	LexA DNA binding domain fusion shuttle and expression vector: multiple cloning site, Amp^R, *col*E1 ori., P_{ADH1}, LexA DNA binding domain sequence, ADE1 transcriptional terminator, 2μ, *TRP1*	S. Fields, S.U.N.Y Stony Brook
pET19b	*E. coli* expression vector; MCS, T7 promoter sequence,6x His-tag coding sequence, Enterokinase cleavage site, T7 transcription termination sequence, Amp^R, *lac*I,*col*E1 ori.	Novagen
pRS316	Yeast-*E. coli* shuttle vector; *URA3*, Amp^R MCS, *CEN6*, *ARS*	Sikorski and Hieter, 1989
YEplac195	Yeast-*E. coli* shuttle vector; *URA3*, Amp^R MCS, 2μ, *lac*Zα	Gietz and Sugino, 1998
pRS1539	Contains a MCS, TAP tag and a *URA3* cassette; *col*E1 ori., Amp^R	G.Riggaut 1999
pB27	Derived from the original pBTM116: LexA DNA binding domain fusion shuttle and expression vector: multiple cloning site, Tet^R, *col*E1 ori., P_{ADH1}, LexA DNA binding domain sequence, ADE1 transcriptional terminator, 2μ, *TRP1*	Hybrigenics

Table 2.10 Modified Plasmids

Plasmid	Features	Source
pBTM116/ *YOL093W*	Modified pBTM116; contains *YOL093W* cloned in frame with the LexA binding site encoding sequence. The construction of this plasmid is detailed in Figure 5.3.	This work
pRS316/ *YOL093W*	Modified pRS316: contains *YOL093W* coding sequence with its wild-type promoter and polyA signal, *CEN6*, *URA3*	This work
YEplac195/ *YOL093W*	Modified YEplac195: contains *YOL093W* coding sequence with its wild-type promoter and polyA signal, 2μ, *URA3*	This work
pRS316/ *Spo21*	Modified pRS316: contains *SPO21* coding *sequence* with 300 bp on either side, CEN6, URA3	A. Neiman, S.U.N.Y Stony Brook
PRS426/ *SPO21*	Modified pRS316: contains *SPO21* coding sequence with 300 bp on either side, 2μ, URA3	A. Neiman, S.U.N.Y Stony Brook
pBL619	Modified pRS316: contains *RFC4* coding sequence with its wild-type promoter and polyA signal, , *CEN6, URA3*	P. Burgers Washington University
pET19b/ *YOL093W*	*E. coli* expression vector used to produce a 6x His-tagged Yol093wp. Expression of Yol093wp is controlled by IPTG-inducible *lac* promoter. MCS; $(His)_6$-Yol093wp; Amp^R	J. Connelly This Lab
pFA6a-13myc -hph	Contains a MCS, 13x myc tag and a hygromycion B-resistance cassette; Amp^R	Longtine, 1998

Table 2.10 Modified Plasmids Continued

Plasmid	Features	Source
pFA6a-GFP - kanMX6	Contains a MCS, GFP tag and a hygromycion B-resistance cassette; *Amp*^{R}	Longtine, 1998
pFA6a-3HA-kanMX6	Contains a MCS and a kanamycin-resistance cassette; *Amp*^{R}	Longtine, 1998
pAG32	Contains a MCS and a hygromycion B -resistance cassette; *Amp*^{R}	Goldstein and McCusker, 1999
pB27/ *YOL093W*	Modified pB27; contains *YOL093W* cloned in frame with the LexA binding site encoding sequence. The construction of this plasmid is detailed in Figure 5.5.	This work

2.2 Microbiological Methods

2.2.1 Growth of Strains

2.2.1.1 Growth of Bacteria

E. coli strains were routinely grown at 37°C in LB medium (Table 2.1). To select or maintain selection for plasmid DNA, the transformed bacteria were grown in medium containing the appropriate antibiotic (Table2.3).

2.2.1.2 Growth of Yeast

Unless otherwise stated, yeast strains were grown at 30°C in YPDA medium (table 2.2). To maintain selection for plasmid DNA, and/or for auxotrophic markers inserted on the genome, cells were grown in the appropriate drop-out medium or in YMM medium (Table 2.2) supplemented with appropriate nutrients (section 2.1.2.4).

2.2.2 Preservation of Strains

2.2.2.1Preservation of Bacteria

E. coli strains were stored for short period of time on solid medium at 4°C. Strains were stored permanently at -70°C in 15% (v/v) glycerol. One milliliter of cell culture was spin-down and resuspended with one milliliter of 15% glycerol. And snap-frozen on dry ice.

2.2.2.2 Preservation of *S. cerevisiae*

Yeast strains were stored for up to two months on solid medium at 4°C. Strains were stored permanently at -70°C in 15% (v/v) glycerol. Yeast cells were grown to mid-logarithmic phase. One milliliter of cell culture was spun down, resuspended with one milliliter of 15% glycerol, and snap-frozen on dry ice.

2.2.3 Yeast Sporulation and Tetrad Dissection

2.2.3.1 Sporulation on Solid Plates

Diploid yeast cells of the strain to be sporulated were grown on YPDA or selective solid medium (Table 2.2). Cells were patched onto solid sporulation medium (Table 2.2) supplemented with the nutrients (section 2.1.2.4) required for growth of the diploid strain. Plates were incubated at 30°C to induce sporulation. After approximately five days, cells were examined microscopically to determine if sporulation occurred and tetrads had formed.

2.2.3.2 Sporulation in Liquid Medium

W303 strains to be sporulated were grown on YPDA (Table 2.2). A colony of cells was transferred to 2 ml of YPA media in a 15-ml glass tube and grown for 18 hours at 30°C. Cells were spun down at 200 rpm for 4 minutes and the YPA media was aspirated and replaced with 2 ml of sporulation medium (Table 2.2) supplemented with the nutrients required for growth of the diploid strain. Cultures were incubated in a rotor for 5-7 days at 30°C to induce sporulation. After approximately five days, cells were examined microscopically to determine if sporulation had occurred and tetrads had formed.

* YPA Medium	2% Potassium Acetate
	2% Peptone
	1% Yeast Extract
* Sporulation Medium	1% Potassium Acetate
	0.02% Raffinose

2.2.3.3 Tetrad Dissection

Upon successful sporulation and tetrad formation, cells were scraped from the sporulation plate with a loop and resuspended in 100 µl of sterile, distilled water. 3 µl of β-glucuronidase (10 units/µl stock solution, Sigma) was added into this suspension, mixed gently and incubated at RT for 25-40 minutes. Upon successful cell wall digestion, 20 µl of the cell suspension was streaked onto solid YPDA plate (Table 2.2) and tetrads were dissected using a Singer MSM series 100 micromanipulator. After dissection, spores were incubated at 30°C for 3-5 days.

2.2.4 Transformation of *E. coli*

2.2.4.1 Preparation of Chemically-competent Cells

E coli DH5α F′ (Table 2.5) cells were grown overnight on solid medium. Then a single colony was inoculated in 5 ml LB medium and grown at 37°C for overnight. Following this, 0.5 ml of this start culture was inoculated into 50 ml LB medium, and 1 ml of 1 M $MgCl_2$ was added. Then incubated at 37°C until the OD_{600} was approximately 0.6. The culture was held on ice for 15 minutes, and transferred into sterile McCautney bottles. Cells were spun down at 4000 rpm for 10minutes (4°C, and resuspended in 1 ml TSB (Table 2.4). The competent cells were transferred in 200 µl aliquots to pre-chilled Eppendorf tubes and stored until required for use at -70°C.

2.2.4.2 Transformation of Chemically-competent Cells

The competent cells aliquots were thawed on ice and up to 10 µl DNA was added into 100 µl of competent cells, and then transferred to a 15 ml tube. The tube was left on ice for 30 minutes before being transferred to 42°C for 2 min. 900 µl of TSB (Table 2.4) and 20 µl of 1 M glucose were then added and the cells were incubated at 37°C for 1 hour. Cells were then pelleted (3000 rpm, RT, Eppendorf

microcentrifuge), and resuspended in 200 µl of LB medium. The cells were then placed on solid LB medium containing a suitable antibiotic. This was placed at 37°C overnight to produce visible colonies.

2.2.5 Transformation of Yeast

Yeast cells were transformed using the method of Gietz *et al.* (Gietz et al., 1992).

2.2.5.1 Standard Yeast Transformation

A single colony of the yeast strain to be transformed was inoculated into 10 ml of YPDA medium and grown at 30°C overnight. The following day, the cells were diluted into 50 ml YPDA to an OD_{600} of 0.1 and incubated at 30°C.

Upon reaching an OD_{600} of 1.0, cells were harvested by centrifugation at 3500 rpm for 5 minutes (MSE Mistral 1000 centrifuge, RT), and washed once in 10 ml of sterile water. Cells were resuspend in 1 ml of 100 mM LiAc and transferred into an Eppendorf tube. Cells were pelleted by centrifugation in a microcentrifuge. Cells were finally resuspend in 250 µl of 100 mM LiAc. 50 µl of cell suspension was mixed with approximately 1 µg of transforming DNA and 50 µg of salmon sperm DNA (Gibco BRL, incubated at 95°C for 10 minutes prior to use). 240 µl of 50 % (w/v) PEG_{3350} and 36 µl of 1 M Lithium acetate, and 18 µl of sterile water were added, mixed well and incubated at 30°C for 30 minutes on a rotating wheel. Follwing this, cell were heat-shocked at 42°C for 20 minutes, then sedimented at 14000 rpm for 5 seconds. The pellet was resuspend in 200 µl of sterile water and placed onto the appropriate solid medium to select for transformants. Plates were incubated at 30°C for 2-3 days.

* X10 LiAc: 1M Lithium acetate

2.2.6 ORF Replacement and Construction of Epitope-tagged Genes in Yeast

2.2.6.1 ORF Replacement in Yeast

Replacement of open reading frames in yeast was performed using the method of Baudin *et at* (Baudin et al., 1993). A linear DNA fragment was generated by PCR (section 2.3.2.9). This PCR template was chosen to contain the relevant DNA sequence required following integration. The primers were designed so that the final PCR product would contain a selectable marker and would be flanked at both ends by approximately 45 bp of sequence identical to the DNA immediately 5′ and 3′ to the coding sequence to be replaced. The PCR product was purified (section 2.3.2.11) and the relevant strain was transformed (section 2.2.5.1). Colonies growing on the appropriate selective plates were re-streaked onto fresh solid medium and the integration was investigated using PCR and, where relevant, Western Blotting (section 2.3.3.8).

2.2.6.2 Construction of Epitope-tagged Genes in Yeast

Epitope-tagged genes were generated using the same principal method that was used for ORF replacement (section 2.2.6.1). To construct an epitope-tagged allele of gene, however, an integration cassette was PCR-generated (section 2.3.2.9) was inserted immediately downstream of the final codon of t the target ORF. The integration cassette was chosen to contain a selectable/auxotrophic marker to select for the integration.

2.2.6.3 Growth Curves

Growth curves analysis was performed on yeast cells. Cells were grown in liquid medium to mid-logarithmic phase at 30°C. Then aliquots of cultures were to inoculate medium to an OD_{600} of 0.1. Cultures were then incubated at 30°C with the growth rate monitored by measuring the OD_{600} at regular intervals.

2.2.6.4 Hydrophobic Spore Isolation in Yeast

Cultures were sporulated in liquid for 5-7 days. The cells were harvested by centrifugation in a microcentrifuge (10 seconds), resuspended at a concentration of approximately 5×10^8 cells/ml in aqueous solutions of 250 units β-glucuronidase (10 units/μl stock solution, Sigma), and incubated at 30°C for 60 minutes until the ascus walls were digested. Cells were centrifuged at 1400*g* for 30 seconds in 1.5-ml polypropylene microcentrifuge tubes. The supernatant was discarded, and the cells were resuspended in 1ml of water, centrifuged, and resuspended in 100 μl of water. Each tube was then agitated for approximately 2 minutes in an upright position, using a Vetox mixer at maximum speed. During this treatment, the spores clumped together and stuck to the walls of the tubes, which were relatively hydrophobic. Vegetative cells did not accumulate on the walls of the tubes and were removed by discarding the aqueous cell suspension and rinsing the tube several times with water. The spores were then resuspended by adding 1 ml of 0.01% Nonidet P-40 (Roche) and sonicating on ice for 3×45 seconds, using a Soniprep 150 (MSE) equipped with a microtip.

2.2.6.5 Meiotic Assays in Yeast

The enriched spores were spread onto YMM-ADE-ARG+CAN, YMM-URA-ARG+CAN, and YMM-LYS-ARG+CAN. Canavanine (CAN) was used in all of the meiotic assays to select for haploid products and against unsporulated diploids. The increased number of papillae on YMM-LYS-ARG+CAN media is indicative of the induction of meiotic heteroallelic recombination. Meiosis I non-disjunction was measured by papillation on YMM-ADE-ARG+CAN. Only strains carrying both homologues of chromosome I was able to grow on YMM-ADE. As the parental diploid could grow on YMM-ADE, canavanine was used to ensure that one was only looking at the haploid products of meiosis. Growth on YMM-URA+CAN was used to assess reciprocal recombination between *URA3-CAN1* and *ura3-1* and *can1-100*.

2.2.7 Yeast Two-hybrid Screen

2.2.7.1 FRYL Library

The FRYL library utilised in the two-hybrid screens described was constructed by M. Froment-Racine in the laboratory of P. Legrain (Institut Pasteur, Paris, France) (Fromont-Racine et al., 1997). The Y187 yeast cells were transformed with the FRYL library DNA, and stored at -80°C.

2.2.7.2 Mating and Collection of Diploids

The bait plasmid was introduced into the appropriate yeast strain (L40ΔG for pBTM116 plasmids) (Table 2.6) and propagated on –W drop-out medium (Table 2.2). Baits cells were grown in –W drop-out liquid medium to an OD_{600} of approximately 0.8. An aliquot of Y187 cells containing the FRYL library was thawed on ice, inoculated into 20 ml of YPDA + Tetracycline (Table 2.2 & 2.3) and incubated at 30°C for 15 minutes, with gentle shaking (approximately 120 rpm). Baits cells equivalent to 80 OD_{600} units (approximately 8×10^8 cells) were mixed with the recovered library-containing Y187 cells, and 1/12 volume of the cells concentrated onto a Millipore filters (47-mm diameter, 0.22 μm pore size). Each filter was washed with 3 ml of YPDA + Tet medium and incubated for 5 hours at 30°C. Cells were collected by washing from the filters with 2 ml of –LWH drop-out medium (Table 2.2). Collected cells were mixed thoroughly and 50 μl was removed for control plates. This 50 μl aliquot was diluted to 1:1000 by three 10-fold serial dilutions in –LWH drop-out medium and 50 μl was plated onto each of –L, -W, and –LW drop-out media (Table 2.2). These plates were incubated at 30°C for 2 days. The remainder of the mated cells were spread onto –LWH + Tet drop-out medium at 250 μl per plate, and incubated 30°C for 3 days.

2.3 Nucleic Acid Methods

2.3.1 General Methods

2.3.1.1 Phenol/chloroform Extraction

Nucleic acids were purified away from protein in an aqueous solution by adding an equal volume of phenol:chloroform:isoamyl alcohol (25:24:1), vortexing for 10 seconds and centrifuging at 14000 rpm for 4 minutes. The upper, aqueous, phase containing the nucleic acid was removed to a fresh tube.

2.3.1.2 Precipitation of Nucleic Acid

Nucleic acids were precipitated from solution by adding 2 volumes of ethanol and 0.1 volumes of 3 M sodium acetate (pH 5.2). This was incubated at -20°C for 30 minutes. Nucleic acids were than pelleted by centrifugation at 14000 rpm for 30 minutes at 4°C, and the pellet washed in 70% (v/v) ethanol. The pellet was then dried and resuspended in an appropriated volume of distilled water.

2.3.2 DNA Methods

2.3.2.1 Small Scale Preparation of Plasmid DNA by Spin Column

Plasmid DNA was prepared using the QIAprep spin miniprep kit (Qiagen), following the manufacturer's instructions. DNA was extracted from 1.5 ml of *E. coli* culture grown to stationary phase, eluted in 30 µl of distilled water and stored at -20°C.

2.3.2.2 Large Scale Preparation of Plasmid DNA by Filtration Column

Plasmid DNA was prepared using the QIAfilter midiprep kit (Qiagen), following the manufacturer's instructions. DNA was extracted from 100ml of *E. coli* culture grown to stationary phase, eluted in 500 µl of distilled water and stored at -20°C.

2.3.2.3 Yeast Genomic DNA preparation

Yeast genomic DNA was prepared using the method of Hoffman and Winston (Hoffman and Winston, 1987).

A single colony of yeast strain was inoculated in 10 ml of the appropriate medium (table 2.2), and incubated at 30°C overnight. Cells were harvest by centrifugation at 3500 rpm for 5 minutes (MSE Mistral 100 centrifuge, RT), and washed with 10ml of distilled, sterile water. Cells were then resuspend in 1 ml of water and transferred into a 1.5 ml tube, and pelleted at 4000 rpm for 10 seconds. 200 µl of glass beads (0.5mm, Biospec Products Inc.), 200 µl of lysis buffer, and 200 µl of phenol:chroroform:isoamyl alcohol (25:24:1) were added. The mixture was vortexed for 4 minutes. After this, 200 µl of distilled water was added. The tube was then centrifuged at 14000 rpm for 5 minutes (RT). The upper phase was removed into a new tube and the nucleic acid precipitated and dried (section 2.3.1.2). For a yeast genomic DNA preparation, the pellet was resuspended in 100 µl of distilled water. Typically, a yield of approximately 0.2 µg /µl is obtained.

* Lysis Buffer: 10 mM Tris-HCl, pH 6.8
1% (w/v) SDS
1 mM EDTA
100 mM NaCl
2% (v/v) Triton X-100

2.3.2.4 Yeast Plasmid Rescure

Plasmid DNA was rescued from yeast cells using the Zymoprep Yeast Plasmid Minipreparation Kit (ZYMO Research), following the manufacturer's instructions. DNA was extracted from 5 ml of yeast culture grown to stationary phase, eluted in 30 µl of distilled water and stored at -20°C. 5 µl of the DNA solution was used for transformation of *E. coli* cells.

2.3.2.5 Restriction Digestion of DNA

Restriction endonuclease digestion of DNA was typically performed in volumes of 20-100 µl. These contained the required quantity of DNA and the appropriate buffer (supplied and recommended by the manufacturer) at X1 concentration. Between 2 to 5 units of restriction enzyme in question were added, ensuring that the total enzyme volume did not exceed 10% of the total reaction volume. The digestion was incubated at the appropriate temperature recommended by the supplier; typically 1-4 hours. The products of the digestion were either analysed by agarose gel electrophoresis (section 2.3.2.6) or extracted (section 2.3.2.7) for further manipulations.

2.3.2.6 Agarose Gel Electrophoresis

DNA fragments produced either by restriction endonuclease digestion (section 2.3.2.5) or generated by PCR (section 2.3.2.9) were analysed typically in 0.8-1.2% (w/v) agarose gels. Gels were prepared by melting agrose in 100 ml of X1 TAE buffer (table 2.4) and adding ethidium bromide to a final concentration of 0.5 µg/ml. Samples to be analysed were added to Ficoll loading buffer and were loaded directly onto the gel. Two hundred volts were supplied across the gel so that the DNA fragments separated with respect to size. The DNA could subsequently be visualized using a UV transilluminator. DNA markers of known molecular size were also loaded on the gel so that DNA fragments could be easily identified.

* X6 Ficoll Loading Buffer: 15% (w/v) Ficoll (Type 400)
0.25% (w/v) Xylene xyanol FF
0.25% (w/v) Bromophenol blue

2.3.2.7 Purification of DNA from Agrose Gels

DNA fragments produced either by restriction endonuclease digestion or generated by PCR were purified by freshly separating DNA fragments by agrose gel electrophoresis (section2.3.2.6) and subsequently isolating the desired DNA band from the agarose gel using the QIAquick gel extraction kit (Qiagen) according to the

manufacturer's instructions. DNA was eluted in 30 µl of distilled water and stored at -20°C.

2.3.2.8 Ligation of DNA Molecules

Ligations were performed in a final volume of 10 µl, containing approximately 25 ng of vector DNA, about 3 times this amount (with respect to the number of moles) of insert DNA, X1 ligation buffer and 200 units of T4 DNA ligase (NEB). Reactions were allowed to proceed at 16°C for 18 hours and stopped by heat-inactivation at 70°C for 15 minutes.

2.3.2.9 Amplification of DNA by the Polymerase Chain Reaction (PCR)

Specific regions of DNA were amplified using the polymerase chain reaction (PCR). Template DNA was either approximately 1 µg of plasmid DNA or yeast genomic DNA using specifically designed primers manufactured commercially. A typical PCR reaction using plasmid as template was as follows:

X10 Polymerase Buffer ($MgCl_2$ plus*)	5 µl
10 mM dNTPs (dATP, dCTP, dTTP, dGTP)	5 µl
Oligonucleotide primer 1 (10 pmol/µl)	3 µl
Oligonucleotide primer 2 (10 pmol/µl)	3 µl
Template DNA (10 ng/µl)	1 µl
DNA polymerase (2 U/µl)	0.5 µl
Sterile distilled water	32.5 µl

*$MgCl_2$ concentrations were adjusted as required to optimise reaction conditions.

PCRs were carried out in a PTC-100 Hot Lid reactor or a DNA Engine Gradient Cycler (Genetic Research Instrumentation Ltd) programmed according to the length of the desired product and the annealing temperature of the oligonucleotide primers being used.

A typical cycling program is show below:

30 cycles of step1-step3:

Step 1	Denaturation	94°C for 20 seconds
Step2	Primer Annealing	40-65°C for 1 minute
Step 3	Extension	72°C for 1 minute#
Step 3	Final Extension	72°C for 10 minutes

This time was extended by one minute for every kb over 1kb of the length of the desired product.

2.3.2.10 PCR from Yeast Colonies

A single colony of yeast was picked with a sterile toothpick and resuspended in 100 μl of distilled water. The cell suspension was boiled for 10 minutes and then placed on ice. 5 μl of this suspension was used in a 20 µl PCR reaction.

2.3.2.11 Purification of PCR Products

DNA fragments generated by PCR (section 2.3.2.9) were purified from oligonucleotide primers, unincorporated nucleotides, polymerases and salts using the QIAquick PCR purification kit (Qiagen), following the manufacturer's guidelines. Purified DNA was eluted in 30 µl of distilled water and stored at -20°C.

2.3.2.12 DNA Sequencing

Plasmid DNA to be sequenced was prepared using the QIAprep spin columns (section 2.3.2.1) and quantified by visualization on an agrose gel (section 2.3.2.6). Genomic DNA to be sequenced was firstly amplified using PCR (section 2.3.2.9) with suitable primers (Table 2.7) and the resulting DNA fragment was purified using the QIAquick PCR purification kit (section 2.3.2.11). Sequencing reactions were then performed using a dRhodamine terminator cycle sequencing kit (Perkin Elmer) in a UNO-Thermoblock reactor (Biometra). A reaction mix was as follows:

Template DNA	250 ng of double-stranded DNA or 100 ng of PCR product
Terminator mix	2 µl
Primer	1.6 pmol
Distilled water	make-up volume to 10 µl

35 cycles as described below were performed:

Step 1: 96°C for 30 seconds

Step 2: 50°C for 15 seconds

Step 3: 60°C for 4 minutes

10 µl of distilled was then added into the reaction mix.

Samples were run on an ABI PRISM 377 DNA Sequencer and the resulting DNA sequence studied using the Gene Jockey II computer program.

2.3.2.13 ^{32}P DNA labelling

DNA oligonucleotides (J26-1, -2, -3, -4, and J26-2-COMP.) were synthesized by MWG-Biotech AG. Labelling reactions were performed at 37°C for 30 minutes. A reaction mix was as follows:

DNA (J26-2)		20 pmol
X10 PNK buffer		4 µl
^{32}P-γ-ATP		3 µl
PNK-ase		4 µl
Distilled water	make-up volume to	40 µl

After incubation, 8 µl of 0.5 M EDTA (pH7.5) was added to stop the reaction. Oligonucleotides were precipitated from solution by adding 2 volumes of ethanol and 0.1 volumes of 3 M sodium acetate (pH 5.2). Nucleic acids were than pelleted by centrifugation at 14000 rpm for 60 minutes at 4°C, and the pellet washed in 70 % (v/v) ethanol. The pellet was then dried and resuspended in 60 µl of TE buffer.

2.3.2.14 Preparation of the ^{32}P-labelled duplex and Holliday Junction

In all constructs, one of the oligos was [γ-^{32}P]-end labelled, and after annealing the products were gel purified. Annealing reactions were performed in a PCR reactor. A reaction mix was as follows:

(1) Duplex

^{32}P-γ-labelled ssDNA (J26-2)	approximately	15 pmol
Oligonucleotides DNA (J26-2-COMP)		50 pmol
NaCl		250 mM
Distilled water	make-up volume to	20 µl

(2) Holiday junction (HJ)

^{32}P-γ-labelled ssDNA (J26-2)	approximately	15 pmol
Oligonucleotides DNA (J26-1)		50 pmol
Oligonucleotides DNA (J26-3)		50 pmol
Oligonucleotides DNA (J26-4)		50 pmol
NaCl		250 mM
Distilled water	make-up volume to	20 µl

The program as described below was performed:

99°C	4 minutes
65°C	10 minutes
37°C	10 minutes
28°C	10 minutes

Samples were purified by loading on a 10% native acryamide gel. The bands were excised and 500 µl of TE buffer was added per tube. Samples were incubated at 30°C overnight then centrifuged at and 12000 rpm for 10 min (4°C) The supernatant was removed into a fresh tube and oligonucleotides were precipitated with ethanol. The pellet was dried and resuspended in 30 µl of TE buffer.

2.4 Protein Methods

2.4.1 Crude Extraction of Total Cellular Protein from Yeast

10 ml of appropriate medium was inoculated with a single colony of yeast strain, and incubated overnight. Cells were harvested centrifugation at 3500 rpm for 4 minutes (Mistral 100 centrifuge, RT). The pellet was resuspended in 100 µl of H_2O and 100 µl of X2 SDS loading buffer, and mixed well. 50 µl of glass beads (0.5 mm) was added and vortexed for 60 seconds. The lysate was incubated at 96°C for 60 seconds and then on ice for 60 seconds. These incubations were repeated for a further two times, after which the tubes were centrifuged at 14000 rpm for 5 minutes. Samples could be stored at -20°C. Samples were heated again at 95°C for 5 minutes before loading 15-20 µl of the sample on a gel.

2.4.2 Large Scale Yeast Whole Cell Extraction Preparation

10 ml of the appropriate medium was inoculated with a single colony of yeast strain, and incubated at 30°C overnight. This was then taken and used to inoculate more volume of medium to OD_{600} of approximately 0.1, and incubated until the OD_{600} was approximately 2. Cells were then centrifuged at 5000 rpm for 5 min (JLA 10.500 rotor, RT) and resuspended in 50 ml of AGK buffer. Cells were sedimented at 3500 rpm for 5 min (Mistral 1000 centrifuge, RT). The supernatant was removed and the resulting cell pellet was weighed. Cells were resuspended in 0.4 cell pellet volume of AGK buffer. DTT was added to a final concentration of 2 mM. Protease inhibitors (Roche) were added just before freezing. The cell suspension was then frozen by adding drop wise into liquid nitrogen. This could be stored at -70°C for one year with no loss of activity.

The frozen cell pellet was then added into a mortar containing liquid nitrogen and ground to a fine powder with occasional additions of liquid nitrogen to ensure the pellet did not thaw. The frozen powder was transferred to a polycarbonate centrifuge tube, and thawed on ice. It was then centrifuged at 17000 rpm for 30 minutes (in a

JA2.50 rotor, at 4°C). The supernatant was transferred to chilled polycarbonate tubes avoiding the lipid layer during transfer. This was then spun in a pre-cooled 70.1 Ti rotor at 40000 rpm for one hour (Beckman, at 4°C). The supernatant was transferred to dialysis membrane with a molecular weight cut-off of approximately 10 kDa. This was placed in 1.5 litre of dialysis buffer and dialysed for 3 hours 4°C, changing the dialysis buffer once. The supernatant was then placed in a falcon tube and stored at -70°C until use.

*AGK buffer: 10 mM HEPES, pH 7.9
1.5 mM $MgCl_2$
200 mM KCl
10% (v/v) Glycerol

*Dialysis buffer: 20 mM HEPES, pH 7.9
0.2 mM EDTA
50 mM KCl
20% (v/v) Glycerol
0.5 mM DTT

2.3.3 Polyacrylamide Gel Electrophoresis (PAGE)

Novex Mini Gels (Protein SDS PAGE)

Protein samples with SDS loading buffer were heated at 95°C for 5 minutes before loading. Samples were then loaded onto a pre-cast 4-12% polyacrylamide gel (Novagen), alongside pre-strained molecular weight markers of known size (NEB) for reference. The gel was subject to electrophoresis in a Novex Mini-cell (Novagen) with X1 MOPS (Table 2.4) as buffer. Electrophoresis was performed at 200V until the bromophenol blue dye front reached the bottom of the gel.

*X2 SDS loading buffer: 100 mM Tris-HCl, pH 6.8
4% (w/v) SDS
20% (v/v) glycerol
200 mM DTT
0.2% (w/v) Bromophenol blue

Classic Gels (Protein SDS PAGE)

Two glass plates were separated by spacers. Resolving gel solution was prepared, poured between the plates, and overlaid with water over the top to prevent oxidation and to help form an even interface between the resolving and stacking gels. The gel was then left to set at room temperature, the water was removed, stacking gel solution was poured and an appropriate comb inserted to create loading wells. After polymerisation, the gel was subject to electrophoresis in a Mini-cell (BIO-RAD), the comb was removed and the wells were washed with X1 running buffer (Table 2.4). Protein samples were boiled for 5 minutes and loaded into the wells. 1X running buffer was poured into the upper and lower buffer chambers. Gels were run at 150V at room temperature until the bromophenol blue dye front reached the bottom of the gel.

* 10 % resolving gel:	375 mM Tris-HCl, pH 8.8
	1% (w/v) SDS
	10% (w/v) Acrylamide/bis-acrylamide (ratio 37.5:1)
	1% (w/v) Ammonium persulfate
	TEMED
* Stacking gel solution:	125 mM Tris-HCl, pH 6.8
	1% (w/v) SDS
	10% (w/v) Acrylamide/bis-acrylamide
	1% (w/v) Ammonium persulfate
	TEMED
* X1 running buffer:	25 mM Tris base
	0.1% (w/v) SDS
	250 mM Glycine

Native DNA-Protein Gels

Two glass plates were separated by spacers. Non-denaturing gel solution was prepared, poured between the plates, and an appropriate comb inserted to create loading wells. The gel was then left to set at room temperature. After polymerisation, the gel was subject to electrophoresis in a Mini-cell (BIO-RAD), the comb was

removed and the wells were washed with X1 TBE buffer (Table 2.4). Protein samples were boiled for 5 minutes and loaded into the wells. X1 running buffer was poured into the upper and lower buffer chambers. Gels were run at 150V at room temperature until the bromophenol blue dye front reached the bottom of the gel.

* 4-6% Non-denaturing gel: 375 mM Tris-HCl, pH 8.8
  4-6% (w/v) Acrylamide/bis-acrylamide (ratio 19:1)
  1% (w/v) Ammonium persulfate
  TEMED

2.3.4 Coomassie Staining of SDS Polyacrylamide Protein Gels

In order to visualise total protein in an SDS polyacrylamide gel, the gel was incubated in coomassie solution for 30 minutes and then destained by incubation for 7-12 hours in destaining solution under constant gentle shaking at room temperature. The destaining solution was replaced frequently. After destaining, the gel was dried on Whatman 3MM paper using a Bio-Rad's Model 583 Gel Dryer.

* Coomassie solution: 0.1% (w/v) Coomassie blue
  50% (v/v) Methanol
  10% (v/v) Acetic acid
* Destaining solution: 10% (v/v) Methanol
  10% (v/v) Acetic acid

2.3.5 Silver Staining of SDS Polyacrylamide Protein Gels

Silver staining of the total protein in an SDS polyacrylamide gel was using the silver staining kit (Pharmacia Biotech) following the manufacturer's guidelines.

2.3.6 GelCode Blue Staining of SDS Polyacrylamide Protein Gels

GelCode Blue staining of the total protein in an SDS polyacrylamide gel was using the GelCode Blue Stain reagent (Pierce) following the manufacturer's guidelines.

This reagent utilizes the colloidal properties of Coomassie for protein staining on polyacrylamide gels. This unique reagent stains only protein and allows bands to be viewed directly on the gel during the staining process.

2.3.7 Mass Spectrometry

Silver- or GelCode Blue-stained proteins were digested in-gel with trypsin. Trypic peptides were sequenced by nanoelectrospray tandem mass sectrometry. Proteins were identified by searching peptide sequence tags against a comprehensive nonredundant protein database using a peptide mass fingerprinting tool from the UCSF Mass Spectrometry Facility (http://prospector.ucsf.edu/ucsfhtml4.0/msfit.htm).

2.3.8 Western Blot

Electrophoretic Transfer of Protein to PVDF Member

Proteins were transferred electrophoretically form the SDS-polyacryamide gel to PVDF membrane (Amersham) using the Novex Mini-cell (Novagen).

Electrophoretic transfer was performed in 1x Western Transfer Buffer at 30V constant for one hour.

* X10 Western Transfer Buffer: 200 mM Tris-HCl, pH 6.8
  1.5 M Glycine

2.3.9 Antibody Binding

Non-specific protein interactions were blocked by incubating the PVDF membrane following transfer at RT for one hour or at 4°C for overnight. Blocking was performed in 25 ml of Blocking Buffer with constant shaking. Primary antiserum (Table 2.8) was diluted to the appropriate concentration in 10ml of Blocking Buffer, added to the blocked membrane and incubated at 4 °C for one hour with constant shaking. The membrane was then washed in 1x TBST three times for 15 minutes each. Secondary antiserum (HRP-conjugated or not) was then diluted in 10 ml of

Blocking Buffer, applied to the membrane and incubated at RT for 60 minutes with constant shaking. The membrane was then washed as detailed above.

* X 1 Blocking Buffer: 1X TBST (Table 2.4)
5% (w/v) dry milk powder (J. S. Sainsbury Ltd)

2.3.10 Enhanced Chemiluminescence (ECL)

3 µl of developer solution (Amersham) was prepared according to manufacturer's instructions, added to the membrane and incubated at RT for 60 seconds. Following incubation, the membrane was placed in Saran wrap and exposed to photographic film. Exposure times varied depending on the strength of the signal, but were typically between 10-60 seconds.

2.3.11 Expression and Purification of His-tagged Recombinant Protein from *E. coli*

Protein Expression

500 millilitres of LB medium (Table 2.1) containing the appropriate antibiotics (Table 2.3) were inoculated with 25 ml overnight culture of the expression plasmid-bearing *E. coli* strain. The culture was grown at 37°C to an OD_{650} value of 0.6. For induction of the expression, IPTG was added to a final concentration of 1mM and the culture was incubated at 37°C for 4 hours. The cells were harvested by centrifugation at 5000 rpm for 10 minutes at 4°C (Beckman JLA 10.500 rotor) and stored at –80°C.

Preparation of Protein Extract

Cells were thawed on ice and resuspended in 3 ml ice-cold binding buffer (500 mM NaCl, 20 mM Tris-HCl, 5 mM imidazole, pH 7.9) per gram cell weight. The suspension was then sonicated in a beaker on ice until the sample was no longer viscous. The lysate was transferred into 1.5 ml Eppendorf tubes and centrifuged at

12,000 rpm for 30 minutes at 4°C. The supernatant was transferred to a universal tube on ice.

Ni–NTA Affinity Purification of the His-tagged Protein

All manipulations were done in the cold room at 4°C. 10 µl of Ni-NTA agarose (Novagen) were loaded and equilibrated with 30 ml of binding buffer for one hour at 4°C. 10 ml of the prepared cell extract was added. The column was then washed with 10 ml of binding buffer and 10ml of wash buffer (500 mM NaCl, 20 mM Tris-HCl, 60 mM imidazole, pH 7.9). The flow through was collected as a batch. Eventually, the His-tagged protein was eluted with 60 ml of elution buffer (1 M imidazole, 500 mM NaCl, 20 mM Tris-HCl, pH 7.9) over an hour and the eluate was collected in fractions of 1 ml and stored at -80°C.

20 ml aliquots of the eluates and the washes were resolved by SDS-polyacrylamide gel electrophoresis (section 2.3.2.6). The total proteins were visualised by coomassie staining (section 2.3.3.4).

2.3.12 DNA-protein Binding Assays

(1) Reactions for Agarose Gels

All binding reactions were carried out at 30°C for 30 minutes. A reaction mix was as follows:

Circular or linear DNA (plasmid pBR322)		1 µg
X10 nuclease buffer		2 µl
NaCl		200 mM
BSA		2 µg
Distilled water	make-up volume to	20 µl

After incubation, samples were visualized on a agarose gel.

(2) Reactions for Native Acrylamide Gels

All binding reactions were carried out at 30°C for 30 minutes. A reaction mix was as follows:

^{32}P-γ-labelled DNA	0.5~2 μl
X10 nuclease buffer	4 μl
NaCl	200 mM
BSA	2 μg
Distilled water	make-up volume to 20 μl

After incubation, load samples on a 4~5% native acrylamide gel.

*Nuclease buffer (X10):	12.5 mM DTT
	20% glycerol
	250 mM Tris (pH 7.5)

2.3.13 DNA Methylation Assays

All methylation reactions were carried out at 30°C for 60 minutes. A reaction mix was as follows:

tRNA (Roche, *E. coli* tRNAs)		630 μg of tRNA
or HJ substrates		or 6.3 μl of HJ DNA
S-adenosylmethionine (SAM) [methyl-^{3}H]		3 μM
NaCl		200 mM
Spermidine		1 mM
Tris-HCl (pH 7.4)		50 mM
$MgCl_2$		5 mM
Elution buffer or protein		2 μl
Distilled water	make-up volume to	20 μl

After incubation, samples were spun down for 10 seconds. 15 μl of samples were spotted on a 2.5-cm circle of Whatman DE81 paper on a vacuum manifold (Millipore). The filter papers were washed with 5 × 1 ml of 0.2 M NH_4HCO_3, 3 × 1

ml of ethanol, and 1ml of diethyl ether. Tritium was determined in 5 ml of a scintillation fluid.

2.3.14 Immunofluorescence for Visualization of GFP and 13Myc-tagged Antibodies

Yeast cells were grown to mid-logarithmic phase, and then Formaldehyde was added directly into the growing medium to final concentration of 3.7%. The mix was further incubated at 30°C for 30 minutes. After fixation, cells were harvested by centrifugation at 3500 rpm for 3 minutes, and washed with 1 ml of 100 mM Kpi (pH7.4, 1.2 M Sorbitol added) (Buffer B). For spheroplasts, cells were resuspended in 1ml of Lyticase (250 μg/ml, dissolved in 100 mM Kpi, pH7.4), and then incubated at 30°C for 40 minutes. Cells were pelleted by centrifugation at 3500 rpm for 1.5 minutes, and washed twice with 1 ml of Buffer B, followed by PBS/Sorbitol. Cells were resuspended in 1 ml of Buffer B. 20 μl of cells were spotted onto a slide coated with polysine (BDH, Polysine coated slides), and incubated for 10 minutes in the humid chamber. The slides were then washed twice with 1 ml of Buffer B, and blocked with 5% milk/PBS at RT for 45 minutes. Milk/PBS was aspirated right before adding primary antibody, and the slide was incubated at 4°C overnight in the humid chamber. After the incubation, the slide was washed twice with 5% milk/PBS before applying secondary antibody and incubated in the dark for one hour in the humid chamber. It was then washed 5 times with 5% milk/PBS. A drop of a mounting medium containing DAPI (Vectashield mounting medium, VECTRA) was added on each well, and a cover slip was applied. The slide was sealed with nail polish, and stored at -20°C. The sections were photoconverted using a conventional fluorescence microscope (Axioskop; Zeiss, Oberkochen, Germany) with a Photometrics SenSys CCD camera (Coherent Life Science).

2.3.15 TAP Tag Purification

IgG Beads Binding

200 µl of IgG agarose bead suspension (SIGMA A2909) was added to column and washed with 5 ml of IPP-150. To every 1 ml of yeast protein extract, 10 µl of 1 M Tris pH8, 20 µl of 5 M NaCl, and 10 µl of 10% NP-40 were added. The mix was then added to column and rotated at 4°C for 2 hours.

TEV Protease Cleavage and Calmodulin Beads Binding

The column was drained by gravity flow, and washed with 30 ml of IPP-150, followed by 10 ml of TEV cleavage buffer. 1 ml of TEV cleavage buffer and approximately 60 units of TEV enzyme (GIBCOBRL) were added into the column. The column was closed and rotated at 4°C overnight. During the incubation, a new calmodulin bead column was prepared for using: 200 µl of calmodulin bead suspension (SIGMA P4385) was added to a column and washed with 5 ml of calmodulin binding buffer (CBB). Eluate was then recovered from the IgG-bead column by gravity flow and collected into the calmodulin column. CBB (3 volumes of eluate) and 1 M $CaCl_2$ (3 µl /ml) were added. The column was closed and rotated at 4°C for 1 hour. The column was then drained by gravity flow and washed with 30 ml of IPP-150 CBB. Proteins were eluted with 200 µl of IPP150 calmodulin elution buffer. 5 fractions were collected. All the fractions were then combined.

2.3.16 Protein Precipitation with Trichloroacetic Acid (TCA)

The eluate was adjusted to 20% TCA with 60% TCA. The mix was then placed on ice for 30 minutes. After incubation, the mix was pelleted at 14000 rpm for 30 minutes at 4°C. The supernatent was removed and kept. The pellet was washed two times with 200 µl of ice-cold acetone, followed by centrifugation at 14000 rpm for 5 minutes at 4°C. The supernatant was removed and the pellet was air-dried. The pellet was resuspended in 25 µl of X1 SDS loading buffer and stored at -20°C.

Buffers:

IPP-150 Buffer:	10 mM Tris pH8
	150 mM NaCl
	0.1% NP-40

TEV Cleavage Buffer:	10 mM Tris pH8
	150 mM NaCl
	0.1% NP-40
	0.5 mM EDTA

*10 mM EDTA was added immediately before use.

Calmodulin Binding Buffer (CBB):	10 mM Tris pH8
	150 mM NaCl
	0.1% NP-40
	1 mM Mg^{2+} Ac
	1 mM Imidazol
	2 mM $CaCl_2$

*β-Mercaptoethanol (BME) was added to final concentration of 0.7% immediately before use.

Calmodulin Elution Buffer (CEB):	10 mM Tris pH8
	150 mM NaCl
	0.1% NP-40
	1 mM Mg^{2+} Ac
	1 mM Imidazol
	10 mM EGTA

*BME was added to final concentration of 0.7% immediately before use.

2.4 Computer Analysis

Yeast database searches were performed on the *Saccharomyces* Genome Database (SGD) network (http://www.yeastgenome.org/).

Protein database search were performed on the NCBI server using the *PSI*-BLAST program (http://www.ncbi.nlm.nih.gov/BLAST).

Pairwise and multiple protein sequence alignments were perform using the EMBL ClustalWu program (http://www.ebi.ac.uk/clustalw/index.html)

The nuclear localization signal (NLS) was predicted using the Columbia University Bioinformatics Center Web Server:
(http://cubic.bioc.columbia.edu/cgi/var/nair/resonline.pl).

3D predictions were performed using the 3D-PSSM Web Server V 2.6.0 program (http://www.sbg.bio.ic.ac.uk/servers/3dpssm).

Sequence identities and similarities were identified using the BOXSHADE 3.21 server (http://www.ch.embnet.org/software/BOX_form.html).

CHAPTER THREE

YOL093W Gene Replacement

3.1 Sequence Analysis of the Yol093w Protein (Yol093wp)

The Yol093w protein is a hypothetical protein comprised of 293 amino acids (Figure 3.1.A). The protein has a predicted molecular weight of 34.5 kDa, and isoelectric point (pI) of 10.03. At the start of this thesis, no functional data was available for this protein.

The protein sequence, as shown in Figure 3.2, contains a predicted nuclear localization signal (NLS) in the N-terminal region, which suggests that Yol093wp might be a nuclear protein. The three-dimensional structure predictions of the protein fragments showed it contained a putative DNA binding domain and a DNA/RNA-binding 3-helical bundle in its C-terminal end (Figure 3.3), but the significance of the

predictions was quite low. The domains were delineated by sequence analysis and there was no experimental data to suggest the function of the Yol093wp. No other recognised protein motifs were identified. Examination of the sequence of Yol093wp therefore did not reveal any clues as to the role of the protein; although it did suggest that Yol093wp might bind to DNA or RNA.

(A) *YOL093W* Chr 15

MSNDEINQNEEKVKRTPPLPPVPEGMSKKQWKKMCKRQRW
EENKAKYNAERRVKKKRLRHERSAKIQEYIDRGEEVPQELIRE
PRINVNQTDSGIEIILDCSFDELMNDKEIVSLSNQVTRAYSANR
RANHFAEIKVAPFDKRLKQRFETTLKNTNYENWNHFKFLPDD
KIMFGDEHISKDKIVYLTADTEEKLEKLEPGMRYIVGGIVDKNR
YKELCLKKAQKMGIPTRRLPIDEYINLEGRRVLTTTHVVQLML
KYFDDHNWKNAFESVLPPRKLDAEAKSASSSPAPKDT

(B)

A.A. Composition		
	no.	%
Ala[A]	15	5.1%
Cys[C]	3	1.0%
Asp[D]	18	6.1%
Glu[E]	29	9.9%
Phe[F]	9	3.1%
Gly[G]	9	3.1%
His[H]	6	2.0%
Ile[I]	18	6.1%
Lys[K]	34	11.6%
Leu[L]	21	7.2%
Met[M]	8	2.7%
Asn[N]	19	6.5%
Pro[P]	16	5.5%
Gln[Q]	10	3.4%
Arg[R]	23	7.8%
Ser[S]	14	4.8%
Thr[T]	13	4.4%
Val[V]	15	5.1%
Trp[W]	4	1.4%
Tyr[Y]	9	3.1%
Total Length	293	

Figure 3.1 Amino Acid Composition of Yol093wp

(A) Amino acid sequence of Yol093wp. (B) Amino acid composition of Yol093wp: no.- number of times a particular amino acid is present in the protein.

PredictNLS Online

(http://cubic.bioc.columbia.edu/cgi/var/nair/resonline.pl)

Input Sequence (NLS's in Red)	MSNDEINQNEEKVKRTPPLPPVPEGMSKKQWKKMCKRQRWEENKAKYNAE RRVKKKRLRHERSAKIQEYIDRGEEVPQELIREPRINVNQTDSGIEIILDCSFDE LMNDKEIVSLSNQVTRAYSANRRANHFAEIKVAPFDKRLKQRFETTLKNTNY ENWNHFKFLPDDKIMFGDEHISKDKIVYLTADTEEKLEKLEPGMRYIVGGIVD KNRYKELCLKKAQKMGIPTRRLPIDEYINLEGRRVLTTTHVVQLMLKYFDDH NWKNAFESVLPPRKLDAEAKSASSSPAPKDT
Sequence Length	293
NLS's found. *No gives position of Motif*	*RVKKKRLR 51*

Statistical data for Nuclear Localization Signals present in the Input Sequence

Generalized NLS (notation)	Type	No with NLS	%Nuc Proteins	%NonNuc Proteins	Protein Swiss Id	Protein Localizations (Swiss anno.)
[RK][PLIV][KR][RK]{2,4}[PLVI]R	Potential [a]	5	100	0	ht31_arath	nuc
					cg2f_human	nuc
					prt3_oncmy	nuc
					prt4_oncmy	nuc
					prtb_oncmy	nuc

a:The potential NLS [RK][PLIV][KR][RK]{2,4}[PLVI]R has been derived from the experimental NLS RIRKKLR

format for NLS motifs:

[KR]	read	**K or R**
G{3}	read	**GGG**
x{3,5}	read	**between 3 and 5 x** where 'x' stands for 'any amino acid'

Figure 3.2 Nuclear Localisation Signal (NLS) Prediction of Yol093wp
The NLS was predicted using the Columbia University Bioinformatics Center Web Server. The proposed NLS is highlighted in red.

(A) **Putative DNA-binding domain**

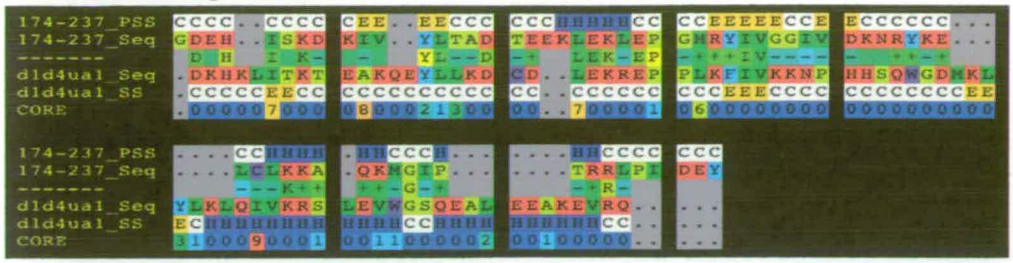

DNA/RNA-binding 3-helical bundle ("Winged helix" DNA-binding domain superfamily)

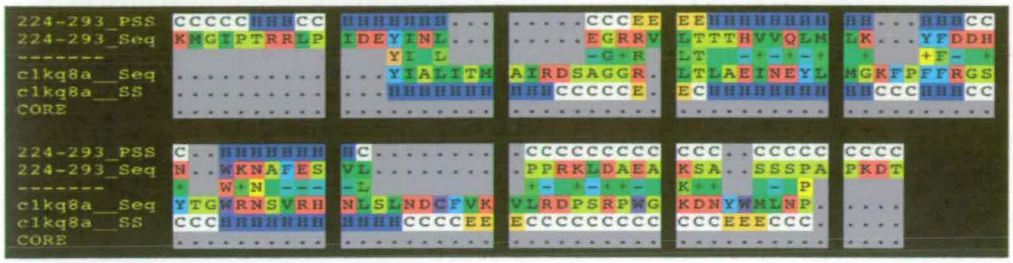

(number)_PSS	Predicted Secondary Structure for your Sequence
(number)_Seq	Your Sequence
(number)_Seq	Library Sequence
(number)_SS	Known Secondary Structure of the Library Sequence (Assigned by STRIDE)
CORE	A measure of the burial and number of contacts made by a residue. (9 very buried/making many contacts, 0 not buried/making few contacts)

(B)

Putative DNA-binding domain

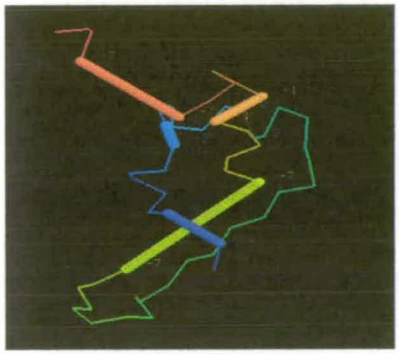

PSSM E-value: 18.6; template length: 75

DNA/RNA-binding 3-helical bundle ("Winged helix" DNA-binding domain superfamily)

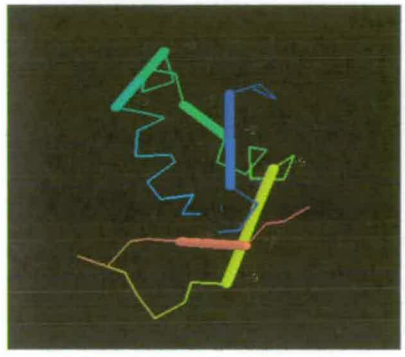

PSSM E-value: 7.75; template length: 75

http://www.sbg.bio.ic.ac.uk/servers/3dpssm/output/a0901141b3bc33a7.job_summary.html
http://www.sbg.bio.ic.ac.uk/servers/3dpssm/output/2a39d5e56250e69a.job_summary.html

Figure 3.3 3D-predictions of Yol093wp Sequence Fragments

Sequences were aligned using the 3D-PSSM Web Server V 2.6.0 program. The models as displayed were coloured from blue → red and N → C. This model was generated directly from the alignment, with no subsequent refinement. It was intended only as a guide. The thick lines represent a deletion in the known library structure, i.e. there are residues in the known structure that are not aligned to residues in the query. The thin lines represent the reverse situation, i.e. thin lines represent an insertion in the known library structure. The numbers appearing at the beginnings and ends of these insertions and deletions represent the number of residues inserted into or deleted from the known structure respectively.

3.2 Gene Replacement of *YOL093W*

3.2.1 Introduction of PCR-based Gene Disruptions in *Saccharomyces cerevisiae*

In *Saccharomyces cerevisiae*, gene deletion and the modification of chromosomal genes by homologous recombination are now standard techniques. A PCR-mediated technique has been developed that allows single-step deletion or epitope tagging of chromosomal genes (Lorenz et al., 1995; Baudin et al., 1993; Lorenz et al., 1995; Wach et al., 1994) (Figure 3.4). In this method, a linear DNA fragment is generated by PCR, that comprises the selectable marker gene, flanked at both ends by approximately 45 base pairs of sequence identical to the DNA immediately 5' and 3' to the coding sequence to be replaced. The amplified DNA is introduced into yeast, and by homologous recombination, the gene can be deleted or epitope tagged. Genes can be replaced directly at high efficiencies in *S. cerevisiae*, permitting the convenient production of numerous altered forms of proteins. These techniques have been exploited extensively in the analysis of general questions in cell biology.

The yeast strains that were used or produced in this work are listed on Table 2.6.

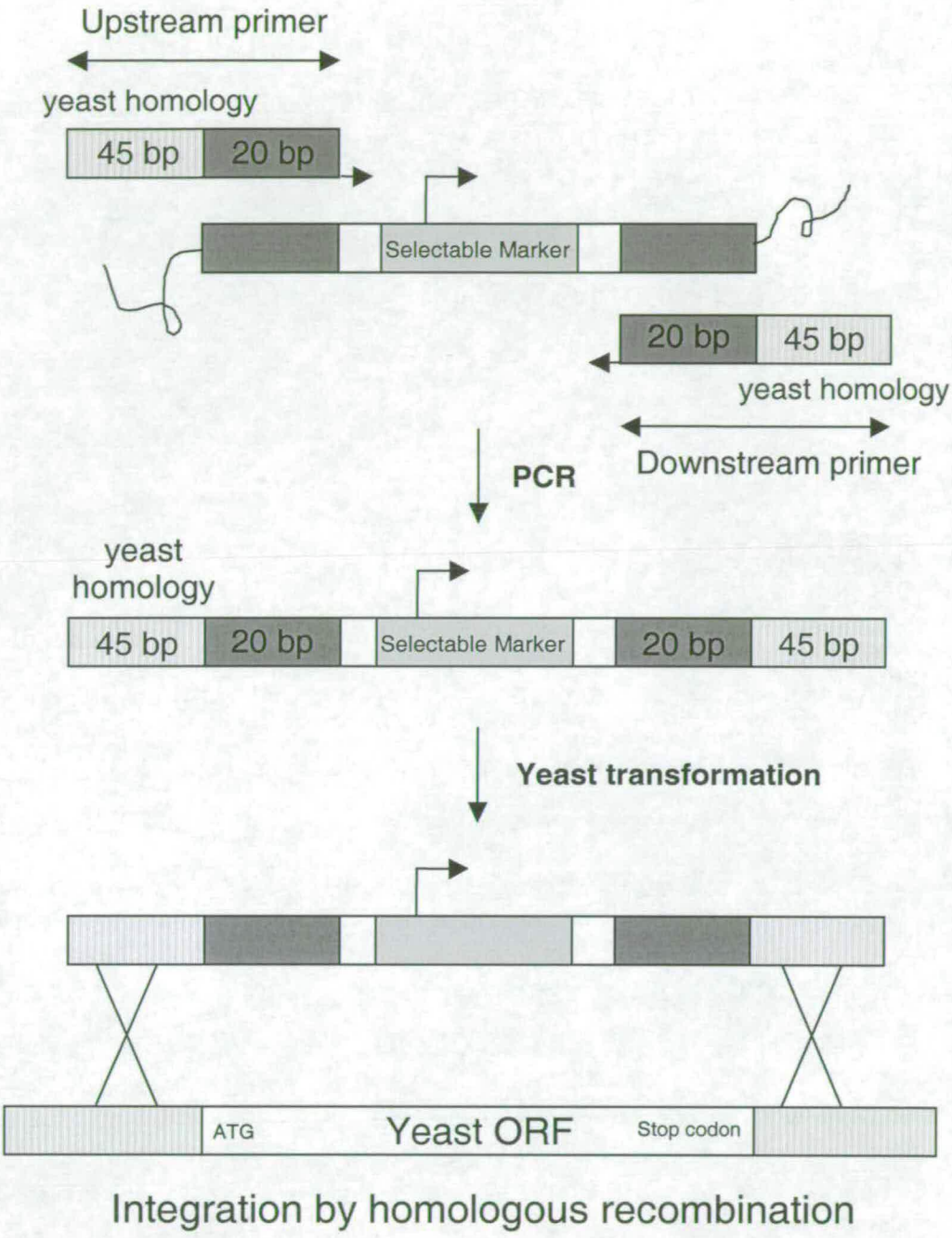

Figure 3.4 Schematic Representation of the Strategy of ORF Deletion from the Chromosome

Oligonucleotide primers were used to amplify the 3HA-kan or hph cassette flanking with 45bp upstream sequence of the stop codon of the ORF, and 45bp downstream sequence of the ORF. PCR product was then introduced into the yeast cells. The cassette was integrated though homologous recombination.

3.2.2 Deletion of *YOL093W* ORF from the BMA38 Genome

3.2.2.1 Deletion of *YOL093W*

As a first step in characterization of *YOL093W*, a gene replacement was performed in yeast. The entire *YOL093W* coding sequence (from ATG to the stop codon) was removed precisely and replaced by the kanamycin (kan) or the hygromycin B (hph) resistance marker using a PCR-based method of direct gene deletion. Using the oligonucleotides YOL093W-KO-1 and YOL093W-KO-2, kan or hph marker gene was amplified by PCR from the plasmid pFA6a-3HA-KanMX6 or pAG32. The diploid yeast strain BMA38(2n) was transformed with the purified linear PCR product containing the kan or the hph resistance marker flanked by approximately 45 base pairs of the *YOL093W* locus at either site, so that integration of the marker gene can occur by homologous recombination. Kan-resistant or hph-resistant clones were streaked out onto fresh YPDA + kan or YPDA+ hph medium for colony purification. Kan- or hph-resistant transformants were then tested for integration of the marker gene at the desired locus by PCR, as shown in Figures 3.5 & 3.6. The following heterozygous *YOL093W* deletion mutants were made: MYY1 (*YOL093W/yol093wΔkan*) and MYY2 (*YOL093W/yol093wΔhph*). The heterozygous mutants were then used as the parental strains for the second knockout of another copy of the *YOL093W* allele, and the homozygous *YOL093W*-deleted mutant, MYY3 (*yol093wΔkan/yol093wΔhph*), was made. PCR analysis (Figures 3.7 & 3.8) and DNA sequencing (Figures 3.9 & 3.10) were used to confirm the gene replacement.

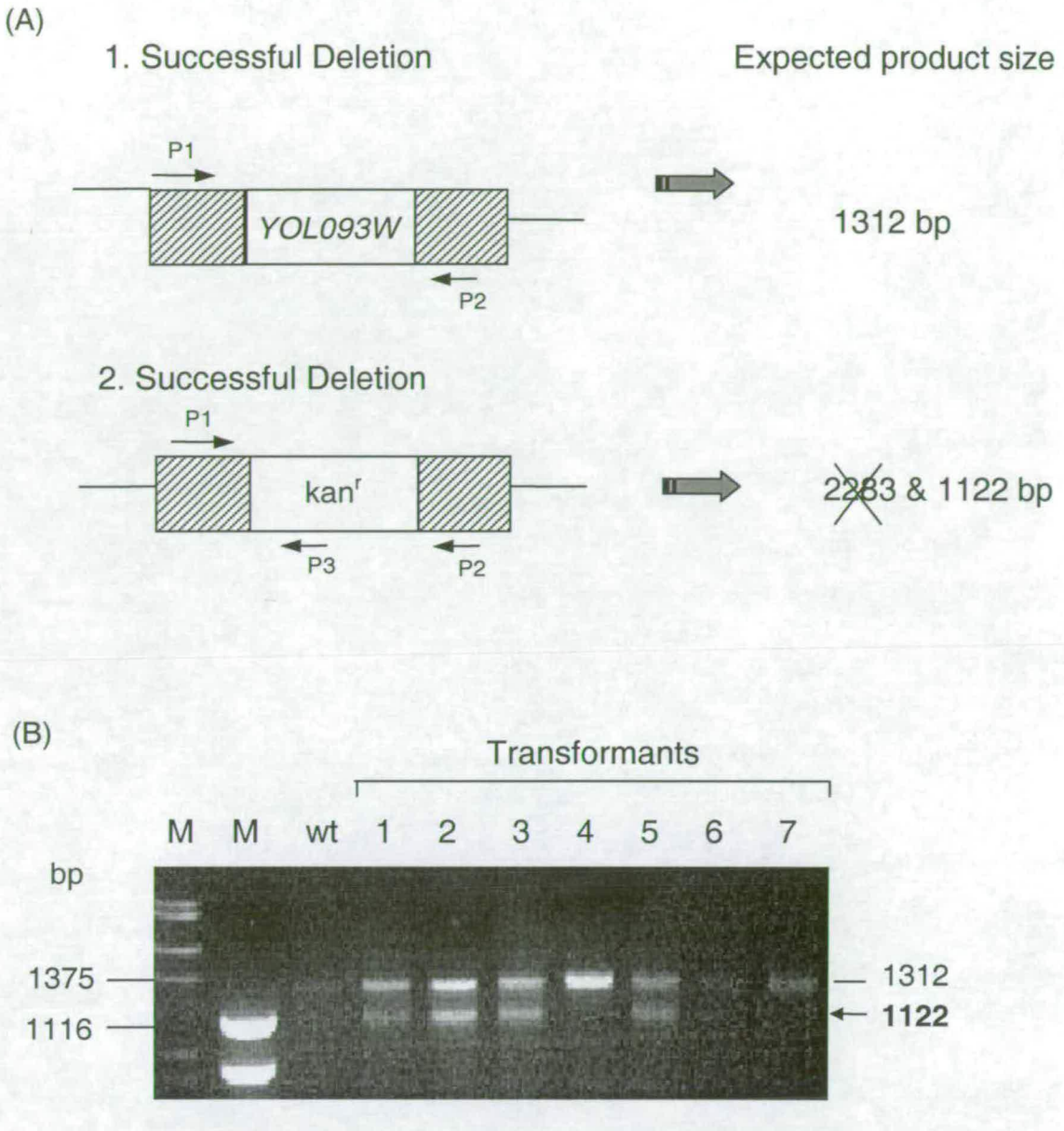

Figure 3.5 PCR Analysis of Heterozygous *YOL093W* ORF Deletion by the Kanamycin Marker

PCR analysis of yeast transformants to confirm integration of the kanamycin (kan) marker into the chromosome. After transformation of BMA38(2n) with a linear PCR product containing the kan marker flanked by approximately 45 base pairs of the *YOL093W* locus at either site, Kan-resistant clones were streaked out onto fresh YPDA+ kan medium for colony purification. Cells from the transformants, and the parental BMA38(2n) were suspended in water, boiled for 10 minutes and used in a PCR using oligonuceotides P1: SC093-TEST-1, P2: SC093-TEST-2, P3: R-Kan as primers. (A) The positions on the template at which the primers anneal are indicated in the upper schematic drawing of the *YOL093W* locus (either wild type, or after kan-integration). The product failed to be amplified by yeast colony PCR has been crossed. (B) The products of PCR reactions. The fragment expected following successful integration of kan cassette into the *YOL093W* locus is indicated. The 3' junction of the gene replacement was also confirmed by PCR with an internal forward primer of the drug-resistant cassette and a reverse primer P2 (data not shown).

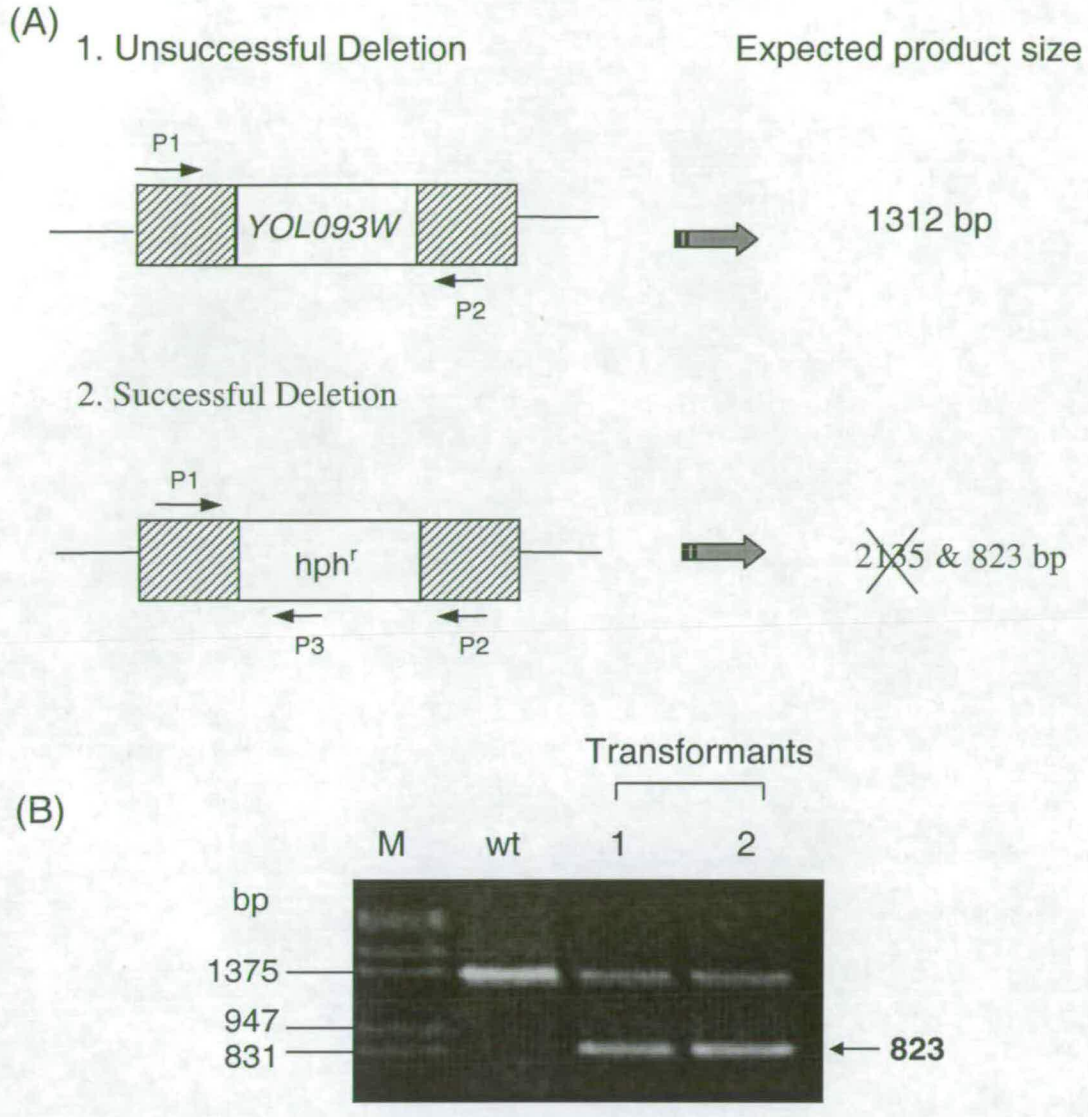

Figure 3.6 PCR Analysis of Heterozygous *YOL093W* ORF Deletion by the Hygromycin B Marker

PCR analysis of yeast transformants to confirm integration of the hygromycin B (hph) marker into the chromosome. After transformation of BMA38 (2n) with a linear PCR product containing the kan marker flanked by approximately 45 base pairs of the *YOL093W* locus at either site, Kan-resistant clones were streaked out onto fresh YPDA+ kan medium for colony purification. Cells from the transformants, and the parental BMA38 (2n) were suspended in water, boiled for 10 minutes and used in a PCR using oligonuceotides P1: SC093-TEST-1, P2:SC093-TEST-2and P3: R-hph as primers. (A) The positions on the template at which the primers anneal are indicated in the upper schematic drawing of the *YOL093W* locus (either wild type, or after kan-integration). The product failed to be amplified by yeast colony PCR has been crossed. (B) The products of PCR reactions. The fragment expected following successful integration of kan cassette into the *YOL093W* locus is indicated. The 3' junction of the gene replacement was also confirmed by PCR with an internal forward primer of the drug-resistant cassette and a reverse primer P2 (data not shown).

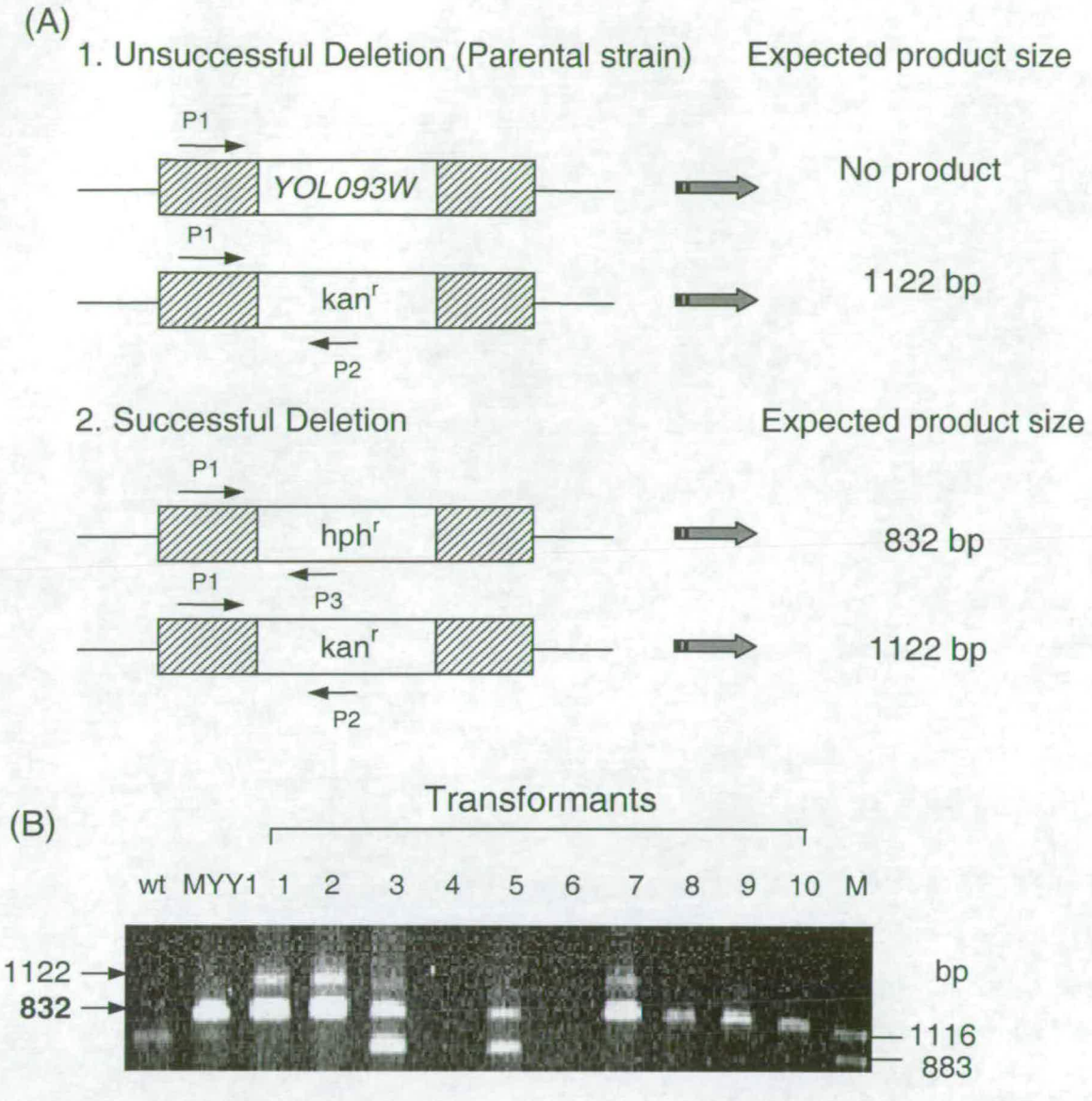

Figure 3.7 Detection of *YOL093W* ORF Deletion from the MYY1 (*YOL093W/yol093wΔKan*) Genome

PCR analysis of the yeast transformants to confirm integration of the hygromycin B (hph) marker into the chromosome. After transformation of MYY1 (*YOL093W/yol093wΔ::kan*) with a linear PCR product containing the hph marker flanked by approximately 45 base pairs of the *YOL093W* locus at either site, hph-resistant clones were streaked out onto fresh YPDA + hph + kan medium for colony purification. Yeast colony PCR was performed using P1: SC093-TEST-1, P2: R-kan and P3: R-hph primers. (A) The positions on the template at which the primers anneal are indicated in the upper schematic drawing of the *YOL093W* locus (either the parental strain or after hph-integration). (B) The products of the PCR reactions. The fragment expected following successful integration of hph cassette into the *YOL093W* locus is indicated. The 3' junction of the gene replacement was also confirmed by PCR with an internal forward primer of the drug-resistant cassette and a reverse primer outside the *YOL093W* locus (data not shown).

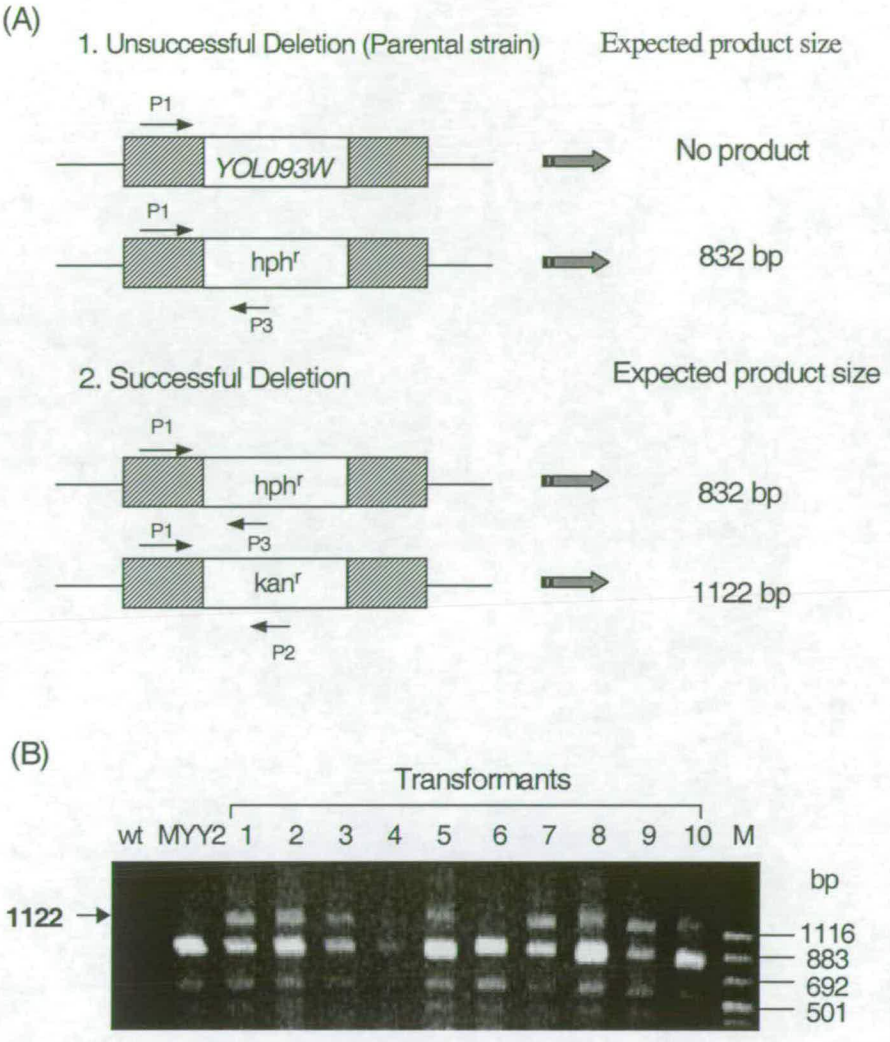

Figure 3.8 Detection of *YOL093W* ORF Deletion from the MYY2 (*YOL093W/yol093wΔhph*) Genome

PCR analysis of the yeast transformants to confirm the integration of the kanamycin (kan) marker into the chromosome. After transformation of MYY2 (*YOL093W/yol093wΔ:hph*) with a linear PCR product containing the kan marker flanked by approximately 45 base pairs of the *YOL093W* locus at either site, Kan-resistant clones were streaked out onto fresh YPDA + kan + hph medium for colony purification. Yeast colony PCR was performed using P1: SC093-TEST-1, P2: R-kan and P3: R-hph primers. (A) The positions on the template at which the primers anneal are indicated in the upper schematic drawing of the *YOL093W* locus (either the parental type or after kan-integration). (B) The products of the PCR reactions. The fragment, which would be expected following successful integration of kan cassette into the *YOL093W* locus is indicated. The 3' junction of the gene replacement was also confirmed by PCR with an internal forward primer of the drug-resistant cassette and a reverse primer outside the *YOL093W* locus (data not shown).

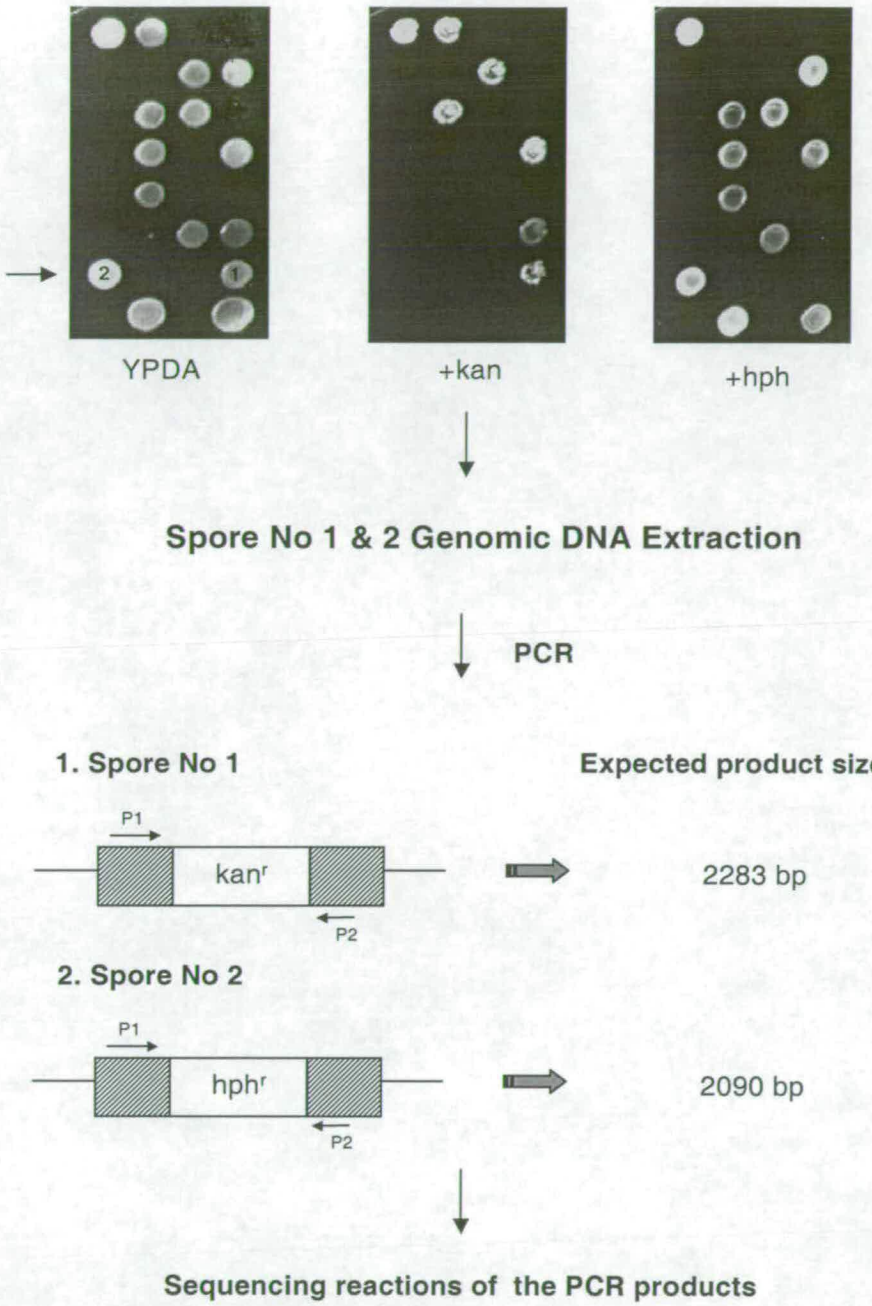

Figure 3.9 Schematic Representation of the Strategy for Sequencing the 5'- and 3'-junctions of *YOL093W* Replacement to Confirm the Gene Deletion

Oligonucleotide primers were used to amplify the cassettes from *YOL093W* deletion genome flanking with 45 bp upstream sequence of the stop codon of the ORF, The 5' and 3' junctions of the PCR products were then sequenced.

Figure 3.10 Sequencing Analysis of *YOL093W* Deletion from the MYY3 (*yol093wΔkan* /*yol093wΔhph*) Genome

Sequencing analysis of the MYY3 spores to confirm integration of the kanamycin (kan) or hygromycin B (hph) marker into the chromosome. The 5' and 3' junctions of the replacement were amplified by PCR, and the PCR products were then assessed by sequence analysis.

3.2.2.2 Tetrad Dissection Analysis of *YOL093W* Deletion Strains

The diploid transformants that had been shown positive for the gene replacement (designated strains MYY1, MYY2 and MYY3) were sporulated. Tetrads were dissected onto YPDA agar plates and separated spores were incubated at 30°C for 3-4 days (Figure 3.11).

Result of the tetrad dissection is shown in figure 3.12. For the heterozygous strain MYY1 (*YOL093W/yol093wΔkan*), out of 43 tetrads dissected, in 38 cases (54.35%) all four spores grew to colonies of comparable size, in 14 cases (30.35%) only 3 spores germinated, in 5 cases (10.87%) two spores grew to colonies, and in 2 cases (4.35%) one spore was viable. For the other heterozygous strain MYY2 (*YOL093W/yol093wΔhph*), in 38 cases (76%) all four spores germinated, leading to two small and two larger colonies for each dissected tetrads. In other 9 cases (18%), three spores germinated. In other 2 cases (4%), two spores grew to colonies, and in the other 1 case (2%), no spore was viable. For the homozygous gene knockout strain MYY3 (*yol093wΔkan/yol093wΔhph*), out of 58 tetrads dissected, in 44 cases (75.86%) only 2 spores grew to colonies, in 10 cases (17.24%) only 1 spores germinated, and in 4 cases (6%) no spore was viable.

These data suggested that *YOL093W* is not essential for cell viability. However, the *YOL093W* double-knockout strain showed lower spore viability, which suggested that *YOL093W* might play a role in meiosis process.

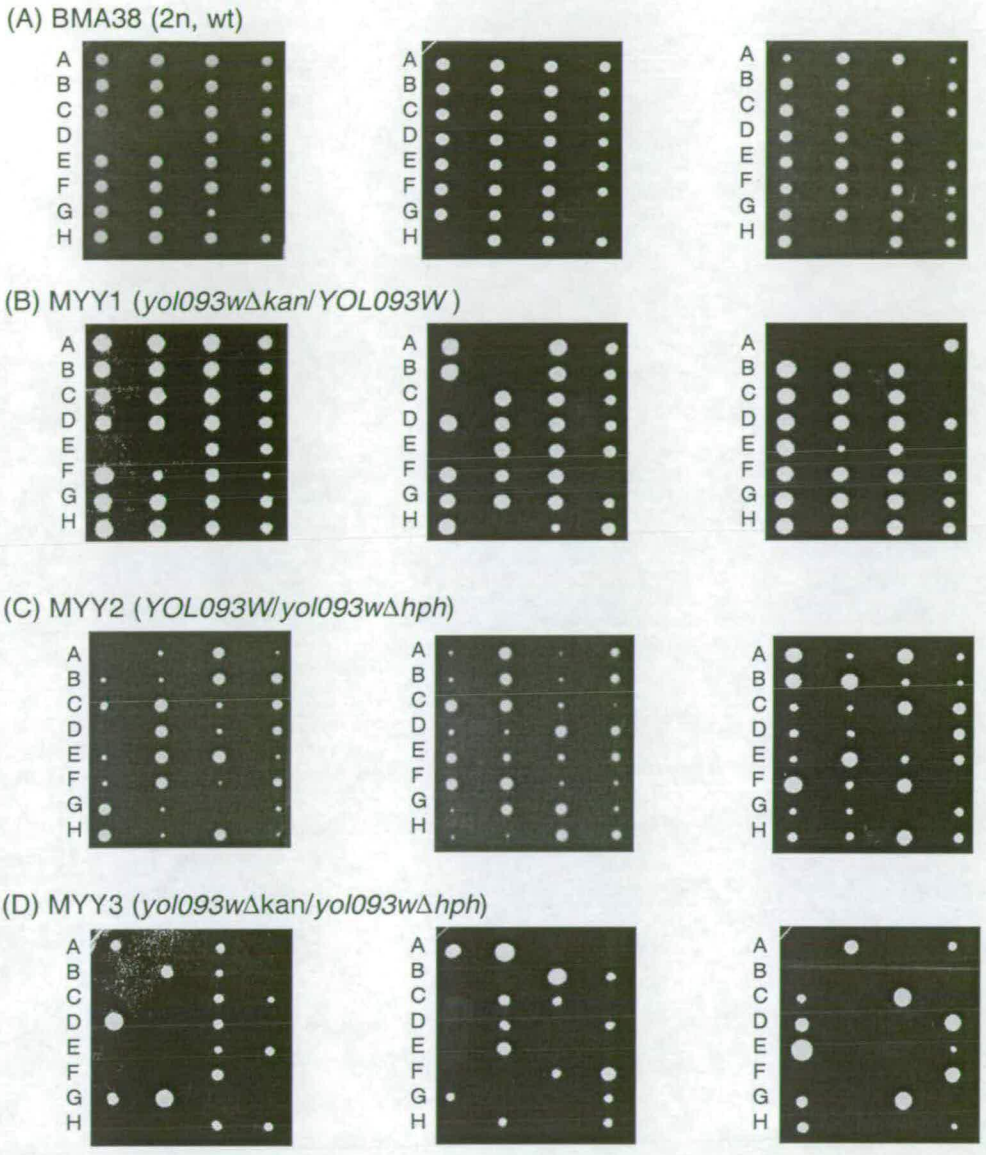

Figure 3.11 Tetrad Dissection Analysis of the Effects of *YOL093W* Deletion

Tetrad analysis of strains (A) BMA38 (wt, *YOL093W/YOL093W*), (B) MYY1 (*YOL093W/yol093wΔkan*), (C) MYY2 (*YOL093W/yol093wΔhph*), and (D) MYY3 (*yol093wΔkan/yol093wΔhph*). Strains were streaked out onto sporulation medium plates. After 5-7 days of inoculation at 30°C, tetrads were dissected onto the YPDA agar plate. Spores were incubated for a few days at 30°C.

(A) BMA38 (2n, wt)

Number of viable spores/tetrad	Number of tetrads	Percentage (%)
0	2	4.65
1	0	0
2	5	11.63
3	11	25.58
4	25	58.14
Total	43	100

(B) MYY1 (*yol093wΔkan / YOL093W*)

Number of viable spores/tetrad	Number of tetrads	Percentage (%)
0	0	0
1	2	4.35
2	5	10.87
3	14	10.35
4	38	54.35
Total	46	100

(C) MYY2 (*YOL093W/ yol093wΔhph*)

Number of viable spores/tetrad	Number of tetrads	Percentage (%)
0	1	2
1	0	0
2	2	4
3	8	18
4	38	76
Total	50	100

(D) MYY3 (*yol093wΔkan / yol093wΔhph*)

Number of viable spores/tetrad	Number of tetrads	Percentage (%)
0	4	6
1	10	17.24
2	44	75.86
3	0	0
4	0	0
Total	58	100

Figure 3.12 Spore Viability of Tetrads in *YOL093W* Deletion Strains

Tetrad dissection analysis of strains (A) BMA38 (B) MYY1 (C) MYY2 and (D) MYY3. Strains were streaked out onto sporulation medium plates. After 5-7 days of inoculation at 30°C, tetrads were dissected onto the YPDA agar plate. Spores were incubated for 3-4 days at 30°C. The spore viability is shown on tables.

3.2.2.3 Temperature-sensitivity Tests of *YOL093W* Deletion Strains

Cells of the spores of MYY3 (*yol093wΔkan/yol093wΔhph*) as well as cells from wild-type spores were serially diluted into microtiter plates and spotted onto YPDA or YPDA + Nocodazole plates using a pronged metal inoculator. The plates were incubated at a range of temperatures for 2-5 days (Figure 3.13). This confirmed that the deletion of *YOL093W* from the genome does not have a visible effect on the cell growth in rich medium.

3.2.2.4 Growth Curves of *YOL093W* Deletion Strains

To study the effect of *YOL093W* deletion on cell growth, the growth rate analysis was performed on the following strains: BMA38 (*YOL093W/YOL093W*), MYY1 (*YOL093W/yol093wΔkan*), MYY2 (*YOL093W/yol093wΔhph*), MYY3 (*yol093wΔkan/yol093wΔhph*), haploid strain MYY2/1(*YOL093W*), and haploid MYY2/2 (*yol093wΔhph*). Cells were inoculated in YPDA medium and incubated at 30°C. The optical density (OD_{600}) of cells was measured at different time points. By comparing the growth rate of these *YOL093W* deletion strains with the wild type strain in Figure 3.14, only the haploid MYY2/2 (hph-resistant spore) showed slightly slow growth, which was seen in the tetrad dissection analysis of MYY2 (section 3.2.2.2). This slow growth might be caused by the hph cassette integration. There was no difference on the growth rate in the other *YOL03W* deletion strains with the

wild-type strain BMA38(2n). Thus it suggested that the deletion of *YOL093W* alleles does not affect cell growth.

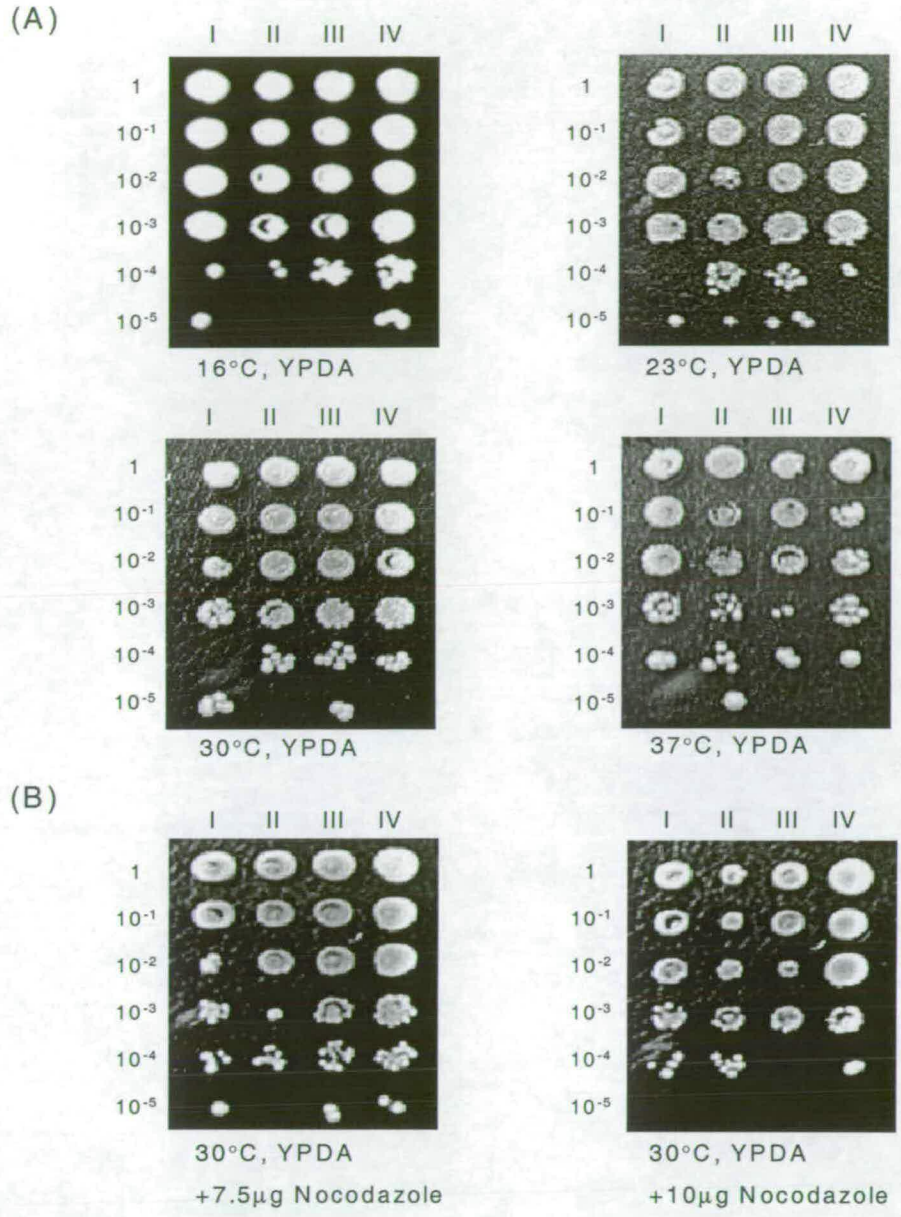

Figure 3.13 Temperature Sensitivity Analysis of the Effects of *YOL093W* Deletion from the Genome

A. Haploid cells deleted for the *YOL093W* locus (II: strain MYY3/1; III: strain MYY3/2) as well as cells from (I) the parental wild-type strain and (IV) the diploid *YOL093W* deletion strain MYY3 were suspended in dilutions in microtiter plates, spotted onto YPDA plates and inculbated at a range of temperatures for a few days. B. Haploid cells deleted for the *YOL093W* locus (strain MYY1) as well as cells from the wild-type spore were suspended in dilutions in microtiter plates, spotted onto YPDA + Nocodazole plates and incubated at 30°C for 3 days. (I: wild-type; II: strain MYY3/1; III: strain MYY3/2; IV: MYY3)

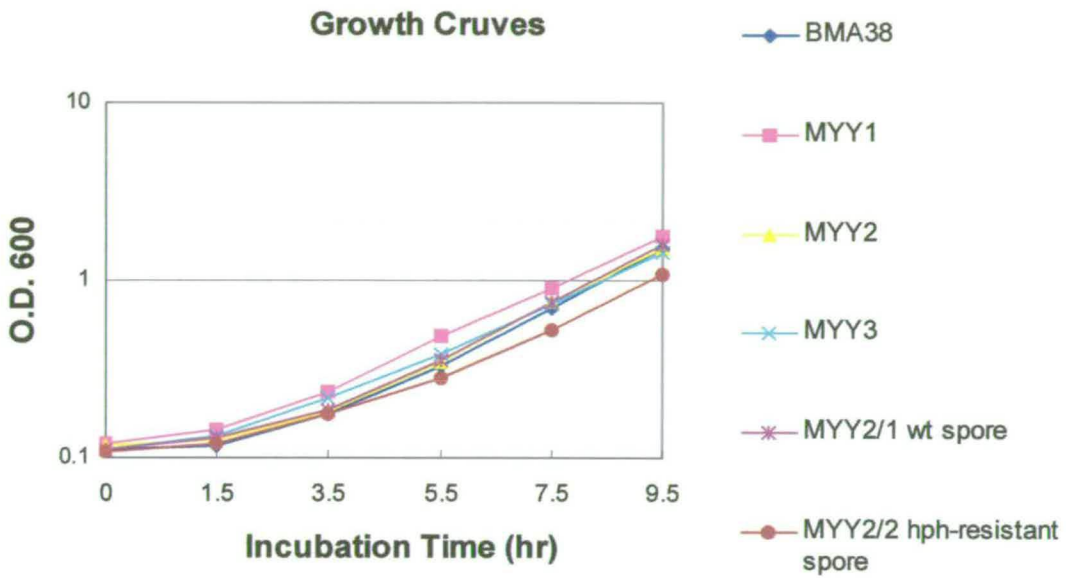

Figure 3.14 Growth Curves of *YOL093W* Deletion Strains
Growth rate analysis of strains BMA38 (*YOL093W/YOL093W*), MYY1 (*YOL093W/yol093wΔkan*), MYY2 (*YOL093W/yol093wΔhph*), MYY3 (*yol093wΔkan/yol093wΔhph*), as well as the haploid strain MYY2/1(*YOL093W*), and MYY2/2 (*yol093wΔhph*) were performed. Cells were inoculated in YPDA medium and incubated at 30°C. Aliquots were removed at regular intervals and the optical density of the cells (OD_{600}) was measured.

3.2.2.5 Drug-resistant Tests of *YOL093W* Deletion Strains

Spores of the tetrad dissection assay were replicated onto YPDA, YPAD + kan, YPDA + hph, and YPDA + kan + hph plates (Figure 3.15). In the cases which all four spores geminated only two spores grew on the selective plates as expected. Interestingly, some spores from the MYY3 strain (*yol093wΔkan/yol093wΔhph*) grew on the YPDA + kan + hph plates (Figure 3.15 C). It showed that these spores possessed two drug-resistant genes, which might suggest non-disjunction events happened during the chromosomal segregation.

3.2.2.6 DAPI Stain of *YOL093W* Deletion Strain

To learn more about the DNA components of spores from *YO093W* deletion strain, the DAPI (4'6-diamidino-2-phenylindole) stain was used to examine the DNA inside tetrads of wild type BMA38(2n) strain as well as MYY3 strain (*yol093wΔkan/yol093wΔhph*) (Figure 3.16). The micrographs showed abnormal DNA components inside *YOL093W* deletion tetrads; various numbers (from 1-4) of DAPI-strained spots were observed form a single tetrad. This result was consistent to the spore viabilities of MYY3 strain (section 3.2.2.2).

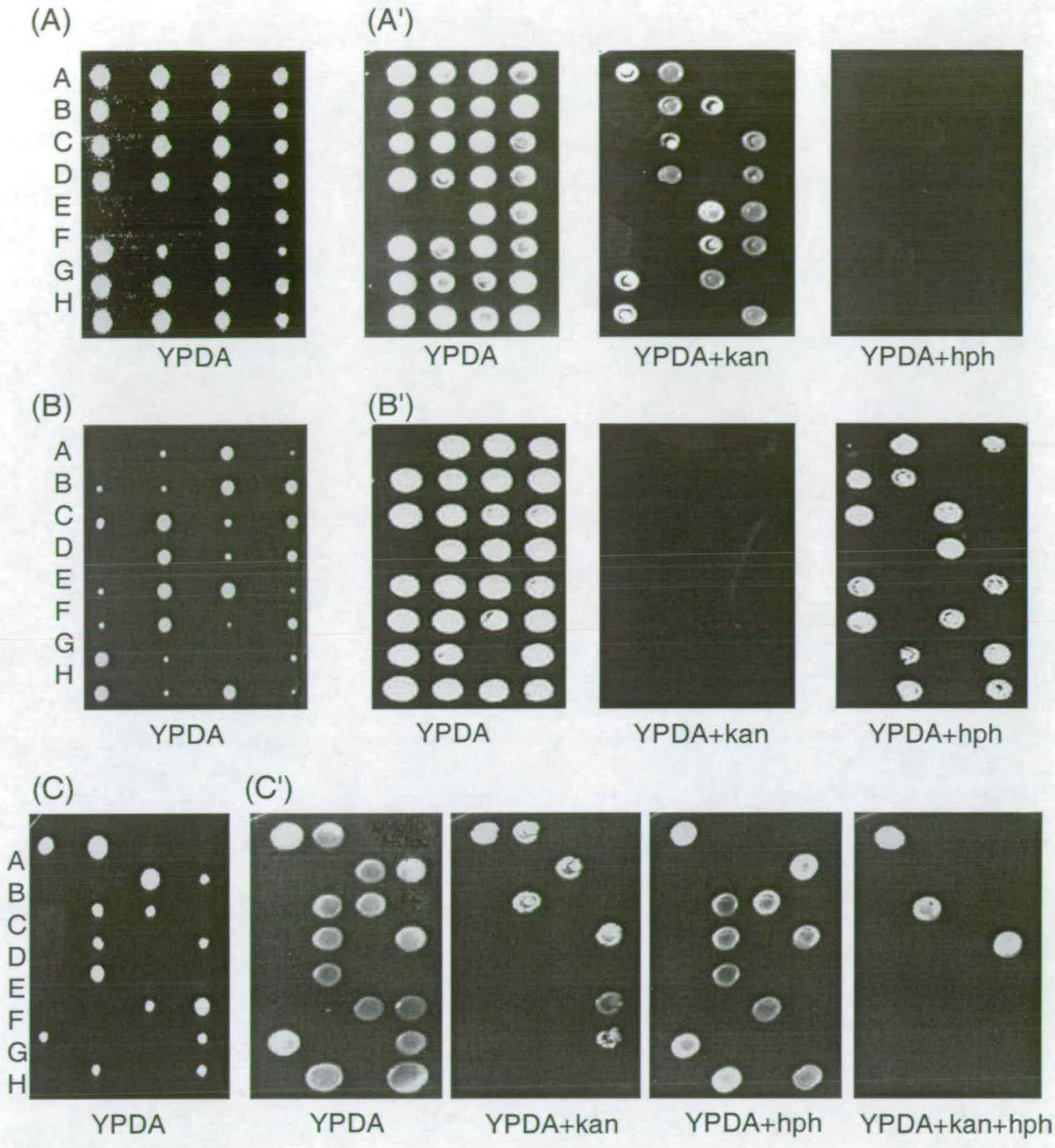

Figure 3.15 Drug Resistance Analysis of the Effects of *YOL093W* Deletion

Haploid cells form (A) MYY1 strain (*yol093wΔkan/YOL093W*), (B) MYY2 strain (*YOL093W/yol093wΔhph*), as well as cells from (C) MYY3 strain (*yol093wΔkan/yol093wΔhph)* were suspended in dilutions in microtiter plates, spotted onto YPDA, YPDA + kan, YPDA + hph plates and incubated at 30°C for a few days (A', B' and C').

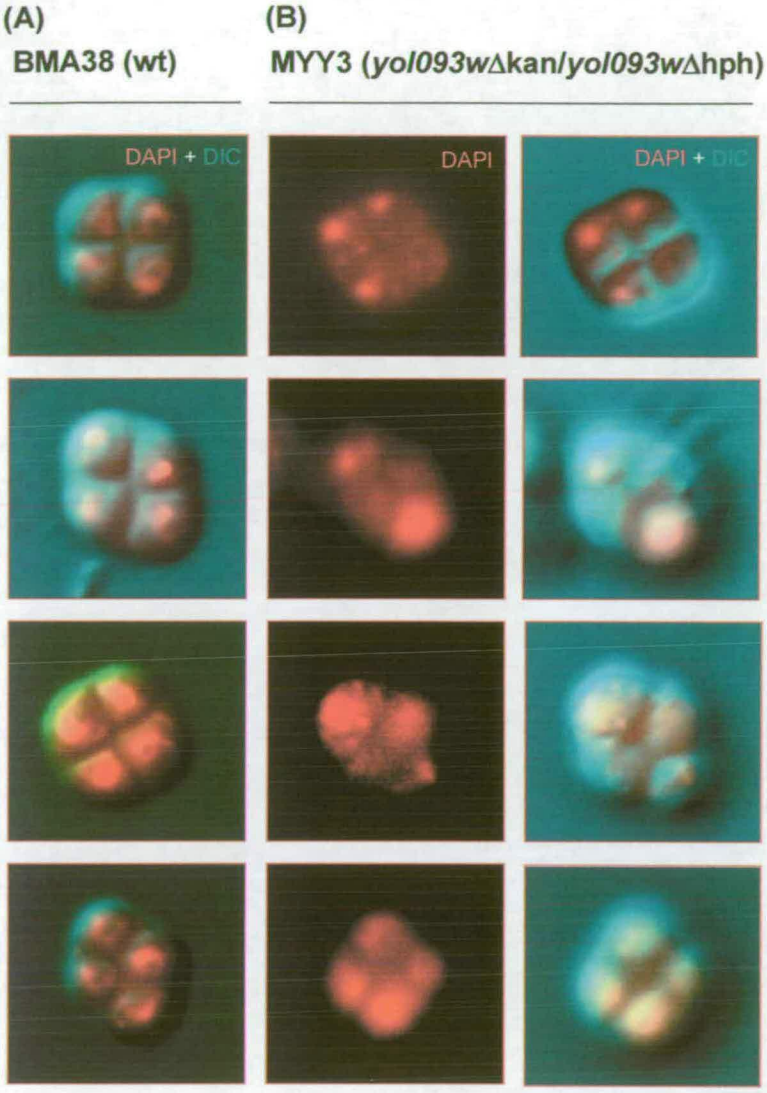

Figure 3.16 DAPI Straining of Tetrads from *YOL093W* Deletion Strain
Tetrad form (A) wild-type BMA38 (*YOL093W/YOL093W*) and (B) MYY3 (*yol093wΔkan/yol093wΔhph*) were strained with DAPI and examined by fluorescence microscopy (X630 magnification). DAPI staining for DNA; DIC represents Differential Interference Contrast image.

3.3 Complementation Tests

3.3.1 Complementation Tests of *YOL093W* Deletion with the Wild-type *YOL093W*

In order to prove that the lower spore viability of MYY3 (*yol093wΔkan/yol093wΔhph*) is in fact due to the deletion of *YOL093W*, complementation of the defect by providing Yol093wp was tested. In parallel, the cross-back experiment was performed.

For the complementation experiments, both *S. cerevisiae* 2μ vectors and centromeric (*CEN*) vectors were used. 2μ vectors contain the origin of the 2μ circle, a multicopy endogenous yeast episome. Centromeric vectors contain an *ARS* origin of replication and one of several centromere loci. Centromeric vectors exist at a low copy number (1 to 2 per cell) and are generally more stable then those based on 2-μm circle origin.

The *YOL093W* ORF along with its endogenous promoter region (500 bp upstream) and its polyA signals (500 bp downstream) were amplified by PCR from the genomic DNA of strain BMA38 using primers *Bam*HI-93W promoter-F and *Eco*RI-93W polyA-R. The PCR product was digested with *Bam*HI and *Eco*RI, and then ligated into the *CEN* plasmid pRS316 or the 2μ plasmid pYEplac195. The construct pRS316/*YOL093W* and pYEplac1956/*YOL093W* were confirmed by enzyme digestion (Figures 3.17 & 3.18).

(A)

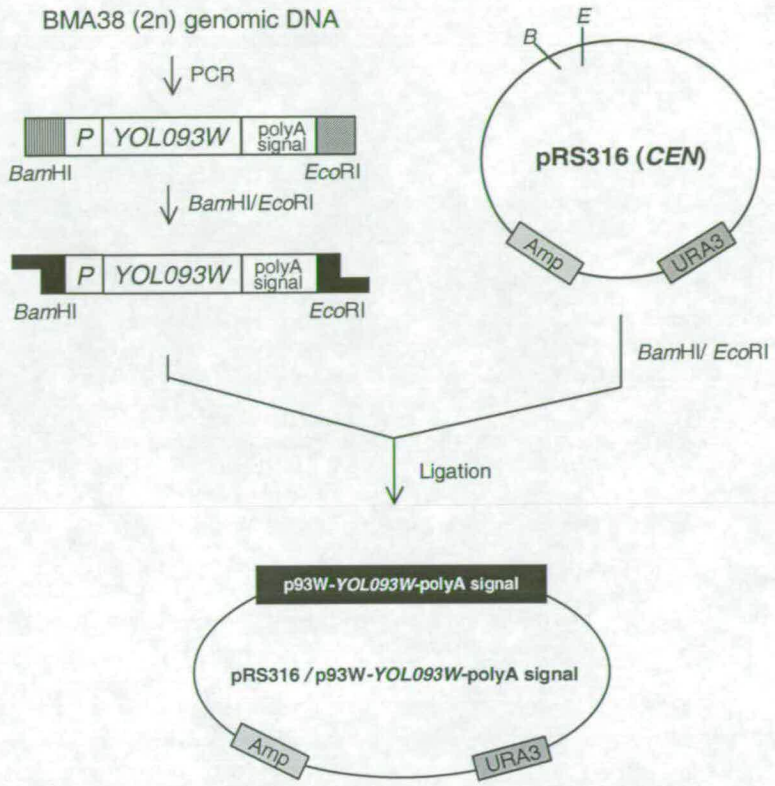

(B)

Figure 3.17 Construction of pRS316/*YOL093W* Plasmid
The *YOL093W* ORF was amplified by PCR from genomic DNA of strain BMA38. The PCR product was digested with *Bam*HI/*Eco*RI, and ligated into the vector pRS316. (A) A schematic representation of the cloning strategy used to construct pRS316/*YOL093W*. (B) The construct was confirmed by the *Bam*I/*Eco*RI enzyme digestion. The arrow indicates the 1894bp DNA fragment, which would be expected following successful construction of pRS316/*YOL093W* is indicated. V: pRS316 vector.

(A)

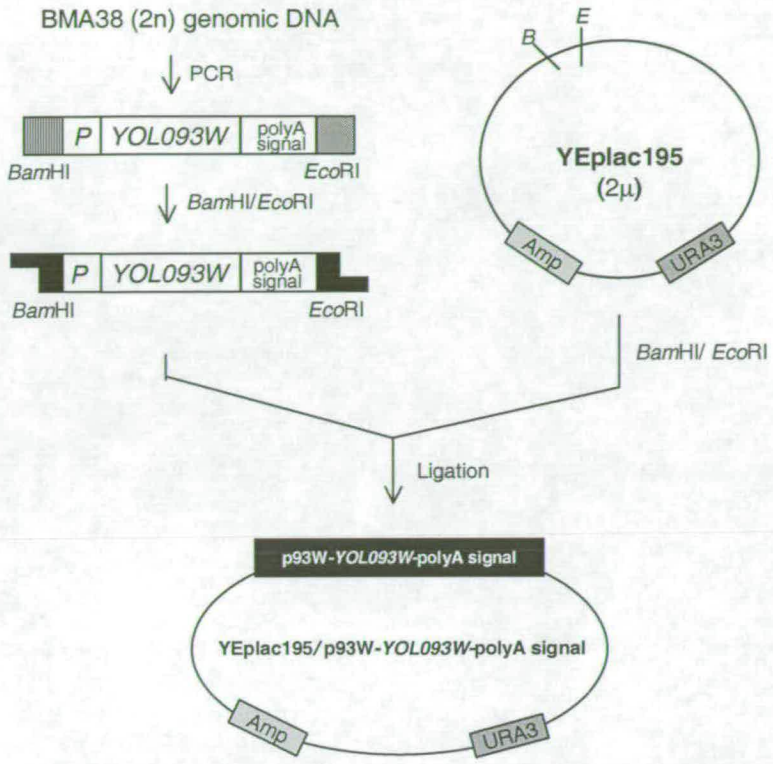

(B)

Figure 3.18 Construction of pYEplac195/*YOL093W* Plasmid
The *YOL093W* ORF was amplified by PCR from genomic DNA of strain BMA38. The PCR product was digested with *Bam*HI/*Eco*RI, and ligated into the vector pRS316. (A) A schematic representation of the cloning strategy used to construct pYEplac195/*YOL093W*. (B) The construct was confirmed by the *Bam*I/*Eco*RI enzyme digestion. The arrow indicates the 1894 bp DNA fragment, which would be expected following successful construction of pYEplac195/*YOL093W* is indicated. V: pYEplac195 vector.

The *CEN* and 2μ constructs were introduced into MYY3 (*yol093wΔkan/yol093wΔhph).* The resultant strains, MYY3/pRS316-p93W-*YOL093W*-polyA and MYY3/pYEplac195-p93W-*YOL093W*-polyA respectively, were than used for tetrad dissection analysis (Figures 3.19 & 3.20).

Surprisingly, transformation of MYY3 with either the *CEN* plasmid pRS316/*YOL093W* or the 2μ plasmid pYEplac1956/*YOL093W* did not complement the low spore viability defect. This suggested that the defect might be not caused by the *YOL093W* deletion, but some other gene. To test this possibility further, the chromosome feature map around *YOL093W* was retrieved from *Saccharomyces* Genome Database (SDG) (Figure 3.21). By identifying the functions of the proteins nearby the *YOL093W*, the *RFC4* and *SPO21* were decided as candidates for complementation experiments.

(A) MYY3 (*yol093wΔkan/yol093wΔhph*)

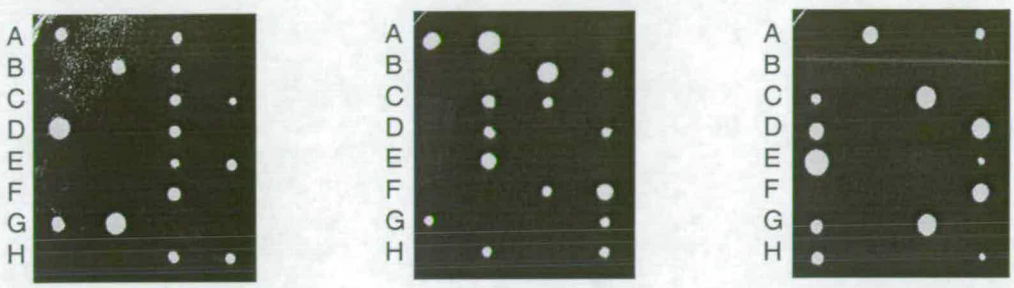

(B) MYY3/pRS316-p93W-*YOL093W*-polyA

Figure 3.19 Complementation Test of *YOL093W* Deletion by the pRS316/*YOL093W* Plasmid

The pRS316/*YOL093W* plasmid was introduced into MYY3 strain (*yol093wΔkan/yol093wΔhph*). Transformants were selected on YMM-U medium, restresked for colony purification. Tetrad dissection analysis of strains (A) BMA38 (*YOL093W/YOL093W*), and (B) MYY3/pRS316-p93W-*YOL093W*-ployA was performed. Strains were streaked out onto sporulation medium plates. After 5-7 days of incubation at 30˚C, tetrads were dissected onto the YPDA agar plate. Spores were incubated for a few days at 30˚C.

(A) MYY3 (*yol093wΔkan/yol093wΔhph*)

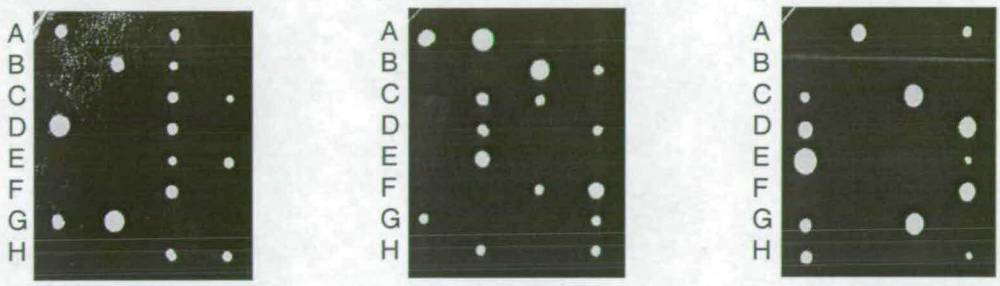

(B) MYY3/YEplac195-p93W-*YOL093W*-polyA

Figure 3.20 Complementation Test of *YOL093W* Deletion by the pYEplac195/*YOL093W* Plasmid

The pYEplac195/*YOL093W* plasmid was introduced into MYY3 strain (*yol093wΔkan/yol093wΔhph*). Transformants were selected on YMM-U medium, restresked for colony purification. Tetrad dissection analysis of strains (A) BMA38 (*YOL093W/YOL093W*), and (B) MYY3/ pYEplac195-p93W-*YOL093W*-ploy A was performed. Strains were streaked out onto sporulation medium plates. After 5-7 days of incubation at 30°C, tetrads were dissected onto the YPDA agar plate. Spores were incubated for a few days at 30°C.

Chromosomal Features Map

Features around YOL093W on chromosome XV
Spanning a region 10kb left and 10kb right
(coordinates 132814 to 153695)

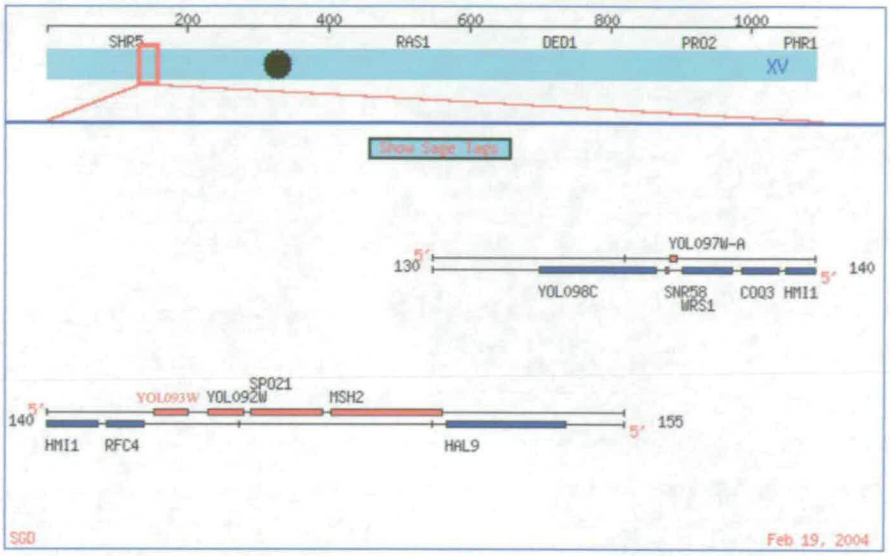

Keys:

- = Represents the chromosome you are viewing
- = Watson strand ORF
- = Crick strand ORF
- = tRNA gene
- = RNA gene
- = Transposon
- = Ribosomal RNA
- = Small Nuclear RNA
- = snoRNA gene
- = LTR of Transposon
- = ARS
- = Dubious ORF
- = X element Core sequence
- = X element Combinatorial Repeats
- = Telomeric Repeat
- = Y' element

Notes:

1. Click on light blue bar to retrieve features left & right
2. Click on any gene or ORF name, any little colorful bar, or centromere to retrieve the corresponding LOCUS entry in SGD
3. A white box in the middle of a blue or red bar indicates that there is an intron in the ORF. The size of the white box represents the length of the intron.
4. For a definition of the features listed in the key please see the glossary.

Figure 3.21 Chromosome Feature Map around *YOL093W*
(http://www.yeastgenome.org/)

3.3.2 Complementation Tests of *YOL093W* Deletion with the Wild-type *SPO21*

The Spo21p is a component of the meiotic outer plaque of the spindle pole body. It is involved in modifying the meiotic outer plaque that is required prior to prospore membrane formation.

The *CEN* plasmid pRS316/*SPO21* and the 2μ plasmid pRS426/*SPO21* plasmid were gifts from Aaron Neiman, SUNY Stony brook, NY, USA. The constructs were introduced into MYY3 strain (*yol093wΔkan/yol093wΔhph*). Transformants were selected on YMM-U medium, restreaked for colony purification. The resultant strains, MYY3/pRS316-*SPO21* and MYY3/pRS426-*SPO21*, were then used for tetrad dissection analysis (Figure 3.22).

Transformation of MYY3 with either the *CEN* plasmid pRS316/*SPO21* or the 2μ plasmid pYEplac1956/*SPO21* did not complement the low spore viability defect. This showed that the defect was not caused by the deletion of *SPO21*.

(A) MYY3 (*yol093wΔkan/yol093wΔhph*)

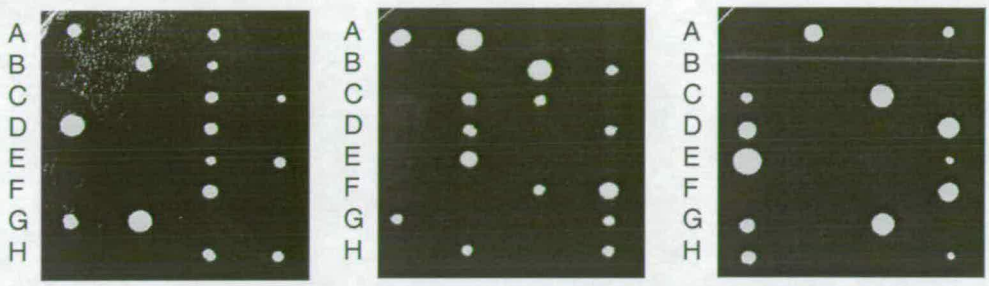

(B) MYY3 (*yol093wΔkan/yol093w*Δhph)/pRS316-*SPO21* (*CEN* plasmid)

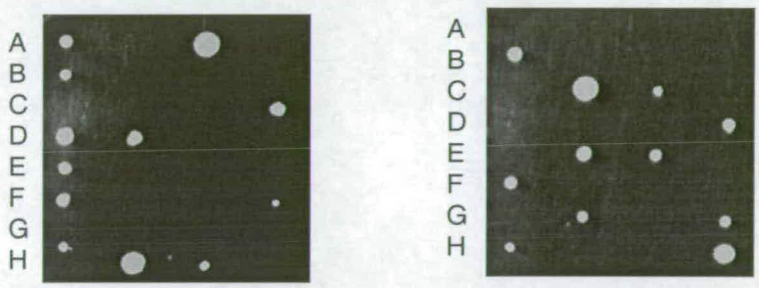

(C) MYY3 (*yol093wΔkan/yol093w*Δhph)/pRS426-*SPO21* (2μ plasmid)

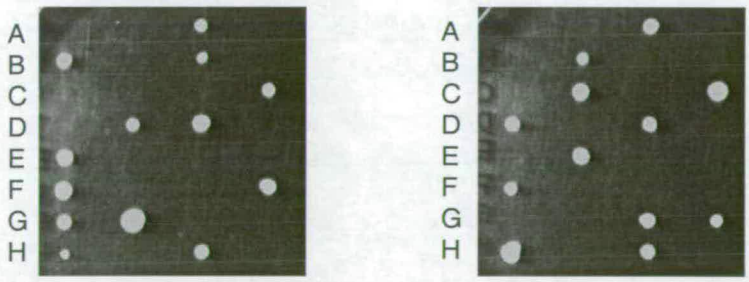

Figure 3.22 Complementation Test of the Low Spore Viability by the pRS316/*SPO21* or pRS426/*SPO21* Plasmid

The pRS316/*SPO21* or pRS426/*SPO21* plasmid was introduced into MYY3 strain (*yol093wΔkan/yol093wΔhph*). Transformants were selected on YMM-U medium, restresked for colony purification. Tetrad dissection analysis of strains (A) BMA38 (*YOL093W/YOL093W,* wt), (B) MYY3/pRS316-*SPO21* and (C) MYY3/pRS426-*SPO21* was performed. Strains were streaked out onto sporulation medium plates. After 5-7 days of incubation at 30°C, tetrads were dissected onto the YPDA agar plate. Spores were incubated for a few days at 30°C.

3.3.3 Complementation Tests of *YOL093W* Deletion with Wild-type *RFC4*

The Rfc4p is a DNA binding protein and ATPase that acts as a processivity factor for DNA polymerases delta and epsilon and loads proliferating cell nuclear antigen (PCNA) on DNA.

The pBL619 (*RFC4, URA3, CEN*) plasmid was a gift from Peter Burgers, Washington University, USA. The plasmid was then introduced into MYY3 strain (*yol093wΔkan/yol093wΔhph*). Transformants were selected on YMM-U medium, restreaked for colony purification. The resultant strain, MYY3/pBL619, was then used for tetrad dissection analysis (Figure 3.23).

Transformation of MYY3 with the *CEN* plasmid pBL619 (*RRC4, URA3, CEN*) did not complement the low spore viability defect. This showed that the defect was not caused by the deletion of *RFC4*.

(A) MYY3 (*yol093wΔkan/yol093wΔhph*)

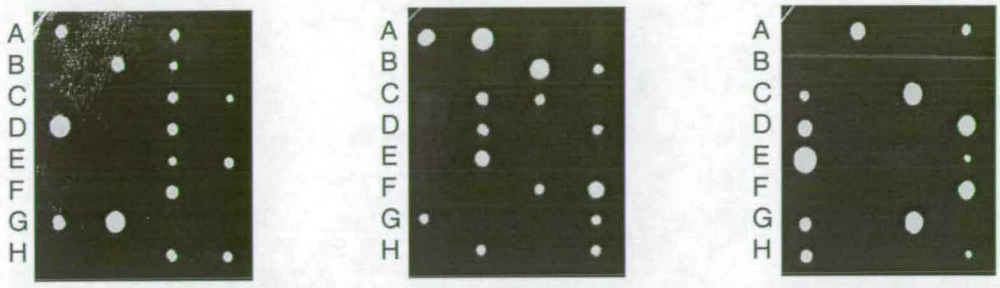

(B) MYY3 (*yol093wΔkan/yol093wΔhph*)/pBL619 (*RFC4, URA3, CEN* plasmid)

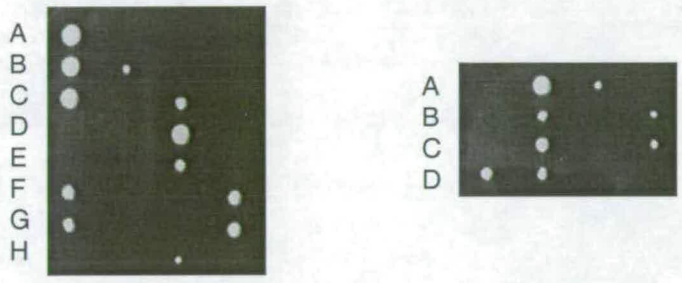

Figure 3.23 Complementation Test of the Low Spore Viability by the pBL619 (*RFC4*) Plasmid

The pBL619 (*RFC4, URA3, CEN*) plasmid was introduced into MYY3 strain (*yol093wΔkan/yol093wΔhph*). Transformants were selected on YMM-U medium, restresked for colony purification. Tetrad analysis of strains (A) BMA38 (*YOL093W/YOL093W*) (B) MYY3/pBL619 was performed. Strains were streaked out onto sporulation medium plates. After 5-7 days of incubation at 30°C, tetrads were dissected onto the YPDA agar plate. Spores were incubated for a few days at 30°C.

3.4 Back-cross Experiments

To check if there was a linked mutation existing in the genome, the back-cross experiments were performed by using the reference strain Y1643 (*YOL093W/yol093wΔkan*) form Euroscrf (Figure 3.24). The haploid MYY3/2 strain (*yol093wΔhph*) was mated with the Y1643 (*yol093wΔkan*), and the resulting diploid strains were streaked onto sporulation medium plates. After incubation at 30°C, the tetrads were dissected onto the YPDA agar plate. Spores were tested for drug resistance, and mating types of hygromycin B-resistant spores were then determined. Hph-resistant spores were then mated with MYY3/1 (*yol093wΔkan*) with the opposite mating types. The final resultant diploid strains were then sporulated and tetrads dissected.

The data from the back-cross experiments did not reveal the expected segregation patterns in the tetrads, which suggested that the low spore viability phenotype was not truly due to the *YOL093W* gene deletion. As when the diploid parent is heterozygous at a locus, a 2:2 segregation of genotypes in the tetrads is expected, the most consistent reasonable explanation for a 2:2 segregation of live to dead spores in the tetrad of *YOL093W* deletion MYY3 strain would be a haplo-lethal mutation either associated with the disruption or more likely a random mutation (not insertion of the marker) somewhere else in the genome.

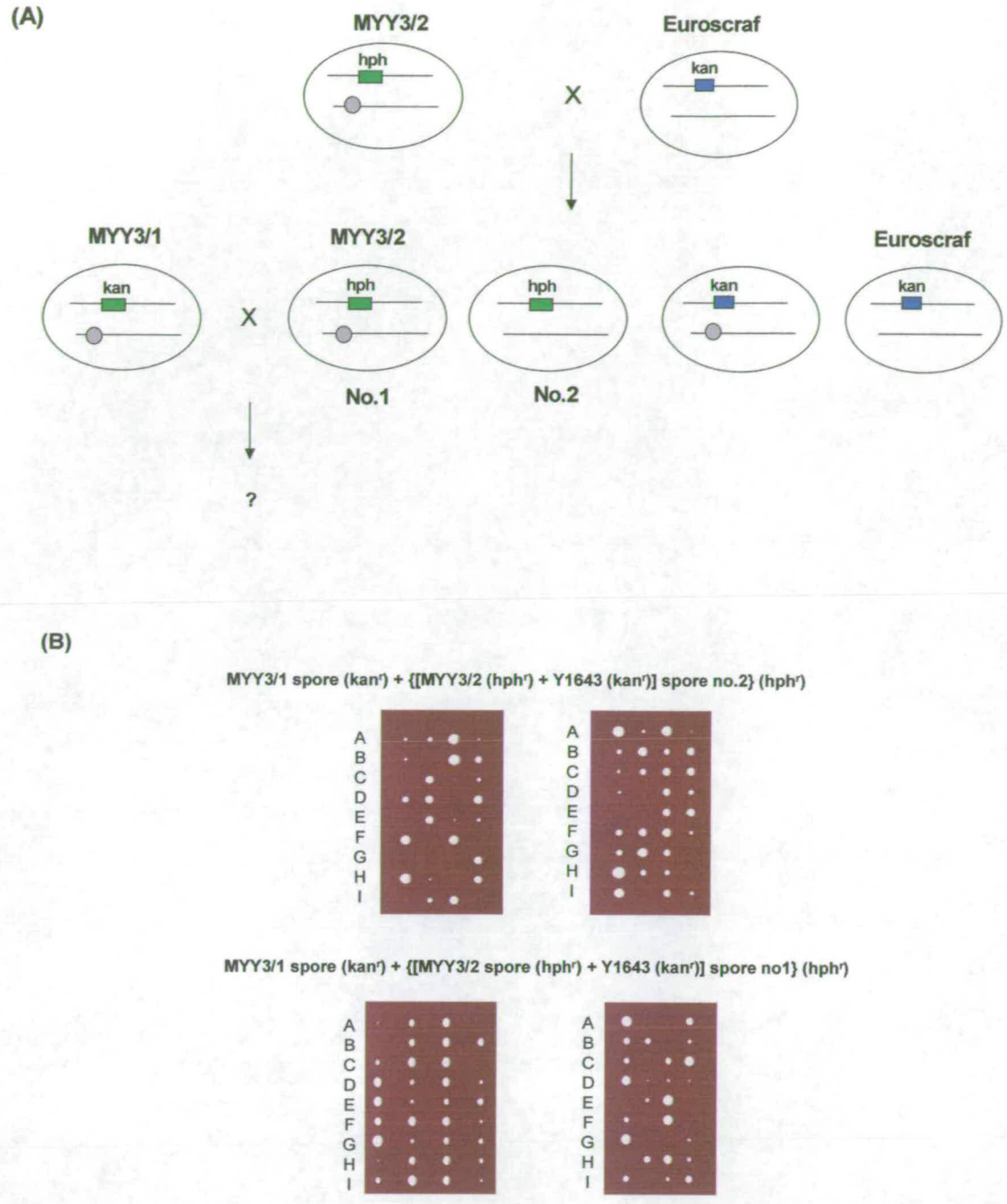

Figure 3.24 Back-cross Experiments of *YOL093W* Deletion Strains
(A) A schematic representation of the back-cross strategy by using the reference strain form Euroscrf (*yol093wΔkan*). The grey circle represents another mutant in the chromosome. (B) Tetrad dissection analysis of the final resultant strains. Diploid strains were streaked out onto sporulation medium plates. After 5 days of incubation at 30°C, tetrads were dissected onto the YPDA agar plate. Spores were incubated for a few days at 30°C.

3.5 Meiotic Assays

3.5.1 Introduction

As Holliday junction resolvases might be involved in meiotic processes, in order to investigate the effects of *YOL093W* deletion on meiosis, meiotic recombination assays were carried out. All assays were performed in derivatives of the Eurofan W303 strain. Two W303 derivative strains EUF153 RAD5$^+$ (MATa, *lys2* nde1-3', *ade1*::*ADE2*, *ade2*, canR, *ura3*-52) and EUF180 RAD5$^+$ (MATα, *lys2* nde1-5', *ADE1*, *ade2*, CANS, *URA3*) were used. Multiple assays can be performed in the EUF153 RAD5$^+$ /EUF180 RAD5$^+$ diploid. The frequency of mitotic and meiotic intragenic recombination can be determined with the *lys2* heteroalleles (Figure 3.25 A), the mitotic and meiotic reciprocal crossover frequencies can be determined with the linked canR *URA3* markers on chromosome V (Figure 3.25 B), and the meiosis I chromosomal non-disjunctions can be followed with the allelic *ADE1*/*ade1*::*ADE2* markers measured (Figure 3.25 C).

3.5.2 Deletion of *YOL093W* from the Genome of EUF153 RAD5$^+$ and EUF180 RAD5$^+$ Strains

3.5.2.1 Gene Deletion

The entire *YOL093W* coding sequence was removed precisely and replaced by the kanamycin (kan) resistance marker using a PCR-based method of direct gene deletion. Using the oligonucleotides YOL093W-KO-1 and YOL093W-KO-2, the kan-resistance marker was amplified by PCR from plasmid pFA6a-3HA-KanMX6. Haploid yeast strain EUF153 RAD5$^+$ or EUF180 RAD5$^+$ was transformed with the

purified linear PCR product containing the kan resistance marker flanked by approximately 45 base pairs of the *YOL093W* locus at either site, so that integration of the marker gene can occur by homologous recombination. Kan-resistant clones were streaked out onto fresh YPDA + kan medium for colony purification. Kan-resistant transformants were then tested for integration of the marker gene at the desired locus by PCR, as shown in Figure 3.26. The following heterozygous *YOL093W* deletion mutants were made: EUF153 RAD5$^+$/*yol093wΔkan* and EUF180 RAD5$^+$/*yol093wΔkan*.

3.5.2.2 Meiotic Assays of *YOL093W* Deletion Strains

The two strains that had been demonstrated positive for the gene replacement were then mated with each other, and YMM-A-U medium was used to select for diploid. The resultant diploid strain was sporulated. Spores were isolated (section 2.2.6.4) and meiotic assays (section 2.2.6.5) were performed. Spores were spread onto YMM-ADE-ARG+CAN, YMM-URA-ARG+CAN, and YMM-LYS-ARG+CAN plates. Canavanine (CAN) was used in all of the meiotic assays to select for haploid products and against unsporulated diploids. The increased number of papillae on YMM-LYS-ARG+CAN media is indicative of the induction of meiotic heteroallelic recombination. Meiosis I non-disjunction was measured by papillation on YMM-ADE-ARG+CAN. Only strains carrying both homologs of chromosome I are able to grow on YMM-ADE. As the parental diploid could grow on YMM-ADE, canavanine was used to ensure that one was only looking at the haploid products of meiosis.

Growth on YMM-URA+CAN was used to assess reciprocal recombination between *URA3-CAN1* and *ura3-1* and *can1-100*.

Results of the meiotic assays are shown in Figure 3.27. 30,000to 250,000 of spores were analysed per experiment. There was no difference between the wild-type strain and *YOL093W* deletion strains on these assays. Both of the strains showed similar frequencies on the meiotic heteroallelic recombination assay, the meiosis I non-disjunction assay, and the reciprocal recombination assay. Therefore, deletion of *YOL093W* does not affect the meiotic recombination process.

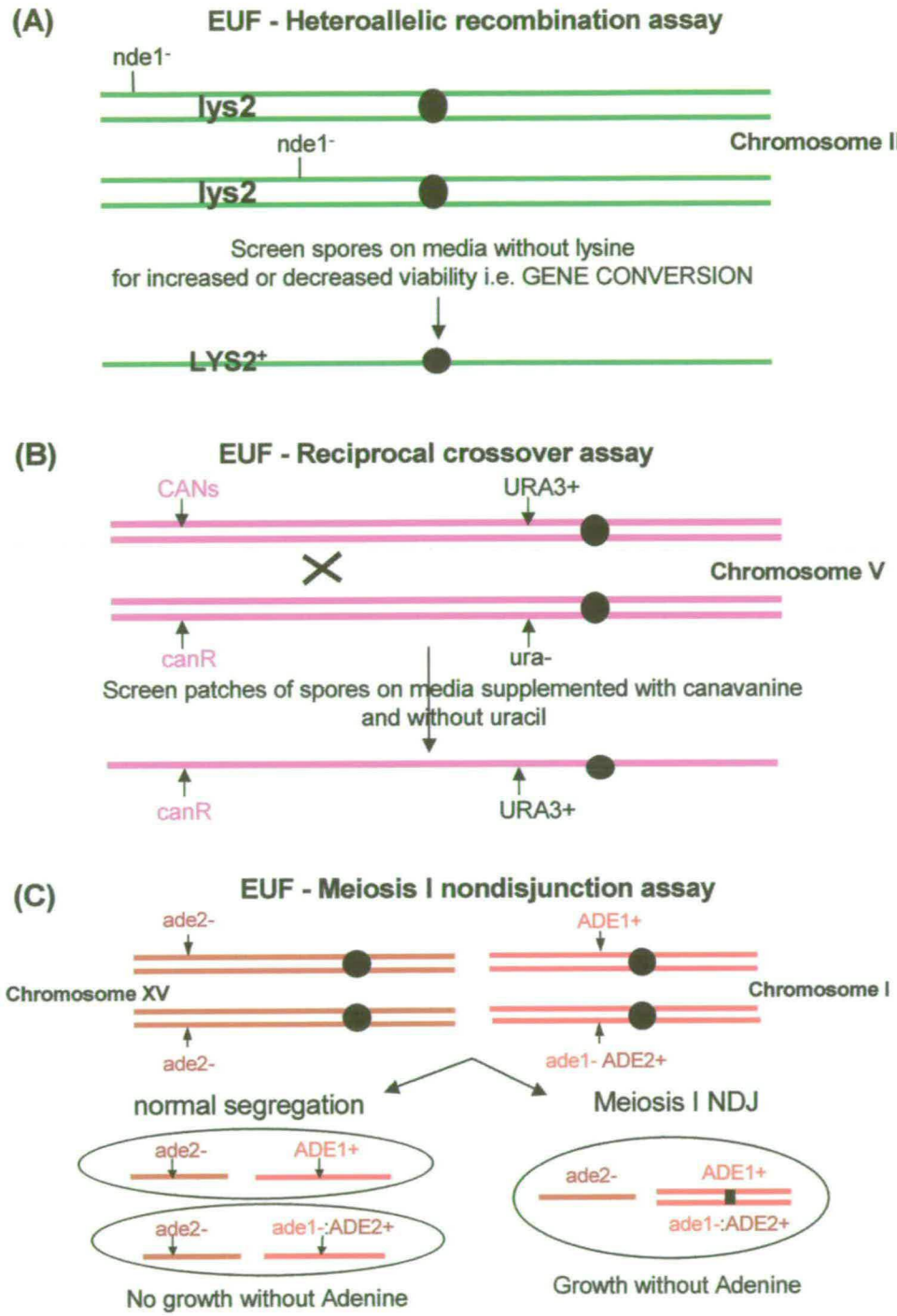

Figure 3.25 EUROFAN W303 Meiotic Assays
(A) Heteroallelic recombination (gene conversion) assay. Note: LYS2 = lysine biothesis. (B) Reciprocal crossover assay. Note: CAN = canavinine resistance (R) /sensitivity (S); URA3 = pyrimidine biosynthesis. (C) Meiosis I nondisjunction assay. Note: ADE1 and ADE2 = purine base metabolic genes.

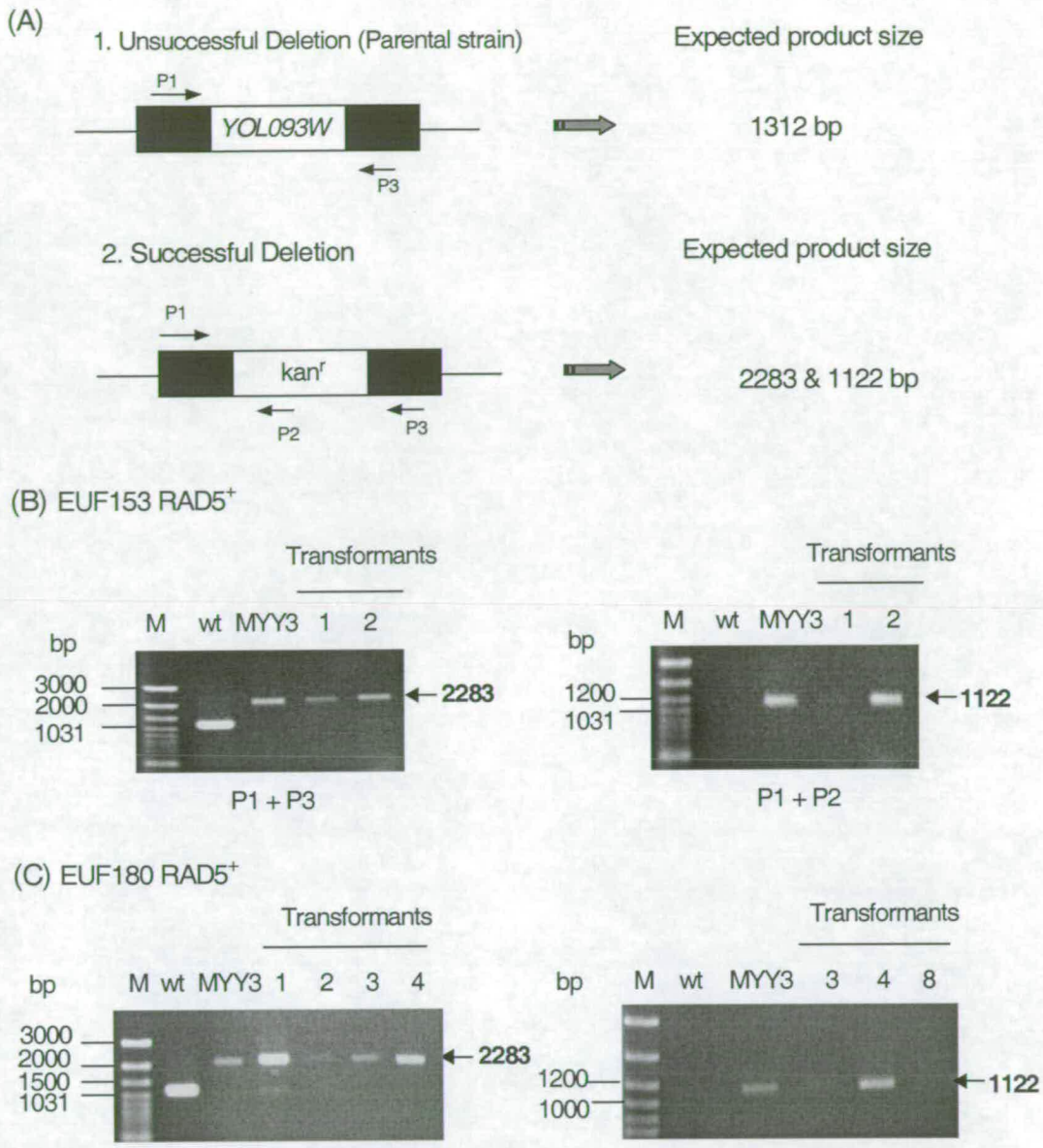

Figure 3.26 Detection of *YOL093W* Deletion from the EUF153 RAD5$^+$ and EUF180 RAD5$^+$ Genome

PCR analysis of the yeast transformants to confirm the integration of the kanamycin (kan) marker into the chromosome. After transformation with a linear PCR product containing the Kan marker flanked by approximately 45 base pairs of the *YOL093W* locus at either site, kan-resistant clones were streaked out onto fresh YPDA + kan for colony purification. Yeast colony PCR was performed using P1: SC093-TEST-1, P2: R-kan and P3: SC093-TEST-2 primers. (A) The positions on the template at which the primers anneal are indicated in the upper schematic drawing of the *YOL093W* locus (either the parental type or after kan-integration). (B & C) The products of the PCR reactions. The fragment, which would be expected following successful integration of kan cassette into the *YOL093W* locus is indicated. The 3' junction of the gene replacement was also confirmed by PCR with an internal forward primer of the drug-resistant cassette and a reverse primer outside the *YOL093W* locus (data not shown).

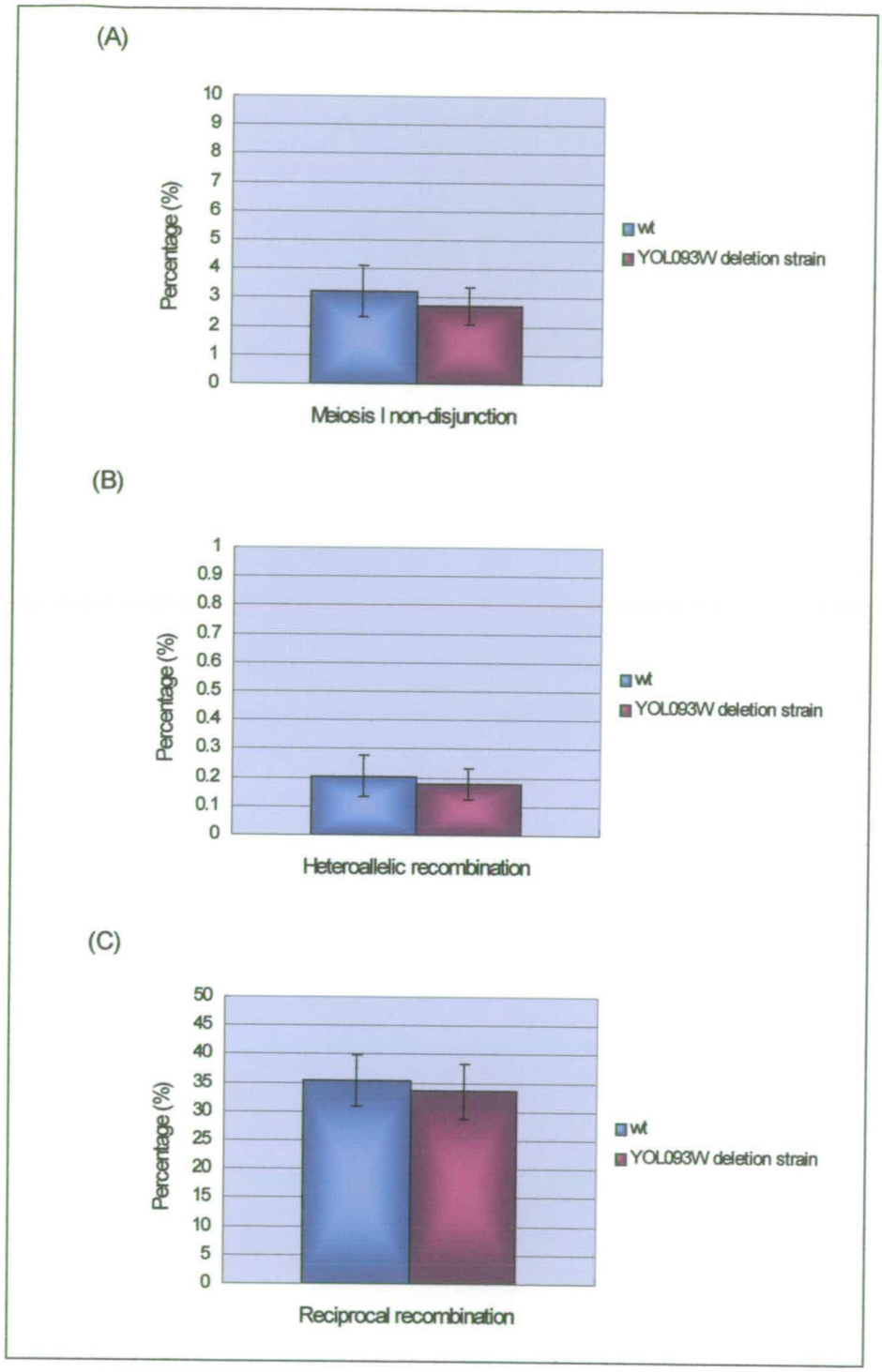

Figure 3.27 Meiotic Assays of *YOL093W* Deletion Strain
Spores were collected and spread onto (A) YMM -ADE -ARG+CAN plates (meiosis I non-disjunction), (B) YMM-LYS-ARG+CAN plates (heteroallelic recombination), and (C) YMM-URA-ARG+CAN plates (reciprocal recombination). Spores were incubated at 30°C for 2-4 days and the colony number was counted. 30,000 to 250,000 of spores were analysed per experiment.

3.6 Gene Replacement of *YOL093W* in W303 Background Strains

In order to check if the low spore viability defect observed in section 3.2.2.2 was caused by deletion of *YOL093W*, gene replacement was also performed in two other yeast strains, MAS386 and BY4743, with a W303 background.

3.6.1 MAS386 Strain

3.6.1.1 *YOL093W* Deletion

The entire *YOL093W* coding sequence was removed precisely and replaced by the kanamycin (kan) marker using a PCR-based method of direct gene deletion. Using the oligonucleotides YOL093W-KO-1 and YOL093W-KO-2, the kan marker was amplified by PCR from plasmid pFA6a-3HA-KanMX6. Diploid yeast strain MAS386(2n) was transformed with the purified linear PCR product containing the kan resistance marker flanked by approximately 45 base pairs of the *YOL093W* locus at either site, so that integration of the marker gene can occur by homologous recombination. Kan-resistant clones were streaked out onto fresh YPDA + kan medium for colony purification. Kan-resistant transformants were then tested for integration of the marker gene at the desired locus by PCR, as shown in Figure 3.28. The following heterozygous *YOL093W* deletion mutant was made: MAS386/*yol093wΔkan* (*YOL093W/yol093wΔkan*). The heterozygous mutant was then used as the parental strain for the second knockout of another copy of the *YOL093W* allele. The gene was replaced by hygromycin B (hph) resistance marker amplified from pAG32 plasmid using primers YOL093W-KO-1 and YOL093W-

KO-2. The homozygous *YOL093W* deletion mutant, MAS386/*yol093wΔkan-yol093wΔhph* (*yol093wΔkan/yol093wΔhph*), was made.

3.6.1.2 Tetrad Dissection of *YOL093W* Deletion Strains

Diploid transformant that showed positive for the gene replacement was sporulated. Tetrads were dissected and separated spores were incubated at 30°C for 3-4 days (Figure 3.29). By comparing with wild-type strain, tetrad dissection assay of *YOL093W*-deleted MAS386 strain showed two large and two small spores phenotype; similar to that was observed in the MMY2 strain (*YOL093W/yol093wΔhph*). As *YOL093W*-deleted MAS386 strain did not show lower spore viability, this suggested that the lower spore viability of MYY3 was not caused solely by the *YOL093W* deletion.

3.6.1.3 Drug-resistant Tests of *YOL093W* Deletion Strains

Spores of tetrad dissection from *YOL093W*-deleted MAS386 strain were replicated onto YPDA, YPAD + kan, YPDA + hph, and YPDA + kan + hph plates (Figure 3.30). In the cases that all four spores germinated, only two spores grew on the selective plates as expected. No spore from the MAS386/*yol093wΔkan-yol093wΔhph* strain grew on the YPDA + kan + hph plates.

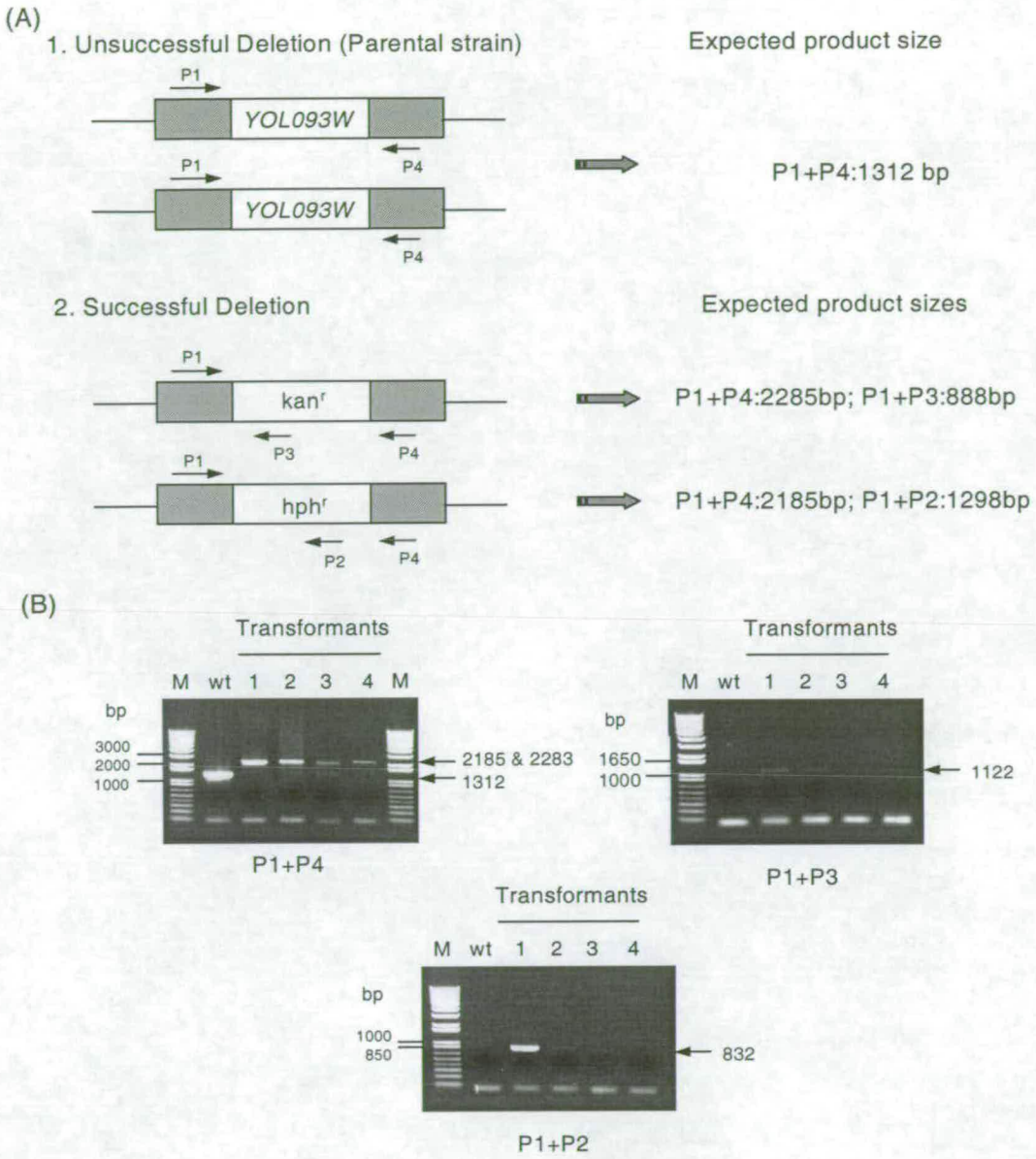

Figure 3.28 Detection of *YOL093W* ORF Deletion from the MAS386 Genome

PCR analysis of the yeast transformants to confirm the integration of the kan and the hph markers into the chromosome. After transformation with a linear PCR product containing the Kan and hph markers flanked by approximately 45 base pairs of the *YOL093W* locus at either site, clones were streaked out onto fresh YPDA + kan + hph medium for colony purification. Yeast colony PCR was performed using P1: SC093-TEST-1, P2: R-kan and P3: R-hph, P4: SC093-TEST-2 primers. (A) The positions on the template at which the primers anneal are indicated in the upper schematic drawing of the *YOL093W* locus (either the parental type or after kan- or hph-integration). (B) The products of the PCR reactions. The fragment, which would be expected following successful integration of kan or hph cassette into the *YOL093W* locus is indicated. The 3' junction of the gene replacement was also confirmed by PCR with an internal forward primer of the drug-resistant cassette and a reverse primer outside the *YOL093W* locus (data not shown).

(A) MAS386 (2n, wt)

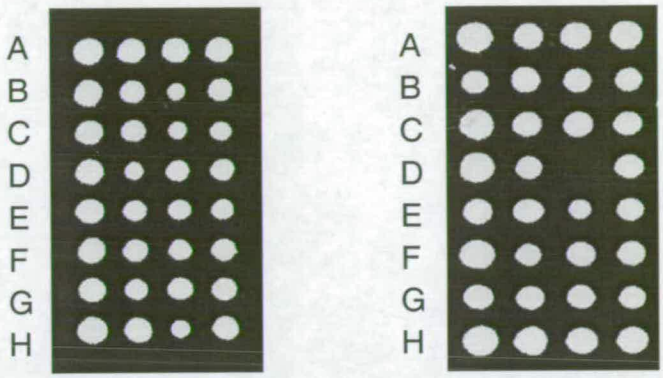

(B) MAS386/*yol093wΔkan-yol093wΔhph* (*yol093wΔkan/yol093wΔhph*)

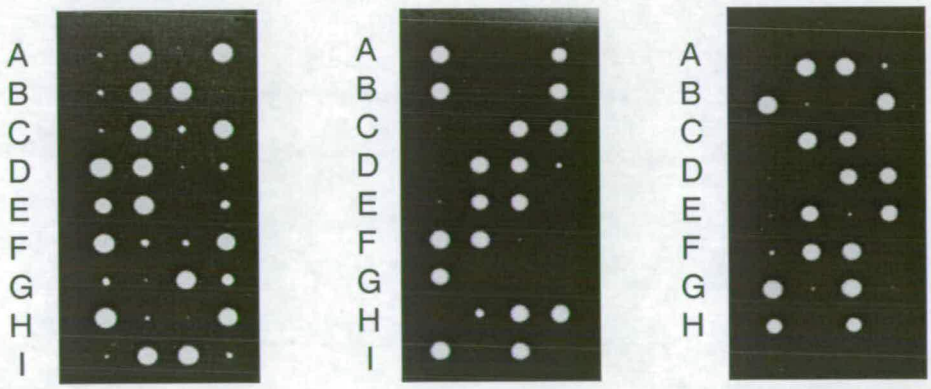

Figure 3.29 Analysis of the Effects of *YOL093W* Deletion in MAS386/*yol093wΔkan-yol093wΔhph* (*yol093wΔkan/yol093wΔhph*)
Tetrad dissection analysis of the *YOL093W* deletion strain as well as cells from the parental wild-type strain MAS386(2n) were streaked onto sporulation plates. After 5 days of incubation at 30˚C, tetrads were dissected onto the YPDA agar plate. Spores were incubated at 30˚C for a few days. (A) wt, MAS386(2n); (B) MAS386/*yol093wΔkan-yol093wΔhph* (*yol093wΔkan/yol093wΔhph*).

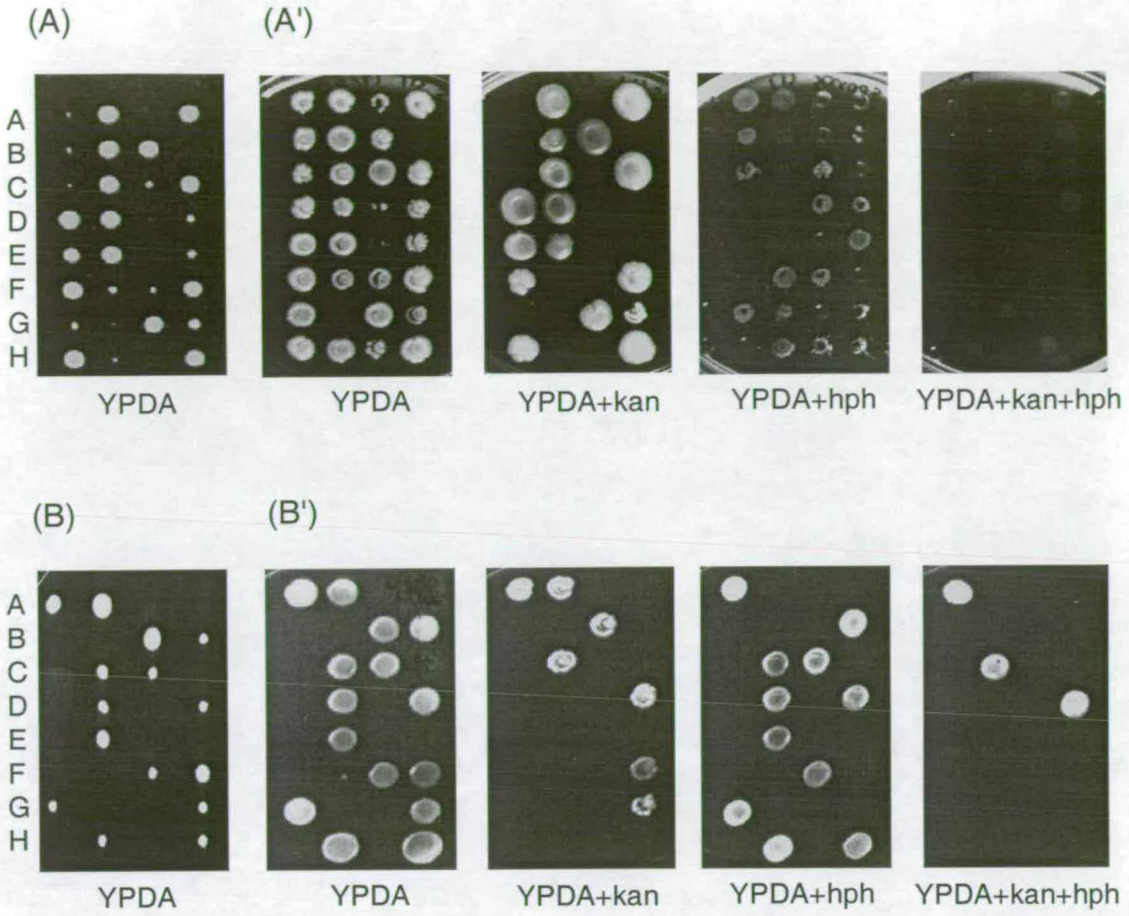

Figure 3.30 Drug Resistance Analysis of *YOL093W* Deletion Spores of MAS386 Strain

Haploid cells MAS386/*yol093wΔkan-yol093wΔhph* were suspended in dilutions in microtiter plates, spotted onto (A) YPDA; (A') YPDA + kan, YPDA + hph, and YPDA + kan + hph plates, and incubated at 30˚C for a few days. (B&B') Results from MYY3 strain (*yol093wΔkan/yol093wΔhph)* as seen in Figure 3.15.

3.6.2 BY4347 Strain

3.6.2.1 *YOL093W* Deletion

YOL093W deletion mutant of parent strain BY4743 was obtained from the EUROFAN strain library. Both homologues of the *YOL093W* coding sequences were replaced with a KanMX4 gene using PCR-mediated gene disruption.

3.6.2.2 Tetrad Dissection of *YOL093W* Deletion Strains

Diploid strain was sporulated. Tetrads were dissected onto YPDA agar plates and the separated spores were incubated at 30°C for 3-4 days (Figure 3.31). By comparing with the wild-type strain, tetrad dissection assay of *YOL093W* deletion BY4743 strain did not show lower spore viability. This also suggested that the lower spore viability observed in the *YOL093W* deletion BMA38(2n) strain was not caused solely by *YOL093W* deletion.

(A) BY4743 (2n, wt)

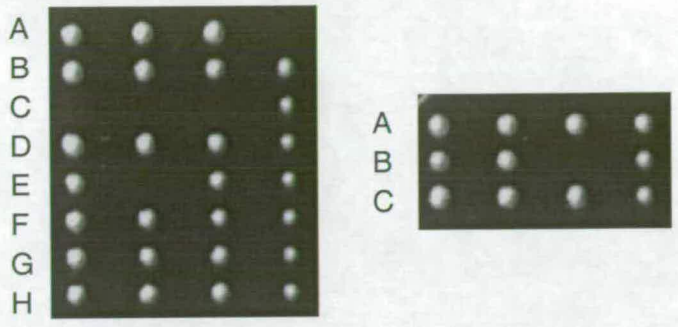

(B) BY4743 Δ *yol093w* (*yol093w*Δkan/ *yol093w*Δkan)

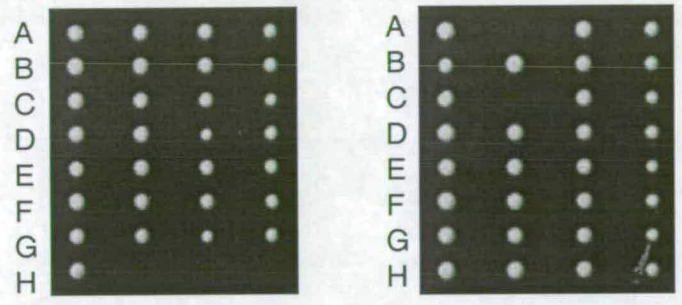

Figure 3.31 Analysis of the Effects of *YOL093W* Deletion in BY4743/*yol093wΔkan-yol093wΔhph* (*yol093wΔkan/yol093wΔhph*)

Tetrad dissection analysis of *YOL093W* deletion strain as well as cells from parental wild-type strain BY4743(2n) were streaked onto sporulation plates. After 5 days of incubation at 30˚C, tetrads were dissected onto the YPDA agar plate. Spores were incubated at 30˚C for a few days. (A) wt, BY4743(2n); (B) BY4743/*yol093wΔkan-yol093wΔhph*.

3.7 Discussion

The deletion of *YOL093W* ORF in BMA38 strain demonstrated that *YOL093W* was not essential for cell viability. Despite *YOL093W* deletion in MYY3 (*yol093wΔkan/yol093wΔhph*) showed lower spore viability and potential non-disjunction phenotypes, transformation of MYY3 with either the *CEN* plasmid pRS316/*YOL093W* or 2μ plasmid pYEplac1956/*YOL093W* did not complement the defect. This suggested that the defect might be not caused by *YOL093W* deletion, but by the interference of another gene in the genome.

Furthermore, the gene replacement of *YOL093W* was also performed in MAS386 and BY4347 strains. By comparing with the wild-type strain, tetrad dissection assays of *YOL093W* deletion strains did not show lower spore viability or non-disjunction phenotypes. This also suggested that the lower spore viability seen in the *YOL093W*-deleted BMA38(2n) strain was not caused by the *YOL093W* deletion. Similar observations were also suggested in the back-cross experiment and the *YOL093W* gene replacement in the other two *S. cerevisiae* strains. This circumstance might be avoided by assessing the phenotype more at the very early stage of experiments. One should check more gene-knockout transformants in order to confirm the phenotype is reproducible and is really due to the gene deletion itself. As any meiotic I segregation defect will give a mixture of tetrads with 4, 2 and 0 viable spores as the major classes, and when the diploid parent is heterozygous at a locus, a 2:2 segregation of genotypes in the tetrads is expected. The most consistent reasonable

explanation for a 2:2 segregation of live to dead spores in the tetrad of *YOL093W* deletion MYY3 would be a haplo-lethal mutation either associated with the disruption or more likely a random mutation (not insertion of the marker) somewhere else in the genome.

CHAPTER FOUR

Tandem Affinity Purification of Yol093wp

4.1 Introduction of Tandem Affinity Purification (TAP) Tag

As part of the general approaches, a Tandem Affinity Purification (TAP) tag was used to study the function of Yolo93wp. The TAP method is a generic procedure to purify proteins expressed at their natural level under native conditions using a novel TAP tag (Rigaut et al., 1999). The TAP tag contains two IgG-binding units of *Staphylococcus aureus* protein A and a Calmodulin-binding peptide (CBP) separated by a cleavage site for tobacco etch virus (TEV) protease. The TAP purification method involves the fusion of the TAP tag to the target protein of interest, either at C- or N-terminus, and the introduction of the construct into the cognate host cell or

organism. TAP-tagged proteins to be expressed in yeast can be constructed using standard cloning strategies and introduced in yeast plasmids or by recombination with an endogenous chromosome. However, the best and fastest way to generate a TAP-tagged protein in yeast is to use PCR-based genomic tagging (Figure 4.1). In brief, a PCR fragment containing a selectable marker and the TAP tag is integrated in the genome such as to fuse the TAP tag and the protein of interest. C-terminal tagging is often preferred because it should maintain expression of the target protein at its natural basal level. However, N-terminal tagging is also possible. By design, it is also possible to truncate the target protein at its N- or C- terminus.

To purify protein complexes it is preferable to maintain expression of the fusion protein at, or close to, its natural level. The fusion protein present in extracts prepared from these cells, as well as associated components, are then recovered by tandem affinity purification (TAP) (Figure 4.2).

The TAP procedure has similar applications to the yeast two-hybrid method (Chapter 5). However, an advantage of the TAP procedure is that, under given conditions, all directly or indirectly interacting components are identified in a single experiment. In addition, the TAP system provides an indication of the approximate stoichiometry of the proteins present in a given complex and allows for direct biochemical analysis of the purified protein(s). In particular, the activity of mutant complexes can easily be analysed. Combined with the highly sensitive mass-spectrometry methods available, the TAP method is useful for identification of proteins interacting with a given target protein (Rigaut et al., 1999).

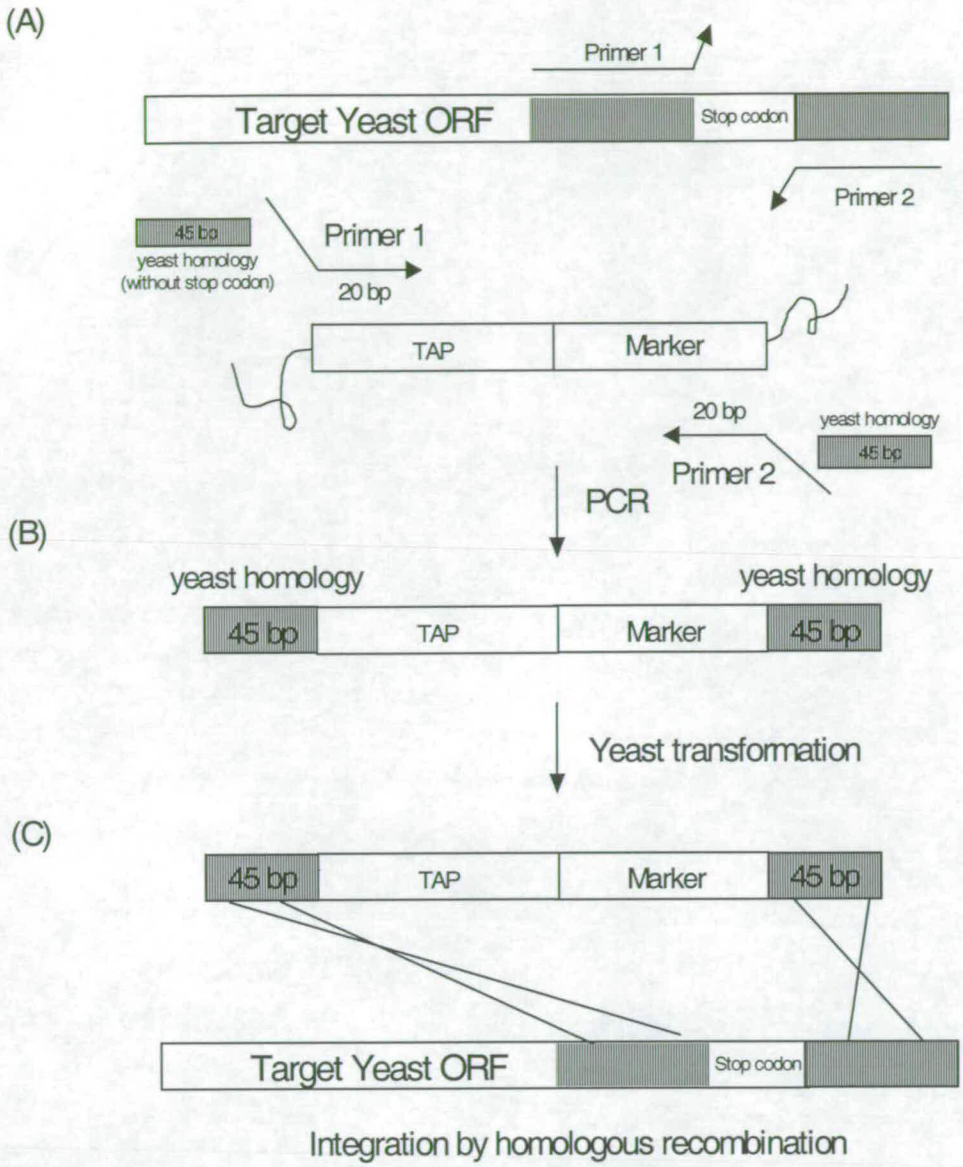

Figure 4.1 Schematic Representation of the PCR-based TAP Genomic Tagging

(A) Two oligonucleotides complementary to the TAP tag-marker cassette at their 3' end and containing the appropriate region of homology with the yeast genome to allow in frame fusion of the TAP tag downstream of the gene of interest are designed. (B) PCR DNA fragments were generated and introduced into yeast cells. (C) Integration of the fragments by homologous recombination in the yeast genome fuses the TAP tag downstream of the gene of interest.

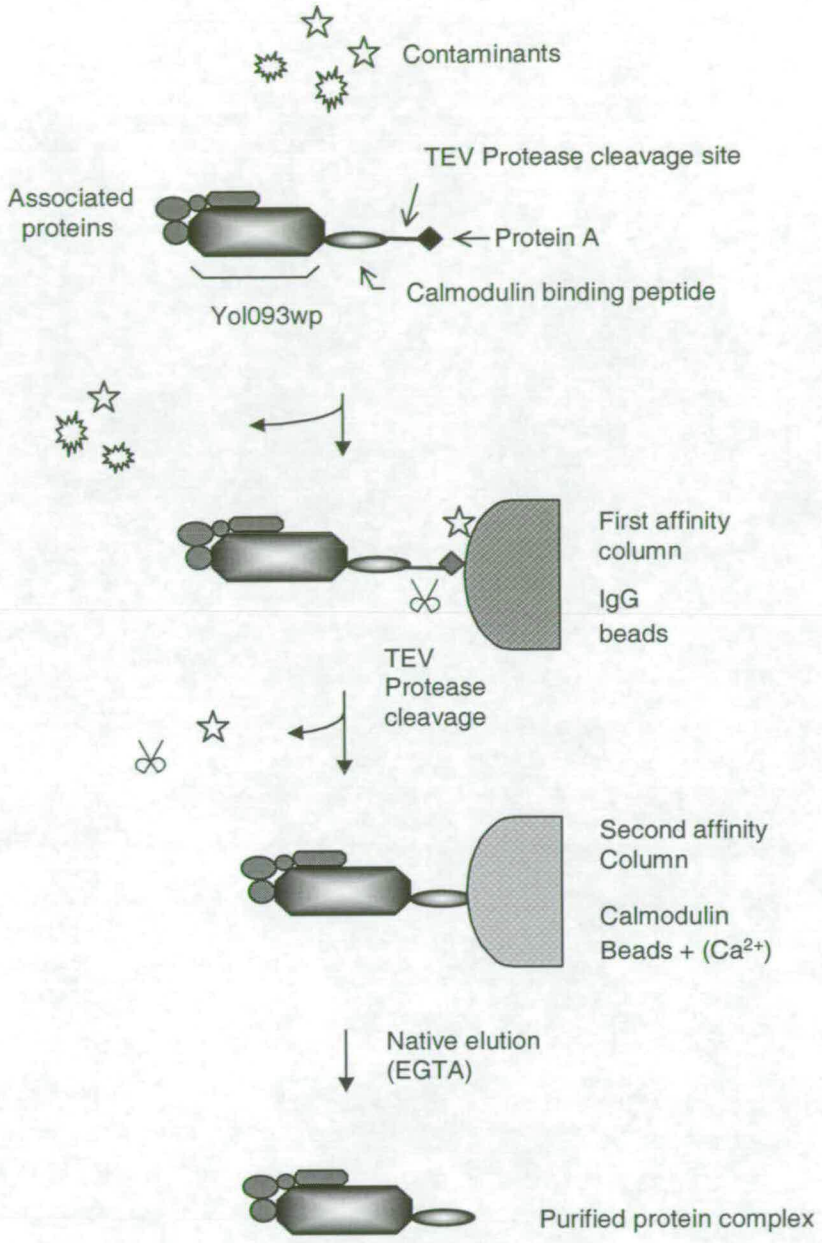

Figure 4.2 Overview of the TAP Protein Purification Procedure (Adapted from Rigaut *et al*, 1999)

The fusion protein and associated components were recovered from cell extracts by affinity selection on an IgG matrix. After washing, the TEV protease was added to release the bound matrix. The eluate was incubated with calmodulin-coated beads in the presence of calcium. This second affinity step was required to remove the TEV protease as well as traces of contaminants remaining after the first affinity selection. After washing, the bound material was released with EGTA. Stars represent contaminant proteins; Scissors represent TEV protease; First affinity column = IgG beads column; Second affinity column = calmodulin beads column.

4.2 TAP Purification of Y0l093wp-TAP in *S. cerevisiae*

4.2.1 Generation of a TAP-tagged Y0l093wp in *S. cerevisiae*

In order to isolate Yol093wp and its associated proteins from yeast cultures that can be used for protein sequencing, a TAP-tagged version of Yol093w was generated. For this purpose the coding sequence of the TAP tag was inserted immediately downstream of the final codon of the *YOL093W* gene. The high efficiency of homologous recombination in yeast bypasses the need to construct a plasmid to fuse the TAP-tag to the protein of interest. A strategy was used to generate DNA fragments to introduce the C-terminal TAP tag into the yeast genome. The pBS1539 plasmid contains the URA3 marker from *Kluyveromyces lactis* adjacent to the TAP cassette as the selectable marker. Two oligonucleotides complementary to the TAP tag-marker cassette at their 3' end and containing the appropriate region of homology with the yeast genome allow in frame fusion of the TAP tag downstream of the gene of interest (Figure 4.1). Integration of the PCR DNA fragment by homologous recombination in the yeast genome fuses the TAP tag downstream of the gene of interest. Transformants are selected using heterologous markers to avoid recombination at the endogenous marker locus.

The haploid BMA38(a) strain was transformed with a linear PCR product containing the TAP tag, which should be inserted immediately downstream of the final codon of the *YOL093W* gene. Uracil prototrophs were then streaked out onto fresh YMM – uracil medium for colony purification. The resultant haploid yeast strain

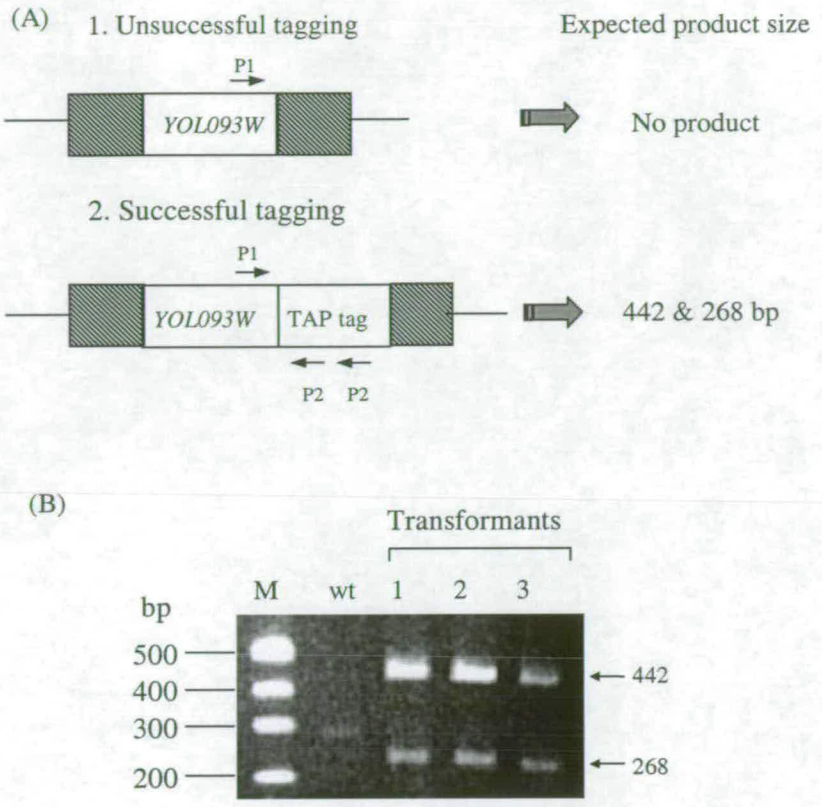

Figure 4.3 PCR on Yeast Transformants to Test for Integration of the TAP Tag into the Chromosome

After transformation of BMA38 (a) strain with a linear PCR product containing the TAP tag, which should be inserted immediately downstream of the final codon of the *YOL093W* gene, uracil prototrophs were streaked out onto fresh YMM – U medium for colony purification. Then cells of the transformants and of the wt parental BMA38(a) were suspended in water, boiled for 10 minutes and used in a PCR using oligonuceotide primers P1: yol093w-TAP-test 1 and P2: R-protein A. The positions on the template at which the primers anneal are indicated in the upper schematic drawing of the *YOL093W* locus (either wild type or after TAP-tagged). The products of PCR reactions are shown in (B). The fragments expected following successful integration of TAP tag cassette into the chromosome are indicated. P2 primer is the reverse sequence of IgG-binding units of protein A, therefore, there are two PCR products.

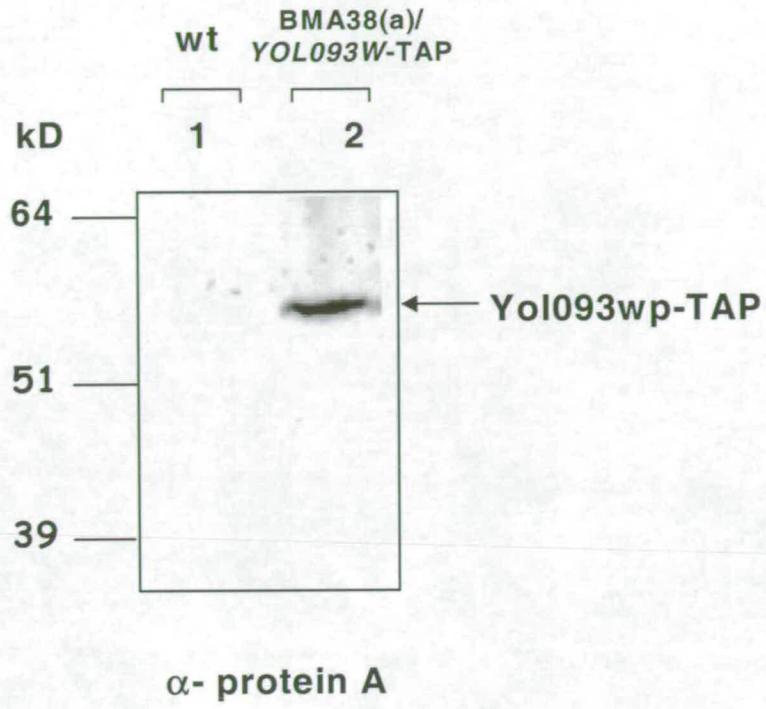

	M.W. (kDa)
Yol093wp	34.5
TAP tag	20
Yol093wp-TAP	54.5

Figure 4.4 Western Blot Analysis of TAP-tagged Yol093wp from BMA38(a)/*YOL093W*-TAP Stain

Crude cell extract was prepared from BMA38(a) (wild type, lane 1) or from MYY4 (lane 2). Proteins were fractionated on a 4-12% SDS-polyacrylamide gel, electroblotted and probed with antibodies against protein A. Immunodetection was with HRP-conjugated anti-rabbit antibodies (Sigma). And proteins were visualized by ECL (Amersham). The position of the TAP-tagged Yol093w (Yol093wp-TAP) is indicated.

4.2.2 Extract Preparation and TAP Purification of a TAP-tagged Yol093wp

Preparation of the extract is a critical step in the purification process, since this step influences the total quantity of the desired protein recovered and the biological activity of the protein. A number of variables determine the success of a protein extraction procedure: the cell lysis method, the presence of protease inhibitors, the choice of buffers, etc (Puig et al., 2001). In this work, a standard procedure (Puig et al., 2001) that has been extensively used in Seraphin's lab (Centre de Génétique Moléculaire, France) was chosen. The fusion protein and associated components were recovered from extracts by affinity selection on an IgG-matrix. After washing, the TEV protease was added to release the bound material. The eluate was then incubated with calmodulin-coated beads in the presence of calcium. This second affinity step is required to remove the TEV protease as well as traces of contaminants remaining after the first affinity selection. After washing, the bound material was released with EGTA (Figure 4.2). Because proteins are purified under native conditions with the TAP method, the purified material can also be used for biochemical analysis and functional assays.

To identify proteins interacting with the Yol093wp, it was desireable to concentrate eluted fractions before loading them on an analytical gel. To achieve this goal, TCA preciptation (Ozols, 1990) was performed. Proteins in the fractions were separated by gradient SDS-PAGE (section 2.3.3.3). Proteins were then stained using PlusOne Silver Staining Kit (Pharmacia Biotech) (Figures 4.5) or GelCode Blue Stain

Reagent (Pierce, Rockford, IL, USA) (Figures 4.6) according to the manufacturer's instructions. GelCode Blue Stain Reagent utilizes the colloidal properties of Coomassie for protein staining on polyacrylamide gels. A typical sensitivity of the GelCode Blue stain is 30-1000 ng protein/band depending on the protein sizes. Silver staining is the most sensitive method for permanent visible staining of proteins in polyacrylamide gels. This visualization technique detects most proteins in the nanogram range, which is 100-fold more sensitive than Coomassie Blue staining. Typical sensitivity of silver staining is 0.2-0.6 ng protein/band. After GelCode Blue or silver staining, bands were excized and analyzed by MALDI-TOF mass spectrometer (done by Edinburgh Protein Interaction Centre Proteomics Facility, University of Edinburgh).

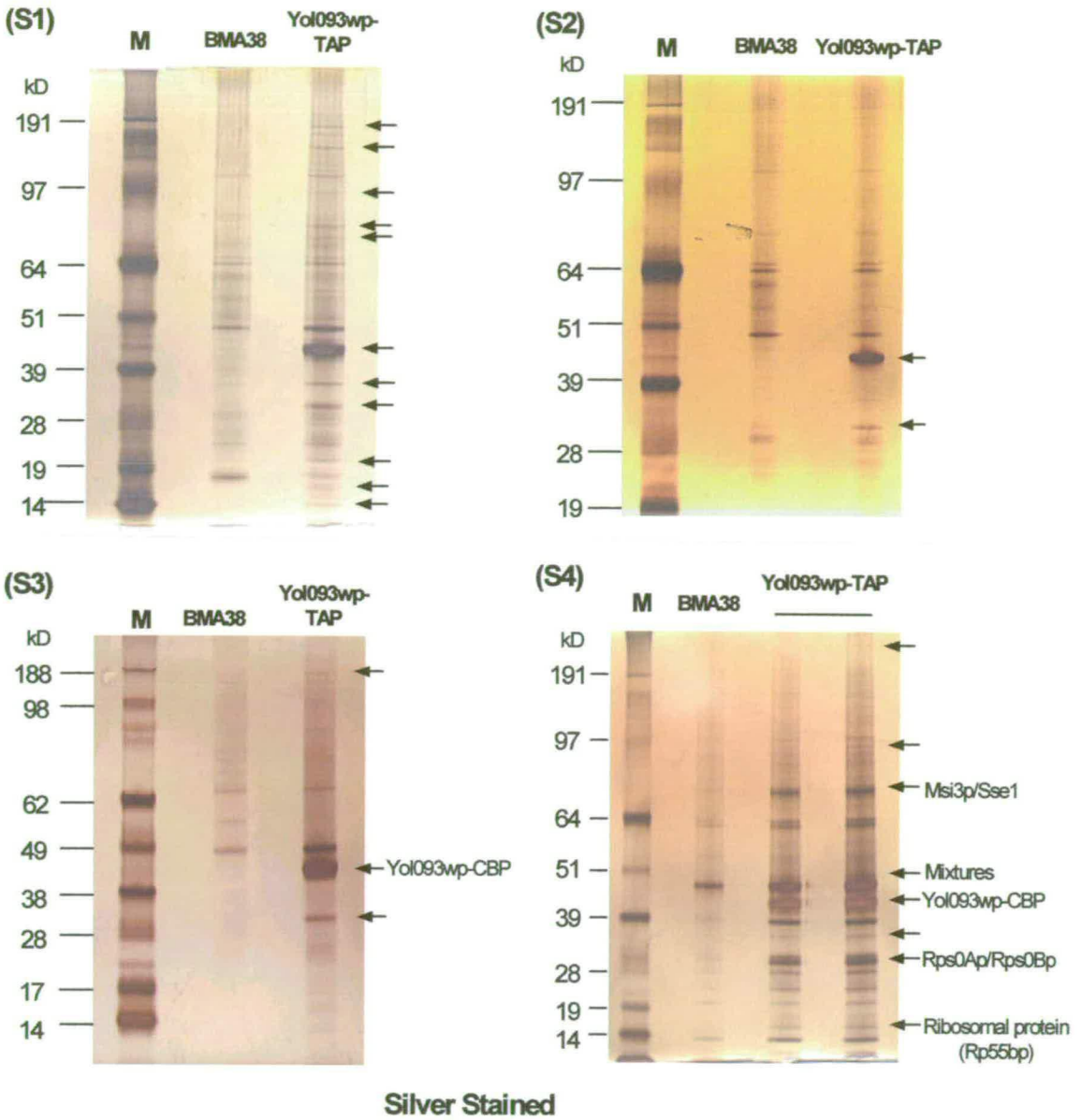

Figure 4.5 Purification of Proteins Associated with Yol093wp by Using a C-terminal TAP Tag (Silver Stained)

Silver-stained gels presenting proteins recovered from purification of the C-terminal TAP-tagged Yol093wp is depicted. The purification was done from 8-16 litres of yeast culture. Lane M represents molecular weight markers. The arrows indicate the samples, which were sent to be assayed by mass spectrometry. The components successfully identified by mass spectrometry are shown on the right.

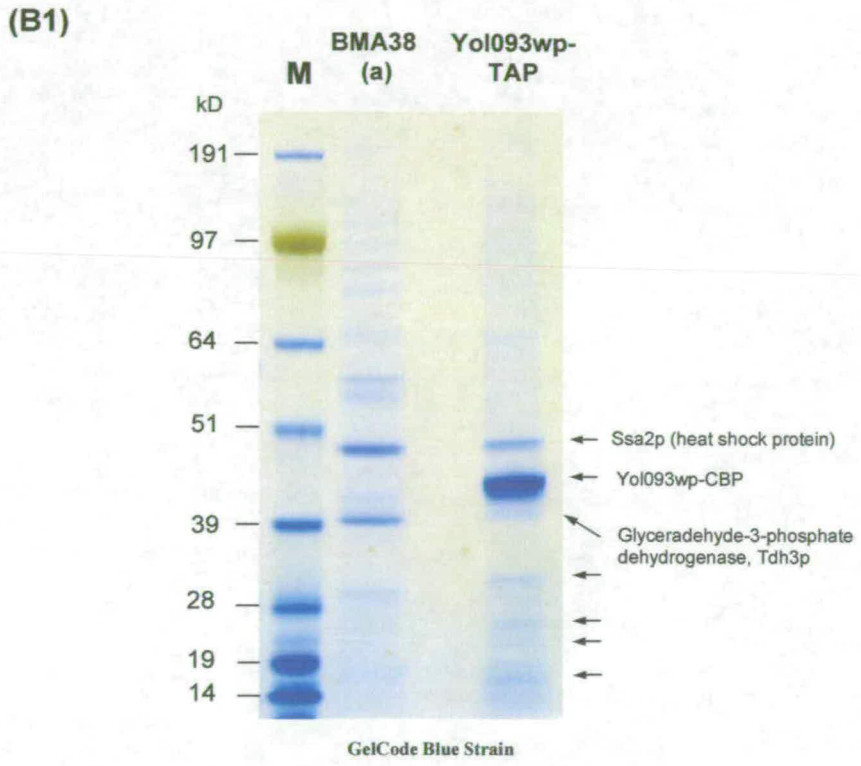

Figure 4.6 Purification of Proteins Associated with Yol093wp by Using a C-terminal TAP Tag (GelCode Blue Stained)

A GelCode Blue-stained gel presenting proteins recovered from purification of the C-terminal TAP-tagged Yol093wp is depicted. The purification was done from 8 litres of yeast culture. Lane M represents molecular weight markers. The arrows indicate the samples, which were sent to be assayed by mass spectrometry. The components successfully identified by mass spectrometry are shown on the right. Additional bands present in the purified fraction may represent contaminants, protein degradation or new subunits of the yeast Yol093wp complex.

4.2.3 Identification of Proteins Functionally Interacting with Yol093wp

Several components of the Yol093wp-TAP complex have been analysed by mass spectrometry. As shown in Figure 4.5, for gel S3, Yol093wp-CBP was identified; for gel S4, Yol093wp-CBP, Sse1p (heat shock protein), and ribosomal proteins, Pr55p and Rps0p were identified; none of the bands from gel S1 and S2 was identified. For gel B1 (Figure 4.6), Yol093wp-CBP, Ssa2p (heat shock protein), and a glyceraldehyde-3-phosphate dehydrogenase (Tdh3p) were identified. In summary, mass spectrometry analysis verified the identity of the purified complex by confirming that 6 of the purified proteins correspond to two heat shock proteins, two ribosomal proteins, Tdh3p, and Yol093wp-CBP itsself (shown in Figure 4.7). In addition, the mass spectrometry data suggested that some bands at the low molecular weight region might be fragments of HSP70.

Sse1p and Ssa2p are members of the 70kDa heat shock protein (HSP70) family. Heat shock proteins are a group of specific proteins that are synthesized by both prokaryotic and eukaryotic cells after they have been exposed to a temperature that is higher than normal. Other stresses, eg. free radical damage, have a similar effect. Many members of the HSP family are not induced but are present in all cells (Mukai et al., 1993).

Rps0Ap and Rps0Bp (also known as: *NAB1A/B*, Nuclear Acid Binding protein) are protein components of the small (40S) ribosomal subunit. They are nearly identical to each other (Demianova et al., 1996) and required for maturation of 18S rRNA.

Deletion of either RPS0 gene reduces growth rate and deletion of both genes is lethal (Ford et al., 1999).

Pr55bp is also a protein component of the small (40S) ribosomal subunit and nearly identical to Rps19Ap and has similarity to rat S19 ribosomal protein (Planta and Mager, 1998).

Tdh3p is one of the glyceraldehyde-3-phosphate dehydrogenases (GAPDH). Glyceraldehyde-3-phosphate dehydrogenase is one of the most abundant proteins in yeast cells (Krebs, 1953). There are three glyceraldehyde-3-phosphate dehydrogenase structural genes per haploid yeast genomes and each structural gene encodes an mRNA (Holland and Holland, 1979); (Holland et al., 1983). All three genes encode catalytically active enzyme and that the genes are expressed at different levels during logarithmic cell growth. The contribution of the TDH1, TDH2, and TDH3 gene products to the total glyceraldehyde-3-phosphate dehydrogenase activity in wild type cells is 10-15, 25-30, and 50-60%, respectively (McAlister and Holland, 1985). Glyceraldehyde-3-phosphate dehydrogenase is a classical glycolytic protein and has been used as a "housekeeping" gene in studies of genetic expression and regulation (Ishitani et al., 2003).

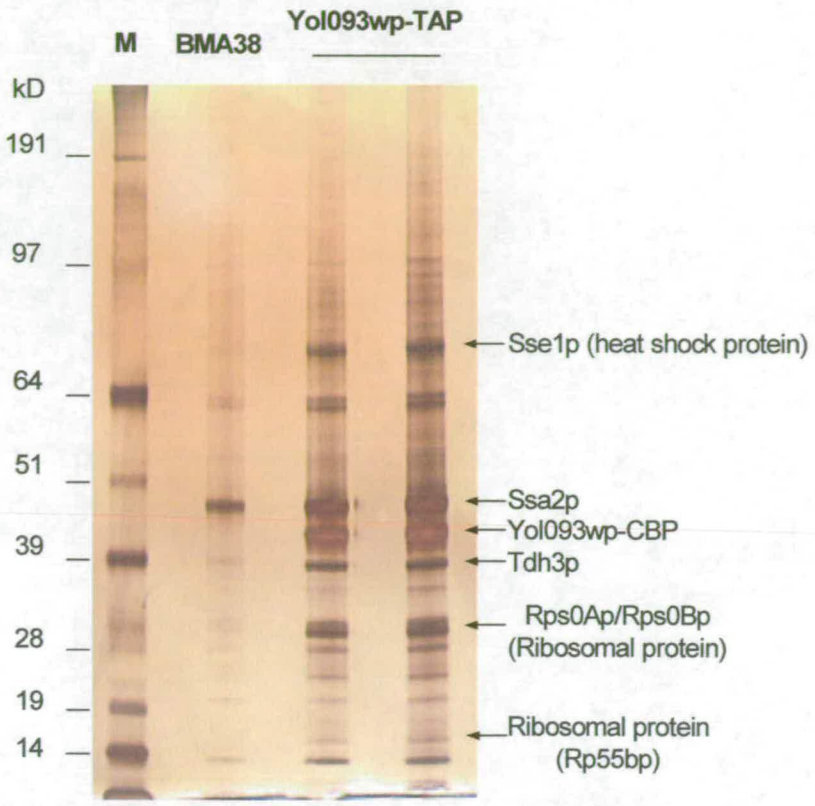

Identity	Mass (kD)	MOWSE Score	% Coverage
Sse1p	77.4	2.31e+6	24
Ssa2p	69.6	6.905e+07	26
Yol093wp	34.5	2.249e+10	62
Tdh3p	35.8	1.512e+07	48
Rpa0A/Bp	27.9	4.291e+04	50
Rp55bp	15.8	8.75e+005	60

Figure 4.7 A Summary of the Results for the TAP Purification of Yol093wp

Proteins were recovered from purification of the C-terminal TAP-tagged Yol093wp. Lane M represents molecular weight markers. The components successfully identified by mass spectrometry are shown on the right of the gel and on the table. The MOWSE score reported by MS-Fit is based on the scoring system described in Pappin *et al*, 1993. % Coverage = the percentage of the protein covered by matched peptides.

4.3 Discussion

In this work, it has been demanstrated that the Yol093w protein was expressed in the TAP-tagged strain, and could be purified followed the TAP purification precedure. However, despite several bands being recovered on SDS-PAGE gels by TAP purification of the Yol093wp complex, only two heat shock proteins, two ribosomal proteins, one glyceraldehyde-3-phosphate dehydrogenase, and Yol093wp-CBP have been identified by the mass spectrometry. Heat-shock and ribosomal proteins are often recognised as contaminant proteins (Gavin et al., 2002). They are highly expressed proteins (Garrels et al., 1997), and in a study of TAP-tagging experiment, they appeared in more than 20 of the TAP purifications (3.5%) (Gavin et al., 2002). Therefore, they were usually considered as the experimental background. However, a DNA/RNA binding domain was found in the Yol093wp sequence analysis (section 3.1), one cannot exclude the possibility that these ribosomal proteins may really interact with Yol093wp *in vivo*. This could be further investigated by other experiments, such as co-immunoprecipitation. Glyceraldehyde-3-phosphate dehydrogenases are constitutively expressed in yeast cells (McAlister and Holland, 1985), and are some of the most abundant proteins in yeast cells (Krebs, 1953). Therefore, it is possible that Tdh3p is also not a natural interactor of Yol093wp.

CHAPTER FIVE

Yeast Two-hybrid Screen of Yol093wp

In conjunction with the TAP tag purification method, the yeast two-hybrid system was used to identify natural interactors of Yol093wp. By comparing results from these two assays, the significance of identified interacting proteins could be revealed.

5. 1 Yeast Two-hybrid System

The two-hybrid system is a genetic assay for detecting protein-protein interactions *in vivo*. The basic concept of the yeast two-hybrid system is to detect the interaction between two proteins via transcriptional activation of one or several reporter genes (Fields and Song, 1989). A classical transcription activator contains a domain that specifically binds to a DNA sequence (the binding domain, BD) and a domain that recruits the transcription machinery (the activation domain, AD). Brent and Ptashne showed that the activation domain of yeast GAL4, a yeast transcription factor, could be fused to the DNA binding domain of *E. coli* LexA to create a functional transcription activator in yeast (Brent and Ptashne, 1985). In the yeast two-hybrid system, these two domains are distinct polypeptides, each fused to a polypeptide, X and Y respectively. The application of the assay requires the co-production of two chimeric fusion proteins within one cell: (a) the bait protein consisting of the BD fused to a protein of interest (X); (b) the prey protein consisting of the AD fused to a protein (Y). Transcription will occur only if X and Y interact with each other (Figure 5.1). The two-hybrid system has been used to investigate the interactions of two proteins or alternatively, by constructing a library of prey fusion proteins, a large number of proteins can be screened to identify proteins which interact with protein X.

The yeast two-hybrid assay has three main applications in the study of protein-protein interactions: (1) It can be used to provide molecular evidence for an interaction suspected between two proteins as a result of genetic or biochemical data, physiological experiments, sequence similarity etc. (2) It can be used to screen a pool

of clones that encode proteins to identify factors which interact with a protein of interest. (3) To define domains or individual amino acid residues which are critical for a particular interaction.

The main advantage of the two-hybrid system is that it is a highly sensitive technique and can detect interactions not revealed by other methods. It is also an *in vivo* assay and therefore the protein components are present in the natural environment of the cell and are not subjected to harsh conditions. A significant advantage of the assay is that, unlike classical genetic screening methods such as synthetic lethal screens, it is not a prerequisite to isolate a conditional lethal mutant of the gene of interest. A two-hybrid screen utilise of the wildtype sequence of the gene and therefore non-essential ORFs and novel genes for which no conditional mutants are available can be analysed. Another beneficial characteristic of the system is that a library screen results in the immediate availability of the gene encoding the interacting protein(s), therefore there is no need for any protein purification steps. In addition, the completion of the yeast genome sequencing project in 1996 allows the rapid identification of interacting factors generated by a two-hybrid screen.

Nevertheless, the yeast two-hybrid system is an indirect genetic assay. Intrinsic limitations of the yeast two-hybrid system include reliance on complex transcriptional activation of reporter genes. Incorrect folding, inappropriate subcellular localization (bait and prey proteins must interact in a nuclear environment), or degradation of chimeric proteins and absence of certain types of

posttranslational modifications in yeast could lead to false negatives. Other properties of the assay may lead to the selection of false positives.

In this study, the two-hybrid system was used to detect proteins that interact with Yol093wp in order to further understand the biological functions of Yol093wp.

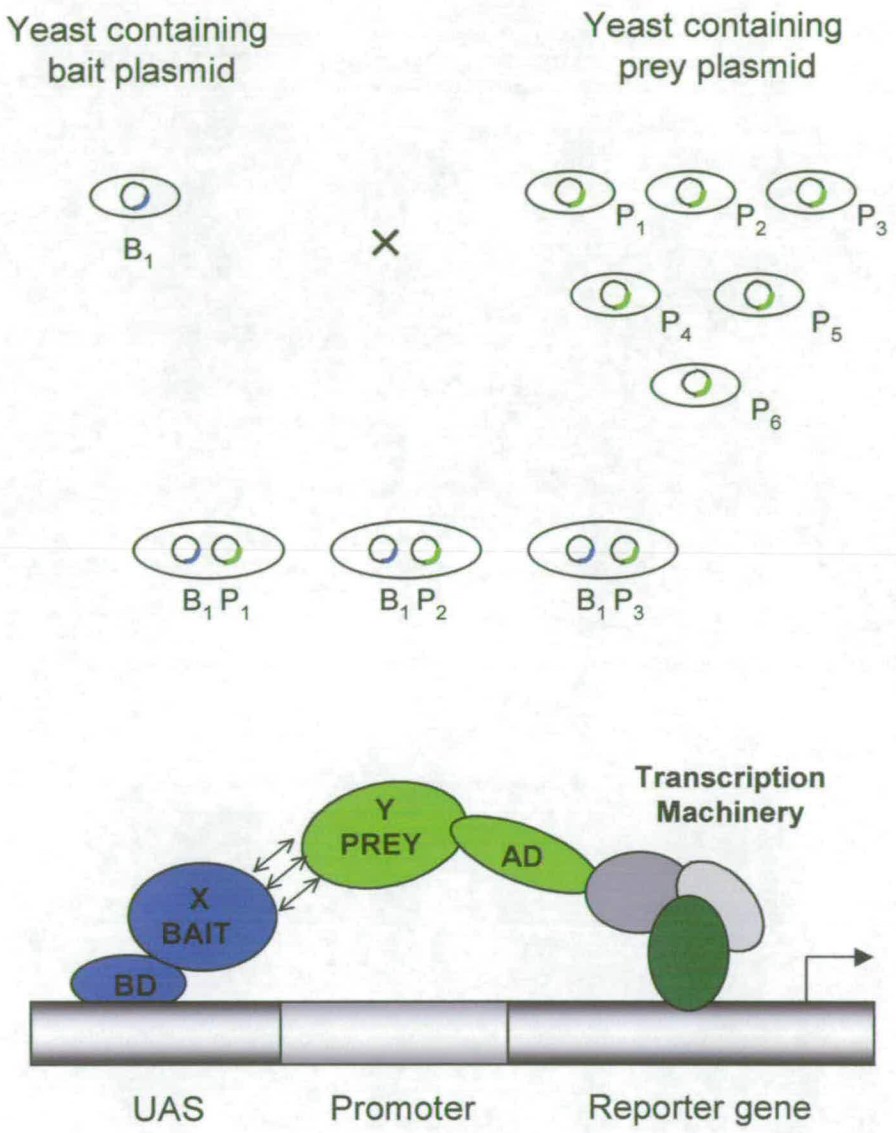

Figure 5.1 General Overview of the Two-hybrid System by Mating
Two hybrid proteins are produced within one cell: the bait fusion, consisting of the DNA-binding domain (BD) of a transcriptional activator fused to a protein of interest X and the prey fusion, consisting of the transcription activation domain (AD) of a transcription factor fused to a protein Y. The interaction between the protein X and Y brings the two previously separated functional domains of a transcription factor together and can thus be monitored through the successful transcription of a reporter gene. This binds to an upstream activation sequence (UAS) of the reporter gene promoter and thereby localises the AD, which is then able to promote transcription.

5. 2 Yeast two-hybrid Screen Analysis of *YOL093W*

5.2.1 Introduction

5.2.1.1 General Strategy

An efficient mating strategy (as shown in the schematic representation below) was used in the study.

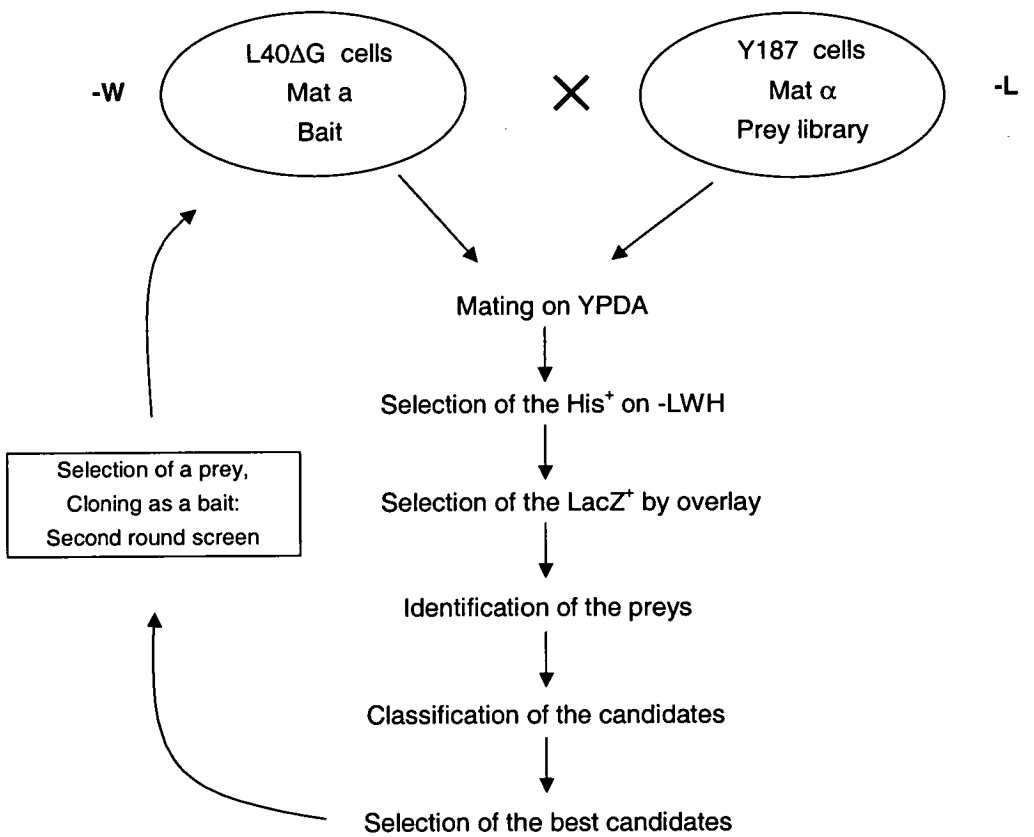

In brief, the L40ΔG (Table 2.6) strain transformed with the bait plasmid and a Y187 (Table2.6) strain transformed with a yeast genomic DNA library (FRYL library, section 5.2.1.3). The mating procedure allows use of selective plates for direct

selection because the two fusion proteins are already produced by the parental cells. No replica plating is required. Prey plasmids from all colonies are sequenced at the Gal4 domain junction and prey fragments are classified according to their heuristic value. The classification of interacting proteins found in a two-hybrid screen allows selecting prey proteins to be used as bait for second-round screens.

5.2.1.2 Bait Plasmid

Bait plasmid was the pBTM116 vector, which encodes a LexA fusion protein. The plasmids were transformed into the L40ΔG strain containing *His3* and *LacZ* reporter genes under the transcriptional control of LexA binding sites (Fromont-Racine et al., 2000).

5.2.1.3 FRYL Library

The FRYL library utilised in the two-hybrid screens described was constructed by M. Froment-Racine in the laboratory of P. Legrain (Institut Pasteur, Paris, France) (Fromont-Racine et al., 1997). The FRYL library is a genomic DNA library composed of random fragments, and all the genomic regions should be present with more or less the same frequency. The library comprises 5×10^6 clones, with randomly generated inserts of an average size of 700 base pairs. Given the size of the yeast genome (12×10^6 bp), a fusion event occurs statistically once every 4 base pairs. Any given ORF should be present in multiple fusion fragments in the library. The Y187 yeast strain was transformed with the FRYL library DNA, and stored at -80°C.

5.2.1.4 Mating Experiment

Two strains were used: Y187, which harbours a sensitive *lazZ* reporter gene for Gal4 binding domain bait proteins, and L40ΔG, which contains the yeast *HIS3* and the bacterial *lacZ* reporter genes under the transcriptional control of *lexA* operators. The *HIS3* gene is required in the yeast histidine biosynthetic pathway and it expression facilites colony growth in the media lacking histidine. 3-aminotriazole (3AT) is an inhibitor of the dehydratase encoded by the *HIS3* gene. The bait-mediated background trans-activation can by reduced by including 3AT in the medium. The *HIS3* gene also enables the selection of positive diploids in the absence of 3AT. The Y187 strain was transformed with the genomic library and L40ΔG cells harboured LexA bait plasmid. The L40ΔG was generated by replacing the entire Gal4 coding sequence in L40 strain with the kanamycin-resistant cassette. Thus Gal4 activation domain-derived libraries transformed into Y187 were used for two-hybrid screens with LexA bait proteins. Diploid cells generated from the L40ΔG strain with Y187 cells contain two *LazZ* genes. The one from the L40ΔG strain was controlled by LexA binding sites and functioned as a reporter gene for LexA baits, and the one from Y187 cells is controlled by Gal4 binding sites and is inactive in these diploid cells.

5.2.1.5 Classification of Prey

To facilitate post-screen analysis, all candidates generated from a two-hybrid screen are classified into one of five categories (Figure5.2, as defined by Fromont-Racine et al., 1997). The A1 category contains the most statistically significant candidates produced by a screen. These ORFs are those for which at least two distinct overlapping fusions are found. The A2, A3, and A4 ORFs are found only a single fusion, even though the same is found several times. The A2 ORFs are fusions starting close to the initiation codon of a yeast ORF, within 150 bases of the in-frame stop codon located upstream of this ORF. The A3 ORFs are fusions containing coding inserts of more than 1000 bases (significantly longer than the mean size of fragments in the library). The A4 category simply corresponds to prey which are found as single fusions and do not qualify for A2 or A3 status. B fusions express nonbiological peptides, i.e., antisense or intergenic regions. Out-of-frame fusions might be selected in the process. They are not discarded as they may encode genuine yeast polypeptides resulting from a frameshifting event.

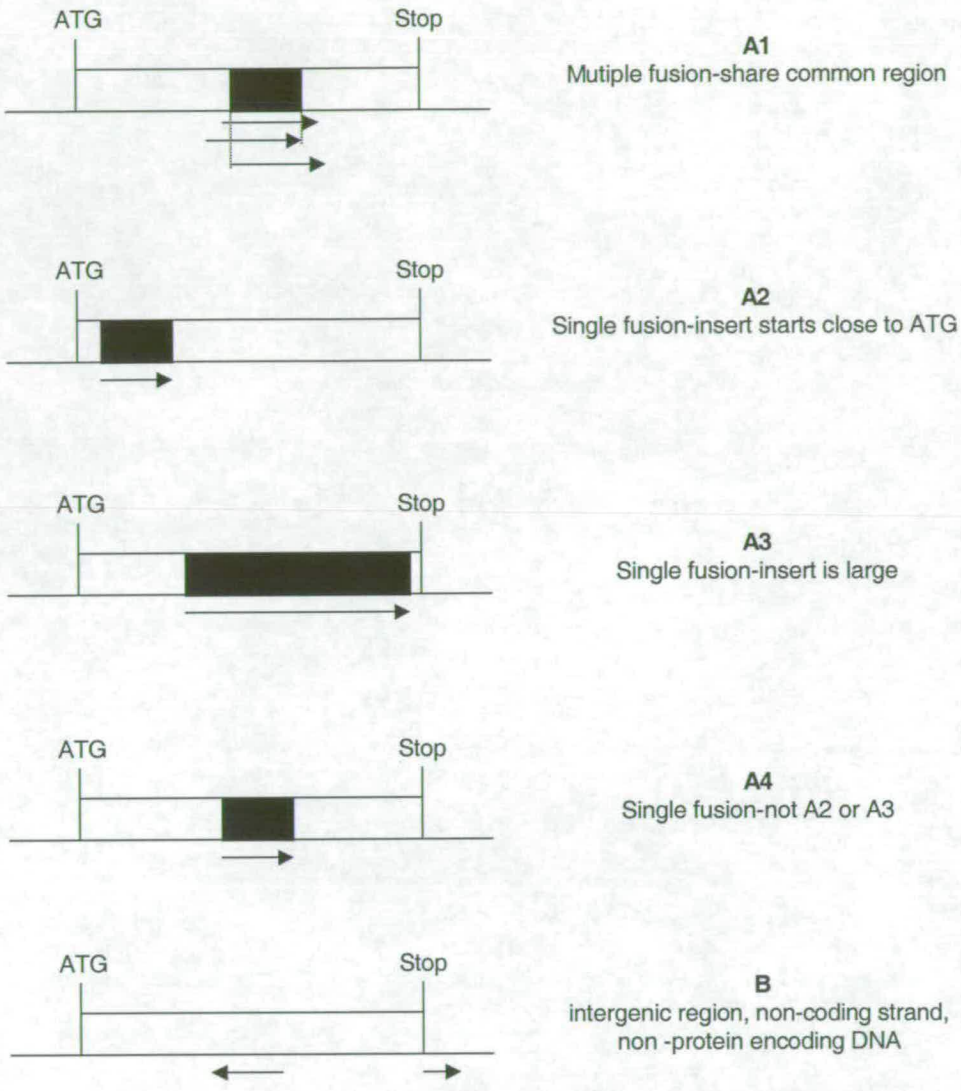

Figure 5.2 Classification of Prey Selected in Two-hybrid Screens
A fragment of a yeast chromosome is depicted, containing an open reading frame (open box). The initiation and termination codons of the ORF are included. The domain is shown (black box). Arrows indicate the position, length and orientation of the isolated fragments. The categories of prey are defined on the right.

5.2.2 Construction of the pBTM116/*YOL093W* Bait Plasmid

The two-hybrid screens performed in this study utilize bait based upon the *E.coli* repressor LexA DNA-binding domain. In order to fuse Yol093w protein to the LexA binding domain, the full-length *YOL093W* open reading frame flanking by restriction enzyme sites was amplified by PCR using yeast genomic DNA of strain BMA38(2n) as a template. The PCR product was cloned into the pBTM116 vector to create pBTM116/*YOL093W*. The construct was confirmed by enzyme digestion (Figure 5.3). This high copy-number plasmid produces the bacterial LexA DNA binding domain-Yol093wp fusion protein under the transcriptional regulation of the constitutive *ADH1* promoter. The 5' vector-insert junction and the entire insert were verified by DNA sequencing (data not shown).

5.2.3 Construction of Yeast Strain Containing pBTM116/*YOL093W* Bait Plasmid

The pBTM116/*YOL093W* plasmid was introduced into yeast strain L40ΔG to make a yeast strain containing bait plasmid (Table 2.6). Transformants were propagated on –W (Tryptophan) drop-out medium. The clone growing on the selective plate were restreaked and investigated by Western blot analysis to confirm the fusion protein was produced (Figure 5.4).

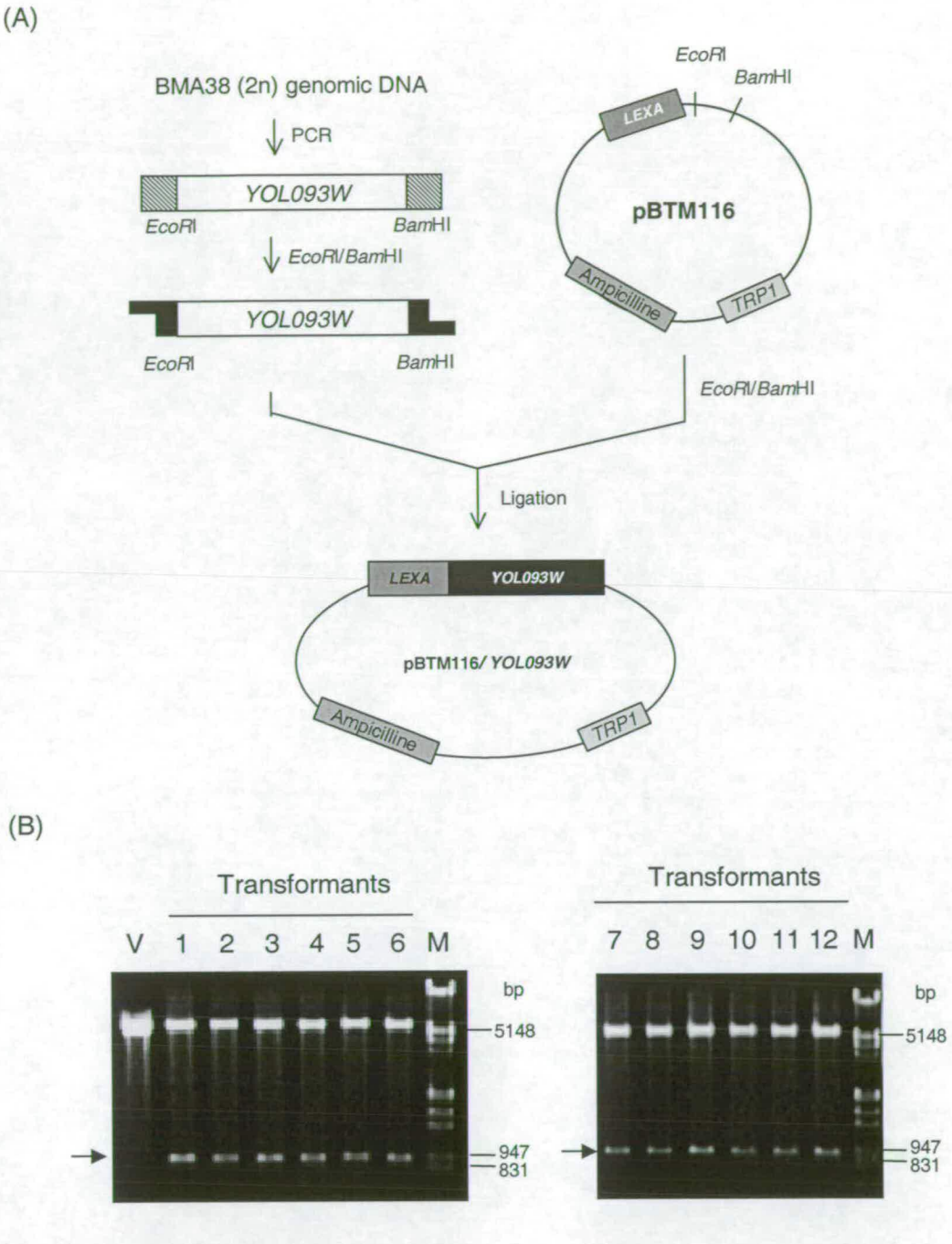

Figure 5.3 Construction of the pBTM116/*YOL093W* Bait Plasmid
The *YOL093W* ORF was amplified by PCR from genomic DNA of strain BMA38(2n). The 900bp PCR product was then digested with *Eco*RI/*Bam*HI, and ligated into the vector pBTM116. (A) A schematic representation of the cloning strategy used to construct pBTM116/*YOL093W*. (B) The construct was confirmed by the *Eco*RI/*Bam*HI enzyme digestion. The arrow indicates the 930 bp DNA fragment, which would be expected following successful construction of pBTM116/ *YOL093W* is indicated. V: pBTM116 vector.

5.2.4 Yeast Two-hybrid Screens with the pBTM116/*YOL093W* Bait Plasmid

The initial two-hybrid screens (section 2.2.7) with the pBTM116/*YOL093W* in this study were performed. The L40ΔG cells harbouring the pBTM116/*YOL093W* bait plasmid were mated with the Y187 cells containing the FRYL library (Jean Beggs laboratory, University of Edinburgh, UK). After four-hour incubation, cells were collected and distributed on –LWH and –LWH+3AT (ranging from 1-50 mM) plates. To determine the mating efficiency, the number of diploids was estimated. For this purpose, an aliquot of cell suspension was diluted by three 10-fold dilutions steps. 50 μl of the 1000-fold dilution were spread onto –L, –W and –LW plates.

Unfortunately, the Y187 cells containing the FRYL library were contaminated. There were two kinds of colonies formed on –LWH+3AT plates with different colours (red and white). The colonies turned into abnormal shape with further incubation. This made the two-hybrid screens with the pBTM116/*YOL093W* bait plasmid impossible to carry out. Consequently, another yeast two-hybrid screen for the other bait plasmid was performed (section 5.2.5).

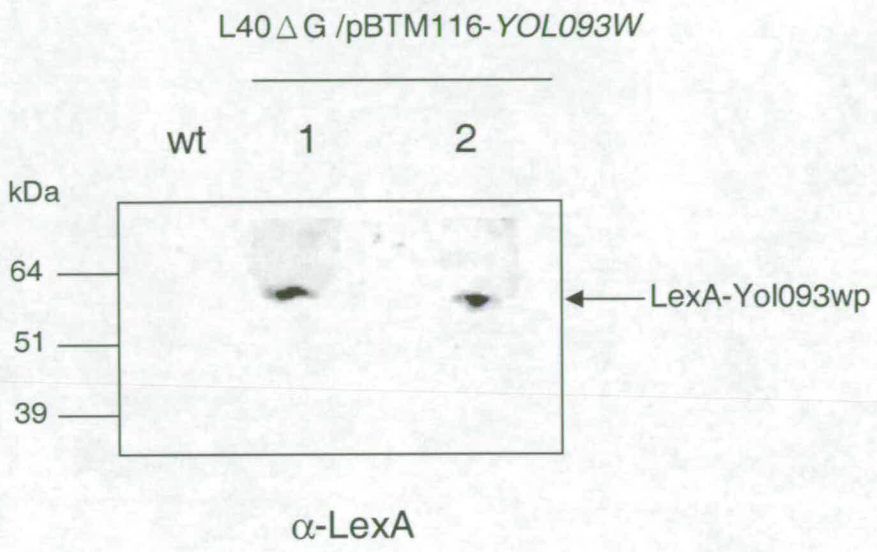

Figure 5.4 Western Analysis of LexA-Yol093wp Fusion Protein from L40 Δ G /pBTM116-*YOL093W*

Crude cell extracts were prepared from L40ΔG (wild type, lane 1) and from L40 Δ G /pBTM116-*YOL093W* (lanes 2 & 3). Proteins were fractionated on a 15% SDS-PAGE gel, electroblotted and probed with antibodies against LexA. Immunodetection was with HRP-conjugated anti-rabbit antibodies. And proteins were visualized by ECL (Amersham). The position of the LexA-Yol093wp fusion protein is indicated.

5.2.5 Construction of the pB27/*YOL093W* Bait Plasmid

The two-hybrid screens performed in this part of study also utilized bait based upon the *E.coli* repressor LexA DNA-binding domain. The full-length *YOL093W* open reading frame flanking by restriction enzyme sites was amplified by PCR using yeast genomic DNA of strain BMA38(2n) as a template. The PCR product was cloned into the pB27 vector to create the pB27/*YOL093W*. The construct was confirmed by enzyme digestion (Figure 5.5). This high copy-number plasmid produces the bacterial LexA DNA binding domain-Yol093wp fusion protein under the transcriptional regulation of the constitutive *ADH1* promoter. The 5' vector-insert junction and the entire insert were verified by DNA sequencing (data not shown).

5.2.6 Yeast Two-hybrid Screens with the pB27/*YOL093W* Bait Plasmid

The two-hybrid screens with the pB27/*YOL093W* were performed by HYBRIGENICS (As a service; a kind gift from Jean Beggs). HYBRIGENICS was set up using the yeast two-hybrid expertise of Pierre Legrain and Jean-Rain for commercial purpose. In this study, fifty million diploid cells were screened.

(A)

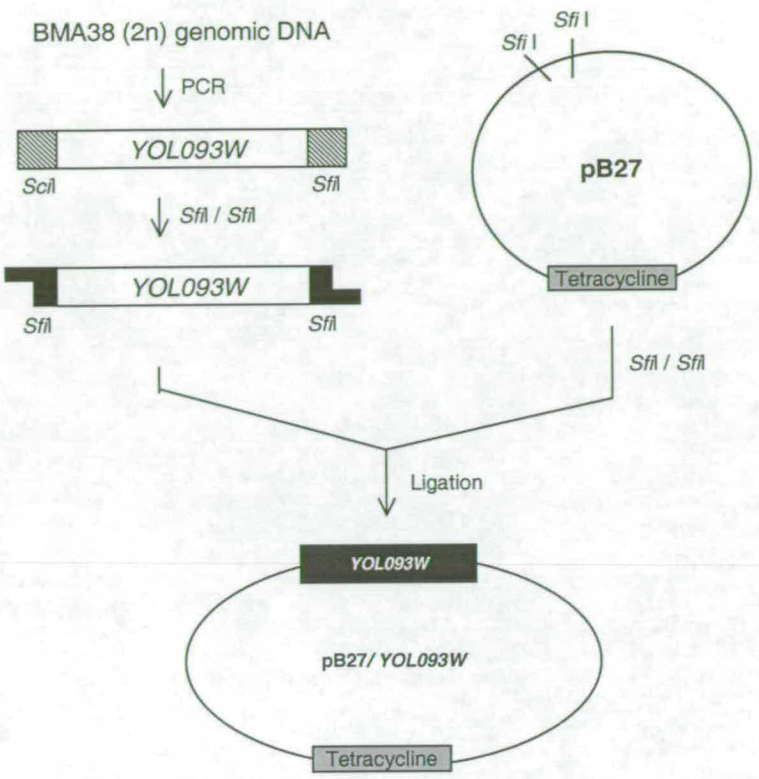

(B)

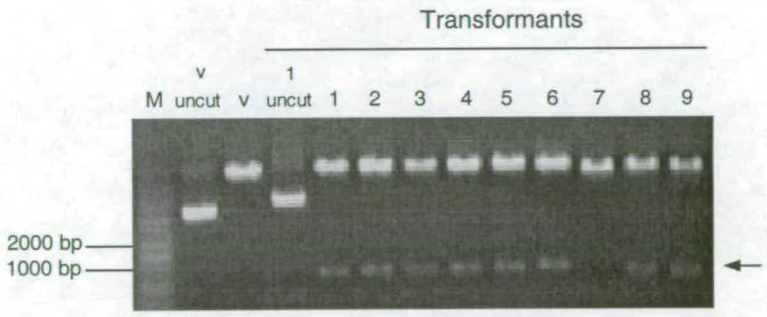

Figure 5.5 Construction of *YOL093W* Bait Plasmid

The *YOL093W* ORF was amplified by PCR from genomic DNA of strain BMA38. The ~900bp PCR product was then cut with *Sfi*I , and ligated into the vector pB27. (A) A schematic representation of the cloning strategy used to construct pB27/*YOL093W*. (B) The construct was confirmed by the *Pst*I/*Eco*RI enzyme digestion. The arrow indicates the ~930 bp DNA fragment, which would be expected following successful construction of pB27/ *YOL093W* is indicated. V: pB27 vector.

5.2.7 Results from the Two-hybrid Screen for the pB27/*YOL093W* Bait Plasmid

The identity and characteristics of the ORF encoded by the prey plasmid resulting from the screen are summarised in Figure 5.6. Only one ORF, *YGR023W (MLT1)*, was identified in the screens. The protein encoded by the *YGR023W* gene was isolated once as an A4 candidate from the screen (section 5.2.1.5). The Mlt1p protein is comprised of 551 amino acids and has a molecular weight of 57.5 kDa. It is involved in cell wall biogenesis. The isolated clone was in the A4 class, so it is possibly the result of non-specific interaction with the bait protein. There was insufficient evidence to suggest that this candidate actually interacts with Yol093wp in the cell and therefore will not be studied further.

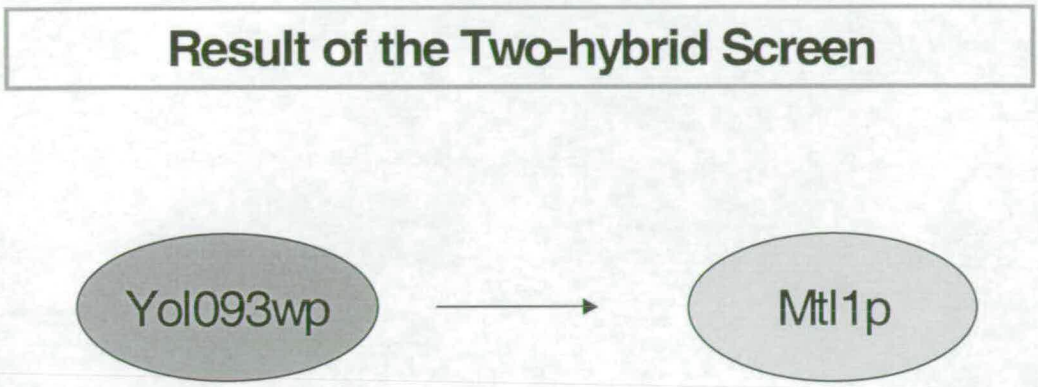

ORF NAME	GENE NAME	nt OF FUSION	ORF SIZE	FREQUENCY IN SCREEN	GATEGORY	OTHER INFORMATION
YGR023W	*MTL1*	612	1656	1	A4	Involved in Cell Wall Biogenesis

Figure 5.6 Result of Two-hybrid Screen with pBT27/*YOL093W*
The ORF and gene names were given by the *Saccharomyces* Genome Database (SGD). Nt of fusion refers to the distance from the start of the coding sequence to the point at which the fusion begins. ORF size is the number of nucleotides from the ATG initiation codon to the termination codon. Frequency in screen refers to the number of identical fusions that were isolated in the screens. The category used is described in Section 5.2.

5. 3 Discussion

In this work, only one protein, Mtl1p, was retrieved in the two-hybrid screens of Yol093wp. The significance of this interaction was relatively low, so that it did not suggest possible biological functions of Yol093wp. The possible reasons for lack of results were: (1) The clone could be under-represented in the library. (2) The library was predominantly small peptides; therefore, some large interactors would never be full length in this library

Ito *et al* (Ito et al., 2001) carried out a comprehensive two-hybrid analysis of the budding yeast proteome. They detected 4,549 interactions. Among them, the *YOL093W* fusion preys were retrieved twice when the *MEC3* was used as the bait in the screens. *MEC3* is involved in checkpoint control and DNA repair. However, this interaction was not included in their core data, which contains 841 interactions with more than 3 Interaction Sequence Tags (IST) hits. Besides, the network they obtained in their screens did include some artefacts. It should be noted that the proteins having numerous interaction partners, some of which are likely caused by noise in the two-hybrid screens. As expected, the proteins with dozens of binding partners should be omitted from the analysis. Therefore, since *MEC3* bait also identified the other 74 prey ORFs in their screens, it indicated some of them were non-specific interactions, and should omitted.

Hazbun *et al* (Hazbun et al., 2003) assigned functions to yeast proteins by integration of technology. From their yeast two hybrid data, when using *YOL093W* as bait

plasmid, the *SML1* and *SMAL1* were isolated twice in the screens. Sml1p is a suppressor of mec lethality (Zhao et al., 1998), and a ribonucleotide reductase inhibitor (Chabes et al., 1999). *Sml1* null mutant is viable and showed the following phenotypes: it suppresses *mec1* or *rad53* lethality; suppresses *mip1-1* at 37°C; suppresses dun1 DNA damage sensitivity; increased resistance to DNA damage; increased dNTP pools (Zhao et al., 1998). The *Sma1* null mutant undergoes meiotic nuclear divisions but does not form spores. Sma1p is involved in spore membrane assembly (Rabitsch et al., 2001). In Hazbun and his colleagues' screens, Sma1p also interacted with 11 other proteins.

All these data may not be conclusive, but they were all indicative of the possibility of Yol093wp involving in DNA metabolism. All of these data may provide clues about the function of Yol093wp.

CHAPTER SIX

Subcellular Localization of Yol093wp

6.1 Introduction

Eukaryotic cells are organized into a complex network of membranes and compartments, which are specialized for various biological functions. Comprehensive knowledge of the location of proteins within these cellular microenvironments is critical for understanding their functions and interactions.

The traditional approach to study protein localization in *Saccharomyces cerevisiae* includes techniques of immunofluorescence microscopy. Tagging a protein with an epitope allows the surveillance of the protein with a specific monoclonal antibody.

This approach can elucidate the cellular location of a tagged protein as well as its size, abundance, posttranslational modifications, and interactions with other proteins. In this study, a myc tag was used to study the cellular location of *YOL093W*. Although these methods have been effectively used to visualize the targeting of specific cellular components, their use can be limited by the requirement for antibodies directed against the target protein. Antibodies against proteins found in low abundance can be difficult to obtain, and the level of detection of this class of protein is relatively insensitive. To circumvent these potential problems, an *Aequorea victoria* green fluorescent protein (GFP) fusion would be used in parallel.

Gene fusions using GFP, in general, heightens the sensitivity of molecular detection. Since the GFP chromophore is formed by autocatalytic cyclization of three amino acids, and fluorescence is triggered by excitation with specific wavelength light, neither invasive sample preparation nor substrate addition is required, making it possible to study protein localization in living cells. In addition, since GFP is relatively small (238 amino acids) and can remain functional even when fused to a target protein, it allows protein localization to be monitored in real time.

6.2 13myc-tagged *YOL093W*

6.2.1 Construction of a 13myc-tagged *YOL093W* Strain

In order to investigate the subcellular localization of Yol093wp, a 13myc-tagged version of the protein was also generated. For constructing 13myc fusion, the PCR-mediated strategy (as shown in Figure 6.1) was used to engineer homology between 13myc tag and the target gene to create in-frame fusions on the chromosome. Yeast strains were generated expressing full-length Yol093w protein, tagged at the C-terminal end with the 13myc tag, from their endogenous promoter by inserting the coding sequence of 13myc in-frame immediately preceding the stop codon of the *YOL093W* ORF. With this strategy, wild-type levels and patterns of protein expression are minimally perturbed.

A pair of oligonucleotides, Yol093w-13myc1 and Yol093w-13myc2, was used to amplify the 13myc tag and a marker from a plasmid template, and the resulting PCR products were introduced into a haploid BMA38(α) yeast strain. Hygromycin B (hph)-resistant colonies were streaked out onto fresh YPDA + hph medium for colony purification. Transformants were assayed by genomic PCR with one primer specific for the GFP tag (primer R-FA6a-MX6) and a second specific for the *YOL093W* ORF (primer Yol093w-TAP-test1) to determine whether the cassette had integrated at the appropriate locus (Figures 6.2). In addition, the 13myc tag integration was also confirmed by Western blot analysis with antibodies against myc to show that cells produce a myc-tagged Yol093wp protein. The cells expressed the

fusion protein at the expected size of the Yol093wp-myc (Figure 6.3). The resultant haploid yeast strains (BMA38(α)/*YOL093W-13MYC*) (Table 2.6) therefore produces C-terminally 13myc-Yol093w protein (Yol093wp-13myc) which is expressed under the control of the endogenous *YOL093W* promoter.

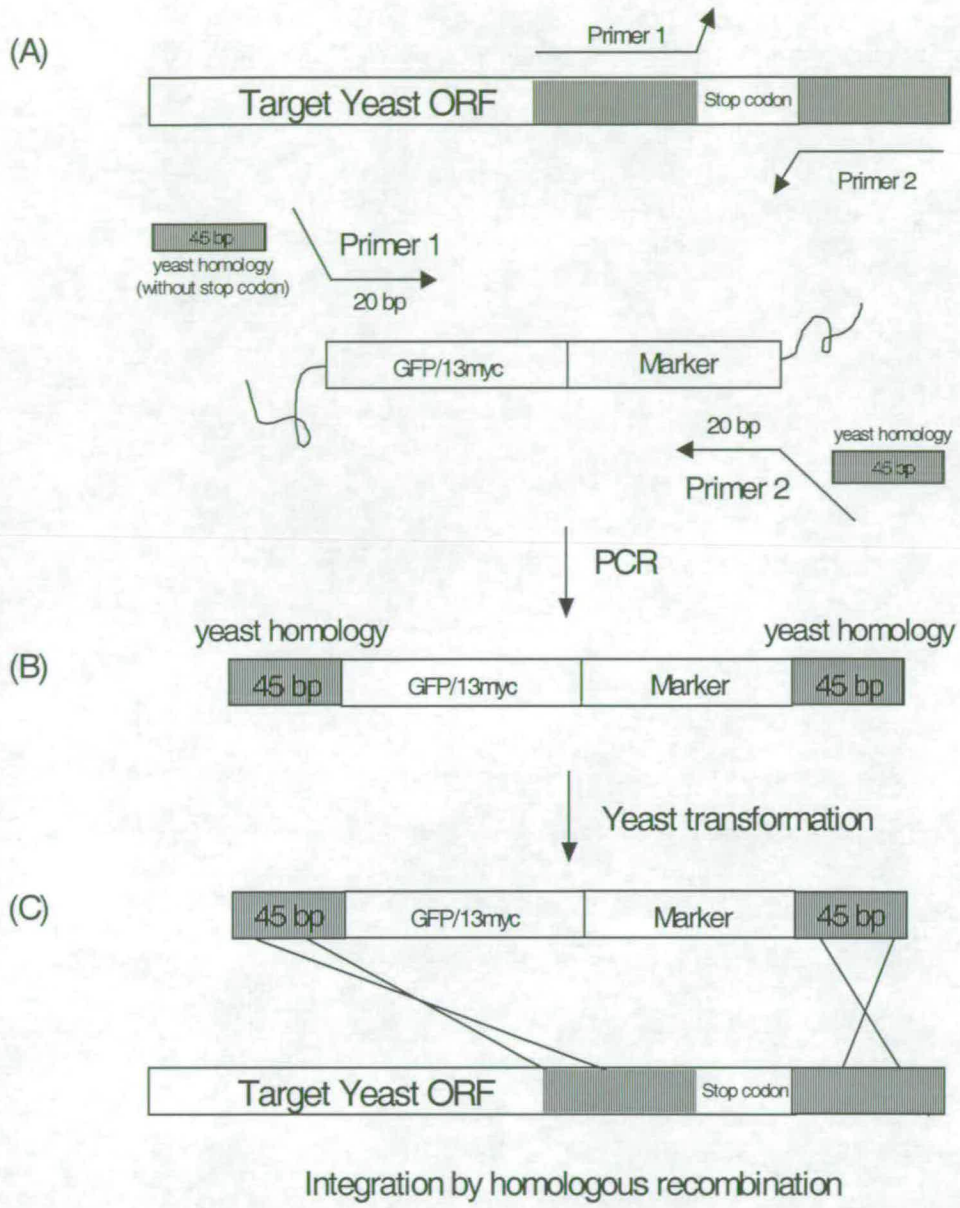

Figure 6.1 Schematic Representation of the Strategy to13myc or GFP Tagging of *YOL093W* on the Chromosome

(A) Oligonucleotide primers Yol093w-13myc1 and Yol093w-13myc2 were used to amplify the GFP or 13myc tag flanking with 45bp upstream sequence of the stop codon of the ORF, and 45bp downstream sequence of the ORF. (B) The PCR product was then transformed into the yeast cells. (C) The tag was integrated though homologous recombination

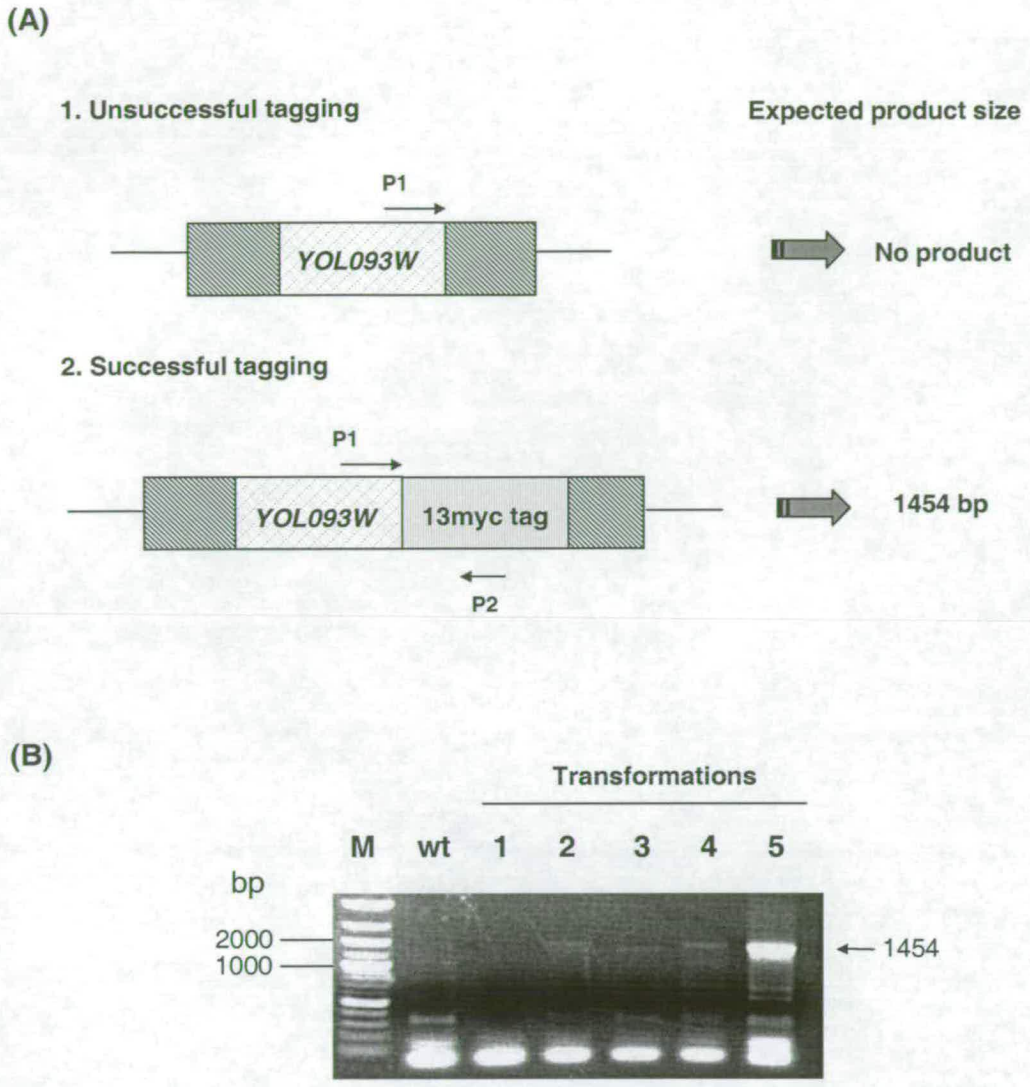

Figure 6.2 PCR on Yeast Transformants to Test the Integration of myc Tag into the Chromosome

After transformation of BMA38(α) strain with a linear PCR product containing the myc tag, which should be inserted immediately downstream of the final codon of the *YOL093W* gene, hph-resistant transformants were streaked out onto fresh YPDA + hph medium for colony purification. Then cells of the transformants and of the wt parental BMA38(α) strain were suspended in water, boiled for 10 minutes and used in a PCR using oligonucleotides primers P1: yol093w-TAP-test 1 and P2: R-hph. (A) The positions on the template at which the primers anneal are indicated in the upper schematic drawing of the *YOL093W* locus (either wild type or after myc-tagged). The products of PCR reactions are shown in (B). The fragments expected following successful integration of myc tag cassette into the chromosome are indicated (lane 1-4 were positive but with weak signal).

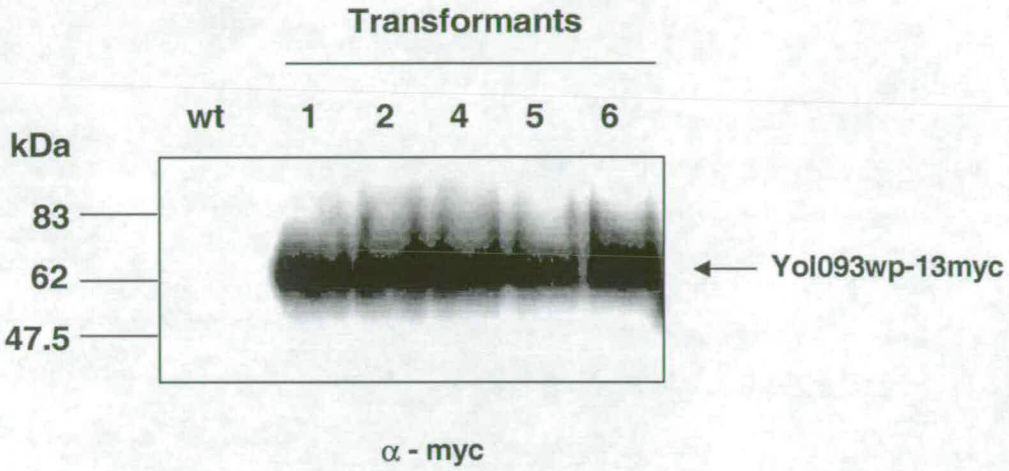

Figure 6.3 Western Blot Analysis of myc-tagged Yol093wp from the Transformants

Crude cell extracts were prepared from BMA38(α) (wild type, lane 1) or from transformants. Proteins were fractionated on a 4-12% SDS-polyacrylamide gel, electroblotted and probed with antibodies against c-myc. Immunodetection was with HRP-conjugated anti-rabbit antibodies. And proteins were visualized by ECL (Amersham). The position of the 13myc-tagged Yol093wp (Yol093wp-13myc) is indicated.

6.2.2 Immunofluorescence (IF) Analysis of the 13myc-tagged *YOL093W* Strain

6.2.2.1 Immunofluorescence Analysis

The strain with 13myc-tagged *YOL093W* was grown to mid-logarithmic phase in medium. The localisation of the fusion protein was visualised by immunofluorescence (IF) techniques. Briefly, cells were fixed with 3.7% formaldehyde and spheroplasted by Lyticase. After incubation with the first antibody against c-myc and the second antibody conjugated with Cy3. DAPI stain (Vectashield mounting medium, VECTRA) was also applied onto the cells. The cells were then visualized using fluorescence microscopy to characterize Yol093wp-13myc fusion protein subcellular localization in *S. cerevisiae* cells.

6.2.2.2 Localization of Yol093wp-13myc Fusion Protein

By using the antibodies against c-myc, and DAPI stain as a marker for the nucleus, the localization of Yol093wp-13myc fusion could be visualized. From the micrographs (shown in Figure 6.4), the fusion protein was co-localized with the DAPI stain, which suggested that the Yol093wp-13myc localized in the nucleus. Some negative anti-myc images might due to the efficency of myc antibody staining.

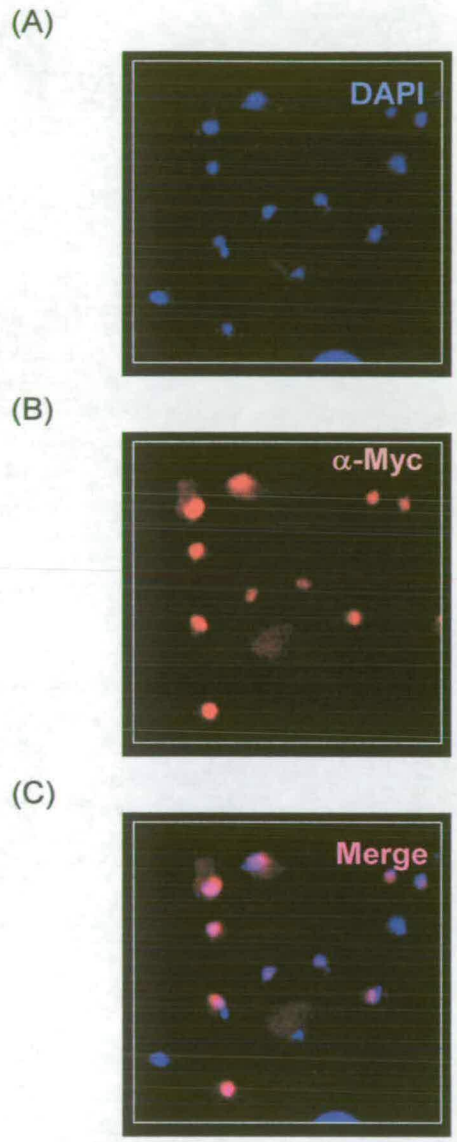

Figure 6.4 Immunofluorescence Staining of 13myc-tagged Yol093wp Strain

The strain with chromosomally 13myc-tagged *YOL093W* was grown to mid-logarithmic phase in medium. Cells were fixed with 3.7% formaldehyde and the localisation of fusion protein was detected by anti-myc antibody and visualized by the microscopy. Cells were strained with DAPI as a marker for the nucleus. (A) DAPI staining for DNA; (B) anti-myc shows the myc protein; (C) merge image.

6.3 GFP-tagged *YOL093W*

6.3.1 Construction of a GFP-tagged *YOL093W* Strain

In order to further clarify the subcellular localization of Yol093wp, a GFP-tagged version of Yol093wp was generated. The GFP may be fused to either the 5' or 3' end of the target gene, to generate either amino- or carboxy-terminal fusions, respectively. This choice is often made by predicting which region of the protein will most likely tolerate the addition of extra amino acids and still remain functional. The strategy chosen in this work, as shown in Figure 6.1, for constructing GFP fusions is to use PCR to engineer homology between GPF and the target gene to create in-frame fusions on the chromosome. Yeast strains were generated expressing full-length Yol093w protein, tagged at the C-terminal end with the GFP tag, from their endogenous promoter by inserting the coding sequence of GFP in-frame immediately preceding the stop codon of the *YOL093W* ORF. With this strategy, wild-type level and pattern of protein expression are minimally perturbed.

We tagged the *YOL093W* ORF in its chromosomal location through oligonucleotide-directed homologous recombination. A pair of oligonucleotides, Yol093w-13myc1 and Yol093w-13myc2, was generated that had homology to the desired chromosomal insertion site at the 5' end of each primer and homology to a vector containing the GFP tag at the 3' end. These primers were used to amplify or GFP tag and a marker from a plasmid template, and the resulting PCR products were transformed into a haploid BMA38(a) yeast strain (Figure 6.1). The selectable marker kanamycin (kan, G418)-resistant colonies were streaked out onto fresh YPDA+ kan medium for colony purification. Transformants were assayed by genomic PCR with one primer

specific for the GFP tag (primer R-FA6a-MX6) and a second specific for the *YOL093W* ORF (primer Yol093w-TAP-test1) to determine whether the cassette had integrated at the appropriate locus (Figure 6.5). The resultant haploid yeast strains (BMA38(a)/*YOL093W-GFP*) (Table 2.6) therefore produces C-terminal GFP-tagged Yol093w protein (Yol093wp-GFP) which is expressed under the control of the endogenous *YOL093W* promoter.

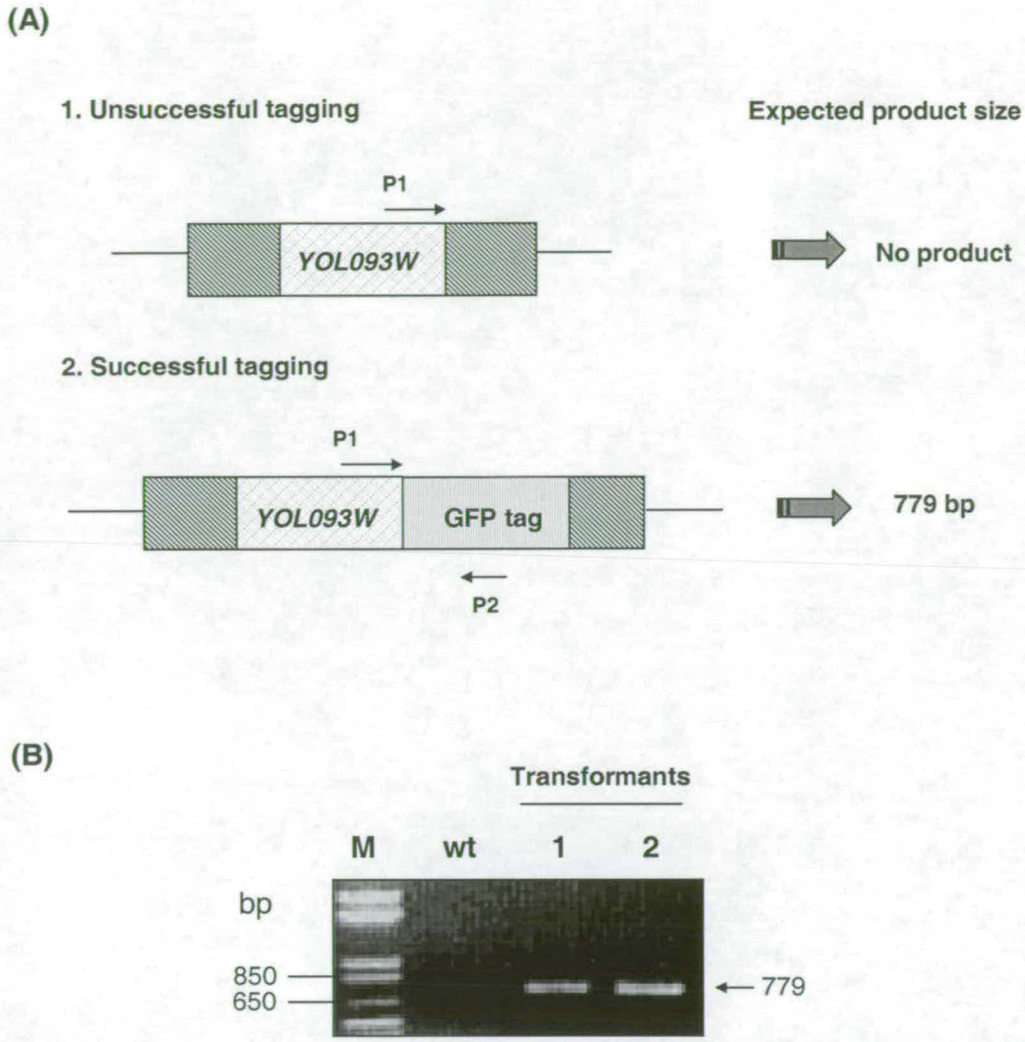

Figure 6.5 PCR on Yeast Transformants to Test the Integration of GFP Tag into the Chromosome

After transformation of BMA38(a) strain with a linear PCR product containing the GFP tag, which should be inserted immediately downstream of the final codon of the *YOL093W* gene, Kan-resistant transformants were streaked out onto fresh YPDA + kan medium for colony purification. Then cells of the transformants and of the wt parental BMA38(a) were suspended in water, boiled for 10 minutes and used in a PCR using oligonucleotides primers P1: yol093w-TAP-test 1 and P2: R-FA6a-MX6. (A) The positions on the template at which the primers anneal are indicated in the upper schematic drawing of the *YOL093W* locus (either wild type or after GFP-tagged). The products of PCR reactions are shown in (B). The fragments expected following successful integration of GFP tag cassette into the chromosome are indicated.

6.3.2 Fluorescence Analysis of the GFP-tagged *YOL093W* Strain

6.3.2.1 Fluorescence Analysis

In this work, GFP signal was monitored in fixed cells. The strain with GFP-tagged *YOL093W* has been analysed using fluorescence microscopy to characterize protein subcellular localization of the protein inside a yeast cell. This strain was grown to mid-logarithmic phase in medium. Cells were fixed with 3.7% formaldehyde, spheroplasted by Lyticase, and visualized by the microscopy. DAPI stain (Vectashield mounting medium, VECTRA) was also applied onto the cells.

6.3.2.2 Localization of Yol093wp-GFP Fusion Protein

By using DAPI as a marker for the nucleus, the localization of a Yol093wp-GFP fusion could be visualized. From the micrographs (shown in Figure 6.6), the fusion protein was co-localized with the DAPI stain, which suggested that Yol093wp-GFP localized in the nucleus. However, one should be aware that the background level expression was quite high, which might influence the interpretations.

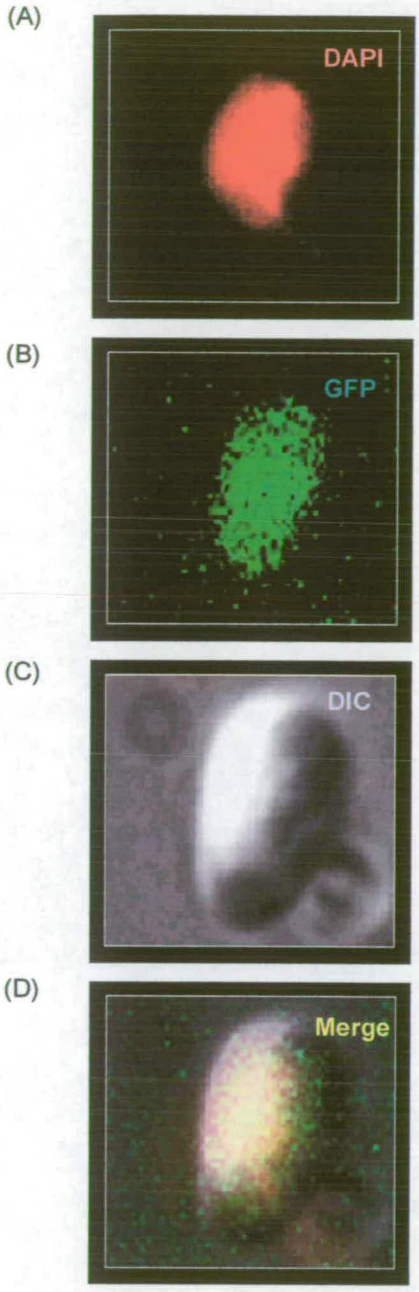

Figure 6.6 Immunofluorescence Staining of GFP-tagged Yol093wp Strain

The strain with chromosomally GFP-tagged *YOL093W* was grown to mid-logarithmic phase in medium. Cells were fixed with 3.7% formaldehyde and the localisation of fusion protein was detected by fluorescence microscopy. Cells were strained with DAPI as a marker for the nucleus. (A) DAPI staining for DNA; (B) GFP image; (C) DIC represents Differential Interference Contrast image; (D) merge image.

6.5 Discussion

In this study, the immunofluorescence micrographs of Yol093w-GFP and Yol093wp-13myc in combination with DAPI straining suggested that the Yol093wp fusion protein was located in the nucleus. The poorer GFP image may be improved by looking at unfixed living cells. The fixation process may affect the apparent location of the GFP protein. However, in conjunction with myc-tagging data, it revealed the localization of Yol093p was in the nucleus.

Huh *et al.* (Huh et al., 2003) described the construction and analysis of a collection of yeast strains expressing full-length, chromosomally tagged GFP fusion proteins. They classified the proteins into 22 distinct subcellular localization categories, and they defined the subcellular localization of Yol093wp-GFP fusion protein was in the nucleus/cytoplasm. From the micrographs they showed on the website (http://yeastgfp.ucsf.edu/displayLocImage.php?loc=15192), one could find that the GFP signal was much stronger inside the nucleus than in the cytoplasm.

CHAPTER SEVEN

Biochemical Assays o Yol093wp

7.1 Expression and Enrichment of His-Yol093w Fusion Protein in *E. coli*

7.1.1 Introduction

To investigate the function of the Yol093wp *in vitro*, the recombinant His-tagged Yol093wp was expressed in *E. coli*. The expression vector used in this work was pET-16b (Navogen). pET vectors are ideal for protein expression in *E. coli* as they allow the gene of interest to be cloned under the control of the T7 promoter, which is not recognized by *E. coli* RNA polymerase (Dubendorff and Studier, 1991).

Therefore, no expression occurs until a source of T7 RNA polymerase is provided, allowing tight control of expression and avoiding plasmid instability due to the toxic effect that many expressed proteins may have on the host. The His•Tag® sequence allows one-step protein enrichment as it binds to divalent cations (Ni^{2+}) that can be immobilized on nitrilotriacetic acid (NTA) resin used for chromatography. The *E. coli* strain BL21 is ideal for protein expression using pET vectors as it carries the T7 RNA polymerase gene under the control of the isopropyl-beta-D-thiogalactopyranoside (IPTG)-inducible *lacUV5* promoter. In addition, the strain is deficient for both *lon* and *ompT* proteases to reduce protein degradation.

7.1.2 Expression of the His-Yol093wp in *E. coli*

The ORF of *YOL093W* was acquired from the American Type Culture Collection (ATCC) as a lambda phage clone. The phage strain was used to amplify the *YOL093W* ORF that was inserted into a multiple cloning site of pET-16b vector (Novagen). The *YOL093W* sequence was fused to an N-terminal His•Tag® (6 His residues) present in the pET-16b vector. The construct, pET-16b/*YOL093W* (Figure 7.1), was prepared by John Connelly (University of Edinburgh). *E. coli* strain BL21 (DE3) pLysS (Novagen, Table 2.5) was transformed with the pET-16b/*YOL093W* construct. Expression of the His-Yol093w fusion protein was induced by addition of IPTG. A high level of expression was obtained after four hours induction. His-Yol093wp was present in the cell supernatant, and therefore was soluble (Philip Jordan, this lab, University of Edinburgh). A mock induction of cells transformed with the pET-16b vector containing no insert was also performed as a negative control.

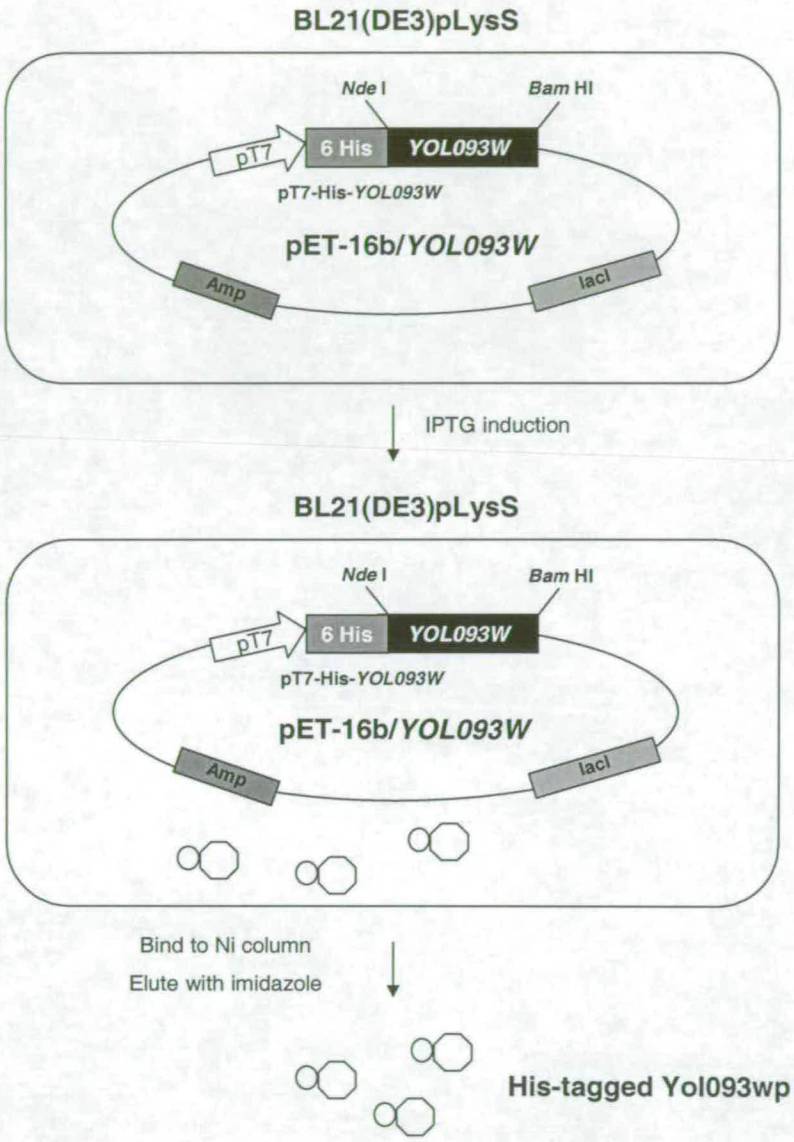

Figure 7.1 Production of Recombinant Yol093wp in *E. coli*
Schematic diagram showing the product and purification of recombinant Yol093wp. Plasmid pET-16b/*YOL093W* was transformed into BL21(DE3)pLysS cells. IPTG was added to induce His-Yol093wp synthesis. The cells were then lysed, and the extract passed down a Ni-NTA column and eluted, resulting enriched Yol093wp. The double circles represent the Ni-NTA column enriched His-Yolo93wp.

7.1.3 Enrichment of His-Yol093wp by Ni-NTA His•Bind® Affinity Chromatography

Cell extracts of His-Yol093wp and the mock control were enriched using Ni-NTA His•Bind® Resin column chromatography (Novagen) (section 2.3.3.11). His-Yol093wp and the mock supernatants were applied to a 10-ml Ni-NTA column that was used for one-step purification of proteins containing His tag sequence by metal chelation chromatography. The His tag sequence bound to Ni^{2+} cations, which were immobilized on the Ni-NTA resin. After this unbound proteins were washed away, His-Yol093wp was recovered by elution with imidazole. An Imidazole ring is part of the structure of histidine. The imidazole rings in the histidine residues of the His tag sequence bind to the nickel ions immobilized by the NTA groups on the matrix. Imidazole itself also can bind to the nickel ions and disrupt the binding of the histidine residues in the His sequence. When imidazole is applied to the Ni-NTA column, it competes with the bound protein resulting in its elution. Non-specific binding can be reduced by including a low concentration of imidazole in the lysis/binding and wash buffer (5-20 mM imidazole). His-Yol093w fusion protein was dissociated from the Ni-NTA resin with imidazole. During a 1000 mM imidazole elution, fractions were collected. 20 µl of each fraction were subjected to SDS-PAGE (section 2.3.3.3.2) and stained with Coomassie blue (section 2.3.3.4). The results are shown in Figure 7.2. Coomassie blue staining revealed that the Yol093wp preparation contained a number of other polypeptides: these could be contaminating proteins or degradation products of Yol093wp itself. Fractions (fr. 13-22) that contained the highest levels of Ni-NTA enriched His-Yol093wp were

combined, and stored at -80°C. Identical fractions of the mock elution were also pooled, and stored at -80°C as a control for further investigation.

(A) His vector only

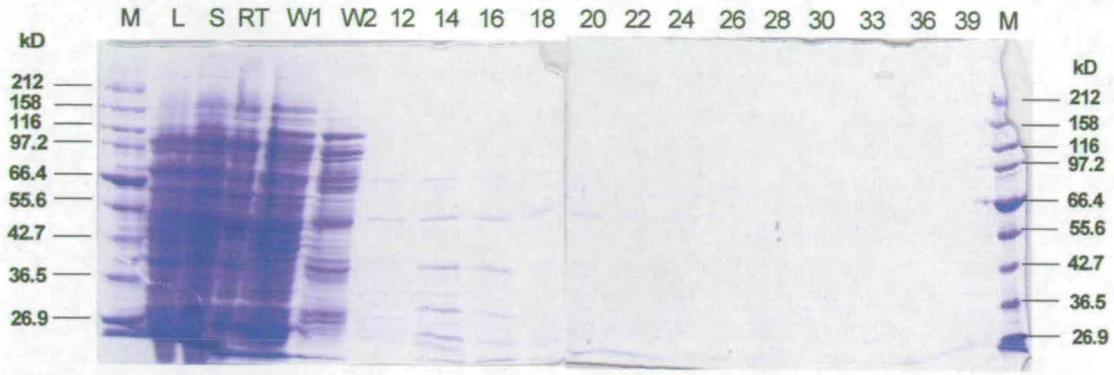

(B) His-Yol093wp

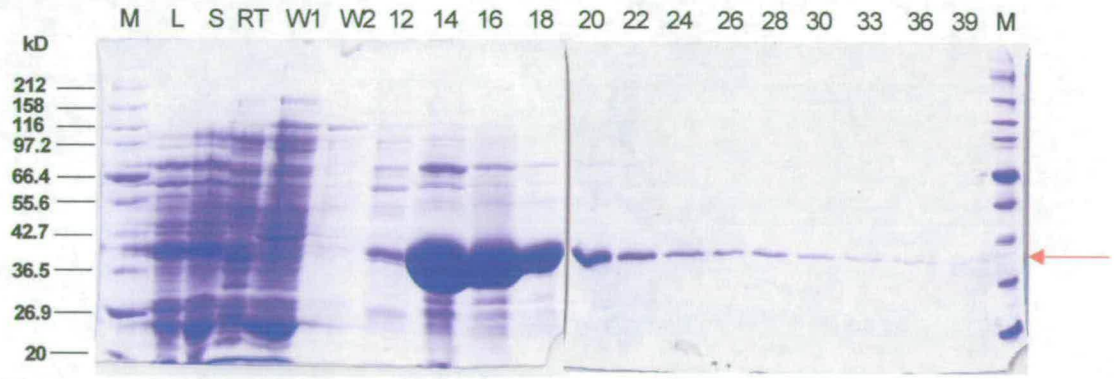

Figure 7.2 Enrichment of His-Yol093wp by Ni-NTA His•Bind® Affinity Chromatography

40 μl of each sample were boiled for 5 minutes, and then 20 μl of samples were assessed by SDS-PAGE. The proteins were visualized by Coomassie blue staining. The enriched His•Tag®-Yol093wp is indicated. M: broad range protein marker; L: cell lysate; RT: Ni-NTA His•Bind Resin cell lysate supernatant run through (5 mM imidazole); W1: Ni-NTA His•Bind Resin binding buffer wash (5 mM imidazole); W2: Ni-NTA His•Bind Resin washing buffer wash (60 mM imidazole); 12-39: elute fractions (1000 mM imidazole).

7.1.4 Concentrating Ni-NTA Enriched His-Yol093wp Fractions by VIVASPIN6 Concentrators

The combined Ni-NTA enriched His-Yol093wp fractions (fr. 13-22), as well as identical fractions of the mock control, were concentrated by VIVASPIN6 concentrator according to the manufacturer's instructions. The VIVASPIN6 concentrators (Vivasceience) are disposable ultrafiltration devices for the concentration and/or purification of biological samples. The concentrator features twin vertical membranes for unparalleled speed and it is with a molecular weight cut-off of 30,000 Da (MWCO 30,000). 20 μl of each of the resulting samples were assessed by SDS-PAGE. Proteins were visualized by Coomassie blue staining (Figure 7.3). It should be noted that the solution volume was only reduced to half and was only reduced to 1/4 for the mock control. This might be because the concentration of Ni-NTA enriched Yol093wp fractions was too high, so that the solution could not run through the membrane totally.

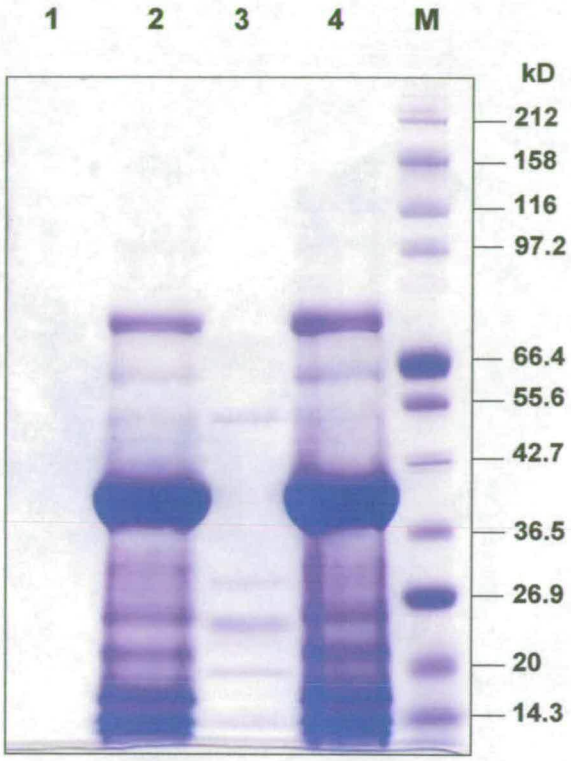

Lane 1: Ni-NTA enriched mock control

Lane 2: Ni-NTA enriched His-Yol093wp

Lane 3: VIVASPIN6 concentrated mock control

Lane 4: VIVASPIN6 concentrated His-Yol093wp

M: Broad range protein marker (NEB)

Figure 7.3 Concentrating Ni-NTA Enriched Yol093wp

40 μl of each sample were boiled for 5 minutes, and then 20 μl of samples were subjected to SDS-PAGE gels. The proteins were visualized by Coomassie blue staining.

7.2 DNA Binding Activity of Ni-NTA Enriched Yol093wp

7.2.1 Double Strand (ds) DNA-Binding Assays Using Agarose Gel Electrophoresis

As the known Holliday junction (HJ) resolvases are metal-ion dependent endonucleases that recognize and cleave four-way DNA junctions (reviewed in (White et al., 1997)), and as mentioned previously in Chapter 3, Yol093wp sequence prediction revealed a DNA binding domain, Ni-NTA enriched His-Yol093wp and VIVASPIN6 concentrated His-Yol093wp were assessed for possible DNA binding activity (section 2.3.3.12).

Circular and linear DNA was used in the assays. As revealed in Figure 7.4, Ni-NTA Yol093wp enrichment caused gel mobility shifts to both double-strand circular and linear DNA substrates run on agarose gels, whereas Ni-NTA mock enrichment did not. This suggested that Ni-NTA enriched Yol093wp had DNA binding properties. It should be noted that Ni-NTA enriched Yol093wp showed more obvious binding shift than VIVASPIN6 concentrated Yol093wp. Additionally, the gel mobility shift was concentration-related. With increased the protein concentration, decreased gel mobility was observed on agarose gels (Figure 7.5).

(A) pBR322 (circular)

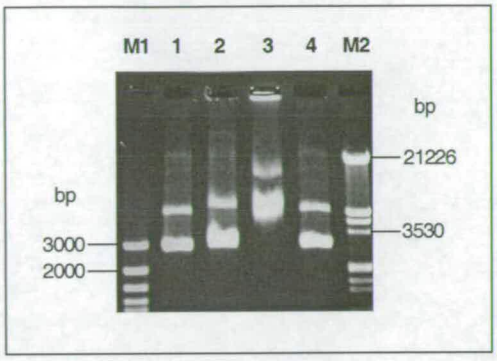

(B) pBR322/*Eco*RI (linear)

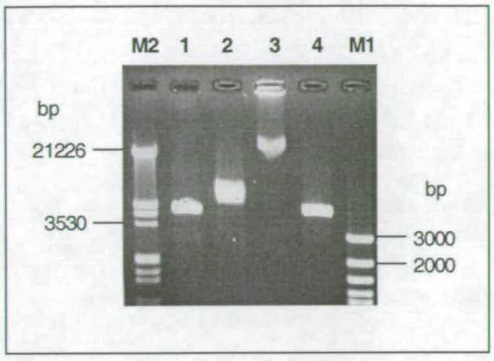

(C) PCR product (linear, 500 bp)

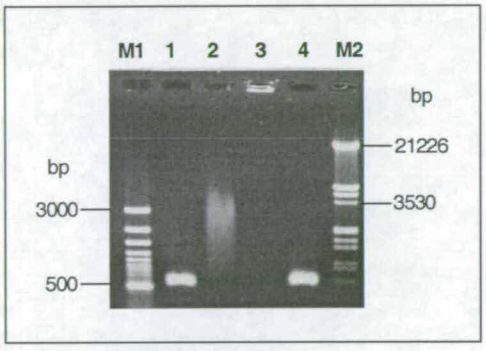

Figure 7.4 dsDNA-Binding Assays Using Agarose Gel Electrophoresis
Binding assays were carried out on ice for 30 minutes with different DNA substrates. (A) pBR322 DNA (NEB, circular) (B) pBR322 DNA digested with *Eco*RI (4316 bp, linear) (C) PCR product (500 bp, linear). The entire reactions were loaded on 0.8% agarose gels. M1: 100 bp DNA ladder; M2: λ DNA/*Eco*RI+*Hind*III marker; Lane1: negative control (DNA substrates + elution buffer); Lane 2: DNA substrates + VIVASPIN6 concentrated Yol093wp (2 μl); Lane 3: DNA substrates + Ni-NTA enriched Yol093wp (2 μl); Lane 4: DNA substrates + Ni-NTA enriched mock proteins (2 μl).

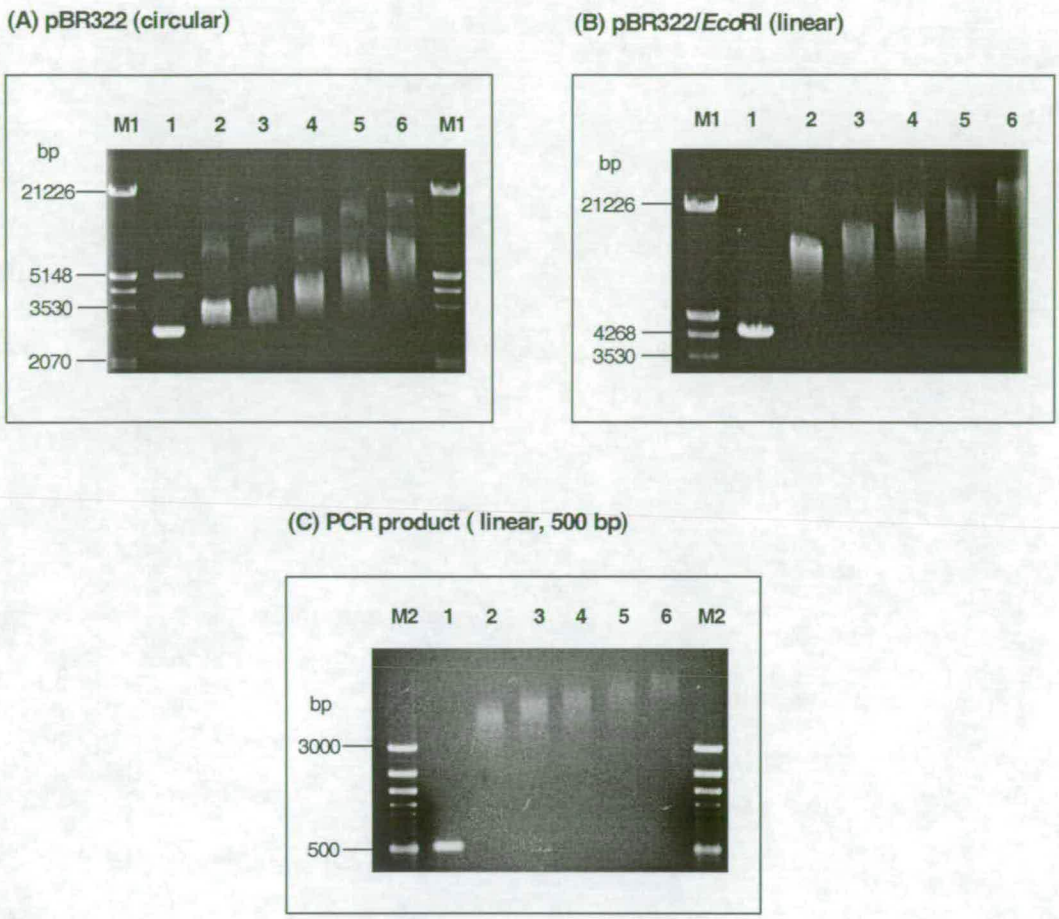

Figure 7.5 DNA Binding Assays with Different Concentrations of Ni-NTA Enriched Yol093wp Using Agarose Gel Electrophoresis

Binding assays were carried out on ice for 30 minutes with different DNA substrates. (A) pBR322 DNA (NEB, circular) (B) pBR322 DNA digested with *Eco*RI (4316 bp, linear) (C) PCR product (500 bp, linear). The entire reactions were loaded on 0.8% agarose gels. M: λ DNA/*Eco*RI+*Hind*III marker; Lane1: negative control (DNA substrates + elution buffer); Lane 2-6: DNA substrates + different concentrations of Ni-NTA enriched Yol093wp (2 μl).

7.2.2 Single Strand (ss) and Double Strand (ds) DNA-binding Assays Using Polyacrylamide Gel Electrophoresis (PAGE)

The gel mobility shift assays were also analysed using non-denaturing polyacrylamide gel electrophoresis (PAGE) (section 2.3.3.3).

To assess the DNA binding ability of Ni-NTA enriched Yol093wp and VIVASPIN6 concentrated Yol093wp, a 60 bp ^{32}P-labelled dsDNA ([γ-^{32}P]-dsDNA) was incubated with various amounts of protein, and gel mobility shift assays performed. In the absence of $MgCl_2$, a Yol093wp-ssDNA and Yol093wp-dsDNA complex that did not enter the gel was observed (Figure 7.6A). It revealed that more binding complex was obtained from Ni-NTA enriched Yol093wp and VIVASPIN6 concentrated Yol093wp, which was similar to the result from agarose assays (Figure 7.4). Therefore, Ni-NTA enriched Yol093wp was used for following assessments.

To know if the binding is specific to Yol093wp extracts, not to the vector itself, a 60 bp [γ-^{32}P]-dsDNA or a mobile [γ-^{32}P]-HJ was incubated with 2 μl of Ni-NTA enriched Yol093wp and Ni-NTA enriched mock control proteins on ice for 30 minutes. It showed that Ni-NTA Yol093wp enrichment caused gel mobility shifts to DNA substrates run on polyacryamide gels, whereas Ni-NTA enriched mock did not (Figure 7.6B); similar to that observed for the assays on agarose gels (Figure 7.4). In addition, as revealed in Figure 7.6C, more binding complexes were formed by increasing amounts of Ni-NTA enriched Yol093wp.

To learn about the DNA-binding preferences of Yol093wp extracts, a 60 nt [γ-^{32}P]-ssDNA or a 60 bp [γ-^{32}P]-dsDNA or a mobile [γ-^{32}P]-HJ was incubated with 2 µl of Ni-NTA enriched Yol093wp on ice for 30 minutes and gel mobility assay was performed. It showed that Ni-NTA Yol093wp extracts bound preferentially to the mobile four-way junction compared to a 60 nt-ssDNA or a 60 bp-dsDNA (Figure 7.6D). The difference is also shown in Figure 7.7.

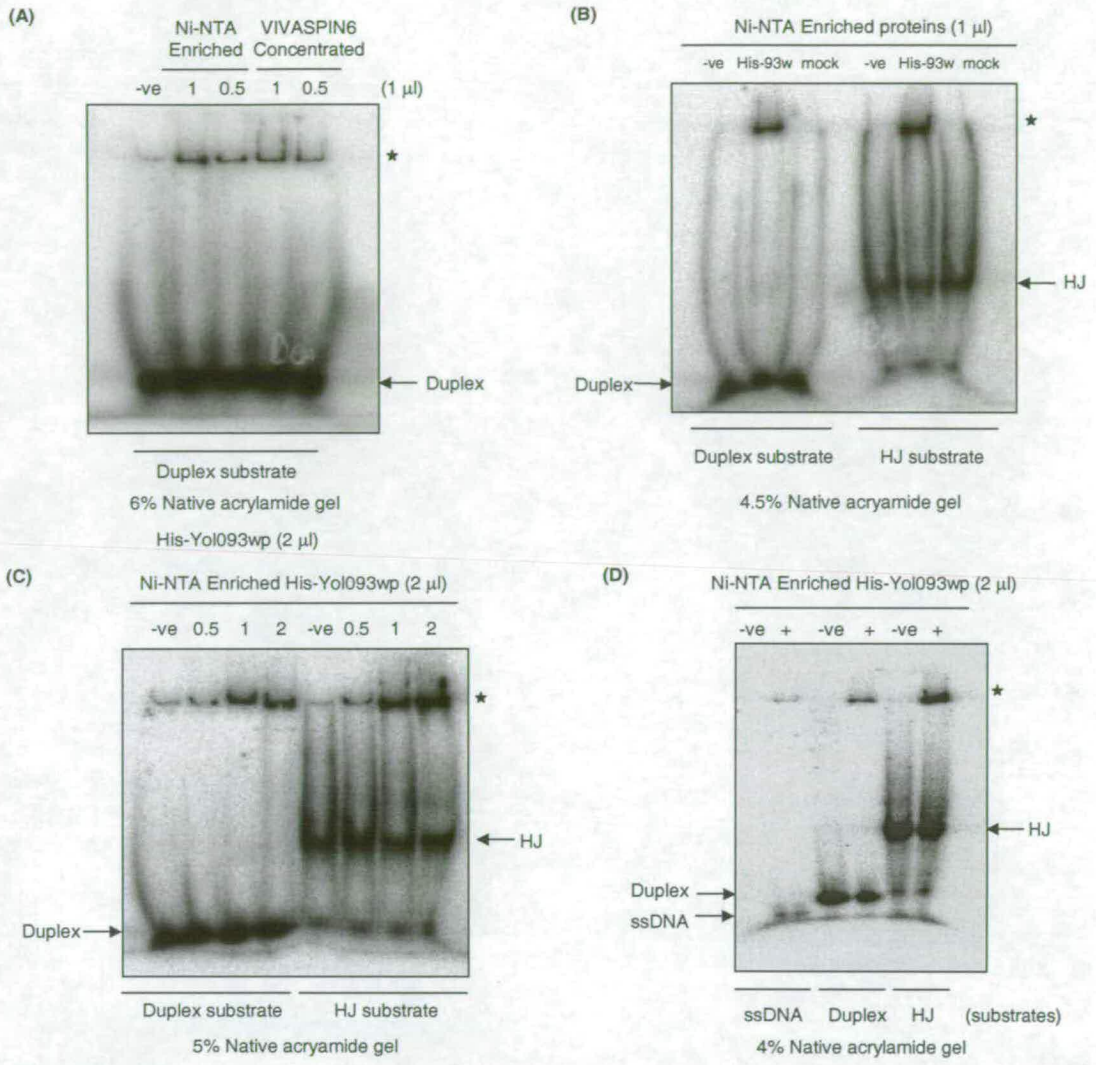

Figure 7.6 Polyacrylamide Gel Electrophoresis of DNA Binding Assays of Yol093wp Extracts (1)

Binding assays were carried out on ice for 30 minutes with various DNA substrates. (A) A 60 bp [γ-^{32}P]-dsDNA was incubated with various amounts of Ni-NTA enriched or VIVASPIN6 concentrated Yol093wp on ice for 30 minutes. (B) A 60 bp [γ-^{32}P]-dsDNA or a [γ-^{32}P]-HJ was incubated with Ni-NTA enriched Yol093wp (1 µl) on ice for 30 minutes. (C) A 60 bp [γ-^{32}P]-dsDNA or a [γ-^{32}P]-HJ was incubated with various amounts of Ni-NTA enriched Yol093wp on ice for 30 minutes. (D) A 60 nt [γ-^{32}P]-ssDNA or a 60 bp [γ-^{32}P]-dsDNA or a mobile [γ-^{32}P]-HJ was incubated with Ni-NTA enriched Yol093wp (2 µl) on ice for 30 minutes. The entire reactions were subjected on 4-6% polyacrylamide gels. -ve: negative control (DNA substrates + elution buffer). The star represents the binding complexes.

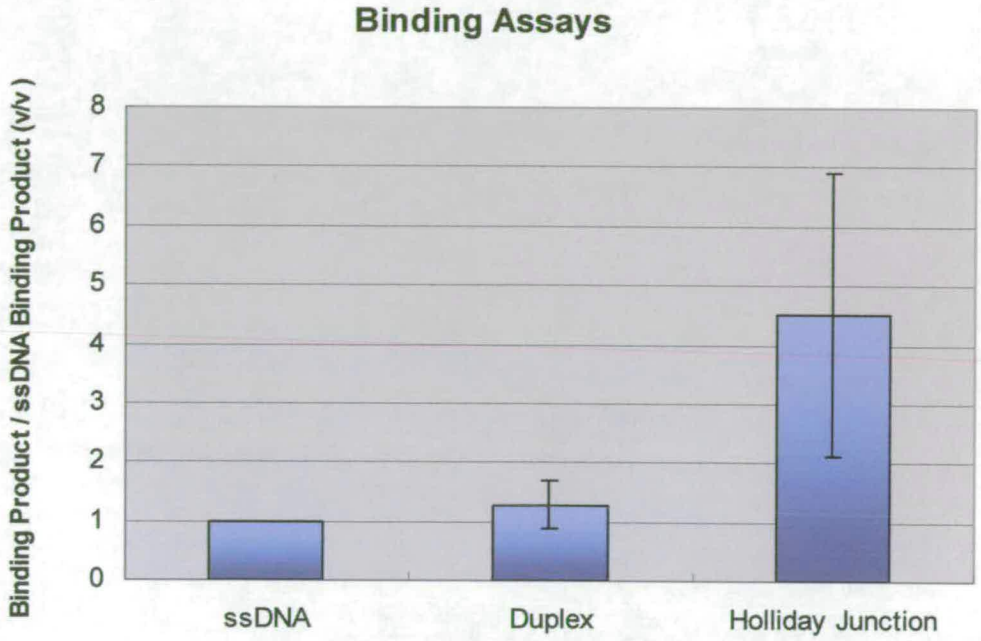

Figure 7.7 A Bar Graph of DNA Binding Assays of Ni-NTA Enriched Yol093wp Using Polyacrylamide Gel Electrophoresis

A 60 nt [γ-^{32}P]-ssDNA or a 60 bp [γ-^{32}P]-dsDNA or a mobile [γ-^{32}P]-HJ was incubated with Ni-NTA enriched Yol093wp (2 μl) on ice for 30 minutes, and gel mobility shift assay was performed. The amounts of substrates and product were determined by ImageQuant program.

As mentioned previously, HJ resolving enzymes are ion-dependent, so the effect of $MgCl_2$ was tested. Furthermore, the effect of *S*-adenosylmethionine (SAM) on the Yol093wp-DNA complexes was also tested (see section 7.3). A 60 nt [γ-^{32}P]-ssDNA or a 60 bp [γ-^{32}P]-dsDNA or a mobile [γ-^{32}P]-HJ was incubated with 2 µl of Ni-NTA enriched Yol093wp in the presence or absence of Mg^{2+} and SAM, and gel mobility shift assay was carried out. In the presence of low (1 mM) and high (10 mM) $MgCl_2$ concentrations, the amounts of the Yol093wp-DNA complexes were similar (Figures 7.7A & B), despite of the amount of Yol093wp-HJ complex was slightly increased in the presence of 5 mM $MgCl_2$ in Figure 7.7A. No difference in the amounts of complexes was detected in the presence or absence of SAM (Figure 7.7B).

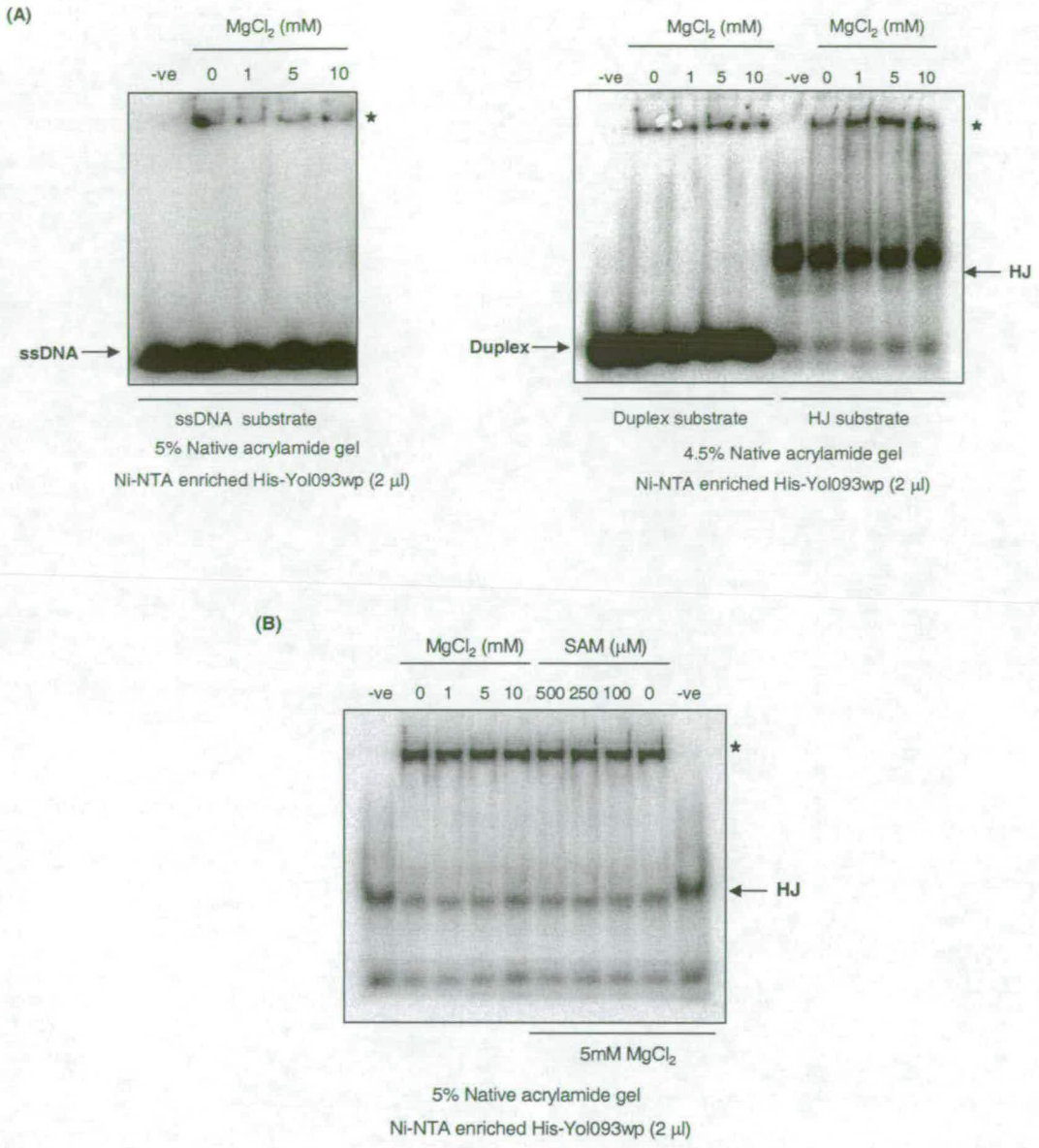

Figure 7.8 DNA Binding Assays of Ni-NTA Yol093wp on Polyacrylamide Gel Electrophoresis (2)

Binding assays were carried out on ice for 30 minutes with different DNA substrates. (A) A 60nt [γ-^{32}P]-ssDNA or a 60bp [γ-^{32}P]-dsDNA or a mobile [γ-^{32}P]-HJ was incubated with Ni-NTA enriched or VIVASPIN6 concentrated Yol093wp (2 µl) with no or the indicated amounts of $MgCl_2$ on ice for 30 minutes. (B) A mobile [γ-^{32}P]-HJ was incubated with Ni-NTA enriched Yol093wp (2 µl) with the indicated amounts of $MgCl_2$ and SAM on ice for 30 minutes. The entire reactions were subjected on 4-6% polyacrylamide gels. -ve: negative control (DNA substrates + elution buffer). The star represents the binding complexes at wells.

7.3 DNA Methylation Activity Assay of Ni-NTA Enriched Yol093wp

Toward the end of this study, Jackman *et al.* revealed that methylation G_9 of yeast $tRNA^{Gly}$ (m^1G_9) is associated with ORF *YOL093W*, named *TRM10* (tRNA methyltransferase) (Jackman et al., 2003). Extracts lacking Trm10p have undetectable levels of m^1G_9 methyltransferase activity but retain normal m^1G_{37} methyltransferase activity. Yeast Trm10p purified from *E. coli* quantitatively modifies the G_9 position of $tRNA^{Gly}$ in the presence of the methyl donor *S*-adenosylmethionine (SAM). Trm10p is responsible *in vivo* for most if not all m^1G_9 modification of tRNAs, based on two results: $tRNA^{Gly}$ purified from a *trm10-Δ/trm10-Δ* strain is lacking detectable m^1G; and a primer extension block occurring at m^1G_9 is removed in *trm10-Δ/trm10-Δ*-derived tRNAs for all 9 m^1G_9-containing species that were testable by this method.

tRNA molecules are extensively modified after transcription. In addition to 5'- and 3'-end maturation, CCA addition, and splicing of introns, all tRNAs contain a number of nucleoside modifications (Bjork, 1995; Grosjean et al., 1997; Hopper and Phizicky, 2003). In *Saccharomyces cerevisiae*, 25 different modifications of base or sugar moieties have been identified within the 34 tRNA species that have been characterized (Sprinzl et al., 1998), and every tRNA molecule has some subset of these modifications, altering nucleoside identity at an average of 11 positions. The identity and position of many of these modifications are highly conserved; however,

despite their widespread conservation, the role that these modifications play in the cell is not fully understood.

One modification of interest is methylation of guanosine (G) at the N-1 position of the base. This modification occurs at two locations in tRNAs. m^1G is found at position 37 in several tRNAs from all three major kingdoms. It is also found at position 9 in several cytoplasmic tRNAs from all eukaryotes that have sequenced tRNAs, in mitochondrial tRNAs from several animal species, in two vertebrate viral tRNAs, and in tRNA from at least one archaeal species (Sprinzl et al., 1998). In the yeast *S. cerevisiae*, m^1G is found at position 9 in 10 tRNAs and at position 37 in 8 tRNAs, with one species, $tRNA^{Pro}$, having m^1G at both positions.

As previously we have shown in this work that Yol093wp extracts had DNA binding activity, methylation assays (section 2.3.3.13) on a mobile HJ with Ni-NTA enriched Yol093wp were performed. As shown in Figure 7.9, by using the purified tRNAs from *E.coli* as a positive control, the Yol093wp (Trm10p) did not reveal DNA (HJ) methylation activity in these assays.

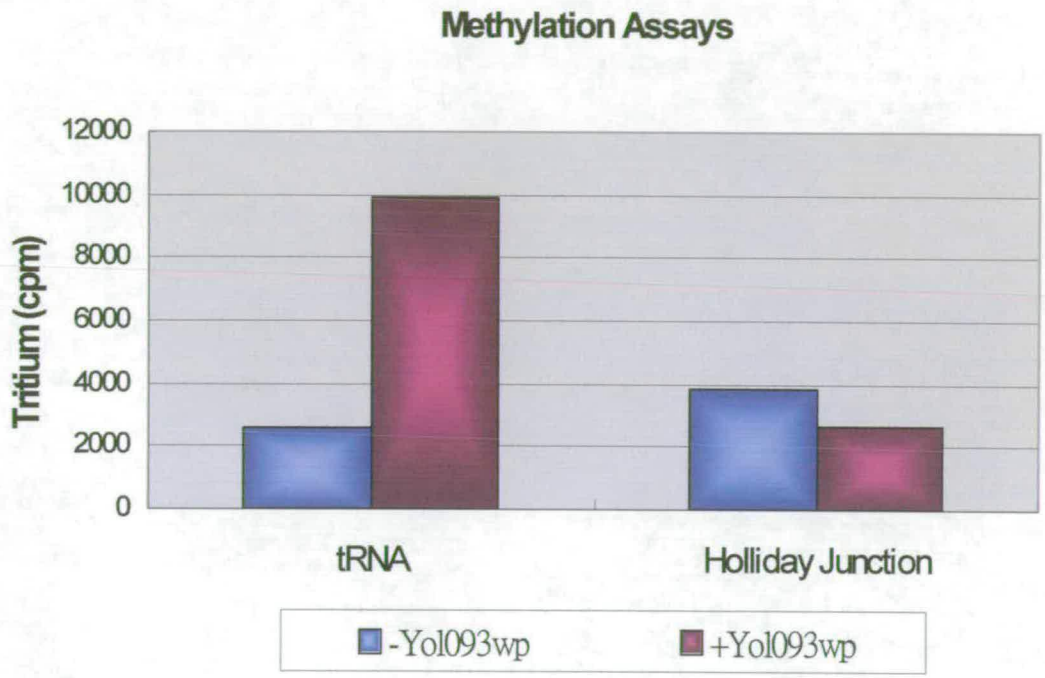

Figure 7.9 Methylation Assays of Ni-NTA Yol093wp Extracts
All methylation reactions were carried out at 30°C for 60 minutes. 2 μl of Ni-NTA Yol093wp was incubated with tRNA or HJ in the presence of 3 μM [methyl-^{3}H]-*S*-adenosylmethionine ([^{3}H]-AdoMet). Samples were then spotted on a 2.5-cm circle of Whatman DE81 paper on a vacuum manifold, and washed with 5 × 1 ml of 0.2 M NH_4HCO_3, 3 × 1 ml of ethanol, and 1 ml of diethyl ether. Tritium was determined in 5 ml of a scintillation fluid.

7.4 Discussion

The *YOL093W* sequence was fused to an N-terminal His tag present in the pET-16b vector, and the His-Yol093w fusion protein was expressed in *E. coli.* Extracts of His-Yol093wp and the mock control were enriched using Ni-NTA His•Bind® Resin column chromatography. The Ni-NTA enriched proteins were then used for biochemical assays.

DNA-binding assays revealed that Ni-NTA enriched Yol093wp caused gel mobility shifts to DNA substrates, whereas Ni-NTA enriched mock did not. This suggested that Ni-NTA enriched Yol093wp might have DNA-binding properties, however, , increasing amounts of Ni-NTA enriched Yol093wp, a decreasing gel mobility shift was observed. It could indicate some protein aggregation might have occurred. It was shown that $MgCl_2$, and *S*-adenosylmethionine (SAM) had no effect on DNA complex formation. Furthermore, the results revealed that Yol093wp extracts bound preferentially to a mobile four-way junction than to a 60 nt-ssDNA or a 60 bp-dsDNA. One should be noted that these experiments were relatively preliminary. Neither the protein concentration nor the molarity of DNA substrates was determined. Therefore, the preferential binding to four-way junctions should be investigated further to elucidate the specificity of this DNA binding. In our methylation assay, Yol093wp extracts did not reveal methylation activity on the mobile four-way junctions using purified tRNAs from *E. coli* MRE 600 as a positive control substrate. As the mechanistic basis for the site specificity and catalysis of m^1G modification by

Yol093wp needs to be further clarified (Jackman et al., 2003), this assay was relatively preliminary.

As the Holliday junction resolvases have junction resolving activity, the enriched Yol093wp could be further investigated for nuclease activity.

CHAPTER EIGHT

Overview

During genetic recombination in meiosis and the repair of DNA strand breaks, DNA molecules become linked at points of strand exchange known as Holliday junctions (Holliday, 1964). Resolution of these DNA structures was postulated by Holliday to be a key event during recombination. Consequently, the search for a DNA endonuclease (resolvase) capable of resolving Holliday junctions has driven research in this field for the last 20 years. Early research was accelerated by new methods to prepare plasmid substrates bearing authentic Holliday junctions and to synthesize structures from oligonucleotides that resemble these junctions. Pioneering work in West's laboratory led to the discovery of a Holliday junction resolvase encoded by the *ruvC* gene in the bacterium *Escherichia coli* (West, 1996). The RuvABC complex has proved a valuable system for understanding movement and resolution of Holliday junctions, but efforts to identify similar activities in eukaryotes have not

been as fruitful. Early efforts to purify a cruciform cleaving activity from yeast resulted in the identification of Cce1p, an enzyme that works in mitochondria (Lockshon et al., 1995). Other studies reported Holliday junction cleavage in extracts of yeast and mammalian tissues, but purification was not sufficient to enable identification of the gene products involved.

Following discovery of the Mus81p-Mms4p (Eme1p) complex in yeast and human cells (Heyer et al., 2003), biologists were optimistic that they had identified the genes encoding the Holliday junction resolvase. Mus81p-Mms4p is a structure-specific endonuclease, which cleaves a variety of branched DNA molecules including Holliday junctions. The discovery that *mus81* homozygous diploid mutants of the fission yeast *Schizosaccharomyces pombe* do not exhibit meiotic crossing over and that this defect is suppressed by expression of the bacterial resolvase RusA provided compelling evidence that Mus81p is the yeast resolvase (Heyer et al., 2003). However, there was concern about the universality of this conclusion given that *mus81* mutants of the budding yeast *Saccharomyces cerevisiae* have no obvious defects in crossing over. Thus, it seemed likely that eukaryotic cells might have another resolvase.

In 2003, two forms of resolvase activity were identified in extracts of cultured human HeLa cells. One was MUS81, and the other co-purified with a branch migration activity. This suggested that the RuvABC resolvasome that cleaves Holliday junctions in bacteria might have a counterpart in eukaryotic cells (Constantinou et al., 2002). The coupled branch migration/resolvase activities (described previously by

West's group) cleave Holliday junctions symmetrically to produce duplex products that can be ligated. In contrast, MUS81-MMS4 preferentially cleaves Y junctions, and the cleavage products from Holliday junctions are not substrates for ligation. Thus, identifying branch migration and resolvase activities in mammalian cells has preoccupied those working on genetic recombination.

In the new work, Liu *et al.* (Liu et al., 2004) follow up on the observation that partially purified HeLa cell fractions catalyze ATP-dependent branch migration and resolution of Holliday junctions. Their most exciting finding is that this activity requires RAD51C, a key recombination/repair protein, but not other proteins known to be involved in resolution or branch migration (MUS81, WRN, or BLM). Depletion of *RAD51C* with a highly specific monoclonal antibody reduced resolution and branch migration to almost background levels; resolvase activity could be reconstituted by adding back recombinant protein complexes containing RAD51C to the depleted fraction. Furthermore, Liu and colleagues discovered that Chinese hamster ovary cell lines lacking RAD51C, or its binding partner XRCC3, had greatly reduced resolvase activity. Together, these *in vitro* results provide compelling evidence that, in eukaryotic cells, the Holliday junction resolvase is either RAD51C itself or another protein that is activated by RAD51C.

RAD51C is a member of a group of proteins called the RAD51 paralog family because they show 20 to 30% sequence identity to RAD51 and to each other (Symington, 2002). The genes encoding the budding yeast Rad51 paralogs, Rad55 and Rad57, were first identified in screens for x-ray-sensitive mutants. Rad55 and

Rad57 are required for spontaneous and double-strand break- induced homologous recombination. Two of the mammalian paralogs, XRCC2 and XRCC3, were identified through genetic studies in which their structural genes were found defective in x-ray-sensitive cell lines. RAD51B, RAD51C, and RAD51D were discovered using polymerase chain reaction and sequence database analysis. All five paralogs have been disrupted in chicken DT40 cell lines--the resulting mutants exhibit defects in genetic recombination and DNA repair (Takata et al., 2001). The paralogs form two complexes: one composed of RAD51C and XRCC3, and the other containing RAD51B, RAD51C, RAD51D, and XRCC2 (Masson et al., 2001). Until recently, the paralogs were thought to act during the early steps of DNA repair by facilitating loading of RAD51 onto single-stranded DNA. This hypothesis was driven by the observation that formation of damage-induced RAD51 subnuclear foci (thought to correspond to sites of DNA repair) is dependent on the paralogs, and that overexpression of RAD51 partially suppresses the DNA-repair defect in paralog mutant cells (Takata et al., 2001). Recent genetic and biochemical studies suggest that the paralogs could also act later during recombination (Brenneman et al., 2002; Yokoyama et al., 2003).

The data that Liu *et al.* present in support of RAD51C being a resolvase or resolvase activator are exciting and persuasive, but certain caveats remain. First, the authors do not show directly that RAD51C cleaves Holliday junctions. *In vitro* studies indicate preferential binding of the RAD51C-XRCC3 complex to single-stranded DNA, which is more suggestive of an early role for this complex in recombination. However, RAD51B does bind to Holliday junctions and could potentially target the

complex to DNA structures formed late during recombination (Yokoyama et al., 2003). Although it remains to be seen whether it is actually RAD51C or an interacting factor that is the resolvase, these studies provide compelling evidence linking the Rad51 paralogs to Holliday junction processing. Without doubt, the exciting findings of Liu and colleagues will spur biochemical and genetic studies of the Rad51 paralog complexes to dissect their late role in recombination, as well as an intensive search for interacting proteins.

In this work, we aimed to identify HJ resolvases through protein sequence alignments. Despite the fact that junction resolvases are structurally diverse with low sequence similarity among any of the known examples, we identified *S. cerevisiae* Yol093wp, a potential HJ resolvase, by the PSI-BLAST search with the sequence of the yeast mitochondrial resolvase Cce1p or Ydc2p. Yol093wp is a highly conserved protein that is widely found in eukaryotes (Figure 1.4). The homologs of the Yol093wp family are poorly related to each other; an observation similar to the families of known resolvases. Besides, the Yol093wp family of proteins is relatively small, which is another characteristic of the known resolvases. As *S. cerevisiae* is recognized as an ideal eukaryotic microorganism for biological studies, and a DNA/RNA binding domain was found at the C-terminal of Yol093wp, Yol093wp was chosen from the family to be investigated in this study.

A variety of general and specific approaches were used to characterize the functions of *YOL093W* in this study. We have shown that His-tagged Yol093wp was expressed and enriched from *E. coli.* Biochemical analysis revealed that Ni-NTA enriched His-

Yol093wp might have DNA binding properties (Chapter 7). However, the gel mobility shift assays showed an indication of protein aggregation. Stoichiometry of binding will be worthy being assessed in the future. One can compete bound dsDNA with HJ DNA. This would help to understand if the protein is DNA binding rather than just aggregating with DNA. Interestingly, *in vitro* studies revealed preferential binding of Yol093wp extracts to the mobile four-way junctions than to a 60 nt-ssDNA or a 60 bp-dsDNA (Chapter 7). The basis of this binding activity is still not known. Further analysis will be required to elucidate the specificity of this DNA binding.

Despite the fact that Jackman *et al.* (Jackman et al., 2003) revealed that cell extracts lacking Yol093wp (named Trm10p) have undetectable levels of m^1G_9 methyltransferase which catalyses the methylation of G residues to m^1G in $tRNA^{Gly}$ at position 9, the role of Trm10 protein still needs to be further clarified. Further studies are required to address the mechanistic basis for the site specificity and catalysis of m^1G modification by Trm10p. A search for homologs of each of two *S. cerevisiae* m^1G methyltransferase proteins (Trm5p and Trm10p) by BLAST yields a distinct family of enzymes for each one. Independent alignments of these two predicted families of m^1G methyltransferases yield core sequences of conserved amino acids within each group; however, none of these blocks of conserved sequence are shared between the two groups of enzymes and their phylogenetic analysis indicates that there might have been functional diversification in this family of proteins. The methyltransferase proteins responsible for m^1G_{37} formation are critical in both bacteria and yeast; *Salmonella typhimurium trmD* mutants and *S. cerevisiae*

trm5 mutants are each severely compromised for growth (Bjork et al., 2001). In contrast, a *trm10*Δ strain does not exhibit any obvious growth defect. Additionally, it is noteworthy that the extended superfamily of Trm5p homologs includes proteins that modify substrates other than tRNA, including rRNA and DNA (Jackman et al., 2003). We previously also revealed that a potential DNA/RNA binding domain was found at the C-terminal of Yol093wp, and showed a preferential binding of the Yol093wp extracts to the mobile DNA four-way junctions which contain G residues at the junctions. These indicate Yol093wp might have various functions in cells in addition to its tRNA methyltransferanse activity. In our methylation assay, Yol093wp extracts did not reveal methylation activity on the mobile four-way junctions using purified tRNAs from *E. coli* MRE 600 as a positive control substrate. As the mechanistic basis for the site specificity and catalysis of m^1G modification by Yol093wp needs to be further clarified (Jackman et al., 2003), this assay was relatively preliminary.

Effect of *YOL093W* deletion on yeast was assessed (Chapter 3). It has been shown that cells lacking Yol093wp have no obvious growth defects under standard growth conditions in rich media. Despite the initial observation that my *YOL093W* deletion MYY3 strain (*yol093wΔkan/yol093wΔhph*) showed lower spore viability and potential non-disjunction phenotypes, unfortunately, transformation of MYY3 with plasmids producing the wild-type Yol093wp did not complement the defect. This suggested that the defect might be not caused by *YOL093W* deletion, but by the interference of another gene in the genome. Similar observations were also suggested in the back-cross experiment and the *YOL093W* gene replacement in the other two *S.*

cerevisiae strains. This circumstance might be avoided by assessing the phenotype more at the very early stage of experiments. One should check more gene-knockout transformants in order to confirm the phenotype is reproducible and is really due to the gene deletion itself. As any meiotic I segregation defect will give a mixture of tetrads with 4, 2 and 0 viable spores as the major classes, and when the diploid parent is heterozygous at a locus, a 2:2 segregation of genotypes in the tetrads is expected. The most consistent reasonable explanation for a 2:2 segregation of live to dead spores in the tetrad of *YOL093W* deletion MYY3 would be a haplo-lethal mutation either associated with the disruption or more likely a random mutation (not insertion of the marker) somewhere else in the genome. Furthermore, meiotic recombination assays were performed in the *YOL093W* deletion strain. No effect on meiotic recombination was revealed.

In this work, the immunofluorescence micrographs of Yol093wp-GFP and Yol093wp-13myc in conjunction with DAPI straining suggested that the Yol093w fusion proteins were located in the nucleus. It is believed that tRNA methylation occurs in the nucleolus, which is not consistent with the observations in this study.

Several general approaches were utilised in this work in order to get more clues about the functions of *YOL093W.* To identify Yol093wp-interacting proteins, a yeast two-hybrid screen and TAP tag purification were used. In the two-hybrid screen, only one protein, Mtl1p, was retrieved with relatively low significance (Chapter 5). The TAP purification of Yol093wp complex showed that the Yol093w protein was expressed in the TAP-tagged strain, and could be purified followed the TAP

purification precedure. However, the proteins that were identified as potential interactors were either common contaminants of TAP-tagging experiments (heat-shock proteins and ribosomal proteins), or a very highly expressed protein (glyceraldehyde-3-phosphate dehydrogenases) (Chapter 5). These data did not generate strong evidence for the *in vivo* interactors of Yol093wp. However, in the other genome-wide two-hybrid analysis showed the interactions between Yol093wp and Mec3p (Ito et al., 2001), Sma1p, or Sml1p (Hazbun et al., 2003). Mec3p is involved in checkpoint control and DNA repair (Foiani et al., 2000). Sml1p is also part of the DNA damage response involved in controlling ribonucleotide reductase (Chabes et al., 1999) and therefore the concentrations of dNTPs (Zhao et al., 1998). Furthermore, Tong *et al.* performed a large-scale study of the yeast genetic interaction network. They showed a synthetic lethal effect between *CDC2* and *YOL093W* (Tong et al., 2004). The *cdc2-1* allele was used in this screen. *CDC2* is a catalytic subunit of DNA polymerase delta and is required for chromosomal DNA replication during mitosis and meiosis (Aguilera and Klein, 1988), intragenic recombination (Gordenin et al., 1992), repair of double strand DNA breaks, and DNA replication during nucleotide excision repair (NER) (Burgers, 1998). Interestingly, if the mutant polymerase causes frequent pausing of replication, then fork reversal may occur and require resolvases for recovery (Grompone et al., 2002). Tong and colleagues also revealed *cdc2-1* had synthetic lethality with genes that were mainly DNA repair, replication, replication checkpoint, and meiotic genes. Among them, there were the putative resolvases: Mms4p (the partner of Mus81p) and Rad57p (the yeast Xrcc3p); checkpoint proteins: Mrc1p, Rad24p, Rad17p and Ddc1p. In fact, Rad17p and Ddc1p interact with Mec3p which is the one

of the interactors of Yol093wp by two hybrid (Kondo et al., 1999); (Ito et al., 2001). It was also shown on the *Schizosaccharomyces pombe GeneDB* that the expression of *S. pombe* Yol093wp is dramatically induced on entry to meiosis. (http://www.genedb.org/genedb/Search?name=SPAC6B12.09&organism=pombe). All these data may not be conclusive, but they were all indicative of the possibility of Yol093wp involving in DNA metabolism. Therefore, in addition to its tRNA methyltransferanse activity, Yol093wp might have various biological function functions in *Sccharomyces cerevisiae*.

References

Aboussekhra, A., Vialard, J. E., Morrison, D. E., de la Torre-Ruiz, M. A., Cernakova, L., Fabre, F. and Lowndes, N. F. (1996). A novel role for the budding yeast RAD9 checkpoint gene in DNA damage-dependent transcription. *Embo J* **15**, 3912-22.

Aguilera, A., Chavez, S. and Malagon, F. (2000). Mitotic recombination in yeast: elements controlling its incidence. *Yeast* **16**, 731-54.

Aguilera, A. and Klein, H. L. (1988). Genetic control of intrachromosomal recombination in Saccharomyces cerevisiae. I. Isolation and genetic characterization of hyper-recombination mutations. *Genetics* **119**, 779-90.

Albala, J. S., Thelen, M. P., Prange, C., Fan, W., Christensen, M., Thompson, L. H. and Lennon, G. G. (1997). Identification of a novel human RAD51 homolog, RAD51B. *Genomics* **46**, 476-9.

Allers, T. and Lichten, M. (2001a). Differential timing and control of noncrossover and crossover recombination during meiosis. *Cell* **106**, 47-57.

Allers, T. and Lichten, M. (2001b). Intermediates of yeast meiotic recombination contain heteroduplex DNA. *Mol Cell* **8**, 225-31.

Amundsen, S. K., Taylor, A. F. and Smith, G. R. (2000). The RecD subunit of the Escherichia coli RecBCD enzyme inhibits RecA loading, homologous recombination, and DNA repair. *Proc Natl Acad Sci U S A* **97**, 7399-404.

Aravind, L. and Koonin, E. V. (2001). Prokaryotic homologs of the eukaryotic DNA-end-binding protein Ku, novel domains in the Ku protein and prediction of a prokaryotic double-strand break repair system. *Genome Res* **11**, 1365-74.

Aravind, L., Makarova, K. S. and Koonin, E. V. (2000). SURVEY AND SUMMARY: holliday junction resolvases and related nucleases: identification of new families, phyletic distribution and evolutionary trajectories. *Nucleic Acids Res* **28**, 3417-32.

Ariyoshi, M., Vassylyev, D. G., Iwasaki, H., Nakamura, H., Shinagawa, H. and Morikawa, K. (1994). Atomic structure of the RuvC resolvase: a holliday junction-specific endonuclease from E. coli. *Cell* **78**, 1063-72.

Arnold, D. A. and Kowalczykowski, S. C. (2000). Facilitated loading of RecA protein is essential to recombination by RecBCD enzyme. *J Biol Chem* **275**, 12261-5.

Aylon, Y. and Kupiec, M. (2003). The checkpoint protein Rad24 of Saccharomyces cerevisiae is involved in processing double-strand break ends and in recombination partner choice. *Mol Cell Biol* **23**, 6585-96.

Aylon, Y. and Kupiec, M. (2004). New insights into the mechanism of homologous recombination in yeast. *Mutat Res* **566**, 231-48.

Bashkirov, V. I., King, J. S., Bashkirova, E. V., Schmuckli-Maurer, J. and Heyer, W. D. (2000). DNA repair protein Rad55 is a terminal substrate of the DNA damage checkpoints. *Mol Cell Biol* **20**, 4393-404.

Baudin, A., Ozier-Kalogeropoulos, O., Denouel, A., Lacroute, F. and Cullin, C. (1993). A simple and efficient method for direct gene deletion in Saccharomyces cerevisiae. *Nucleic Acids Res* **21**, 3329-30.

Bianco, P. R. and Kowalczykowski, S. C. (1997). The recombination hotspot Chi is recognized by the translocating RecBCD enzyme as the single strand of DNA containing the sequence 5'-GCTGGTGG-3'. *Proc Natl Acad Sci U S A* **94**, 6706-11.

Bianco, P. R., Tracy, R. B. and Kowalczykowski, S. C. (1998). DNA strand exchange proteins: a biochemical and physical comparison. *Front Biosci* **3**, D570-603.

Bishop, D. K. and Zickler, D. (2004). Early decision; meiotic crossover interference prior to stable strand exchange and synapsis. *Cell* **117**, 9-15.

Bjork, G. R. (1995). Genetic dissection of synthesis and function of modified nucleosides in bacterial transfer RNA. *Prog Nucleic Acid Res Mol Biol* **50**, 263-338.

Bjork, G. R., Jacobsson, K., Nilsson, K., Johansson, M. J., Bystrom, A. S. and Persson, O. P. (2001). A primordial tRNA modification required for the evolution of life? *Embo J* **20**, 231-9.

Boddy, M. N., Gaillard, P. H., McDonald, W. H., Shanahan, P., Yates, J. R., 3rd and Russell, P. (2001). Mus81-Eme1 are essential components of a Holliday junction resolvase. *Cell* **107**, 537-48.

Boddy, M. N., Lopez-Girona, A., Shanahan, P., Interthal, H., Heyer, W. D. and Russell, P. (2000). Damage tolerance protein Mus81 associates with the FHA1 domain of checkpoint kinase Cds1. *Mol Cell Biol* **20**, 8758-66.

Bond, C. S., Kvaratskhelia, M., Richard, D., White, M. F. and Hunter, W. N. (2001). Structure of Hjc, a Holliday junction resolvase, from Sulfolobus solfataricus. *Proc Natl Acad Sci U S A* **98**, 5509-14.

Borner, G. V., Kleckner, N. and Hunter, N. (2004). Crossover/noncrossover differentiation, synaptonemal complex formation, and regulatory surveillance at the leptotene/zygotene transition of meiosis. *Cell* **117**, 29-45.

Brenneman, M. A., Wagener, B. M., Miller, C. A., Allen, C. and Nickoloff, J. A. (2002). XRCC3 controls the fidelity of homologous recombination: roles for XRCC3 in late stages of recombination. *Mol Cell* **10**, 387-95.

Brent, R. and Ptashne, M. (1985). A eukaryotic transcriptional activator bearing the DNA specificity of a prokaryotic repressor. *Cell* **43**, 729-36.

Burgers, P. M. (1998). Eukaryotic DNA polymerases in DNA replication and DNA repair. *Chromosoma* **107**, 218-27.

Capaldo, F. N., Ramsey, G. and Barbour, S. D. (1974). Analysis of the growth of recombination-deficient strains of Escherichia coli K-12. *J Bacteriol* **118**, 242-9.

Carr, A. M. (2002). DNA structure dependent checkpoints as regulators of DNA repair. *DNA Repair (Amst)* **1**, 983-94.

Cartwright, R., Dunn, A. M., Simpson, P. J., Tambini, C. E. and Thacker, J. (1998). Isolation of novel human and mouse genes of the recA/RAD51 recombination-repair gene family. *Nucleic Acids Res* **26**, 1653-9.

Ceschini, S., Keeley, A., McAlister, M. S., Oram, M., Phelan, J., Pearl, L. H., Tsaneva, I. R. and Barrett, T. E. (2001). Crystal structure of the fission yeast mitochondrial Holliday junction resolvase Ydc2. *Embo J* **20**, 6601-11.

Chabes, A., Domkin, V. and Thelander, L. (1999). Yeast Sml1, a protein inhibitor of ribonucleotide reductase. *J Biol Chem* **274**, 36679-83.

Chen, L., Trujillo, K., Ramos, W., Sung, P. and Tomkinson, A. E. (2001). Promotion of Dnl4-catalyzed DNA end-joining by the Rad50/Mre11/Xrs2 and Hdf1/Hdf2 complexes. *Mol Cell* **8**, 1105-15.

Clyne, R. K., Katis, V. L., Jessop, L., Benjamin, K. R., Herskowitz, I., Lichten, M. and Nasmyth, K. (2003). Polo-like kinase Cdc5 promotes chiasmata formation and cosegregation of sister centromeres at meiosis I. *Nat Cell Biol* **5**, 480-5.

Constantinou, A., Chen, X. B., McGowan, C. H. and West, S. C. (2002). Holliday junction resolution in human cells: two junction endonucleases with distinct substrate specificities. *Embo J* **21**, 5577-85.

Constantinou, A., Davies, A. A. and West, S. C. (2001). Branch migration and Holliday junction resolution catalyzed by activities from mammalian cells. *Cell* **104**, 259-68.

Cox, M. M. (1999). Recombinational DNA repair in bacteria and the RecA protein. *Prog Nucleic Acid Res Mol Biol* **63**, 311-66.

Cox, M. M. (2001). Historical overview: searching for replication help in all of the rec places. *Proc Natl Acad Sci U S A* **98**, 8173-80.

Critchlow, S. E. and Jackson, S. P. (1998). DNA end-joining: from yeast to man. *Trends Biochem Sci* **23**, 394-8.

Davies, A. A. and West, S. C. (1998). Formation of RuvABC-Holliday junction complexes in vitro. *Curr Biol* **8**, 725-7.

de Jager, M., van Noort, J., van Gent, D. C., Dekker, C., Kanaar, R. and Wyman, C. (2001). Human Rad50/Mre11 is a flexible complex that can tether DNA ends. *Mol Cell* **8**, 1129-35.

De Los Santos, T., Hunter, N., Lee, C., Larkin, B., Loidl, J. and Hollingsworth, N. M. (2003). The mus81/mms4 endonuclease acts independently of double-holliday junction resolution to promote a distinct subset of crossovers during meiosis in budding yeast. *Genetics* **164**, 81-94.

de los Santos, T., Loidl, J., Larkin, B. and Hollingsworth, N. M. (2001). A role for MMS4 in the processing of recombination intermediates during meiosis in Saccharomyces cerevisiae. *Genetics* **159**, 1511-25.

Deans, B., Griffin, C. S., Maconochie, M. and Thacker, J. (2000). Xrcc2 is required for genetic stability, embryonic neurogenesis and viability in mice. *Embo J* **19**, 6675-85.

Demianova, M., Formosa, T. G. and Ellis, S. R. (1996). Yeast proteins related to the p40/laminin receptor precursor are essential components of the 40 S ribosomal subunit. *J Biol Chem* **271**, 11383-91.

Doe, C. L., Ahn, J. S., Dixon, J. and Whitby, M. C. (2002). Mus81-Eme1 and Rqh1 involvement in processing stalled and collapsed replication forks. *J Biol Chem* **277**, 32753-9.
Doherty, A. J., Jackson, S. P. and Weller, G. R. (2001). Identification of bacterial homologues of the Ku DNA repair proteins. *FEBS Lett* **500**, 186-8.

Dosanjh, M. K., Collins, D. W., Fan, W., Lennon, G. G., Albala, J. S., Shen, Z. and Schild, D. (1998). Isolation and characterization of RAD51C, a new human member of the RAD51 family of related genes. *Nucleic Acids Res* **26**, 1179-84.

Dubendorff, J. W. and Studier, F. W. (1991). Controlling basal expression in an inducible T7 expression system by blocking the target T7 promoter with lac repressor. *J Mol Biol* **219**, 45-59.

Elborough, K. M. and West, S. C. (1988). Specific binding of cruciform DNA structures by a protein from human extracts. *Nucleic Acids Res* **16**, 3603-16.

Engebrecht, J., Hirsch, J. and Roeder, G. S. (1990). Meiotic gene conversion and crossing over: their relationship to each other and to chromosome synapsis and segregation. *Cell* **62**, 927-37.

Essers, J., Hendriks, R. W., Swagemakers, S. M., Troelstra, C., de Wit, J., Bootsma, D., Hoeijmakers, J. H. and Kanaar, R. (1997). Disruption of mouse RAD54 reduces ionizing radiation resistance and homologous recombination. *Cell* **89**, 195-204.

Essers, J., van Steeg, H., de Wit, J., Swagemakers, S. M., Vermeij, M., Hoeijmakers, J. H. and Kanaar, R. (2000). Homologous and non-homologous recombination differentially affect DNA damage repair in mice. *Embo J* **19**, 1703-10.

Fields, S. and Song, O. (1989). A novel genetic system to detect protein-protein interactions. *Nature* **340**, 245-6.

Foiani, M., Pellicioli, A., Lopes, M., Lucca, C., Ferrari, M., Liberi, G., Muzi Falconi, M. and Plevani, P. (2000). DNA damage checkpoints and DNA replication controls in Saccharomyces cerevisiae. *Mutat Res* **451**, 187-96.

Ford, C. L., Randal-Whitis, L. and Ellis, S. R. (1999). Yeast proteins related to the p40/laminin receptor precursor are required for 20S ribosomal RNA processing and the maturation of 40S ribosomal subunits. *Cancer Res* **59**, 704-10.

Friedberge, E. C., Walker, G. C., Siede, W. (1995). DNA repair and mutagenesis. *American Society for Microbiology, Washington, DC.*

Fromont-Racine, M., Mayes, A. E., Brunet-Simon, A., Rain, J. C., Colley, A., Dix, I., Decourty, L., Joly, N., Ricard, F., Beggs, J. D. et al. (2000). Genome-wide protein interaction screens reveal functional networks involving Sm-like proteins. *Yeast* **17**, 95-110.

Fromont-Racine, M., Rain, J. C. and Legrain, P. (1997). Toward a functional analysis of the yeast genome through exhaustive two-hybrid screens. *Nat Genet* **16**, 277-82.

Fung, J. C., Rockmill, B., Odell, M. and Roeder, G. S. (2004). Imposition of crossover interference through the nonrandom distribution of synapsis initiation complexes. *Cell* **116**, 795-802.

Game, J. C. and Mortimer, R. K. (1974). A genetic study of x-ray sensitive mutants in yeast. *Mutat Res* **24**, 281-92.

Garcia, A. D., Aravind, L., Koonin, E. V. and Moss, B. (2000). Bacterial-type DNA holliday junction resolvases in eukaryotic viruses. *Proc Natl Acad Sci U S A* **97**, 8926-31.

Gardner, R., Putnam, C. W. and Weinert, T. (1999). RAD53, DUN1 and PDS1 define two parallel G2/M checkpoint pathways in budding yeast. *Embo J* **18**, 3173-85.

Garrels, J. I., McLaughlin, C. S., Warner, J. R., Futcher, B., Latter, G. I., Kobayashi, R., Schwender, B., Volpe, T., Anderson, D. S., Mesquita-Fuentes, R. et al. (1997). Proteome studies of Saccharomyces cerevisiae: identification and characterization of abundant proteins. *Electrophoresis* **18**, 1347-60.

Gavin, A. C., Bosche, M., Krause, R., Grandi, P., Marzioch, M., Bauer, A., Schultz, J., Rick, J. M., Michon, A. M., Cruciat, C. M. et al. (2002). Functional organization of the yeast proteome by systematic analysis of protein complexes. *Nature* **415**, 141-7.

Gietz, D., St Jean, A., Woods, R. A. and Schiestl, R. H. (1992). Improved method for high efficiency transformation of intact yeast cells. *Nucleic Acids Res* **20**, 1425.

Gietz, R. D. and Sugino, A. (1988). New yeast-Escherichia coli shuttle vectors constructed with in vitro mutagenized yeast genes lacking six-base pair restriction sites. *Gene* **74**, 527-34.
Gilbert, C. S., Green, C. M. and Lowndes, N. F. (2001). Budding yeast Rad9 is an ATP-dependent Rad53 activating machine. *Mol Cell* **8**, 129-36.

Gilbertson, L. A. and Stahl, F. W. (1996). A test of the double-strand break repair model for meiotic recombination in Saccharomyces cerevisiae. *Genetics* **144**, 27-41.

Goldstein, A. L. and McCusker, J. H. (1999). Three new dominant drug resistance cassettes for gene disruption in Saccharomyces cerevisiae. *Yeast* **15**, 1541-53.

Gordenin, D. A., Malkova, A. L., Peterzen, A., Kulikov, V. N., Pavlov, Y. I., Perkins, E. and Resnick, M. A. (1992). Transposon Tn5 excision in yeast: influence of DNA polymerases alpha, delta, and epsilon and repair genes. *Proc Natl Acad Sci U S A* **89**, 3785-9.

Green, C. M., Erdjument-Bromage, H., Tempst, P. and Lowndes, N. F. (2000). A novel Rad24 checkpoint protein complex closely related to replication factor C. *Curr Biol* **10**, 39-42.

Grompone, G., Seigneur, M., Ehrlich, S. D. and Michel, B. (2002). Replication fork reversal in DNA polymerase III mutants of Escherichia coli: a role for the beta clamp. *Mol Microbiol* **44**, 1331-9.

Grosjean, H., Szweykowska-Kulinska, Z., Motorin, Y., Fasiolo, F. and Simos, G. (1997). Intron-dependent enzymatic formation of modified nucleosides in eukaryotic tRNAs: a review. *Biochimie* **79**, 293-302.

Guldener, U., Heck, S., Fielder, T., Beinhauer, J. and Hegemann, J. H. (1996). A new efficient gene disruption cassette for repeated use in budding yeast. *Nucleic Acids Res* **24**, 2519-24.

Haber, J. E. (1999). DNA recombination: the replication connection. *Trends Biochem Sci* **24**, 271-5.

Haber, J. E. and Heyer, W. D. (2001). The fuss about Mus81. *Cell* **107**, 551-4.

Hadden, J. M., Convery, M. A., Declais, A. C., Lilley, D. M. and Phillips, S. E. (2001). Crystal structure of the Holliday junction resolving enzyme T7 endonuclease I. *Nat Struct Biol* **8**, 62-7.

Harmon, F. G. and Kowalczykowski, S. C. (1998). RecQ helicase, in concert with RecA and SSB proteins, initiates and disrupts DNA recombination. *Genes Dev* **12**, 1134-44.

Hartwell, L. H. and Weinert, T. A. (1989). Checkpoints: controls that ensure the order of cell cycle events. *Science* **246**, 629-34.

Hazbun, T. R., Malmstrom, L., Anderson, S., Graczyk, B. J., Fox, B., Riffle, M., Sundin, B. A., Aranda, J. D., McDonald, W. H., Chiu, C. H. et al. (2003). Assigning function to yeast proteins by integration of technologies. *Mol Cell* **12**, 1353-65.

Hendrickson, E. A. (1997). Cell-cycle regulation of mammalian DNA double-strand-break repair. *Am J Hum Genet* **61**, 795-800.

Heyer, W. D. (2004). Recombination: Holliday junction resolution and crossover formation. *Curr Biol* **14**, R56-8.

Heyer, W. D., Ehmsen, K. T. and Solinger, J. A. (2003). Holliday junctions in the eukaryotic nucleus: resolution in sight? *Trends Biochem Sci* **28**, 548-57.

Hoffman, C. S. and Winston, F. (1987). A ten-minute DNA preparation from yeast efficiently releases autonomous plasmids for transformation of Escherichia coli. *Gene* **57**, 267-72.

Holland, J. P., Labieniec, L., Swimmer, C. and Holland, M. J. (1983). Homologous nucleotide sequences at the 5' termini of messenger RNAs synthesized from the yeast enolase and glyceraldehyde-3-phosphate dehydrogenase gene families. The primary structure of a third yeast glyceraldehyde-3-phosphate dehydrogenase gene. *J Biol Chem* **258**, 5291-9.

Holland, M. J. and Holland, J. P. (1979). Isolation and characterization of a gene coding for glyceraldehyde-3-phosphate dehydrogenase from Saccharomyces cerevisiae. *J Biol Chem* **254**, 5466-74.

Hollenberg, S. M., Sternglanz, R., Cheng, P. F. and Weintraub, H. (1995). Identification of a new family of tissue-specific basic helix-loop-helix proteins with a two-hybrid system. *Mol Cell Biol* **15**, 3813-22.

Holliday, R. (1964). A mechanism for gene conversion in fungi. *Genet Res* **5**, 282-304.
Hopper, A. K. and Phizicky, E. M. (2003). tRNA transfers to the limelight. *Genes Dev* **17**, 162-80.

Huh, W. K., Falvo, J. V., Gerke, L. C., Carroll, A. S., Howson, R. W., Weissman, J. S. and O'Shea, E. K. (2003). Global analysis of protein localization in budding yeast. *Nature* **425**, 686-91.

Hunter, N. and Kleckner, N. (2001). The single-end invasion: an asymmetric intermediate at the double-strand break to double-holliday junction transition of meiotic recombination. *Cell* **106**, 59-70.

Interthal, H. and Heyer, W. D. (2000). MUS81 encodes a novel helix-hairpin-helix protein involved in the response to UV- and methylation-induced DNA damage in Saccharomyces cerevisiae. *Mol Gen Genet* **263**, 812-27.

Ishitani, R., Tajima, H., Takata, H., Tsuchiya, K., Kuwae, T., Yamada, M., Takahashi, H., Tatton, N. A. and Katsube, N. (2003). Proapoptotic protein glyceraldehyde-3-phosphate dehydrogenase: a possible site of action of antiapoptotic drugs. *Prog Neuropsychopharmacol Biol Psychiatry* **27**, 291-301.

Ito, T., Chiba, T., Ozawa, R., Yoshida, M., Hattori, M. and Sakaki, Y. (2001). A comprehensive two-hybrid analysis to explore the yeast protein interactome. *Proc Natl Acad Sci U S A* **98**, 4569-74.

Jackman, J. E., Montange, R. K., Malik, H. S. and Phizicky, E. M. (2003). Identification of the yeast gene encoding the tRNA m1G methyltransferase responsible for modification at position 9. *Rna* **9**, 574-85.

Jackson, S. P. (1999). Colworth Medal lecture. Detection, repair and signalling of DNA double-strand breaks. *Biochem Soc Trans* **27**, 1-13.

Jeggo, P. A.[a] (1998). Identification of genes involved in repair of DNA double-strand breaks in mammalian cells. *Radiat Res* **150**, S80-91.

Jeggo, P. A.[b] (1998). DNA breakage and repair. *Adv Genet* **38**, 185-218.

Johnson, R. D. and Jasin, M. (2001). Double-strand-break-induced homologous recombination in mammalian cells. *Biochem Soc Trans* **29**, 196-201.

Kaliraman, V., Mullen, J. R., Fricke, W. M., Bastin-Shanower, S. A. and Brill, S. J. (2001). Functional overlap between Sgs1-Top3 and the Mms4-Mus81 endonuclease. *Genes Dev* **15**, 2730-40.

Kanaar, R., Hoeijmakers, J. H. and van Gent, D. C. (1998). Molecular mechanisms of DNA double strand break repair. *Trends Cell Biol* **8**, 483-9.

Kiser, G. L. and Weinert, T. A. (1996). Distinct roles of yeast MEC and RAD checkpoint genes in transcriptional induction after DNA damage and implications for function. *Mol Biol Cell* **7**, 703-18.

Kogoma, T. (1997). Stable DNA replication: interplay between DNA replication, homologous recombination, and transcription. *Microbiol Mol Biol Rev* **61**, 212-38.

Kondo, T., Matsumoto, K. and Sugimoto, K. (1999). Role of a complex containing Rad17, Mec3, and Ddc1 in the yeast DNA damage checkpoint pathway. *Mol Cell Biol* **19**, 1136-43.

Kondo, T., Wakayama, T., Naiki, T., Matsumoto, K. and Sugimoto, K. (2001). Recruitment of Mec1 and Ddc1 checkpoint proteins to double-strand breaks through distinct mechanisms. *Science* **294**, 867-70.

Kowalczykowski, S. C. (2000). Initiation of genetic recombination and recombination-dependent replication. *Trends Biochem Sci* **25**, 156-65.

Kowalczykowski, S. C., Dixon, D. A., Eggleston, A. K., Lauder, S. D. and Rehrauer, W. M. (1994). Biochemistry of homologous recombination in Escherichia coli. *Microbiol Rev* **58**, 401-65.

Krebs, E. G. (1953). Yeast Glyceraldehyde-3-phosphate dehydrogenase. I. Electrophoresis of fractions precipitated by nucleic acid. *J Biol Chem* **200**, 471-8.

Kuzminov, A. (2001). DNA replication meets genetic exchange: chromosomal damage and its repair by homologous recombination. *Proc Natl Acad Sci U S A* **98**, 8461-8.

Langle-Rouault, F. and Jacobs, E. (1995). A method for performing precise alterations in the yeast genome using a recycable selectable marker. *Nucleic Acids Res* **23**, 3079-81.

Leasure, C. S., Chandler, J., Gilbert, D. J., Householder, D. B., Stephens, R., Copeland, N. G., Jenkins, N. A. and Sharan, S. K. (2001). Sequence, chromosomal location and expression analysis of the murine homologue of human RAD51L2/RAD51C. *Gene* **271**, 59-67.

Liang, F., Han, M., Romanienko, P. J. and Jasin, M. (1998). Homology-directed repair is a major double-strand break repair pathway in mammalian cells. *Proc Natl Acad Sci U S A* **95**, 5172-7.

Lilley, D. M. and White, M. F. (2000). Resolving the relationships of resolving enzymes. *Proc Natl Acad Sci U S A* **97**, 9351-3.

Lilley, D. M. and White, M. F. (2001). The junction-resolving enzymes. *Nat Rev Mol Cell Biol* **2**, 433-43.

Lim, D. S. and Hasty, P. (1996). A mutation in mouse rad51 results in an early embryonic lethal that is suppressed by a mutation in p53. *Mol Cell Biol* **16**, 7133-43.

Lindahl, T. a. W., S.C. (1995). DNA repair and recombination. *Chapman & Hall, London, UK.*

Liu, N., Lamerdin, J. E., Tebbs, R. S., Schild, D., Tucker, J. D., Shen, M. R., Brookman, K. W., Siciliano, M. J., Walter, C. A., Fan, W. et al. (1998). XRCC2 and XRCC3, new human Rad51-family members, promote chromosome stability and protect against DNA cross-links and other damages. *Mol Cell* **1**, 783-93.

Liu, Y., Masson, J. Y., Shah, R., O'Regan, P. and West, S. C. (2004). RAD51C is required for Holliday junction processing in mammalian cells. *Science* **303**, 243-6.

Lloyd, R. G. a. L., K. B. (1996). Homologous recombination, in Escherichia coli and Salmonella: cellular and molecular biology. *ASM Press, Washington, D. C.*, p2236-2255.

Lockshon, D., Zweifel, S. G., Freeman-Cook, L. L., Lorimer, H. E., Brewer, B. J. and Fangman, W. L. (1995). A role for recombination junctions in the segregation of mitochondrial DNA in yeast. *Cell* **81**, 947-55.

Longtine, M. S., McKenzie, A., 3rd, Demarini, D. J., Shah, N. G., Wach, A., Brachat, A., Philippsen, P. and Pringle, J. R. (1998). Additional modules for versatile and economical PCR-based gene deletion and modification in Saccharomyces cerevisiae. *Yeast* **14**, 953-61.

Lorenz, M. C., Muir, R. S., Lim, E., McElver, J., Weber, S. C. and Heitman, J. (1995). Gene disruption with PCR products in Saccharomyces cerevisiae. *Gene* **158**, 113-7.

Luo, G., Yao, M. S., Bender, C. F., Mills, M., Bladl, A. R., Bradley, A. and Petrini, J. H. (1999). Disruption of mRad50 causes embryonic stem cell lethality, abnormal embryonic development, and sensitivity to ionizing radiation. *Proc Natl Acad Sci U S A* **96**, 7376-81.

Mahdi, A. A., Sharples, G. J., Mandal, T. N. and Lloyd, R. G. (1996). Holliday junction resolvases encoded by homologous rusA genes in Escherichia coli K-12 and phage 82. *J Mol Biol* **257**, 561-73.

Masson, J. Y., Tarsounas, M. C., Stasiak, A. Z., Stasiak, A., Shah, R., McIlwraith, M. J., Benson, F. E. and West, S. C. (2001). Identification and purification of two distinct complexes containing the five RAD51 paralogs. *Genes Dev* **15**, 3296-307.

McAlister, L. and Holland, M. J. (1985). Differential expression of the three yeast glyceraldehyde-3-phosphate dehydrogenase genes. *J Biol Chem* **260**, 15019-27.

Melo, J. and Toczyski, D. (2002). A unified view of the DNA-damage checkpoint. *Curr Opin Cell Biol* **14**, 237-45.

Meyer, R. R. and Laine, P. S. (1990). The single-stranded DNA-binding protein of Escherichia coli. *Microbiol Rev* **54**, 342-80.

Morimatsu, K. and Kowalczykowski, S. C. (2003). RecFOR proteins load RecA protein onto gapped DNA to accelerate DNA strand exchange: a universal step of recombinational repair. *Mol Cell* **11**, 1337-47.

Morita, T., Yoshimura, Y., Yamamoto, A., Murata, K., Mori, M., Yamamoto, H. and Matsushiro, A. (1993). A mouse homolog of the Escherichia coli recA and Saccharomyces cerevisiae RAD51 genes. *Proc Natl Acad Sci U S A* **90**, 6577-80.

Morrison, C. and Takeda, S. (2000). Genetic analysis of homologous DNA recombination in vertebrate somatic cells. *Int J Biochem Cell Biol* **32**, 817-31.

Mukai, H., Kuno, T., Tanaka, H., Hirata, D., Miyakawa, T. and Tanaka, C. (1993). Isolation and characterization of SSE1 and SSE2, new members of the yeast HSP70 multigene family. *Gene* **132**, 57-66.

Naiki, T., Shimomura, T., Kondo, T., Matsumoto, K. and Sugimoto, K. (2000). Rfc5, in cooperation with rad24, controls DNA damage checkpoints throughout the cell cycle in Saccharomyces cerevisiae. *Mol Cell Biol* **20**, 5888-96.

Nassif, N., Penney, J., Pal, S., Engels, W. R. and Gloor, G. B. (1994). Efficient copying of nonhomologous sequences from ectopic sites via P-element-induced gap repair. *Mol Cell Biol* **14**, 1613-25.

Niedernhofer, L. J., Essers, J., Weeda, G., Beverloo, B., de Wit, J., Muijtjens, M., Odijk, H., Hoeijmakers, J. H. and Kanaar, R. (2001). The structure-specific endonuclease Ercc1-Xpf is required for targeted gene replacement in embryonic stem cells. *Embo J* **20**, 6540-9.

Nishino, T., Komori, K., Tsuchiya, D., Ishino, Y. and Morikawa, K. (2001). Crystal structure of the archaeal holliday junction resolvase Hjc and implications for DNA recognition. *Structure (Camb)* **9**, 197-204.

Ochiai, M., Ubagai, T., Kawamori, T., Imai, H., Sugimura, T. and Nakagama, H. (2001). High susceptibility of Scid mice to colon carcinogenesis induced by azoxymethane indicates a possible caretaker role for DNA-dependent protein kinase. *Carcinogenesis* **22**, 1551-5.

Osman, F., Dixon, J., Doe, C. L. and Whitby, M. C. (2003). Generating crossovers by resolution of nicked Holliday junctions: a role for Mus81-Eme1 in meiosis. *Mol Cell* **12**, 761-74.

Ozols, J. (1990). Amino acid analysis. *Methods Enzymol* **182**, 587-601.

Paciotti, V., Lucchini, G., Plevani, P. and Longhese, M. P. (1998). Mec1p is essential for phosphorylation of the yeast DNA damage checkpoint protein Ddc1p, which physically interacts with Mec3p. *Embo J* **17**, 4199-209.

Paques, F. and Haber, J. E. (1999). Multiple pathways of recombination induced by double-strand breaks in Saccharomyces cerevisiae. *Microbiol Mol Biol Rev* **63**, 349-404.

Park, M. S. (1995). Expression of human RAD52 confers resistance to ionizing radiation in mammalian cells. *J Biol Chem* **270**, 15467-70.

Parsons, C. A., Stasiak, A. and West, S. C. (1995). The E.coli RuvAB proteins branch migrate Holliday junctions through heterologous DNA sequences in a reaction facilitated by SSB. *Embo J* **14**, 5736-44.

Pastink, A., Eeken, J. C. and Lohman, P. H. (2001). Genomic integrity and the repair of double-strand DNA breaks. *Mutat Res* **480-481**, 37-50.

Pastink, A. and Lohman, P. H. (1999). Repair and consequences of double-strand breaks in DNA. *Mutat Res* **428**, 141-56.

Paull, T. T. and Gellert, M. (2000). A mechanistic basis for Mre11-directed DNA joining at microhomologies. *Proc Natl Acad Sci U S A* **97**, 6409-14.

Petes, T. D., Detloff, P., Jinks-Robertson, S., Judd, S. R., Kupiec, M., Nag, D., Stapleton, A., Symington, L. S., Vincent, A. and White, M. (1989). Recombination in yeast and the recombinant DNA technology. *Genome* **31**, 536-40.

Petrini, J. H., Walsh, M. E., DiMare, C., Chen, X. N., Korenberg, J. R. and Weaver, D. T. (1995). Isolation and characterization of the human MRE11 homologue. *Genomics* **29**, 80-6.

Pittman, D. L. and Schimenti, J. C. (2000). Midgestation lethality in mice deficient for the RecA-related gene, Rad51d/Rad51l3. *Genesis* **26**, 167-73.

Pittman, D. L., Weinberg, L. R. and Schimenti, J. C. (1998). Identification, characterization, and genetic mapping of Rad51d, a new mouse and human RAD51/RecA-related gene. *Genomics* **49**, 103-11.

Planta, R. J. and Mager, W. H. (1998). The list of cytoplasmic ribosomal proteins of Saccharomyces cerevisiae. *Yeast* **14**, 471-7.

Porter, S. E., White, M. A. and Petes, T. D. (1993). Genetic evidence that the meiotic recombination hotspot at the HIS4 locus of Saccharomyces cerevisiae does not represent a site for a symmetrically processed double-strand break. *Genetics* **134**, 5-19.

Puig, O., Caspary, F., Rigaut, G., Rutz, B., Bouveret, E., Bragado-Nilsson, E., Wilm, M. and Seraphin, B. (2001). The tandem affinity purification (TAP) method: a general procedure of protein complex purification. *Methods* **24**, 218-29.

Raaijmakers, H., Vix, O., Toro, I., Golz, S., Kemper, B. and Suck, D. (1999). X-ray structure of T4 endonuclease VII: a DNA junction resolvase with a novel fold and unusual domain-swapped dimer architecture. *Embo J* **18**, 1447-58.

Rabitsch, K. P., Toth, A., Galova, M., Schleiffer, A., Schaffner, G., Aigner, E., Rupp, C., Penkner, A. M., Moreno-Borchart, A. C., Primig, M. et al. (2001). A screen for genes required for meiosis and spore formation based on whole-genome expression. *Curr Biol* **11**, 1001-9.

Rafferty, J. B., Bolt, E. L., Muranova, T. A., Sedelnikova, S. E., Leonard, P., Pasquo, A., Baker, P. J., Rice, D. W., Sharples, G. J. and Lloyd, R. G. (2003). The structure of Escherichia coli RusA endonuclease reveals a new Holliday junction DNA binding fold. *Structure (Camb)* **11**, 1557-67.

Rafferty, J. B., Sedelnikova, S. E., Hargreaves, D., Artymiuk, P. J., Baker, P. J., Sharples, G. J., Mahdi, A. A., Lloyd, R. G. and Rice, D. W. (1996). Crystal structure of DNA recombination protein RuvA and a model for its binding to the Holliday junction. *Science* **274**, 415-21.

Riballo, E., Doherty, A. J., Dai, Y., Stiff, T., Oettinger, M. A., Jeggo, P. A. and Kysela, B. (2001). Cellular and biochemical impact of a mutation in DNA ligase IV conferring clinical radiosensitivity. *J Biol Chem* **276**, 31124-32.

Rigaut, G., Shevchenko, A., Rutz, B., Wilm, M., Mann, M. and Seraphin, B. (1999). A generic protein purification method for protein complex characterization and proteome exploration. *Nat Biotechnol* **17**, 1030-2.

Rijkers, T., Van Den Ouweland, J., Morolli, B., Rolink, A. G., Baarends, W. M., Van Sloun, P. P., Lohman, P. H. and Pastink, A. (1998). Targeted inactivation of mouse RAD52 reduces homologous recombination but not resistance to ionizing radiation. *Mol Cell Biol* **18**, 6423-9.

Roca, A. I. and Cox, M. M. (1997). RecA protein: structure, function, and role in recombinational DNA repair. *Prog Nucleic Acid Res Mol Biol* **56**, 129-223.

Roeder, G. S. (1997). Meiotic chromosomes: it takes two to tango. *Genes Dev* **11**, 2600-21.

Roman, L. J., Dixon, D. A. and Kowalczykowski, S. C. (1991). RecBCD-dependent joint molecule formation promoted by the Escherichia coli RecA and SSB proteins. *Proc Natl Acad Sci U S A* **88**, 3367-71.

Rouse, J. and Jackson, S. P. (2002). Lcd1p recruits Mec1p to DNA lesions in vitro and in vivo. *Mol Cell* **9**, 857-69.

Schwartz, M. F., Duong, J. K., Sun, Z., Morrow, J. S., Pradhan, D. and Stern, D. F. (2002). Rad9 phosphorylation sites couple Rad53 to the Saccharomyces cerevisiae DNA damage checkpoint. *Mol Cell* **9**, 1055-65.

Scott, K. L. and Plon, S. E. (2003). Loss of Sin3/Rpd3 histone deacetylase restores the DNA damage response in checkpoint-deficient strains of Saccharomyces cerevisiae. *Mol Cell Biol* **23**, 4522-31.

Shinohara, A., Ogawa, H., Matsuda, Y., Ushio, N., Ikeo, K. and Ogawa, T. (1993). Cloning of human, mouse and fission yeast recombination genes homologous to RAD51 and recA. *Nat Genet* **4**, 239-43.

Shu, Z., Smith, S., Wang, L., Rice, M. C. and Kmiec, E. B. (1999). Disruption of muREC2/RAD51L1 in mice results in early embryonic lethality which can Be partially rescued in a p53(-/-) background. *Mol Cell Biol* **19**, 8686-93.

Siede, W., Friedl, A. A., Dianova, I., Eckardt-Schupp, F. and Friedberg, E. C. (1996). The Saccharomyces cerevisiae Ku autoantigen homologue affects radiosensitivity only in the absence of homologous recombination. *Genetics* **142**, 91-102.

Sikorski, R. S. and Hieter, P. (1989). A system of shuttle vectors and yeast host strains designed for efficient manipulation of DNA in Saccharomyces cerevisiae. *Genetics* **122**, 19-27.

Smith, P. J. a. J., C. (2000). DNA recombination and repair. *Oxford University Press, Oxford, UK.*

Sprinzl, M., Horn, C., Brown, M., Ioudovitch, A. and Steinberg, S. (1998). Compilation of tRNA sequences and sequences of tRNA genes. *Nucleic Acids Res* **26**, 148-53.

Storlazzi, A., Xu, L., Schwacha, A. and Kleckner, N. (1996). Synaptonemal complex (SC) component Zip1 plays a role in meiotic recombination independent of SC polymerization along the chromosomes. *Proc Natl Acad Sci U S A* **93**, 9043-8.

Strathern, J. N., Klar, A. J., Hicks, J. B., Abraham, J. A., Ivy, J. M., Nasmyth, K. A. and McGill, C. (1982). Homothallic switching of yeast mating type cassettes is initiated by a double-stranded cut in the MAT locus. *Cell* **31**, 183-92.

Sung, P., Trujillo, K. M. and Van Komen, S. (2000). Recombination factors of Saccharomyces cerevisiae. *Mutat Res* **451**, 257-75.

Symington, L. S. (2002). Role of RAD52 epistasis group genes in homologous recombination and double-strand break repair. *Microbiol Mol Biol Rev* **66**, 630-70, table of contents.

Szostak, J. W., Orr-Weaver, T. L., Rothstein, R. J. and Stahl, F. W. (1983). The double-strand-break repair model for recombination. *Cell* **33**, 25-35.

Takata, M., Sasaki, M. S., Sonoda, E., Morrison, C., Hashimoto, M., Utsumi, H., Yamaguchi-Iwai, Y., Shinohara, A. and Takeda, S. (1998). Homologous recombination and non-homologous end-joining pathways of DNA double-strand break repair have overlapping roles in the maintenance of chromosomal integrity in vertebrate cells. *Embo J* **17**, 5497-508.

Takata, M., Sasaki, M. S., Tachiiri, S., Fukushima, T., Sonoda, E., Schild, D., Thompson, L. H. and Takeda, S. (2001). Chromosome instability and defective recombinational repair in knockout mutants of the five Rad51 paralogs. *Mol Cell Biol* **21**, 2858-66.

Tambini, C. E., George, A. M., Rommens, J. M., Tsui, L. C., Scherer, S. W. and Thacker, J. (1997). The XRCC2 DNA repair gene: identification of a positional candidate. *Genomics* **41**, 84-92.

Tanaka, K., Hiramoto, T., Fukuda, T. and Miyagawa, K. (2000). A novel human rad54 homologue, Rad54B, associates with Rad51. *J Biol Chem* **275**, 26316-21.

Tebbs, R. S., Zhao, Y., Tucker, J. D., Scheerer, J. B., Siciliano, M. J., Hwang, M., Liu, N., Legerski, R. J. and Thompson, L. H. (1995). Correction of chromosomal instability and sensitivity to diverse mutagens by a cloned cDNA of the XRCC3 DNA repair gene. *Proc Natl Acad Sci U S A* **92**, 6354-8.

Thacker, J. (1986). The nature of mutants induced by ionising radiation in cultured hamster cells. III. Molecular characterization of HPRT-deficient mutants induced by gamma-rays or alpha-particles showing that the majority have deletions of all or part of the hprt gene. *Mutat Res* **160**, 267-75.

Thompson, L. H. and Schild, D. (1999). The contribution of homologous recombination in preserving genome integrity in mammalian cells. *Biochimie* **81**, 87-105.

Thompson, L. H. and Schild, D. (2001). Homologous recombinational repair of DNA ensures mammalian chromosome stability. *Mutat Res* **477**, 131-53.

Tong, A. H., Lesage, G., Bader, G. D., Ding, H., Xu, H., Xin, X., Young, J., Berriz, G. F., Brost, R. L., Chang, M. et al. (2004). Global mapping of the yeast genetic interaction network. *Science* **303**, 808-13.

Tsukamoto, Y. and Ikeda, H. (1998). Double-strand break repair mediated by DNA end-joining. *Genes Cells* **3**, 135-44.

Tsuzuki, T., Fujii, Y., Sakumi, K., Tominaga, Y., Nakao, K., Sekiguchi, M., Matsushiro, A., Yoshimura, Y. and MoritaT. (1996). Targeted disruption of the Rad51 gene leads to lethality in embryonic mice. *Proc Natl Acad Sci U S A* **93**, 6236-40.

Umezu, K. and Kolodner, R. D. (1994). Protein interactions in genetic recombination in Escherichia coli. Interactions involving RecO and RecR overcome the inhibition of RecA by single-stranded DNA-binding protein. *J Biol Chem* **269**, 30005-13.

van den Bosch, M., Lohman, P. H. and Pastink, A. (2002). DNA double-strand break repair by homologous recombination. *Biol Chem* **383**, 873-92.

van Gool, A. J., Hajibagheri, N. M., Stasiak, A. and West, S. C. (1999). Assembly of the Escherichia coli RuvABC resolvasome directs the orientation of holliday junction resolution. *Genes Dev* **13**, 1861-70.

van Gool, A. J., Shah, R., Mezard, C. and West, S. C. (1998). Functional interactions between the holliday junction resolvase and the branch migration motor of Escherichia coli. *Embo J* **17**, 1838-45.

Venclovas, C., Colvin, M. E. and Thelen, M. P. (2002). Molecular modeling-based analysis of interactions in the RFC-dependent clamp-loading process. *Protein Sci* **11**, 2403-16.

Venclovas, C. and Siksnys, V. (1995). Different enzymes with similar structures involved in Mg(2+)-mediated polynucleotidyl transfer. *Nat Struct Biol* **2**, 838-41.

Wach, A., Brachat, A., Pohlmann, R. and Philippsen, P. (1994). New heterologous modules for classical or PCR-based gene disruptions in Saccharomyces cerevisiae. *Yeast* **10**, 1793-808.

Weiner, B. M. and Kleckner, N. (1994). Chromosome pairing via multiple interstitial interactions before and during meiosis in yeast. *Cell* **77**, 977-91.

West, S. C. (1992). Enzymes and molecular mechanisms of genetic recombination. *Annu Rev Biochem* **61**, 603-40.

West, S. C. (1996). The RuvABC proteins and Holliday junction processing in Escherichia coli. *J Bacteriol* **178**, 1237-41.

West, S. C. (1997). Processing of recombination intermediates by the RuvABC proteins. *Annu Rev Genet* **31**, 213-44.

Whitby, M. C., Bolt, E. L., Chan, S. N. and Lloyd, R. G. (1996). Interactions between RuvA and RuvC at Holliday junctions: inhibition of junction cleavage and formation of a RuvA-RuvC-DNA complex. *J Mol Biol* **264**, 878-90.

Whitby, M. C. and Lloyd, R. G. (1998). Targeting Holliday junctions by the RecG branch migration protein of Escherichia coli. *J Biol Chem* **273**, 19729-39.

White, M. F., Giraud-Panis, M. J., Pohler, J. R. and Lilley, D. M. (1997). Recognition and manipulation of branched DNA structure by junction-resolving enzymes. *J Mol Biol* **269**, 647-64.

Yokoyama, H., Kurumizaka, H., Ikawa, S., Yokoyama, S. and Shibata, T. (2003). Holliday junction binding activity of the human Rad51B protein. *J Biol Chem* **278**, 2767-72.
Yu, X., West, S. C. and Egelman, E. H. (1997). Structure and subunit composition of the RuvAB-Holliday junction complex. *J Mol Biol* **266**, 217-22.

Zerbib, D., Mezard, C., George, H. and West, S. C. (1998). Coordinated actions of RuvABC in Holliday junction processing. *J Mol Biol* **281**, 621-30.

Zhao, X., Muller, E. G. and Rothstein, R. (1998). A suppressor of two essential checkpoint genes identifies a novel protein that negatively affects dNTP pools. *Mol Cell* **2**, 329-40.

Zou, L., Cortez, D. and Elledge, S. J. (2002). Regulation of ATR substrate selection by Rad17-dependent loading of Rad9 complexes onto chromatin. *Genes Dev* **16**, 198-208.